TECHNISCHE UNIVERSITÄT WIEN

Dissertation

Synthesis of Secondary Cell Wall Polysaccharide Fragments of *Paenibacillus Alvei*

ausgeführt zum Zwecke der Erlangung des akademischen Grades eines Doktors der technischen Wissenschaften unter der Leitung von

Associate Prof. Dipl.-Ing. Dr.techn. Michael Schnürch

Institut für Angewandte Synthesechemie

Technische Universität Wien

und unter der Mitbetreuung von

Univ.-Prof. i.R. Dipl.-Ing. Dr.techn. Paul Kosma

Institut für Organische Chemie

Universität für Bodenkultur Wien

eingereicht an der Technischen Universität Wien

Fakultät für Technische Chemie

von

Dipl.-Ing. Charlie Lim

Wien, 18.01.2024

“Come, faeries, take me out of this dull house!

Let me have all the freedom I have lost –

Work when I will and idle when I will!

Faeries, come take me out of this dull world,

For I would ride with you upon the wind,

Run on the top of the dishevelled tide,

And dance upon the mountains like a flame”

– William Butler Yeats, The Land of Heart´s Desire

Acknowledgments

The roads you need to travel are packed with adventures and obstacles, and will diverge into many paths. You will experience joy, hope, disappointment, good and bad. A mission towards Mount Doom. And as Bilbo tells Frodo: “It's a dangerous business, Frodo, going out of your door. You step into the Road, and if you don't keep your feet, there is no knowing where you might be swept off to.”[1] The road was worth traveling.

In times of despair, I received strong support from friends, mentors and family. They were the light shining bright, when the shadow was strong. Expressing my gratitude towards all supportive people would extend beyond the scope of these pages, but I want to briefly highlight the most important contributions in arbitrary sequence.

My mother. Thank you for the patience, education and good upbringing.

Chea Ung and Meng Duong.

Ingrid Meidl, for your unwavering support, advices and believe.

Werner Frantsits, for the encouragement and support. Without you, I would have never made it that far.

Andreas Berger. My best friend, half my life. You are my Samwise Gamgee. You lifted me, when I couldn´t reach. You are unrivaled.

Melanie Zitka, for all the good memories. It´s always quality time with you. The next bikepacking trips will surely come.

Johannes Werner. For being a phenomenal friend. We are two minds in sync.

Marco Prusa. Friends since the first day of Freshman year. Thank you for the memories.

Konstantin Raabe and Eva-Sophie Schönegger. You are awesome.

[1] J.R.R Tolkien, The Fellowship of the Ring

Julia Schwarz, Bernadette Dangl and Sepand. For all the Sunday social rides on our bikes.

Maximillian Thier and Stefan Fallmann. For all the super hard rides on our bikes. Pain is gain.

Tuesday Train Ride Group. Thank you for all the training sessions. Watt is everything!

Patrick Böhm, Michael Gülly, Fabian Janisch, Philipp Schlögl, David Radakovits.

All the women I dated and broke up with. Thank you for the fun memories.

My fellow colleagues and staff at Boku. The ´Italian gang´, the ´Asian fraction´, the ´German speakers´ and many more.

Fiona Hager-Mair and Cordula Stefanovic. For the biological support.

Markus Blaukopf. Thank you for the support in both scientific and organizational issues. Without you, the institute would be less than what it is now.

Fabian Pfrengle. For providing a productive environment.

Michael Schnürch. For the supervision and support from TU Wien.

Christina Schäffer. Thank you for the possibility to work in this exciting project, and the kind and ambitious environment.

Paul Kosma. Thank you for the highly competent and professional supervision, combined with a good personality.

Abstract

The Gram-positive prokaryote *Paenibacillus alvei* uses the anionic-charged surface of Secondary Cell Wall Polymers (SCWPs) to non-covalently bind S-layer proteins (SpaA) to form a two-dimensional para-crystalline lattice. The SCWPs of *Paenibacillus Alvei* are stoichiometrically defined polymers, based on [4,6-Pyr-ManNAc-β-(1→4)-GlcNAc] repeats of ~11 units that are β-(1→3) linked wherein the pyruvate provides the decisive negative charge. Previous co-crystallization studies with synthetic mono, di- and trisaccharides revealed that SpaA-ligand binding is driven by a terminal pyruvate.

In continuation of these studies, the total synthesis towards tetrasaccharide ligands 4,6-Pyr-β-D-ManNAc-(1→4)-β-D-GlcNAc-(1→3)-4,6-Pyr-β-D-ManNAc-(1→4)-β-D-GlcNAc with terminal and full pyruvylation substitution was investigated. The challenging β-D-ManNAc-(1→4)-GlcNAc glycosidic bond was established *via* hydrogen-bond mediated aglycon delivery (HAD) pathway for the first time, to the best of my knowledge. The glycosylation of the central disaccharide precursor using an 2-azido-protected thioglycoside donor and a 3-*O*-picoloyl protected acceptor, however, could only be achieved in modest yield and low ß-stereoselectivity. The basic nature of the picoloyl group also gave difficulties during anomeric allyl group deprotection, as it quenched any Lewis- or Brønsted-acidic reagents. The 2+2 glycosylation *via* *N*-phenyl trifluoroacetimidate donor yielded a fully orthogonally protected tetrasaccharide in good yield but was surprisingly accompanied by an elimination side product. Deprotection of the tetrasaccharide needs to be elaborated as several challenges with different protocols were faced during azide group deprotection towards SpaA ligands (target compounds I). The orthogonality of the tetrasaccharide key intermediate allows pyrophosphate introduction at the reducing end for biological pyruvyltransferase studies (target compounds II).

UDP-ManNAc (43 mg) was re-synthesized to investigate the biosynthesis pathway of SCWPs.

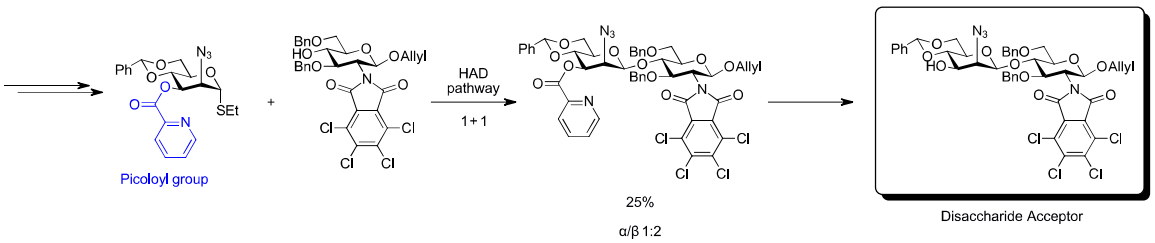

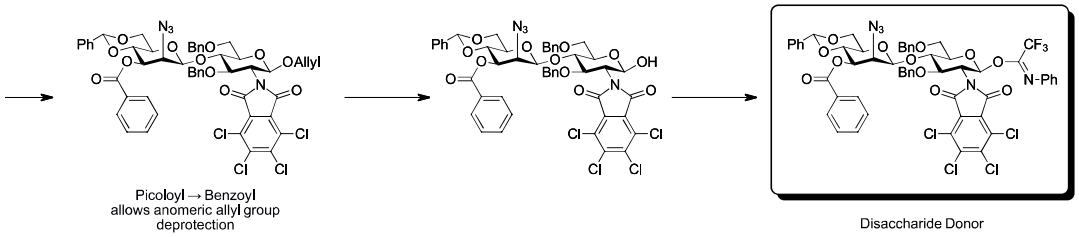

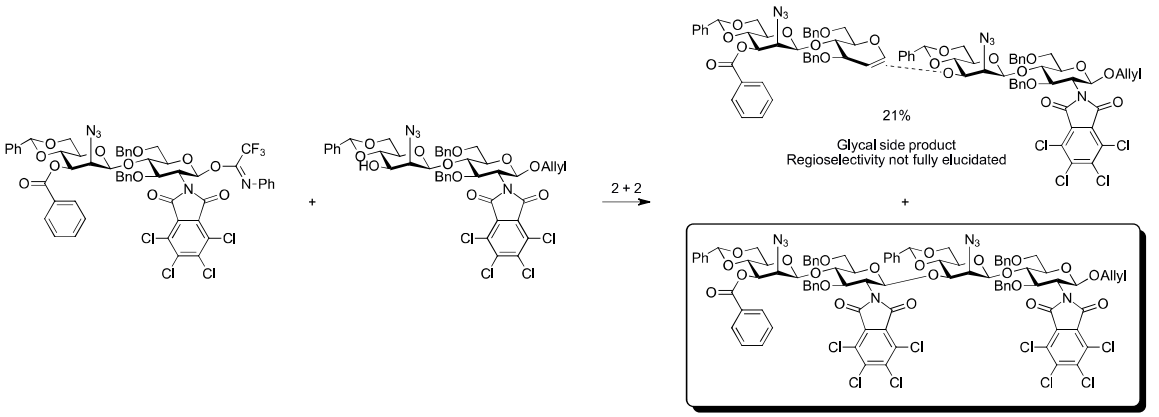

Challenging azide group reduction/*N*-acetylation

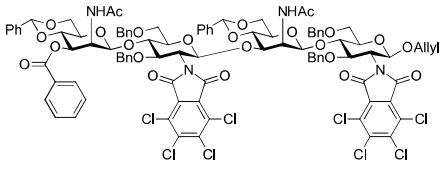

Target Compounds I

for SpaA-ligand binding studies

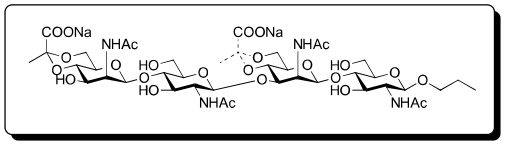

Target Compounds II

for biological studies

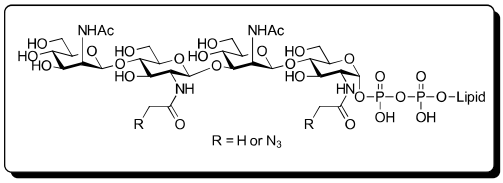

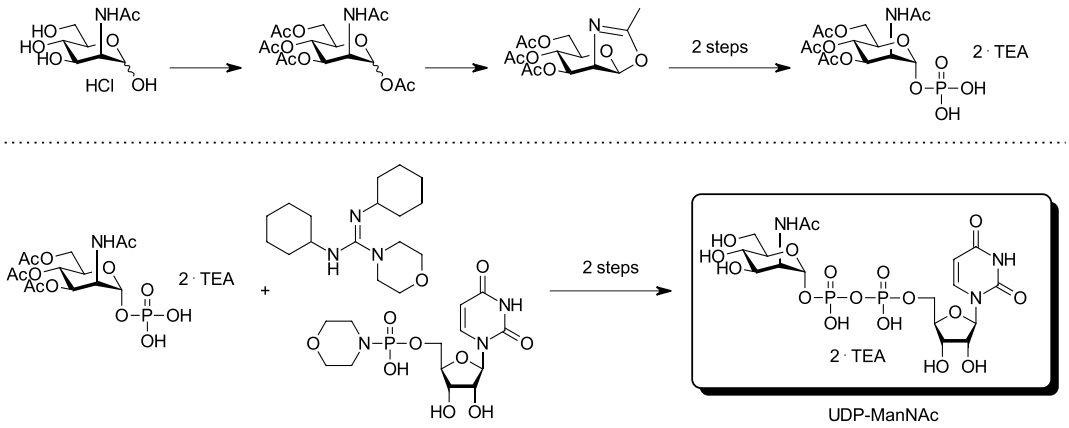

Key

All compounds synthesized in this thesis are labeled with bold Arabic numbers. Intermediates are indicated with bold Roman numbers. Byproducts generated in reactions or compounds that are intended to be grouped together are labeled with bold Arabic numbers followed by bold Latin characters.

Table of Contents

1 List of abbreviations

Ac	Acetyl
Ac_2O	Acetic anhydride
ACN	Acetonitrile
AcOH	Acetic acid
AgOTf	Silver triflate
AllOH	Allylic alcohol
Ar	Aromatic protons
Bn	Benzyl
Bz	Benzoyl
BzCl	Benzoyl chloride
ClAcCl	Chloroacetyl chloride
CLIP-HSQC	clean inphase HSQC
CSA	Camphor sulfonic acid
$Cu(OAc)_2$	Copper(II) acetate
d	Doublet
DBDMH	1,3-dibromo-5,5-dimethylhydantoin
DCE	Dichloroethane
DCM	Dichloromethane
dd	doublet of doublets
DMAP	4-Dimethylaminopyridine
DMF	Dimethylformamide
DMSO	Dimethylsulfoxide
DMTST	Dimethyl(methylthio)sulfonium trifluoromethanesulfonate
equ. / eq.	equivalent
Et_3SiH	Triethylsilane
GlcNAc	*N*-Acetyl glucosamine
GroP	glycerolphosphate
HILIC	Hydrophilic interaction liquid chromatography
HMBC	Heteronuclear multiple-bond correlation spectroscopy
HPLC	High Performance Liquid Chromatography

HPTLC	High Performance Thin-Layer Chromatography
HSQC	Heteronuclear single quantum coherence spectroscopy
LC-MS	Liquid Chromatography - Mass Spectrometry
LTA	Lipoteichoic acid
ManNAc	*N*-Acetyl mannosamine
MeOH	Methanol
MS	Molecular sieves
NaOMe	Sodium methoxide
NIS	*N*-Iodosuccinimide
NMR	Nuclear magnetic resonance
NOESY	Nuclear Overhauser Enhancement Spectroscopy
N-Phth	*N*-Phthaloyl
N-TCA	*N*-Trichloroacetyl
N-TCP	*N*-Tetrachlorophthaloyl
PMe_3	Trimethylphosphine
PPh_3	Triphenylphosphine
RboP	ribitolphosphate
rt	room temperature / ambient temperature
s	Singlet
SCWP	Secondary Cell Wall Polymer
soln.	solution
t	Time or Triplet
TA	Teichoic acid
TBAF	Tetra-*N*-butylammonium fluoride
^{t}BuOH	tert-Butanol
TCA-Imidate	Trichloroacetimidate
TCPA	Tetrachlorophthalic anhydride
TEA	Triethylamine
TFA	Trifluoroacetic acid
TfOH	Triflic acid
THF	Tetrahydrofuran
TLC	Thin-Layer Chromatography
TMS	Trimethylsilyl

TMSOTf	Trimethylsilyl triflate
TUA	Teichuronic acid
WTA	Wall Teichoic Acid

2 Introduction

2.1 Prokaryotic cell wall

The cell wall of prokaryotes features a complex and mesh-like structure, consisting mainly of the extracellular peptidoglycan.[1] The backbone of the peptidoglycan is made up of two linear polymers of Mur*N*Ac/Glc*N*Ac repeats that are β-(1→4) glycosylated.[2] The backbone strands are cross-linked *via* oligopeptides by transpeptidases and in case of some Gram-positive bacteria, the oligopeptide incorporates a glycin interbridge.[3] The cell wall must be strong enough to withstand the high intracellular pressure and any environmental impact (such as simple lysis), but simultaneously should be flexible enough for cellular development.[1] The cell wall is responsible for bacterial survival, but is absent in eukaryotes.[2] The latter fact makes the cell wall historically an attractive target for antibiotics (such as the β-lactam antibiotics that target transpeptidases) and is underlined by the resurging interest in bacterial cell wall.[1]

The cell envelope of Gram-positive and Gram-negative bacteria both have a peptidoglycan layer, but are differentiated by their additional layering.[4]

Gram-negative bacteria (e.g. *Escherichia Coli*) have three principal layers; the inner membrane, the peptidoglycan and the outer membrane.[5] The outer membrane functions as an additional protective and stabilizing layer.[4]

Gram-positive bacteria (e.g. *Staphylococcus aureus*, *Bacillus subtilis*) lack any outer membrane organelle, but the peptidoglycan layer is much thicker (30 – 100 nm) than in Gram-negative prokaryotes (few nm).[4] The thickness gives the cell the ability to withstand the intracellular pressure. Intertwined into the peptidoglycan layer are polysaccharides (covalently or not).[4] Due to their secondary role, these polysaccharides are termed ´secondary cell wall polymers´ (SCWP).[6–8]

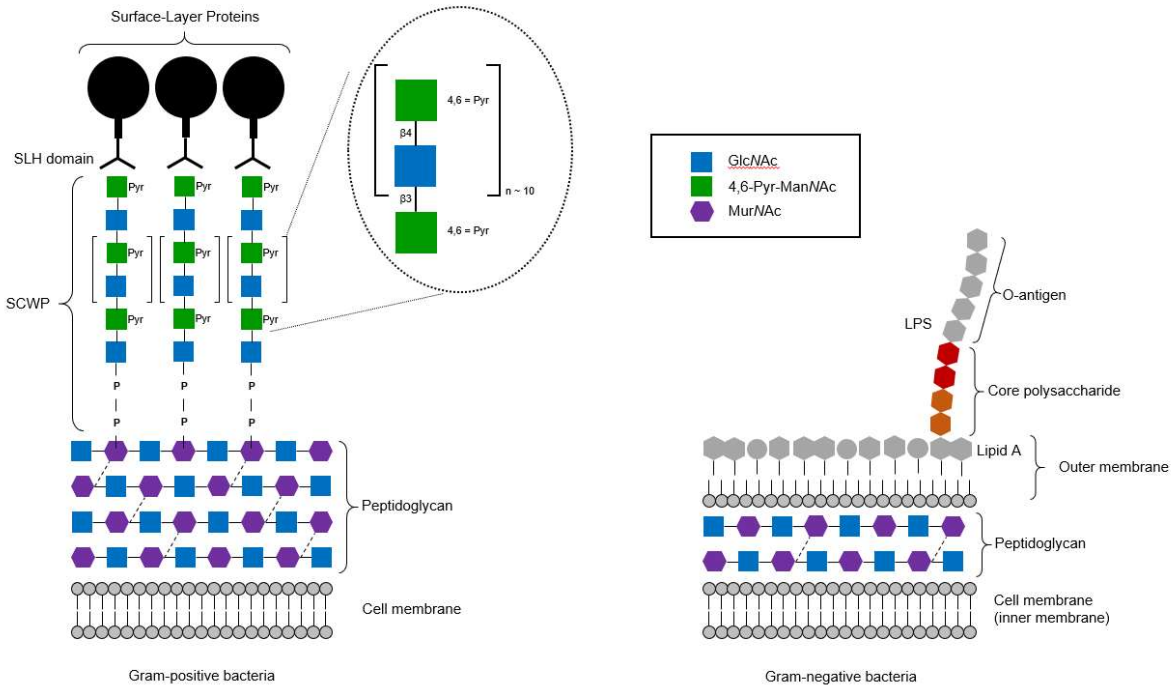

Figure 1: Prokaryotic cell wall layering of (left) Gram-positive [4] (i.e. *Paenibacillus Alvei* [9]) and (right) Gram-negative [5] bacteria

2.2 Prokaryotic Surface-Layer Proteins

The outermost layer of the cell envelope of Gram-positive bacteria are often decorated with surface-layer proteins. These proteinaceous surface-layers (S-layers) are constructed from subunits that self-organize into two-dimensional para-crystalline lattices that are 2-20 nm in thickness.[9–17] For example, the cell envelope of *Paenibacillus Alvei* CCM 2051^T (ATCC 6344; DSM 29) is completely covered with an oblique proteinaceous S-layer lattice.[18] Analysis *via* electron microscopy revealed an oblique lattice with lattice constants of 10.0 and 7.9 nm.[18] SDS-PAGE and PAS staining reaction revealed that the lattice is composed of mono- and di-glycosylated S-layer proteins (Figure 2).[19] The characterization of S-layers from various *Bacillaceae* revealed lattice spacings varying from 8.6 nm to 17.0 nm and the lattice types span from oblique, square to hexagonal.[20] S-layers were first detected *via* electron microscope in 1952[21] and decades of research proved that these protein arrays are common within the cell wall of prokaryotes.[22] A common characteristic of S-layers among prokaryotes is yet to be elucidated, but S-layers are assumed to have a variety of species-specific functions, including cell shaping, structural maintenance, environmental protection, host adhesion, filtering and virulence.[9,23–35]

Evidently, understanding the structure and attachment of S-layer (glyco)proteins to the cell wall facilitates the development of (new) antibiotics and potentially break the barrier towards biotechnological exploitation in drug delivery and vaccine design.[31,36–42]

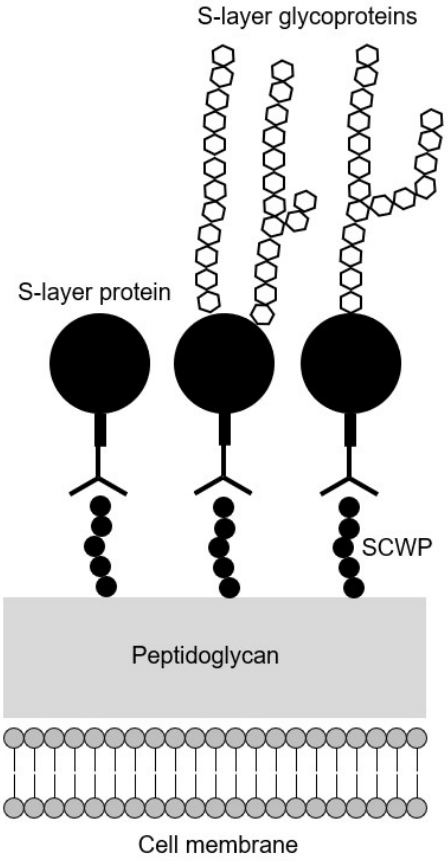

Figure 2: Roughly 20% of S-layer proteins are glycosylated[19]

2.3 Secondary Cell Wall Polymers

As described previously (Chapter 2.1 and 2.2), the cell envelope of Gram-positive prokaryotes is composed of the cell membrane, a thick layer of peptidoglycan and S-layer (glyco)proteins on the surface. In-between are located the secondary cell wall polymers (SCWP) that act as an anchor to stick the (glyco)proteins to the cell wall. These polysaccharides are of big variety and many of them are covalently linked to the peptidoglycan.[8] Based on their composition, the secondary cell wall polymers can be classified into three categories:

i. Teichoic acids[43]
ii. Teichuronic acids[44–46]
iii. Other neutral or acidic polysaccharides not assignable as teichoic or teichuronic acids[47,48]

2.3.1 Teichoic acids

Teichoic acids (TAs) are highly diverse anionic polysaccharides with ribitol (RboP) or glycerol (GroP) phosphodiester repeats that impart a negatively charged polymer surface.[49] Teichoic acids are divided into wall teichoic acids (WTA) and lipoteichoic acids (LTA).[43] They are differentiated in how they are bound to the cell envelope. (Figure 3)

Wall teichoic acids are constructed from a highly conserved linkage repeat units.[47,50,51] The linkage unit is composed of a disaccharide head group (Man*N*Ac-β-(1→4)-Glc*N*Ac-1P) and a 4-*O*-polyGroP (n ~ 1-3) and is tethered to the 6-*O*-MurNAc of the peptidoglycan *via* a α-1-phosphodiester bond.[47,50,51]

The structural diversity of WTAs comes from the variety of the repeat units (up to 60 repeats) that can even differ within a species (i.e. *B. subtilis*).[49,51–54] The polyribitol (polyRboP) and polyglycerol (polyGroP) chains are made up from four types of repeat units (Figure 4).[49,51–54]

The substitution pattern (D-alanyl, glycosyl) on the free hydroxy groups of the polyol repeat units heavily define the properties and functions of the WTA.[51]

Lipoteichoic acids share similar structural characteristics as wall teichoic acids, but with some alterations.[4] The decisive difference is that they are not bound to the

peptidoglycan, but are attached to the glycolipids of the cell membrane.[4] The polyol chains are shorter and thus do not extend (much) beyond the peptidoglycan.[4]

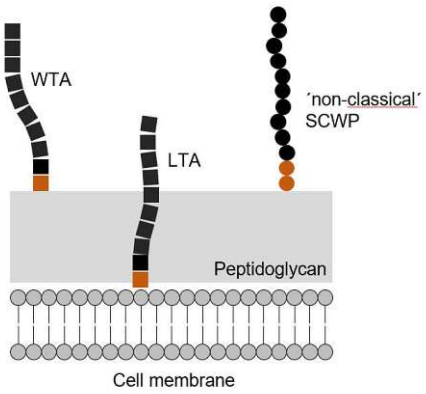

Figure 3: How various SCWPs (WTA[47,50,51], LTA[4], non-classical SCWP[38,55,56]) anchor to the cell wall

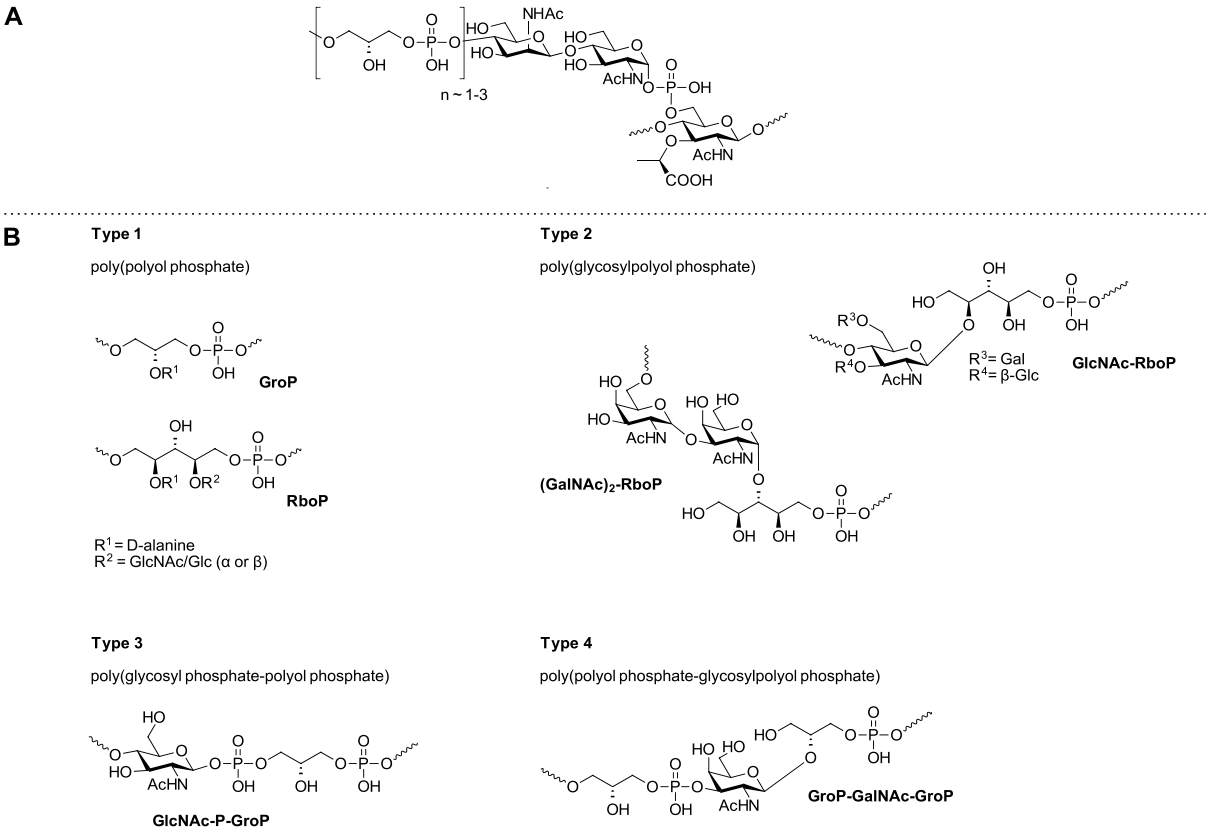

Figure 4: (A) WTA linkage unit (B) WTA repeat units[49,52]

2.3.2 Teichuronic acids

Teichuronic acids (TUA) are in general less investigated than teichoic acids.[57–59] TUA are anionic polysaccharides with uronic acids (carboxyls) imparting the negative charge on the surface.[57–59] *Micrococcus luteus* is a Gram-positive bacterium with TUA chains composed with almost up to 100 disaccharide repeat units.[57–59] The repeat unit is [→4)-β-D-ManNAcA*p*-(1→6)-α-D-Glc*p*-(1→]$_{n<100}$ and the polysaccharide is covalently attached to the peptidoglycan *via* an oligosaccharide and phosphate.[57] (Figure 5)

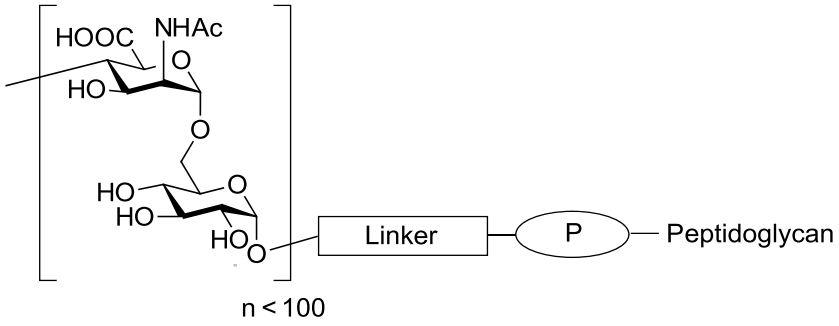

Figure 5: Structural composition of TUA in *M. luteus*[57]

2.3.3 Non-classical Secondary Cell Wall Polymers

Preliminary research focusing on glycosylated S-layer proteins within the laboratory of collaborating partner Prof. Dr. Christina Schäffer has revealed the existence of new secondary cell wall polymers.[38,55,56] In the course of S-layer (glyco)protein purification of *Bacillaceae* cell walls[60], minor amounts of conjugates were isolated that were initially thought of as a second set of S-layer (glyco)proteins[61–65]. Further purification and separation unmasked these glycan structures as non-classical SCWPs and are classified as ´Other neutral or acidic polysaccharides not assignable as TAs or TUAs.[8]

Like teichoic acids, non-classical secondary cell wall polymers of *Bacillaceae* can differ greatly between organisms, but are highly conserved within a species.[8,35] As highlighted by Schäffer *et al*, these SCWPs have varying carbohydrate constituents such as Glc*p*NAc, Man*p*NAc, Gal*p*NAc, Man*p*-2,3-diNAcA, Glc*p* and Rib*f* with pyruvates, phosphates and acetates as non-carbohydrate modifications.[8,35] According to the group of Schäffer, the polysaccharides can be classified into three groups depending on their features.[8,35]

2.3.3.1 Group 1 of non-classical SCWP

Paenibacillus alvei CCM2051^T features a repeat unit of [ManNAc-(1→4)-β-GlcNAc] in its linear backbone that are β-(1→3) glycosylated.[64] The reducing end is attached *via* an α-1-pyrophosphate to the 6-*O*-MurNAc of the peptidoglycan.[64] Every disaccharide motif has a 4,6-pyruvate at the ManNAc moiety, giving the SCWP it´s anionic surface charge.[64] The ManNAc-GlcNAc building block is a common motif in other non-classical and teichoic acid SCWPs.[47] Pyruvate-containing non-classical SCWPs are also found in *Lysinibacillus sphaericus* (formerly *Bacillus sphaericus*)[64] and *Bacillus anthracis*.[66] The ManNAc-GlcNAc repeat moiety is also reported in neutral SCWPs. Examples are *Thermoanaerobacterium thermosaccharolyctium* D120-70[61] and E207-71[67], where the completely missing pyruvate is substituted by a ribofuranose side chain on every second repeat unit. (Figure 6)

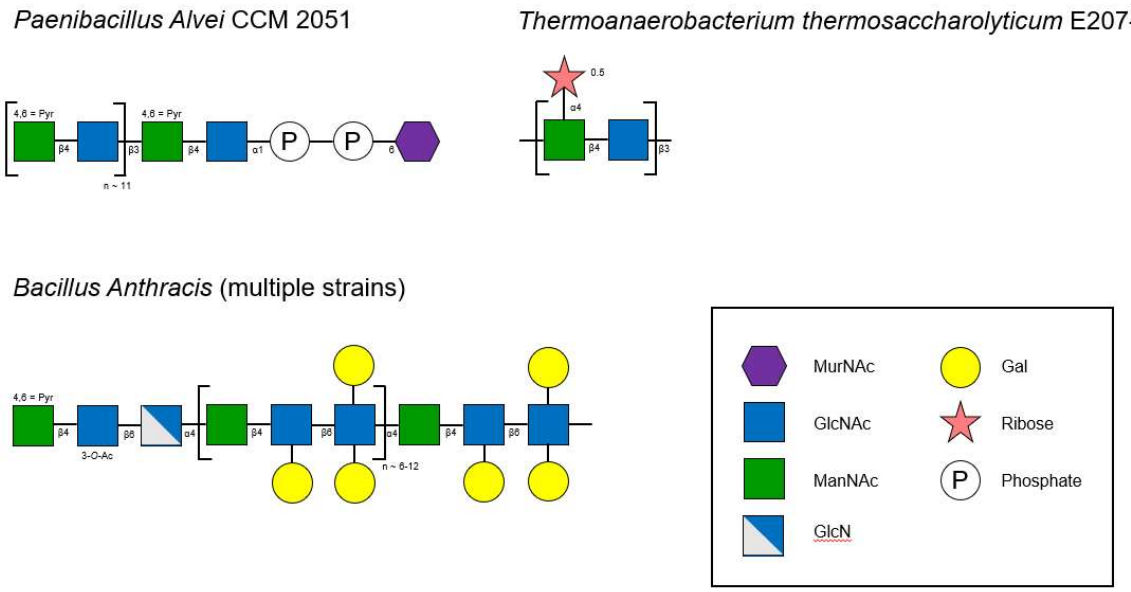

Figure 6: Structural composition of selected non-classical SCWPs of group 1 (*P. alvei*[61] and *B. anthracis*[67])

2.3.3.2 Group 2 of non-classical SCWP

The SCWP of *Geobacillus stearothermophilius* NRS 2004/3a and many of its wild-type strains feature a tetrasaccharide building block with an average repeat of 6 units.[62,63] It was the first SCWP of a S-layer (glyco)protein of which the structural composition was elucidated.[62,63] The polymer owes it´s negative charge to carboxyl groups on the uronic acid moieties.[62,63] The SCWP is attached to the peptidoglycan *via* a 6-*O*-pyrophosphate linkage to the MurNAc residues of which 20-25% are substituted.[62,63]

The SCWP of *Anoxybacillus tepidamans* GS5-97^T (formerly *Geobacillus tepidamans*) has the same linear backbone as *Geobacillus stearothermophilius* with altered substitution on the carboxyl groups, resulting in a neutral character of the polymer.[68] The SCWP is attached to the peptidoglycan *via* a common phosphodiester linkage to the 6-*O*-MurNAc.[68] (Figure 7)

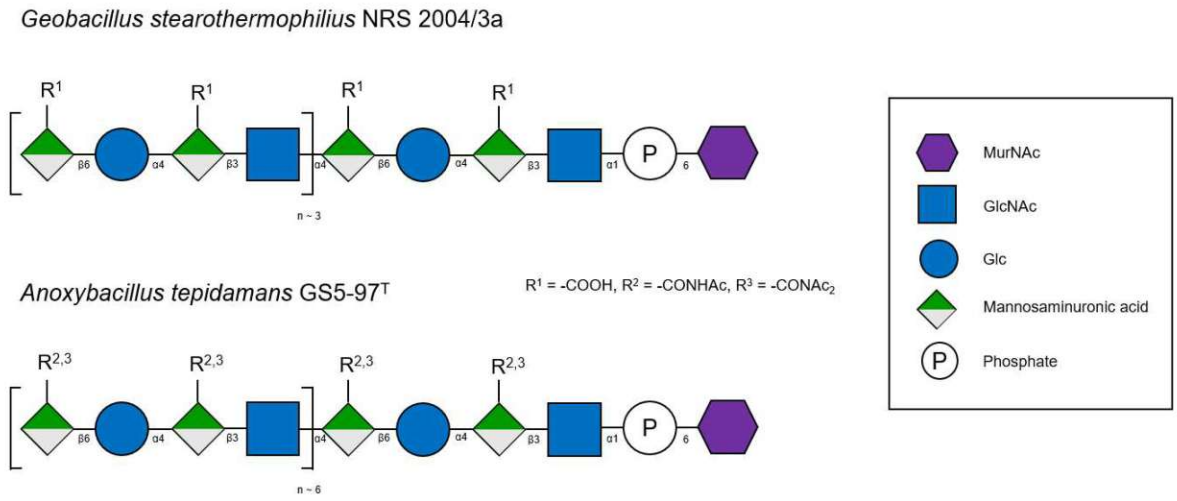

Figure 7: Structure of group 2 non-classical SCWPs[38,63,68–70]

2.3.3.3 Group 3 of non-classical SCWP

The charge-neutral SCWP from *Aneurinibacillus thermoaerophilus* DSM 10155 features a biantennary oligosaccharide structure with defined chain length.[11,65,71] The polysaccharide is composed of a trisaccharide repeat of [→3)-α-D-GlcNAc-(1→3)-β-D-ManNAc-(1→4)-β-D-GalNAc-(1→].[65] Such biantennary polysaccharide structures are more common in eukaryotes rather than in prokaryotes.[65] The SCWP from *G. stearothermophilius* PV72/p2 with a pentasaccharide repeat of →4)-[β-D-Glc*N*Ac-(1→3)]$_{0.3}$-β-D-Man*N*AcA-(1→4)-β-D-Glc*N*/*N*Ac-(1→6)-[4,6-(S)-Pyr-α-D-Man*N*Ac-(1→4)]-α-D-Glc*N*Ac-(1→ also displays a branched structure.[72,73] Chemical exposure with hydrofluoric acid for cleavage of the peptidoglycan-linkage has led to loss of information on the linkage region, extent of pyruvate substitution and proof for *N*-deacetylated glycoses.[72,73] The SCWP contains (S)-configured pyruvates on the ManNAc residues, resembling the group 1 of non-classical SCWPs.[72,73] The pyruvate substitution does not appear within the linear backbone, but rather in the branches extending from the α-D-GlcNAc residues that start at ManNAcA moieties.[72,73]

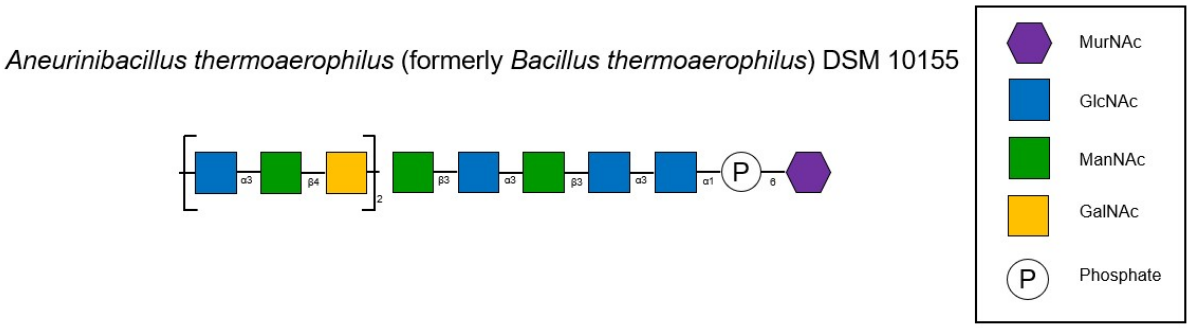

Figure 8: Biantennary structure of *Aneurinibacillus thermoaerophilus* DSM 10155[11,65,71]

These anionic secondary cell wall polymers make up substantial amounts of prokaryotic cell walls.[6,74,75] For example, teichoic and teichuronic acids account for 10-60% of the cell wall mass.[6,74,75]

S-layer (glyco)proteins of *Bacillaceae* make up to 15% of the cell wall and the corresponding SCWPs represent 7-15% of the underlying peptidoglycan.[60]

A distinct function of the negative surface of SCWPs, neatly expressed as a continuum of anionic charge[51], is yet to be elucidated, but is associated with several proposed functions.[6,44,76–79]

- Binding of (divalent) cations
- Regulation of the equilibrium of metal ions for membrane functionality
- Binding of proteins
- Folding of proteins (extracellular and metallo-)
- Source of phosphate in case of phosphate deficiency
- Interaction with lytic enzymes (cell wall)
- Barrier (diffusion of nutrients and metabolites)

2.4 Binding interactions of non-classical SCWPs and S-layer proteins

S-layer (glyco)proteins can be covalently or non-covalently attached to various components of the cell wall. For example, the plasma membrane in archaea[31,80,81], the peptidoglycan in Gram-positive prokaryotes[8,25,31,82] and the lipopolysaccharide in Gram-negative[33,83,84] bacteria.[9] S-layer (glyco)protein attachment to the cell wall is best described for Gram-positive bacteria, where non-classical SCWPs (covalently linked to the peptidoglycan, see Chapter 2.3) bind the glycoconjugates *via* non-covalent mechanisms.[8,35] The binding mechanism is based on the interaction of a S-layer homology domain (SLH domain) at the termini of the protein (i.e. S-layer protein

or other extracellular protein) with the SCWP (Figure 1).[13,31,33,85–87] The domain family SLH accounts 14,079 sequences (SLH domains) distributed over 651 bacterial species, indicating early development of SLH-SCWP binding interaction in the realm of prokaryotes.[88,89]

Paenibacillus alvei CCM 2051^T was selected as model organism to fully elucidate the structural and molecular basis of anchoring the S-layer protein SpaA *via* its fully defined non-classical SCWP (Figure 6).[18,35,64,90] The SLH domain of SpaA, present as a triplicate at the N-terminus, features a conserved TRAE motif in SLH1, TVEE in SLH2 and TRAQ in SLH3, the latter two being variants of TRAE.[9] These variations lead to unequal SCWP binding contribution and mutation of the three motifs to TAAA yielded 37%, 88% and 50% of the original binding affinity.[82,91] The SLH domain is followed by a C-terminus region that is believed to provide shelter for the domains. The binding interaction SLH-SCWP depends on the negative charge imparted by the pyruvates of the SCWP.[64,66,88] Within the TRAE motif, the arginine residue was shown to be pivotal for interaction with the pyruvate.[82,85,92]

2.5 Proposed Biosynthesis Pathway

The group of Schäffer[91] has previously reported the identification (transcription analysis) of the *spaA* gene coding of *Paenibacillus alvei* CCM 2051^T. In the course of which, seven sequences (*orf1*, *csaB*, *tagA*, *tagO*, *slhA, spaA* and *orf7*) were found to be presumably involved in the biosynthesis of the pyruvylated SCWP. The sequences were analyzed *via* database comparison and in the following, *csaB*, *tagA* and *tagO* are discussed briefly.[91]

CsaB shows high similarity to pyruvyltransferases (CsaB) in other *Bacillus* homologues.[91] The necessity of CsaB for the pyruvylation of SCWPs was shown in case of *Bacillus anthracis* and *Thermus thermophilus*.[66,88] The simultaneous presence of CsaB and SLH domains in various *Bacillus* strains underlines the importance and conservation of interaction of SLH domains with pyruvylated SCWPs across prokaryotes.[66,88] The presence of *csaB* obviously indicates its role as pyruvyltransferases CsaB in *Paenibacillus alvei* CCM 2051^T.[64]

TagA and *TagO* encode the glycosyltransferases TagA and TagO in various *Bacillus* species.[91] TagA (ManNAc transferase) and TagO (GlcNAc transferase) are responsible for the construction of the GlcNAc-ManNAc disaccharide moiety of the

linkage unit in teichoic acids.[93,94] As a ManNAc-GlcNAc repeat unit is present in the SCWP of *P. alvei* CCM 2051^T, it was obvious to assess similar roles in the SCWP biosynthesis of *P. alvei*.[91]

The *in vitro* functional characterization of the enzymatic steps by Hager *et al.*[95] utilizing recombinant, tagged enzymes TagA and CsaB unveiled TagA as an inverting UDP-α-D-ManNAc:GlcNAc-lipid carrier transferase and CsaB as a pyruvyltransferase. The pyruvyltransferase was shown to be only active on a lipid-linked pyrophosphate.[95] The study included a synthetic acceptor 11-phenoxyundecyl-diphosphoryl-α-D-GlcNAc (provided by the group of Inka Brockhausen)[94,96], UDP-α-D-ManNAc and phosphoenolpyruvate (PEP) as donor substrates.

Furthermore, the recombinant UDP-GlcNAc-2-epimerase of *P. alvei* was used to circumvent the tedious (re-)synthesis of the nucleotide sugar.[95] The epimerization rate of the recombinant enzyme of 9.5% was within the range of previous publications.[97–99]

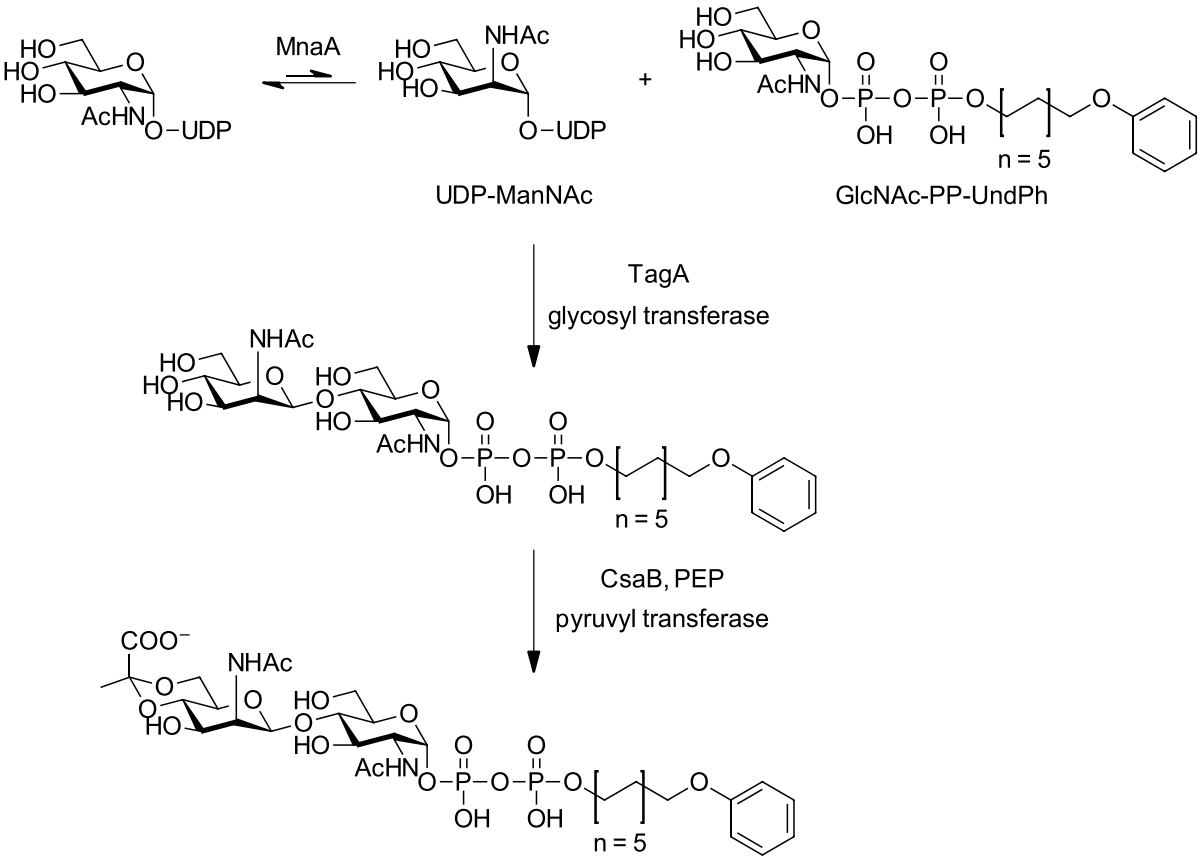

Scheme 1: One-pot cascade reaction towards lipid-linked SCWP precursor[95]

To compensate the low epimerization rate, the three enzymes (MnaA, TagA, CsaB) were successfully utilized in a one-pot cascade reaction to yield the pyruvylated lipid-linked disaccharide monomer.[95] (Scheme 1)

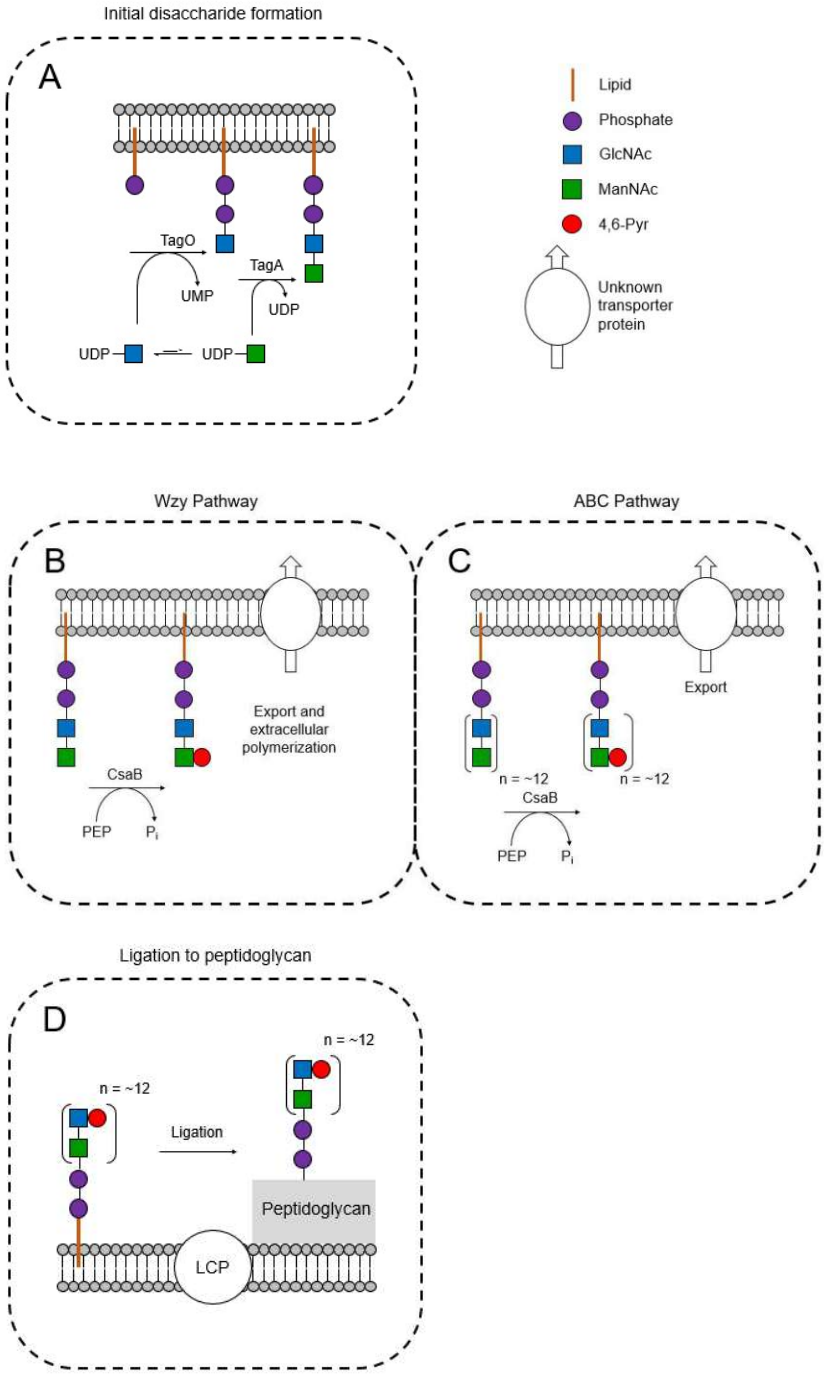

Figure 9: (A) Highly conserved disaccharide formation in SCWP biosynthesis (B and C) Two proposed pathways of SCWP pyruvylation (D) Ligation of SCWP from cell membrane to peptidoglycan

The proposed biosynthesis pathway (Figure 9) can be grouped into three stages. In stage A, the initial disaccharide repeat unit is constructed by the glycosyltransferases TagO and TagA. This step is highly conserved among SCWP biosynthesis across many prokaryotes.[52] The stages B and C represent the suggested steps of pyruvylation. Pyruvylation might occur at the stage of the lipid-linked disaccharide monomer (stage B); termed Wzy pathway in reference to the Wzx/Wzy enzyme (i.e. *B. anthracis*) that is believed to be responsible for translocation and polymerization outside of the cytoplasm.[100–104] Chateau *et al.* proposed in 2020 a combination of intracellular and extracellular glycosylation mechanism in *Bacillus anthracis*.[105,106]

Pyruvylation also might occur at the stage of the lipid-linked polymer (stage C), followed by translocation of the SCWP to the extracellular space; termed ABC pathway in reference to wall teichoic acid biosynthesis.[52,107] In WTA synthesis, the ABC transporter (ATP-binding cassette) is composed of two enzymes (TagGH and TarGH) that translocate the polymer starting from the non-reducing end or from the linkage unit.[52,107,108]

The final ligation of the polymer from the cell membrane to the peptidoglycan at the extracytoplasmic face is catalyzed by LCP transferase (LytR-CpsA-Psr); a conserved class of phosphotransferases in bacteria that is involved in the ligation process within SCWP biosynthesis.[109,110] The exact mechanism and functions of LCP transferases are yet to be elucidated, but there are indications that LCP requires a lipid-phosphate bound polymer. The lipid carrier is released during ligation and resumes as acceptor for polymer construction.[109] The group of Schäffer has reviewed the current knowledge (2021) on LytR-CpsA-Psr Glycopolymer Transferases and its potential for novel antibiotics.[109]

2.6 *Paenibacillus alvei* as well tractable model

Paenibacillus alvei CCM 2051T is a mesophilic Gram-positive prokaryote and is known for being a secondary invader of honeybee colonies that are infected with the European foulbrood, caused by *Melissococcus pluton*.[111,112] The bacterium is fully covered with a S-layer glycoprotein that crystallizes in an oblique lattice (Chapter 2.2).[18] The surface glycoprotein SpaA of *P. alvei* is an excellent platform to study SLH-SCWP binding interaction as *in vivo* and *in vitro* studies can be performed.[112] Furthermore, the SCWP of *P. alvei* is stoichiometrically defined and does not display

any distinct terminal unit and murein linkage during the biosynthesis.[64] (Chapter 2.3.3.1) Together with the availability of pure recombinant pyruvyl transferase (r*Pa*CsaB)[95] and an established quantitative pyruvylation assay in the group of Schäffer[95,113], these characteristics make *Paenibacillus alvei* CCM 2051^T a well tractable model.

2.7 Preliminary work

In cooperation with the groups of Christina Schäffer and Stephen V. Evans, four synthetic ligands – mimicking fragments of the SCWP of *P. alvei* – were previously synthesized and co-crystallized with $SpaA_{SLH}$ to investigate the molecular basis of the SCWP-protein interactions.[9,24]

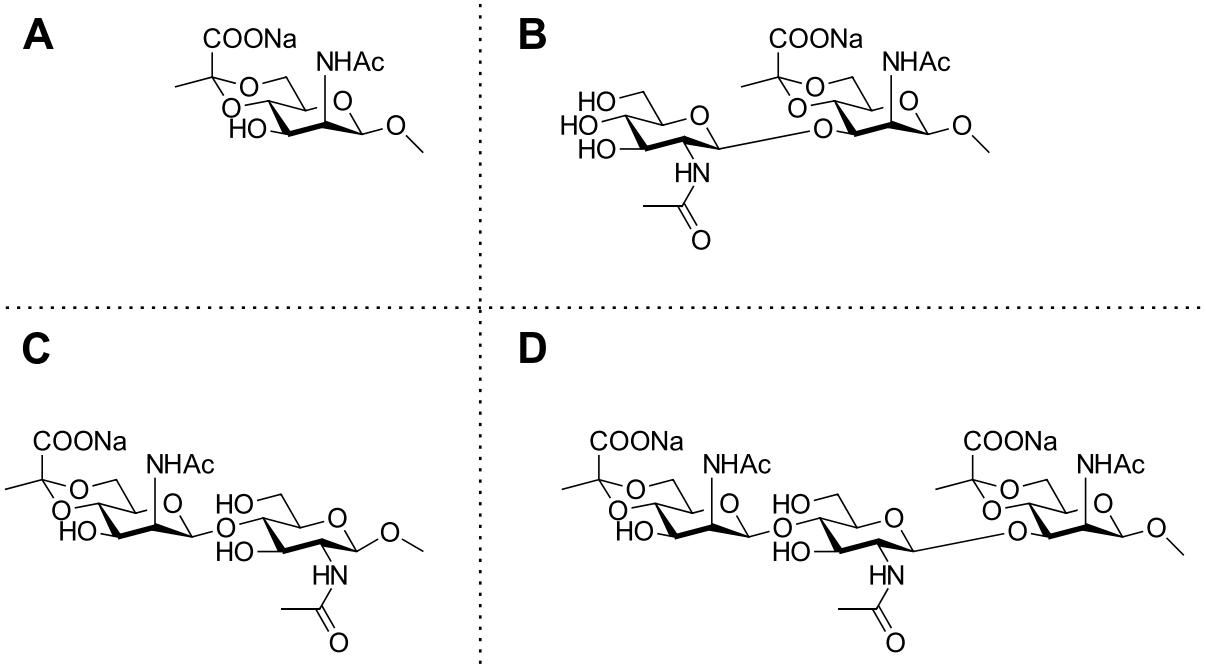

Figure 10: Synthetic SCWP fragments of *P. alvei*[9,24,114]

The three conserved TRAE, TVEE and TRAQ motifs of SpaA (Chapter 2.5) are located near and unequally contribute to the three grooves G1, G2 and G3 harbored by the three SLH domains (SLH1, SLH2, SLH3).[9,24] The co-crystal structure of synthetic monosaccharide 4,6-Pyr-β-D-ManNAcOMe (Figure 10A) with wild-type $SpaA_{SLH}$ uncovered ligand binding in a narrow pocket of G2 composed of conserved residues of all three SLH domains.[9] (Figure 11) The pyruvate is bound deeply into the pocket *via* salt bridge interactions (Arg, Lys) and H-bonds (Gln, Gly amides).[9] The hydrophobic moiety of the ManNAc shows stacking interaction with a Trp residue.[9]

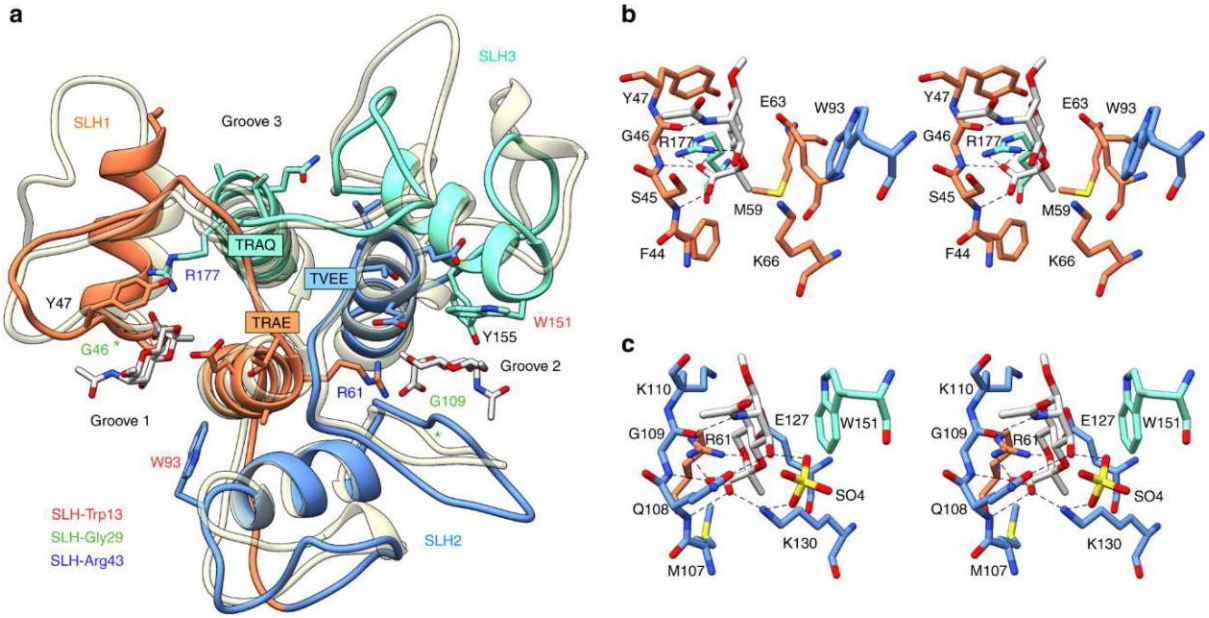

Figure 11: (a) Ribbon diagram of SpaA$_{SLH}$ with monosaccharide ligand (PDB 6CWI); overlapped by Sap from *B. anthracis* (PDB 3PYW) in tan (b) Stereo views of monosaccharide ligand in G1 (c) and G2. "Structural basis of cell wall anchoring by SLH domains in *Paenibacillus alvei*." by "Blackler, R.J., López-Guzmán, A., Hager, F.F. *et al.*" in "*Nat Commun* **9**, 3120 (2018)" is licensed under Creative Commons Attribution 4.0 International License (no changes were made to the image)

Further analysis of the binding interaction *via* isothermal titration calorimetry (ITC) in solution between SpaA$_{SLH}$ and 4,6-Pyr-β-D-ManNAcOMe (Figure 10A) unveiled 1:1 binding stoichiometry (K_D = 29 nM), indicating high preference for G2 in wild-type SpaA$_{SLH}$.[9]

The mutation of a conserved glycine residue to alanine (G109A) resulted in inactivation of the G2 binding site and facilitated G1 binding for the monosaccharide.[9] (Figure 10A) The G1 binding affinity was one order of a magnitude less than in case of G2 binding.[9] The mutations of two conserved glycine residues (G46A, G109A) suppressed any ligand-binding and no binding in G3 was observed.[9] The ability of S-layer protein SpaA$_{SLH}$ to utilize two grooves with different preferences (G2, G1) for binding may spark a first glance on how S-layer carrying prokaryotes may avoid strain during cell growth and division.[9]

The internal disaccharide repeat β-D-GlcNAc-(1→3)-4,6-Pyr-β-D-ManNAcOMe (Figure 10B) displayed no binding affinity to SpaA$_{SLH}$ by ITC, indicating the necessity for a terminal pyruvate.[9] Despite the lack of interaction *via* ITC in solution, the successful co-crystallization of the internal repeat with SpaA$_{SLH}$ revealed higher binding affinity in crystalline environment.[9] Hereby, the 4,6-Pyr-ManNAc moiety binds

to G2 while the GlcNAc moiety is aligned in two different conformations with no H-bonds to the protein.[9] The protein displays some disorder in its structure in proximity to the GlcNAc moiety to clear room for the GlcNAc face.[9]

The next leading questions were to elucidate the (binding) interactions of subsequent repeat units – such as the role of internal pyruvates and the acceptance of longer fragments in G2 and G1.[9,24] The terminal disaccharide 4,6-Pyr-β-D-ManNAc-(1→4)-β-D-GlcNAcOMe[114] (Figure 10C) and trisaccharide 4,6-Pyr-β-D-ManNAc-(1→4)-β-D-GlcNAc-(1→3)-4,6-Pyr-β-D-ManNAcOMe (Figure 10D) were synthesized and binding affinity was determined *via* ITC analysis and co-crystallization with wildtype-SpaA$_{SLH}$ and mutants (SpaA$_{SLH}$/G109A and SpaA$_{SLH}$/G46A/G109A).[24]

Table 1: ITC binding analysis (20 °C) for ligands with terminal pyruvate (Figure 10) *SpaA$_{SLH}$ **SpaA$_{SLH}$/G109A ***SpaA$_{SLH}$/G46A/G109A [9,24]

Ligand	Protein variant	-TΔS (kJ/mol)	ΔH (kJ/mol)	ΔG (kJ/mol)	Stoichiometry	K_D (nM)
4D	wildtype*	-18.70 ± 5.57	-27.14 ± 3.29	-45.84 ± 2.29	1.16 ± 0.10	4.7
	single**	-15.99 ± 1.00	-20.92 ± 0.57	-36.91 ± 0.47	1.44 ± 0.25	260
	double***	n.a.	n.a.	n.a.	n.a.	n.a.
4C	wildtype*	-9.95 ± 2.08	-30.36 ± 1.64	-40.31 ± 0.65	1.20 ± 0.16	64
	single**	-15.74 ± 1.35	-20.95 ± 1.51	-36.70 ± 0.20	1.30 ± 0.19	288
	double***	n.a.	n.a.	n.a.	n.a.	n.a.
1A	wildtype*	45.74 ± 16.01	-87.85 ± 15.62	-42.10 ± 0.65	0.91 ± 0.04	29
	single**	13.33 ± 7.0	-50.64 ± 7.29	-37.31 ± 0.33	0.92 ± 0.04	226
	double***	n.a.	n.a.	n.a.	n.a.	n.a.

All three terminal pyruvylated ligands showed 1:1 binding stoichiometry (Table 1).[9,24] The disaccharide displays a greater dissociation constant (lower binding affinity) than the monosaccharide for the wildtype protein, while the trisaccharide features an opposite trend ($K_{D,tri} < K_{D,mono} < K_{D,di}$).[9,24] The dissociation constants for the single mutant SpaA$_{SLH}$/G109A are as expected higher and no binding was observed in case of the double mutant SpaA$_{SLH}$/G46A/G109A.[9,24] The Gibbs energy of the three ligands are within similar range, for both wildtype and single mutant.[9,24]

The co-crystallization structure of disaccharide-SpaA$_{SLH}$ revealed the analogical pocket binding pattern as in case of the monosaccharide.[9,24] The glycosidic bond is located outside the pocket and the GlcNAc moiety is facing away from the binding site

with no direct interactions with the protein.[9,24] In accordance with the mono- and disaccharide, the co-crystal structure of trisaccharide-SpaA$_{SLH}$ utilizes the terminal ManNAc residue as anchoring point.[9,24] The GlcNAc and ManNAc moieties are located outside the binding pocket and form indirect contact with the protein surface *via* water molecules.[9,24]

2.8 Aim of this work

To definitely confirm that SpaA$_{SLH}$-SCWP binding preferably depends on the terminal pyruvate, the tetrasaccharides A (Figure 12) containing two ManNAc-GlcNAc repeat units with different pyruvate substitution were selected as main targets. The orthogonality of the protecting group pattern was selected to allow further construction towards lipid-pyrophosphate carrying polysaccharides B (Figure 12).

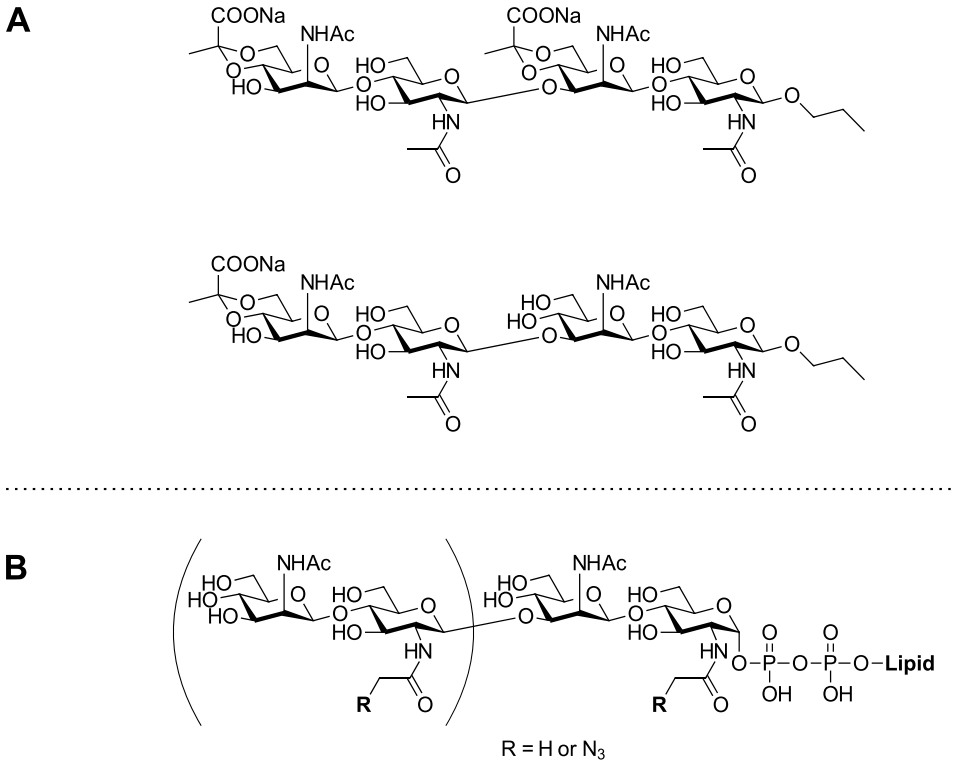

Figure 12: Target compounds

The lipid-pyrophosphate tetrasaccharides B (Figure 12) are intended for pyruvylation studies with recombinant r*Pa*CsaB to investigate the polymerization pathway (ABC pathway vs Wzy pathway; Chapter 2.5). The equatorial *N*-acetyls may be equipped with azides for biorthogonal monitoring *via* click-reaction.

3 Results and discussion

3.1 Retrosynthetic analysis

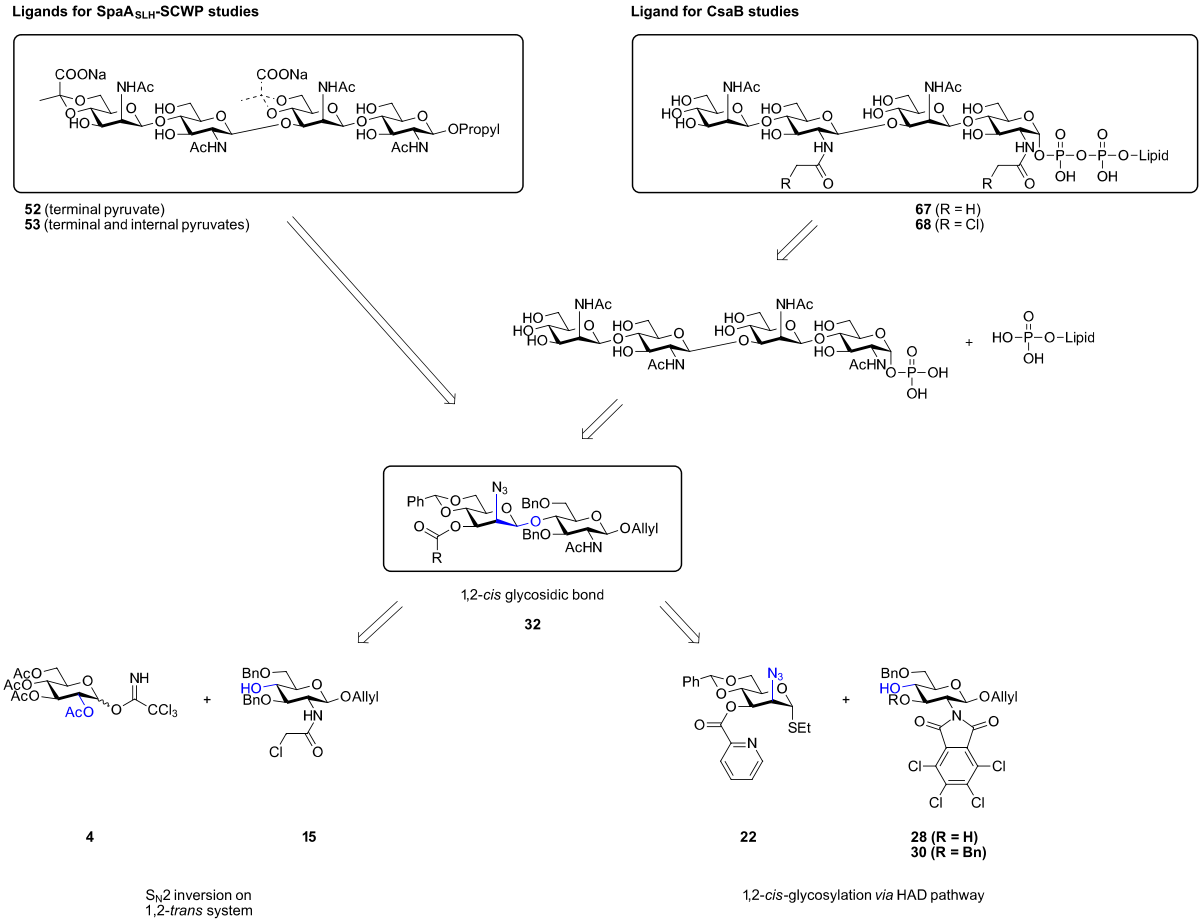

Scheme 2: Retrosynthetic approach towards ligand targets for crystallization and pyruvylation studies

The main targets **47** and **48**, intended for SpaA$_{SLH}$-SCWP co-crystallization experiments, as well as pyruvylation targets **67** and **68**, can be reduced to mutual disaccharide **32**. The key intermediate **32** features a fully orthogonally protecting group pattern that allows further manipulations on the non-reducing and reducing ends – enabling elongation and pyrophosphate linkage formation.

The decisive structural considerations are the construction of the β-(1→4) mannosidic linkage within the ManNAc-GlcNAc repeat units, the β-(1→3) glycosidic bond between the repeat units, the pyrophosphate linkage, the order of pyruvylation and the sequence of protecting group manipulations.

3.1.1 Approaches towards β-ManNAc linkage

The difficulty of β-mannosylation is fueled by the strong anomeric effect that facilitates α-formation, the neighboring group participation and the steric repulsion induced by the axial C_2-substitution.[115] The plethora of methodologies towards the synthesis of β-mannosidic linkages has experienced significant growth in the past two decades[116], but still remains one of the biggest challenges in the realm of carbohydrate chemistry.[115] The general scope[115] of β-mannosylation includes indirect procedures (e.g. C_2-inversion, C_2-oxidation-reduction, intramolecular aglycone delivery – IAD, anomeric alkylation)[117,118] and direct procedures (e.g. Crich´s 4,6-*O*-benzylidene thioglycosides/sulfoxides, hydrogen-bond mediated aglycon delivery – HAD) that have been used with varying success to afford amino β-mannosidic linkages (β-ManNAc).[119–121] (Scheme 3)

The C_2-inversion is a classic approach to β-mannosamine bonds that involves a 1,2-*trans* glycosylation facilitated by neighboring group participation, followed by C_2-inversion within the donor moiety.[122] This method has also been applied to the synthesis of the disaccharide ligand (Figure 10B).[114]

Another route towards diastereoselective glycosylation is *via* hydrogen-bond mediated aglycon delivery (HAD) pathway that utilizes remote group participation.[123] The HAD pathway is, like Crich´s approach[121], a direct glycosylation procedure, but has been applied with more success to construct β-mannosamine bonds.[123] This procedure requires a non-participating group at the C_2-position and 2-azido-2-deoxy-mannosamine derivatives are applied most commonly that can be introduced *via* diazotransfer reaction on mannosamine[124–126] or classical C_2-inversion[127,128] from glucose.[115] Crich´s method was used to construct a β-D-ManNAc-(1→4)-GlcNAc linkage within the total synthesis towards a secondary cell wall polymer fragment of *Bacillus anthracis* but yielded an α/β ratio of 1:1.1.[129] To my knowledge, the HAD pathway has yet not been applied to build a β-D-ManNAc-(1→4)-GlcNAc linkage.

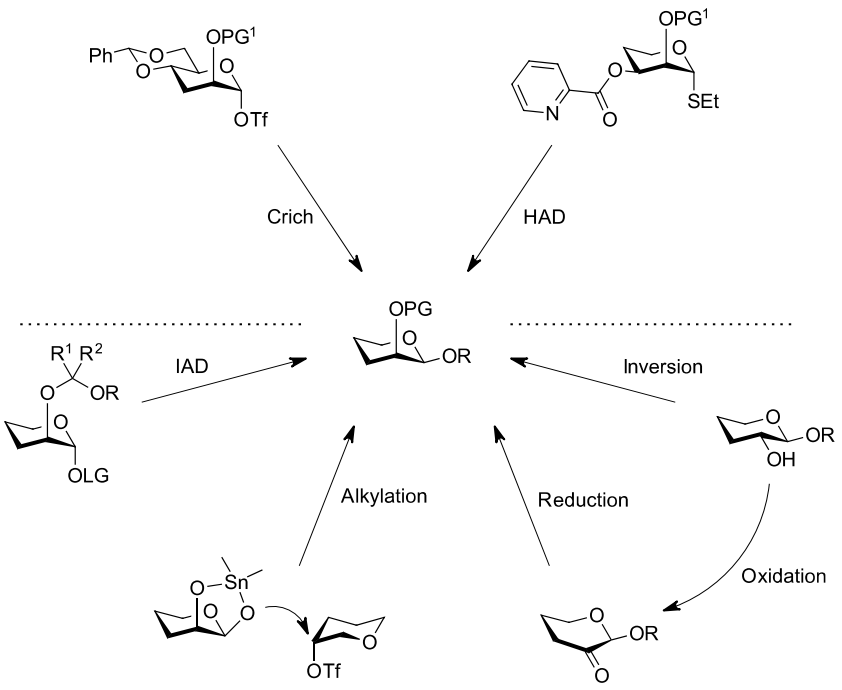

Scheme 3: Selected methodologies for β-mannosylation[115]

For the decisive β-D-ManNAc-(1→4)-GlcNAc glycosidic bond, the established C_2-inversion[122] and the HAD pathway[123] were chosen due to its proven methodology or novelty, respectively.

3.2 Approach *via* C_2-inversion

3.2.1 Synthesis towards donor

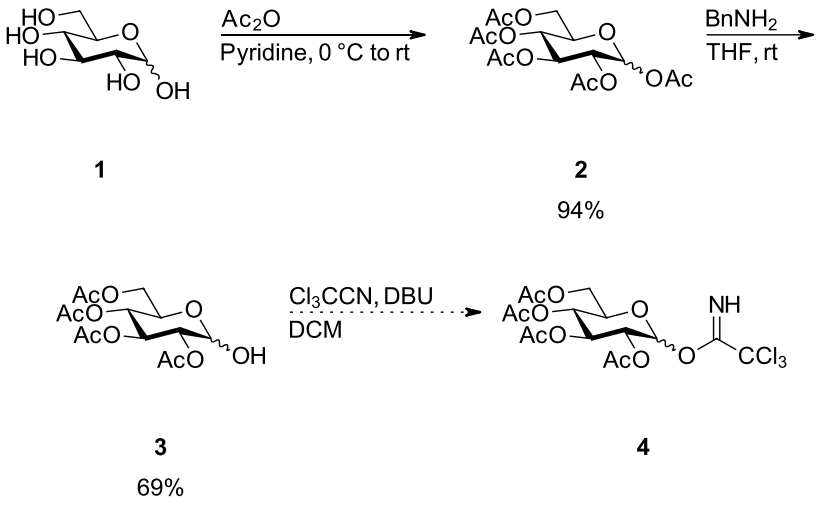

Scheme 4: Synthesis towards donor **4** (C_2-inversion)

According to a literature procedure[130], donor **4** is prepared from D-glucose **1** through peracetylation under standard conditions to give **2** with 94% yield, followed by anomeric deprotection with benzyl amine to yield 69% of hemiacetal **3**. The final imidate leaving group was not installed due to the incomplete acceptor synthesis **15**. (Chapter 3.2.2)

3.2.2 Attempted synthesis of acceptor

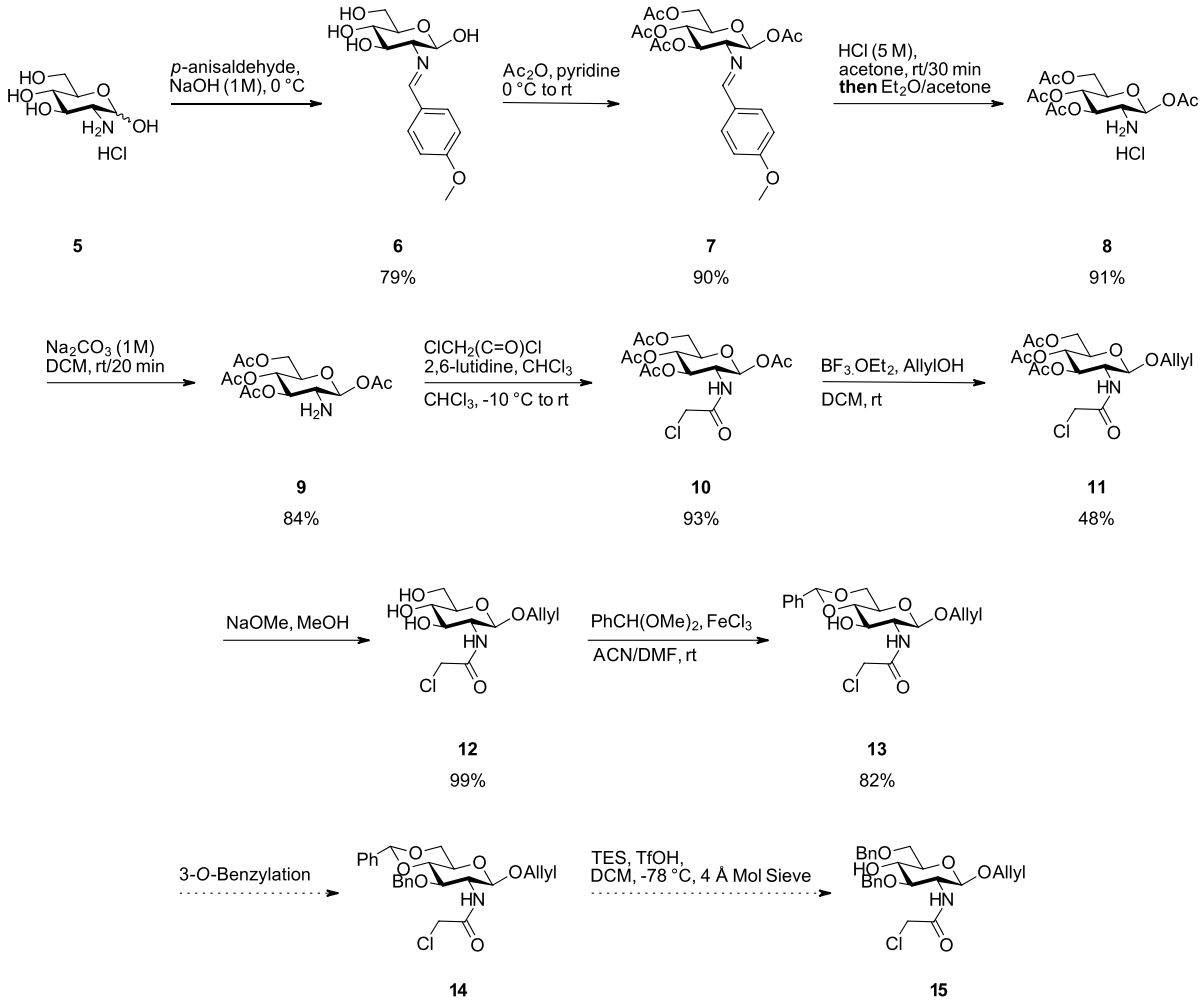

Scheme 5: Synthesis towards acceptor **15**

The literature-unknown acceptor **15**, decorated with an *N*-chloroacetyl group, allows for either azide installation (bioorthogonal click reaction for monitoring) or reduction to the native *N*-acetyl group. The chloroacetyl group was also intended to improve solubility in organic solvents, as amino sugars are very polar compounds.

The forward synthesis towards common building block **9** follows established protocols.[131,132]

Glucosamine hydrochloride **5** was *N*-protected with *p*-anisaldehyde to yield the imine **6** with 79%, followed by peracetylation using standard conditions to give 90% yield of **7**. The temporary *N*-protective group was removed *via* treatment with hydrochloric acid to yield 91% of **8** as a hydrochloride salt and stirring against aqueous sodium carbonate gave 84% yield of the free amine **9**.[131,132]

The free amine was *N*-protected with chloroacetyl chloride[133] to obtain **10** and the anomeric allyl glycoside **11** was afforded with 48% yield *via* transglycosylation with boron trifluoride etherate[134]. The transglycosylation utilizing boron trifluoride etherate as Lewis promoter proved to be superior in terms of yield, α/β ratio (1:15 vs 1:4) and aqueous work up, compared to ferric(III) chloride as promoter. In case of the latter promoter, aqueous work up gives the insoluble ferric hydroxide that has to be removed *via* filtration.

Compound **11** was de-acetylated to **12** and Lewis acid promoted 4,6-*O*-benzylidene protection gave **13** with 99% and 82% yields, respectively. Due to the high polarity of the amino sugars, dimethylformamide was added as a co-solvent in the latter protection step.

Subsequent benzylation of **13** *via* Williamson etherification indicated full consumption of the starting material according to TLC. Flash column chromatography and analysis *via* TLC and LC-MS (column: C4, profile: 20%→100% in 20 min) indicated the formation of several byproducts, but the desired product was not isolated. According to NMR analysis, the *N*-benzylation byproduct was isolated in small quantities. The N-H of the amino group might be more prone to deprotonation than the neighboring alcohol through stabilization *via* hydrogen-bond formation. Vice versa, byproduct formation through ring-closure *via* nucleophilic attack from the 3-alkoxide to the chloroacetyl group could also have been possible. (Scheme 6) The substitution of sodium hydride with potassium hydroxide or the less basic silver oxide did not lead to any conversion according to TLC and LC-MS (column: C4, 5%→100% in 20 min) in both cases after prolonged reaction times. (Scheme 6) The benzyl bromide was filtered over basic aluminum oxide prior to use.

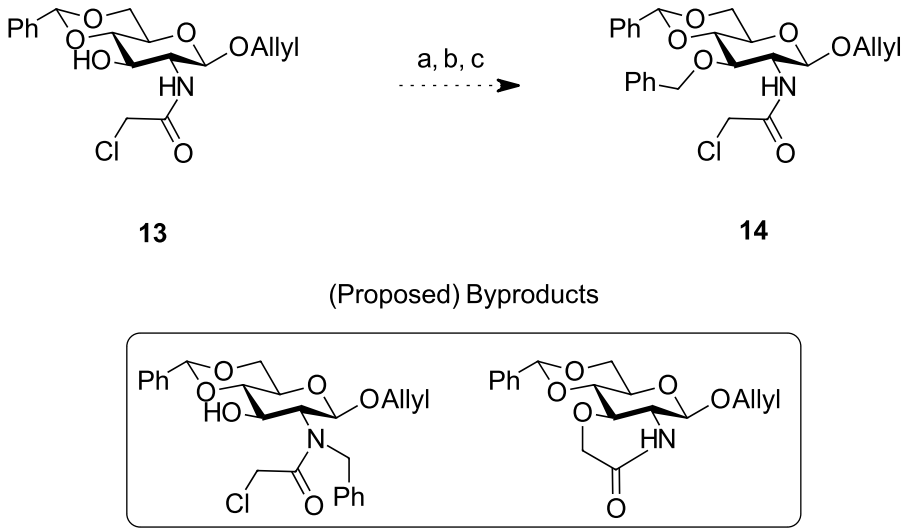

Scheme 6: Attempted Williamson etherification on **13** (a. BnBr, NaH, DMF b. Ag_2O, BnBr, DMF c. KOH, BnBr, DMF)

Wang *et al.*[135] reported the regioselective one-pot protection of glucose to yield various protected compounds, but the procedure was not applied to any amino sugars in the original publication. (Scheme 7) A preceding per-*O*-silylation step provides the intermediates with the necessary regioselective reactivity and improved solubility.[135] Depending on the following reaction sequence, a variety of protected monosaccharides are accessible.[135] The reaction sequence to fully protected glucose derivatives involves the trimethylsilyl triflate catalyzed benzylidene formation, followed by reductive benzylation.[135] The remaining 2-*O*-silyl group is cleaved *via* treatment with tetrabutylammonium fluoride and is protected by an ester or ether group.[135] (Scheme 7) An adaptation of this procedure was applied to compound **12**, but only partially protected intermediates were obtained in presence of excess reagent according to TLC and NMR analysis. The reaction was not further investigated. The silylation of compound **13** did not give any conversion according to TLC. (Scheme 8)

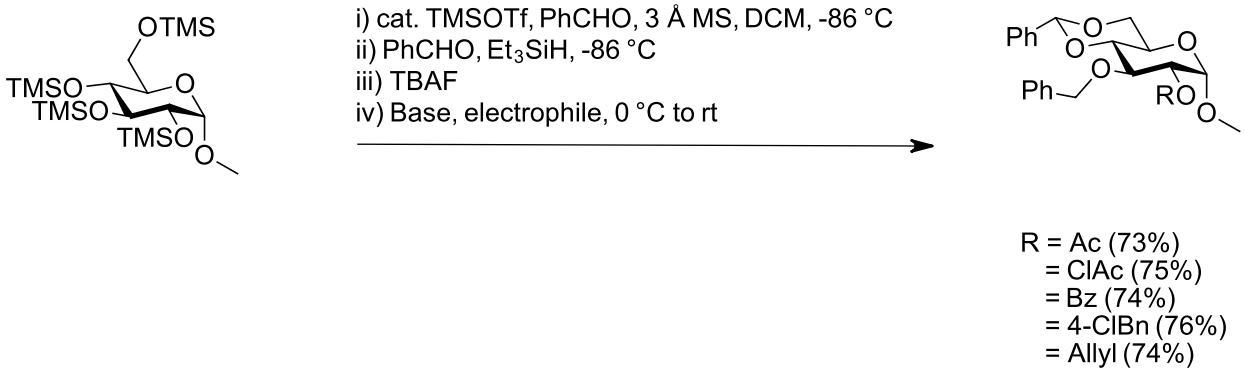

Scheme 7: Selected examples of regioselective one-pot protection[135]

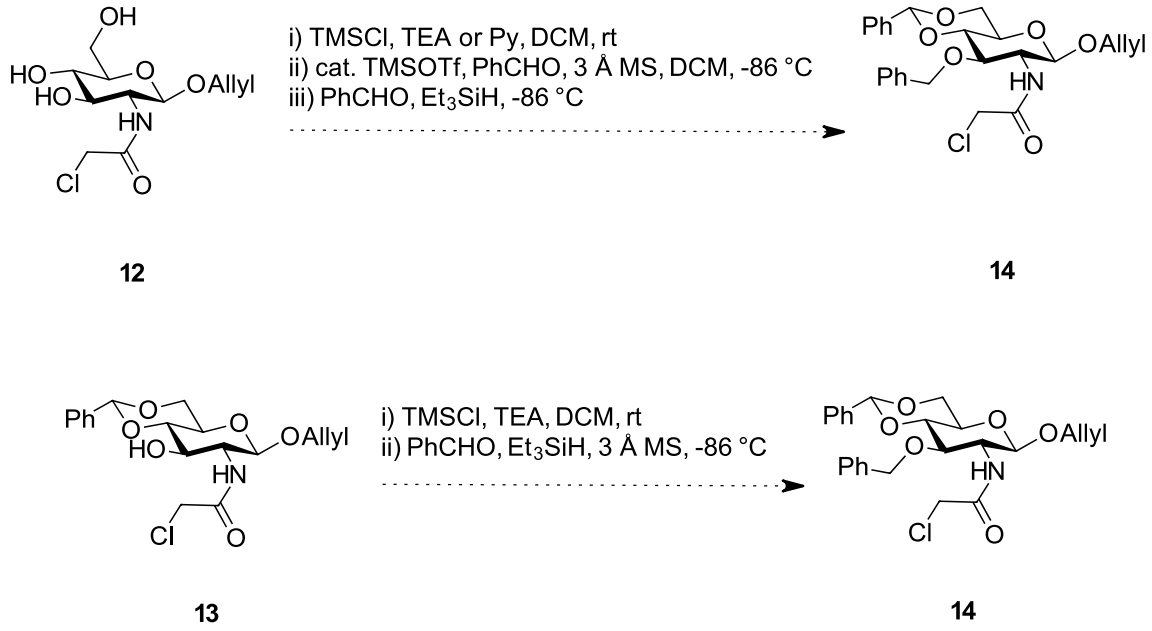

Scheme 8: Attempted (regioselective) protection on compounds **12** and **13**[135]

We reasoned that basic procedures may facilitate byproduct formation. Benzyl imidates, such as benzyl trichloroacetimidate or benzyl *N*-phenyl-2,2,2-trifluoroacetimidate, have been reported to give benzyl ethers under non-basic conditions utilizing trimethylsilyl triflate as promoter.[136–138] Benzyl *N*-phenyl-2,2,2-trifluoroacetimidate is a variation of Yu´s glycosyl donor, bench-stable for months and less prone to rearrangement than benzyl trichloroacetimidate.[138,139] The reagent is synthesized from benzyl alcohol (dry), *N*-phenyl trifluoroacetimidoyl chloride and potassium carbonate in quantitative yields.[138] (Scheme 9) The benzylation of **13** in dichloromethane/acetonitrile gave a suspension at 0 °C that solubilized at ambient temperature. Monitoring *via* TLC and LC-MS indicated minor amounts of the product mass that could also have been *N*-benzylated product. The reaction was repeated

solely in acetonitrile, but due to insolubility no conversion was observed at any time and temperature.[138] (Scheme 9)

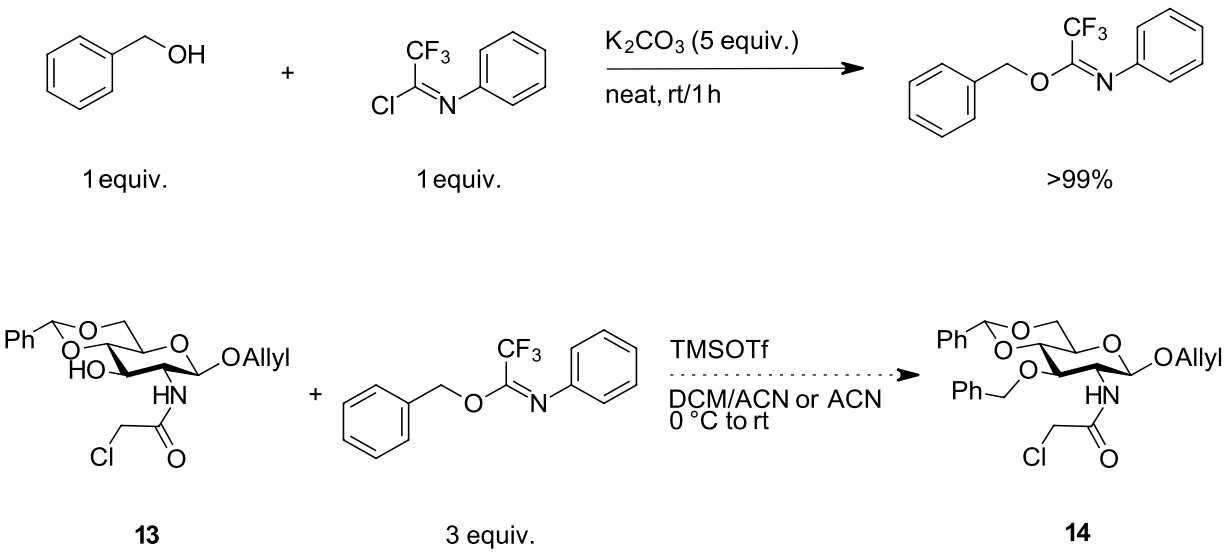

Scheme 9: Attempted alkylation utilizing benzyl N-phenyltrifluoroacetimidate[138]

3.3 The reactivity of *N*-acylglucosamine derivatives

The group of Nicola Pohl[140] investigated the regioselective 4,6-di-*O*-benzylation of glucosamine derivatives with the 3-OH remaining unprotected. (Table 2) A sterically demanding *N*-protecting group, like Phth (phthaloyl)[141,142] or TCP (tetrachlorophthaloyl)[143], would facilitate the 4,6-di-*O*-benzylation and mask the 3-OH, but would simultaneously decrease the reactivity of the 3-OH towards glycosylation.[140] The literature reports that glycosylation preferably favors the 4-OH over the 3-OH in case of bulky 2-*N*-protection, while less sterically demanding groups (i.e. azido, acetyl, 2,2,2-trichloroethylcarbonate) give a mix of regioisomers.[144–146] To suppress benzylation on the 3-*O*-position while keeping its reactivity intact, a *N*-trichloroacetyl (TCA) protective group was chosen by the group of Pohl.[140] Surprised by the lack of efficient benzylation procedures for 4,6-di-*O*-benzyl-*N*-TCA glucosamine derivatives, the group screened various benzylation conditions.[140] The decisive strategy was to exploit the different chemical stability of *O*-acyl and *N*-acyl protecting groups.[140] To facilitate regioselectivity, tetrahydrofuran was used as solvent with lower polarity.[140,147] The addition of a phase-transfer catalyst like 15-crown-5 allowed the use of a milder base and prevent possible *N*-TCA cleavage. [140,148] (Table 2; Entry 1) In cases where the amino functionality is completely masked, 3,4,6-tri-*O*-benzylation products were predominantly obtained – indicating that the free N-H may suppress reactivity on the 3-OH position. (Table 2; Entries 2-6)[140] The 2-azido substrate gave exclusively tribenzylated product in two hours, while *N*-benzylation was observed with mono-protected amino groups (Table 2; Entries 1-2) and *N*-diacetyl group (Table 2; Entry 3) that reacted further to give also the tetrabenzylated byproduct.[140] This is in accordance with our results, as we also isolated the *N*-benzylated byproduct. (Chapter 3.2.2)

Table 2: Regioselective benzylation *via* phase-transfer catalysis by the group of Pohl; conditions: NaOH (powdered, 12 equiv.), 15-crown-5 (0.05 equiv. of base), BnBr (3 equiv.), THF (10 ml/mmol), rt/20 h (or 2 h for entry 5)[140]

Entry	Substrate	Dibenzylated product	Tribenzylated product	Tetrabenzylated product
1	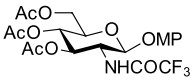	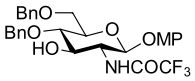 **53%**		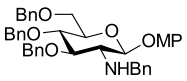 **20%**
2	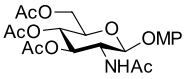		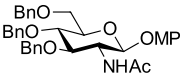 **35%**	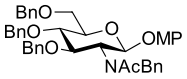 **33%**
3	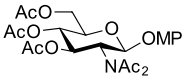		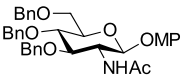 **16%**	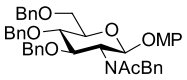 **49%**
4	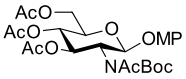		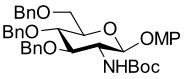 **66%**	
5	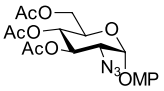		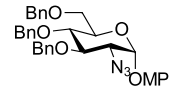 **92%**	
6	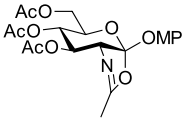		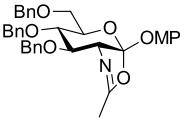 **45%**	
7	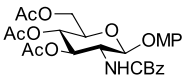		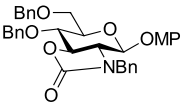 **36%**	
8	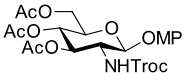		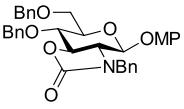 **60%**	

In case of the desired *N*-TCA substrate (Table 2; Entry 1), the regioselective 4,6-di-*O*-benzylation was successful but was accompanied by tetrabenzylated byproduct.[140] The additional *N*-benzylation might mask the amino functionality and facilitate 3-*O*-benzylation.

The group of David Crich investigated the reactivity of glucosamine sugars as nucleophiles/glycosyl acceptors in a comparative study.[149] The relative reactivities of different amino protective groups (*N*-acetyl, 2-azido, *N*-phthaloyl) were evaluated in glycosylation reactions with phenyl 2,3-di-*O*-benzyl-4,6-*O*-benzylidene-1-deoxy-1-thio-α-D-mannopyranoside sulfoxide as donor. [149] (Scheme 10) The glycosyl acceptors were first reacted with the sulfoxide donors separately and then an equimolar mix of the three acceptors were reacted.[149] (Scheme 10) The one-pot competition experiment showed that the reactivity of the 2-azido acceptor was one order of magnitude greater than the *N*-acetyl group, while the *N*-phthaloyl group showed a threefold greater reactivity.[149] The results are in accordance with the "common knowledge" that the 4-OH of *N*-acetylglucosamine derivatives are poor nucleophiles.[149,150] The glycosylation with corresponding imides (*N*,*N*-di-acetyl and *N*-benzyl-*N*-acetyl) (Scheme 11) gave higher yields compared to the *N*-acetyl acceptor, but the partial imide hydrolysis complicated the product isolation.[149] The bidentate *N*-phthaloyl protecting group proves to be superior to the *N*,*N*-di-acetyl and *N*-benzyl-*N*-acetyl derivatives in terms of imide stability and ease of NMR characterization due to rotamers.[149] These results are a clear indication that the lack of reactivity is induced by inter- and/or intramolecular hydrogen-bond interactions.[149]

The poor reactivity of *N*-acyl glucosamines at the 3- and 4-OH position is a consequence of intra- and intermolecular hydrogen-bond interactions and full-protection of the amino functionality is an obvious circumvention to facilitate reactivity and solubility.[140,149]

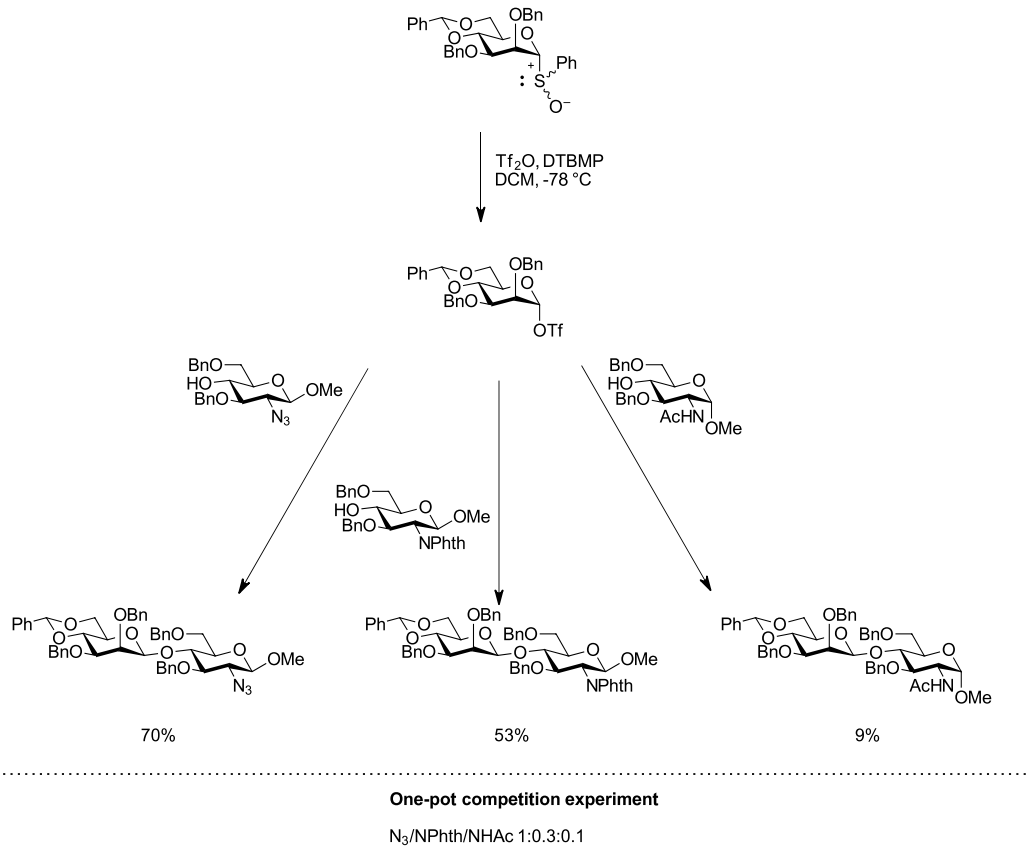

Scheme 10: *N*-protected glucosamine acceptors in 4-*O*-glycosylation[149]

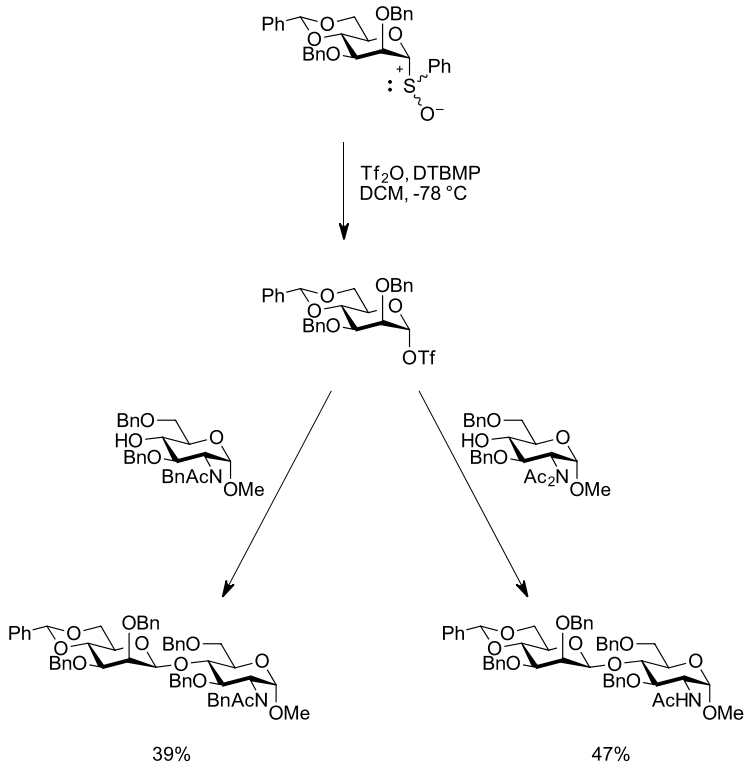

Scheme 11: *N,N*-di-acetyl and *N*-acetyl-*N*-benzyl protected glucosamine acceptors[149]

3.4 Approach *via* diastereoselective HAD pathway

The group of Demchenko has investigated the diastereoselective glycosylation towards β-mannosides through remote-group participation of a 3-*O*-picoloyl group in a 2-azido protected donor.[123] The picoloyl group directs the glycosyl acceptor *via* hydrogen-bond interaction to the anomeric center to form the 1,2-*cis* glycosidic bond.[123] (Scheme 12) The mechanism of the reaction pathway, termed hydrogen-bond mediated aglycon delivery (HAD) pathway, is not fully elucidated.[123] The group showed that the typical 4,6-*O*-benzylidene protective group is not required to facilitate β-manno selectivity.[123,151]

The scope of used glycosyl acceptors covers various tribenzylated methyl α-D-glucopyranosides, but no glucosamine derivatives.[123] (Table 3) The yield was not affected in case of tenfold dilution, but shifted the α/β ratio in favor for the desired 1,2-*cis* product.[123] (Table 3)

Table 3: β-Mannosylation *via* HAD pathway
(conditions: NIS/TfOH, 1,2-DCE, 4 Å MS, -30 °C to rt)[123]

Entry	Donor	Product	
1		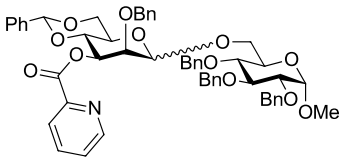	82%; α/β 1:5.0 (50 mM) 97%; α/β 1:21 (5 mM)
2	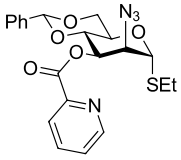	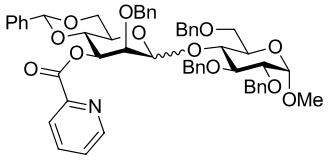	81%; α/β 1:11 (50 mM) 69%; α/β 1:14 (5 mM)
3		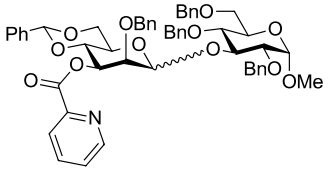	76%; α/β 1:6.0 (50 mM) 61%; α/β 1:11 (5 mM)
4		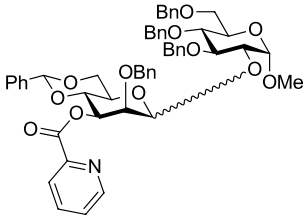	86%; α/β 1:9.0 (50 mM) 87%; α/β 1:25 (5 mM)

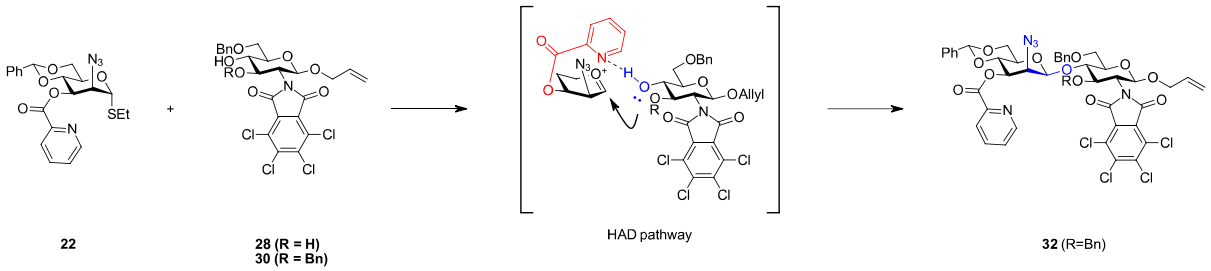

Scheme 12: Donor/Acceptor system for the diastereoselective approach towards β-D-ManNAc-(1→4)-GlcNAc linkage[123]

The *N*-phthaloyl (or related *N*-tetrachlorophthaloyl) and especially the 2-azido protecting groups were proven to be superior in glycosylation than the *N*-acetyl derivative.[149] (Chapter 3.3) The sterically demanding *N*-tetrachlorophthaloyl (TCP) protecting group was chosen due to its orthogonality to the 2-azido group of the glycosyl donor, the literature-reported regioselectivity for 4-*O*- over 3-*O*-glycosylation (potentially dismissing the need for 3-*O*-protection)[143], vastly improved solubility in organic solvents and ease of cleavage compared to the related *N*-phthaloyl group.[152] (Scheme 12, Scheme 13)

Scheme 13: Glycosyl acceptor targets **28** and **30**

3.4.1 Synthesis of monosaccharide donor

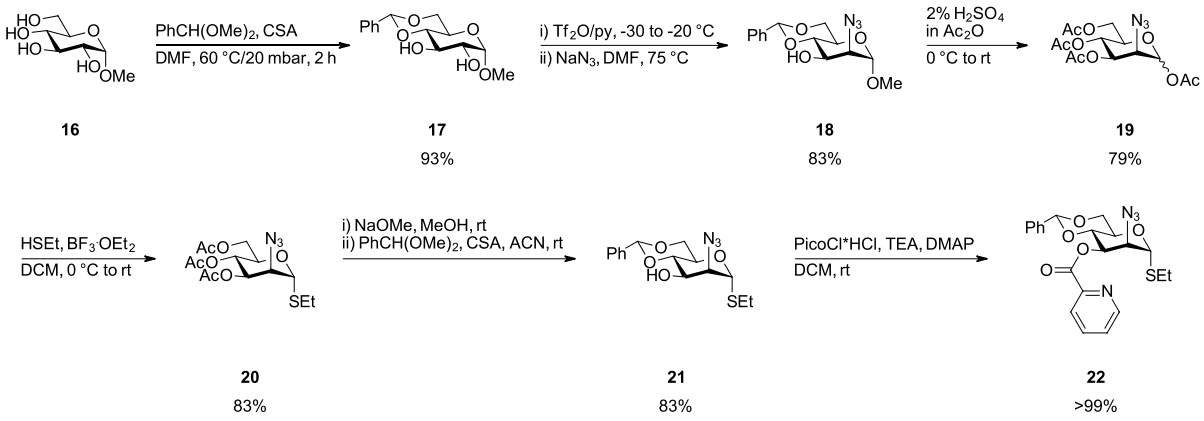

Scheme 14: Synthesis towards donor **22**

The synthesis towards **22** followed a procedure from the group of Demchenko.[123] Starting from commercial methyl α-D-glucopyranoside **16**, compound **17** was obtained *via* trans-acetalisation in dimethylformamide on the rotary evaporator.[153,154] The formed methanol was distilled at 60 °C/20 mbar to shift the equilibrium in favor of the product. The 2-azido group was introduced *via* the classical C_2-sulfonation-inversion reaction sequence to give compound **18**.[115,155,156] The regioselectivity during the sulfonation was obtained at low temperatures ranging from -30 °C to -20 °C with 1.05 equivalents of trifluoromethanesulfonic anhydride, followed by S_N2 reaction with sodium azide.[157] Acetalysis and peracetylation in acetic anhydride with 2% sulfuric acid gave the 1,3,4,6-tetra-*O*-acetyl compound **19**.[158] Lewis-acid promoted transglycosylation with ethanethiol yielded **20** with an α/β ratio of 6:1.[158] De-acetylation under Zemplen condition and subsequent Brønsted-acid catalyzed 4,6-*O*-benzylidene protection yielded **21**.[123] Final 3-*O*-picoloyl protection *via* the corresponding acid chloride gave the desired donor **22** with over 99% yield.[123]

3.4.2 Synthesis of monosaccharide acceptors

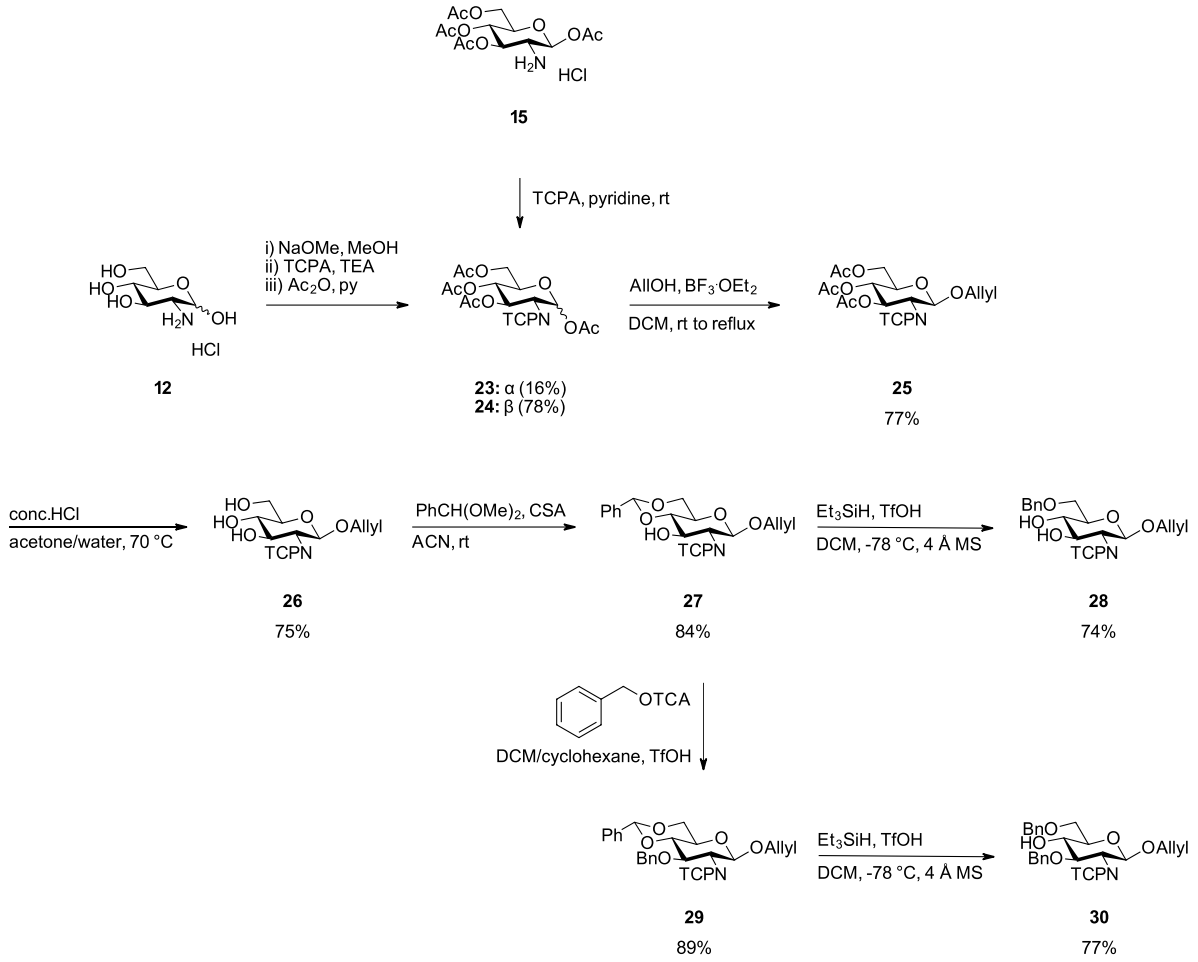

Scheme 15: Synthesis towards glycosyl acceptors **28** and **30**

Compound **23** was synthesized from **5** in a three-step one-pot reaction sequence.[159–163] Glucosamine hydrochloride was treated with one equivalent of sodium methoxide to yield the free base that was *N*-protected with tetrachlorophthalic anhydride. Subsequent peracetylation afforded fully protected **23** in α-configuration with overall 16% yield. The *N*-TCP protection of 1,3,4,6-tetra-*O*-acetyl-glucosamine hydrochloride **8** gave **24** in β-configuration with 78% yield.[143] The latter route towards 1,3,4,6-tetra-*O*-acetyl-*N*-TCP-D-glucopyranose proved to be more reliable and high-yielding than the one-pot sequence.[143] The literature-unknown allyl glycoside **25** was obtained in a Lewis-acid catalyzed transglycosylation reaction. Initial synthesis with ferric(III) chloride yielded **25** with 73% after an inconvenient work up procedure to remove the insoluble ferric(III) hydroxide.[164] The use of boron trifluoride etherate indicated 50% conversion according to TLC at ambient temperature.[165] Full consumption was obtained after further stirring at elevated oil bath temperature of 60 °C to yield **25** with

77% yield. De-acetylation of **25** under standard Zemplen conditions at ambient temperature gave two evenly intensive spots according to TLC. The crude NMR analysis indicated the product and the mono-cleavage of the *N*-tetrachlorophthaloyl group as byproduct. The highly base-labile nature[152] of the *N*-TCP protective group was also observed by the group of Magnusson[143] in a similar building block with a *p*-methoxyphenyl group as anomeric protecting group. The group applied optimized conditions of Zemplen (large volume of 0.018 M sodium methoxide in methanol under 15 minutes) to yield up to 86% yield of the corresponding triol.[143] This procedure was not applied to **25**, as it seemed too unreliable. Deprotection using milder magnesium hydroxide in methanol at ambient temperature gave pre-dominantly the mono-cleaved byproduct, emphasizing the base-labile nature.[166–168] As basic conditions would also facilitate acetyl migration to the 2-position, acidic hydrolysis was investigated. Compound **25**, dissolved in acetone/water, was treated with an excess of concentrated hydrochloric acid (14.5 equivalents) at 70 °C for roughly 15 hours to obtain the desired triol **26** in 75% yield.[169] The *N*-TCP group was not affected under these harsh conditions. The acetalisation towards the 4,6-*O*-benzylidene protected **27** was achieved under standard conditions. Compound **27** served as intermediate towards the synthesis of glycosyl acceptors **28** and **30**. Reductive ring-opening of **27** with triethylsilane and triflic acid under dry conditions and low temperatures gave **28**.[170] In some cases, the mono-silylated byproducts (3-*O*-TMS and 4-*O*-TMS) were observed in varying quantities. The byproducts were isolated and characterized, and de-silylation *via* a tetrabutylammonium fluoride-mediated procedure afforded the final glycosyl acceptor **28**.[171] (Scheme 16) The 3-*O*-benzylation of glucosamine derivative **27** was finally accessible under acidic conditions *via* benzyl trichloroacetimidate.[172] The 0.06 equivalents of triflic acid and the basic nature of the molecular sieves may provide almost neutral conditions in this benzylation. The following reductive ring-opening of **29** with triethylsilane gave the glycosyl acceptor **30**.[170] No silylated byproducts were observed. In contrast to the ring-opening of **28**, the triethylsilane and the starting material were pre-stirred with the molecular sieves at ambient temperature, before addition of the triflic acid at -78 °C. The water content of the used reagent might have been responsible for byproduct formation during the ring-opening of **27**, as in this case the reagent was added right before the acid.

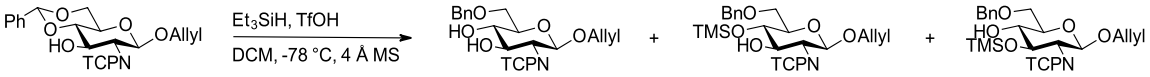

27 **28** **28a** **28b**

Scheme 16: Mix of product and silylated byproducts in the ring-opening of **27**

3.4.3 Attempted diastereo- and regioselective glycosylation

The reactivity of the 3-OH group in 2-amino sugars can be attenuated in presence of sterically bulky *N*-protecting groups like phthaloyl[173] or tetrachlorophthaloyl.[174] In case of unprotected 3- and 4-*O*-positions, bulky *N*-protected glycosyl acceptors might allow regioselectivity in glycosylation reactions.

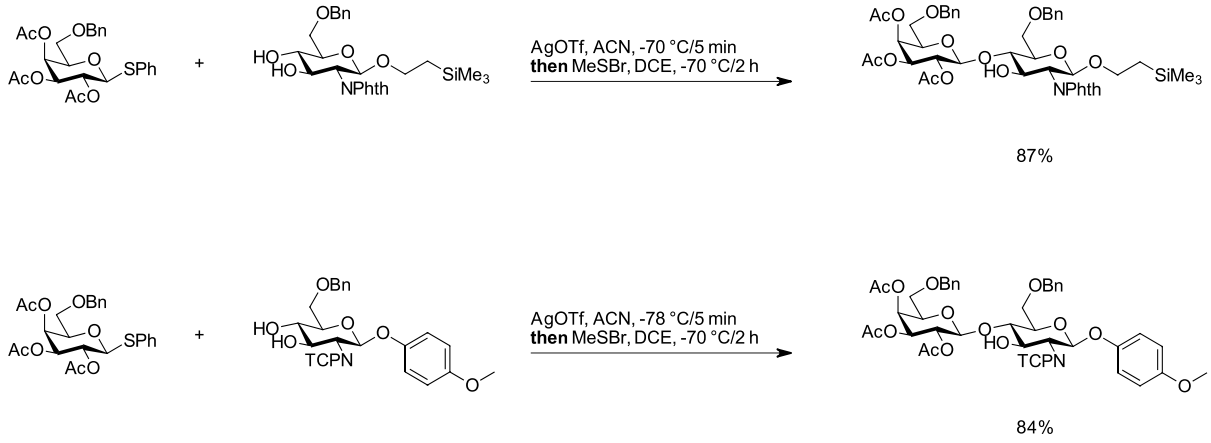

Scheme 17: Regioselective 4-*O*-β-galactosylation with *N*-phthaloyl glucosamine acceptor[143]

The group of Magnusson[143] has exploited the sterically hindered 3-*O*-position towards regioselective galactosylation. (Scheme 17) The use of phthaloyl and tetrachlorophthaloyl groups gave both the same results with a thiophenyl galactosyl donor under sulfenyl activation.[143] The 1→3 linked disaccharide was not observed according to TLC and by NMR.[143]

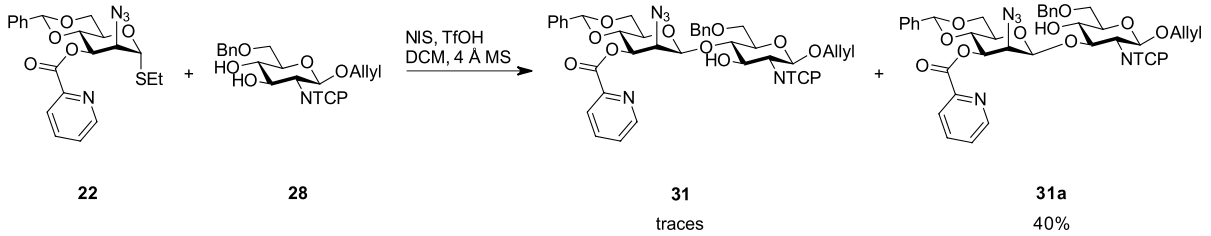

Scheme 18: Attempted regioselective β-mannosylation

In our attempts towards regioselective glycosylation, the reactions of donor **22** with acceptor **28** gave, to our surprise, pre-dominantly the 3-*O*-linked disaccharide **31a** in β-configuration. (Scheme 18) The β-(1→3) linkage was determined *via* the H_{1A}-C_{3B} correlation in the HMBC spectrum (Figure 13) and the corresponding coupling constant of $^{1}J_{C1A,H1A}$ = 163 Hz in the CLIP-HSQC (Figure 14).[175]

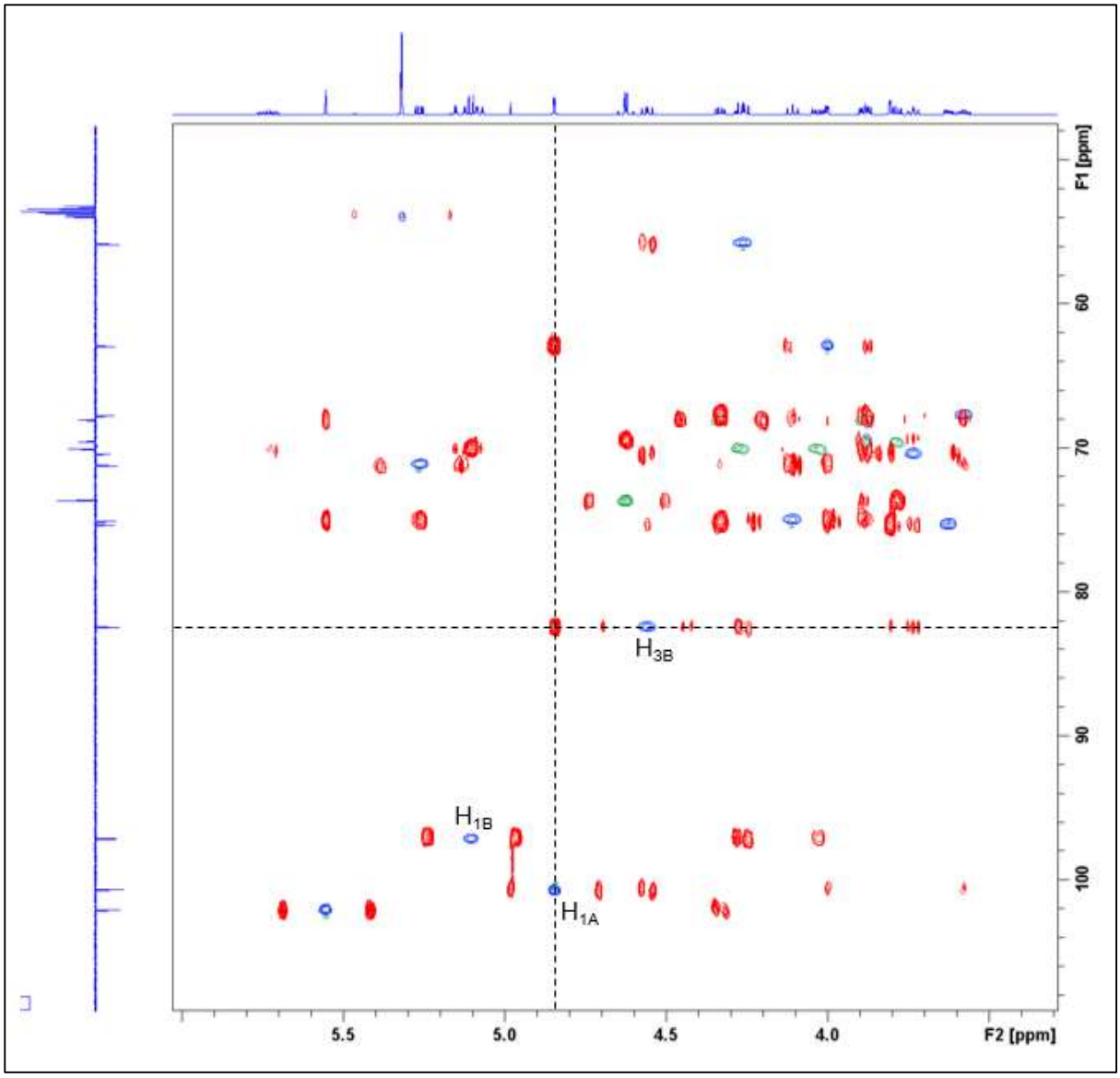

Figure 13: HSQC-HMBC overlay of **31a**

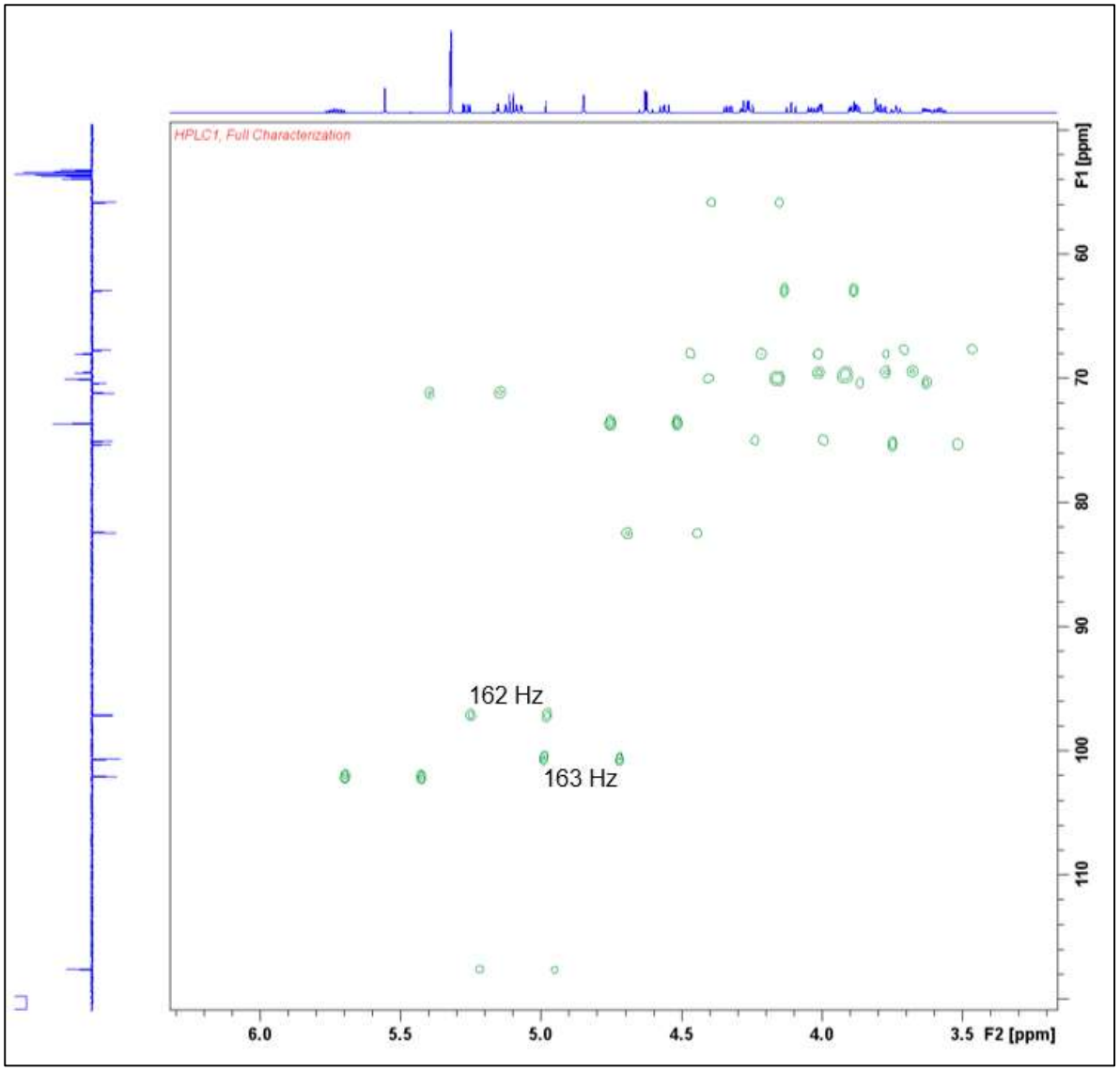

Figure 14: CLIP-HSQC of **31a** with coupling values for the anomeric protons

The reactions were promoted by *N*-iodosuccinimide (2.4 equiv.) and triflic acid (0.4 equiv.) and a purple discoloration at -7 °C indicated the start of the glycosylation. The donor **22** (1.2 – 1.4 equiv.) was used in excess, but the acceptor **28** was never fully consumed even at ambient temperature. (Figure 15) The monitoring *via* TLC indicated pre-dominantly the formation of one compound. Isolation *via* flash column chromatography gave the undesired 3-*O*-linked byproduct with yields up to 40%. The LC-MS analysis of the minor accompanying spots detected the mass of **31/31a**, possibly indicating traces of the desired 4-*O*-regioisomer. Prolonged reaction time for roughly 15 hours facilitated byproduct formation and decomposition. (Figure 16)

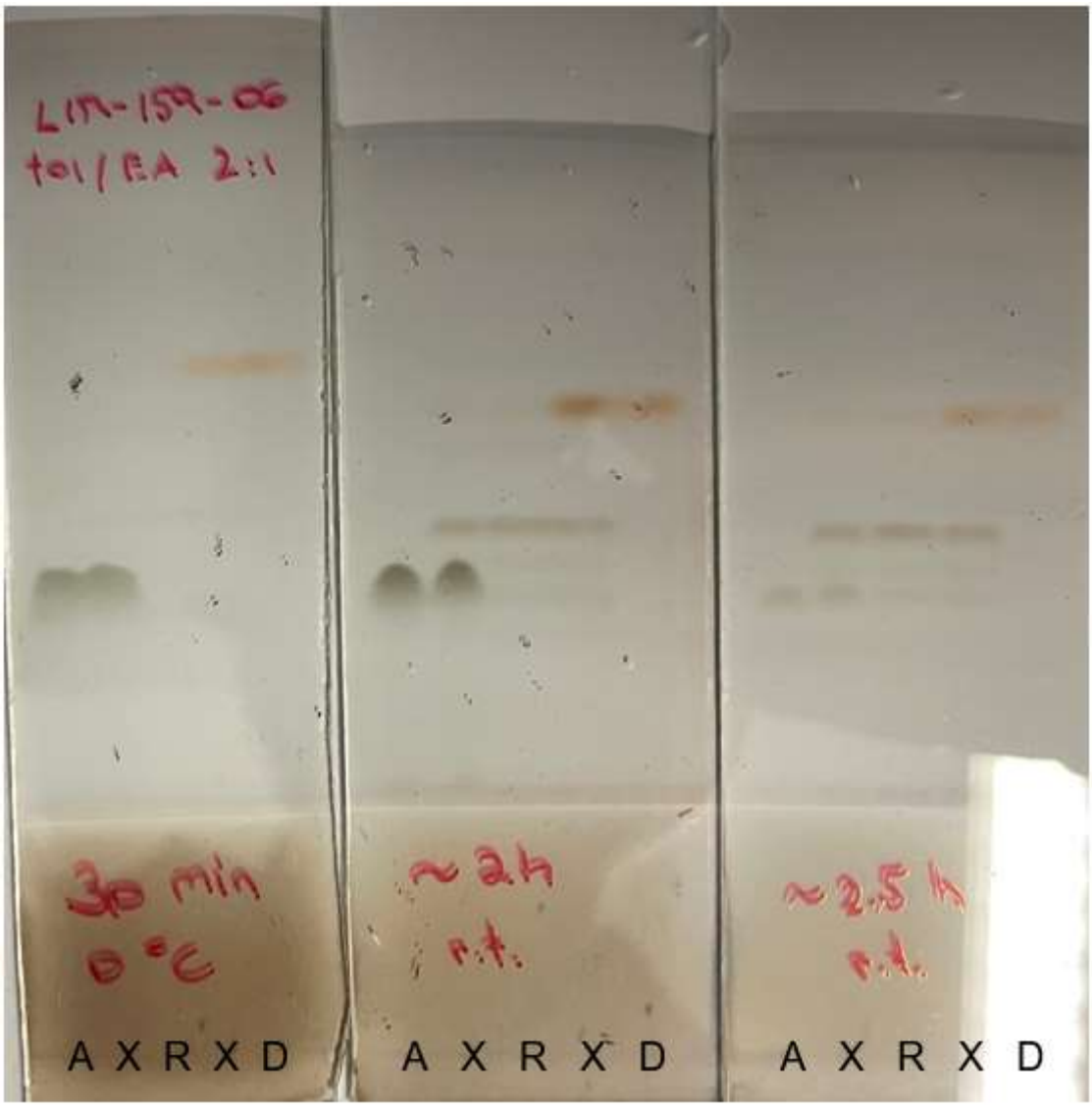

Figure 15: Selected TLC of attempted regioselective glycosylation (A = Acceptor, X = Co-Spot of adjacent spots, R = Reaction, D = Donor)

Figure 16: Stirring at ambient temperature for 15 hours did not facilitate full consumption (A = Acceptor, R = Reaction, D = Donor, X = Co-spots of adjacent spots)

The preference for the 3-OH position despite the steric hindrance induced by the bulky *N*-TCP group in **28** might be attributed to the lower reactivity of the 4-OH position compared to the 3-OH group.[149] (Chapter 3.3) An increase of the glycosyl donor reactivity may induce regioselectivity. Sulfenyl reagents are strong promoters that activate thioglycosides at -78 °C in a fast and clean way[176–180] and this promoter has also been used by the group of Magnusson.[143] (Scheme 17: Regioselective 4-*O*-β-galactosylation with *N*-phthaloyl glucosamine acceptor[143]) *p*-Toluenesulfenyl chloride (*p*-TolSCl)[180] was used as alternative sulfenyl promoter to methanesulfenyl bromide due to its lower volatility and better stability. It is synthesized from *p*-thiocresol in *n*-hexane by adding sulfuryl chloride at 0 °C.[180,181] The resulting sulfenyl chloride was distilled from the crude reaction mixture in a short-path distillation apparatus at 51 °C/0.13 mbar after the solvent was removed in *vacuo*. The reagent was obtained as an intensive red liquid and all operations were strictly executed under argon atmosphere. (Scheme 19)

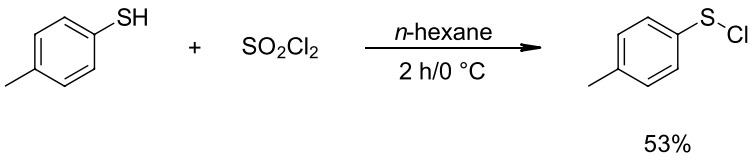

53%

Purification *via* distillation at 51 °C/0.13 mbar

Scheme 19: Synthesis of *p*-TolSCl promoter[180]

The donor **22** and acceptor **28** (1.5 equiv.) were pre-stirred with 4 Å molecular sieves, before silver triflate (2.5 equiv.) in acetonitrile was added. After additional stirring for 20 min under exclusion of light, *p*-toluenesulfenyl chloride was added at -75 °C to form the actual promoter *p*-toluenesulfenyl triflate.[180] (Scheme 20)

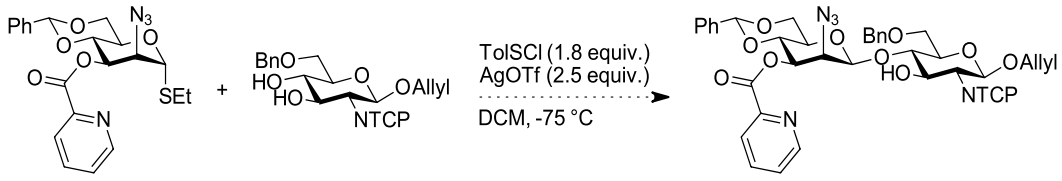

11 **28** **31**

Scheme 20: Thioglycoside activation with *p*-toluenesulfenyl chloride[180]

The monitoring of the reaction *via* HPTLC (Figure 17) indicated pre-dominantly the formation of a spot closely above the acceptor that was accompanied by an intensive baseline spot. A minor compound with similar retention to the 3-*O*-linked byproduct **31a** was also observed. Prolonged reaction time (15 hours) and ambient temperature did not facilitate consumption of the donor, but the acceptor was fully consumed. The baseline spot and the major byproduct increased with further reaction progress, but the donor remained unchanged. The crude NMR analysis indicated the complete absence of any allyl signal. Further analysis *via* LC-MS (HILIC, C5) indicated electrophilic addition byproducts and the corresponding cyclic sulfonium ion. (Scheme 21) These terminal chlorinated thioether structures are S-LOST compounds, derivatives of sulfur mustard[182], and are known for their cytotoxicity and vesicant behavior.[182,183] The intramolecular nucleophilic attack of the thioether gives the sulfonium ion that alkylates nucleotides, making S-LOST structures toxic for cells and facilitating cancer development.[183]

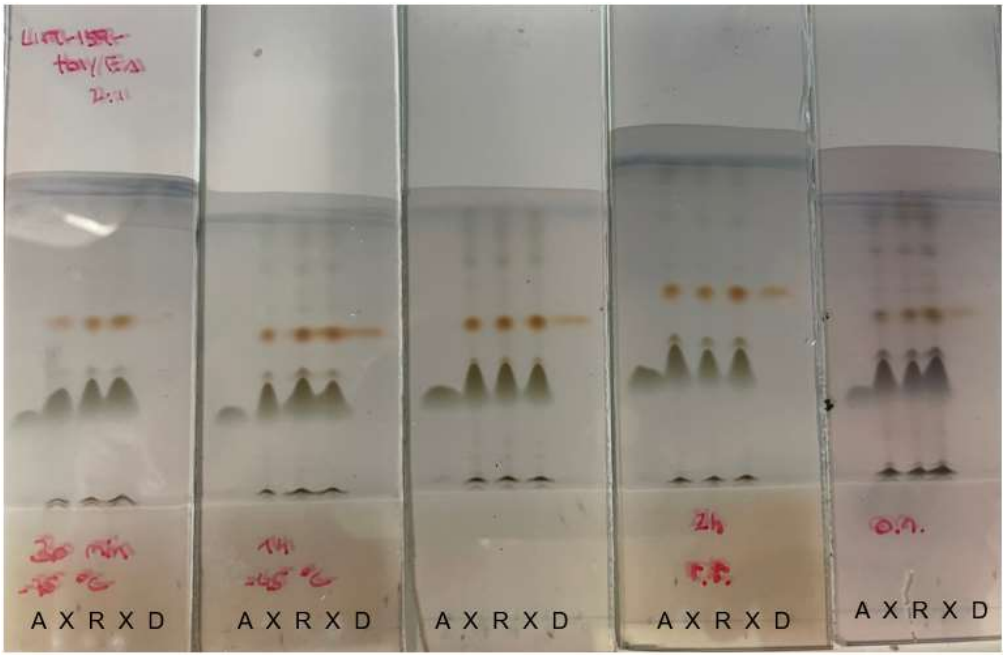

Figure 17: TLC monitoring of sulfenyl promoted thioglycoside activation – TLC samples were taken in fresh capillaries and were instantly quenched by tipping the capillary into a solution of dichloromethane/triethylamine (A = Acceptor, R = Reaction, D = Donor, X = Co-spots of adjacent spots)

The electrophilic addition could be circumvented *via* pre-activation[184] of the donor **22** with equimolar amounts of *p*-toluenesulfenyl chloride at -78 °C, then warming up to facilitate complete transformation to the anomeric α-triflate. Addition of the glycosyl acceptor **28** at -78 °C might then give more regioselectivity.

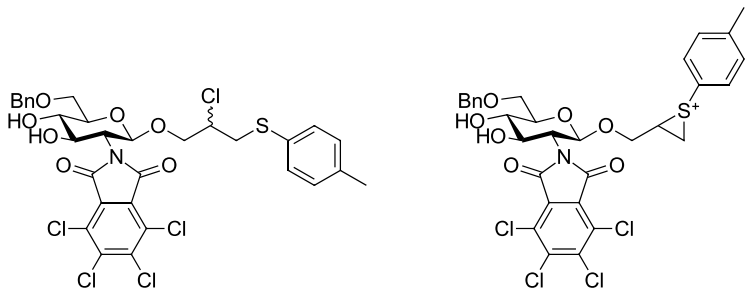

Scheme 21: Structures indicated by LC-MS analysis

Further glycosylation experiments with acceptor **28** were discontinued due to the lack of regioselectivity and occurrence of side reactions.

3.4.4 Key disaccharide intermediate **32**

3.4.4.1 Activation with *N*-iodosuccinimide and triflic acid

The initial glycosylation (Scheme 22) of donor **22** (1.5 equiv.) and 4,6-di-*O*-benzylated acceptor **30** (10.5 mg, 23.7 µmol, 1.0 equiv.) with *N*-iodosuccinimide (1.7 equiv.) and triflic acid (0.6 equiv.) at -70 °C to 5 °C in dichloromethane (0.08 M) did not yield any purple discoloration from the iodine formed during the glycosylation.[123] Further addition of reagents (1.7 equiv. of *N*-iodosuccinimide and 0.6 equiv. of triflic acid) at -50 °C and warming up to 5 °C yielded a dark crude mixture. The monitoring *via* TLC indicated pre-dominantly starting materials that were accompanied by several compounds (including a faint baseline spot indicating degradation). (Figure 18) The reaction was quenched at this point.

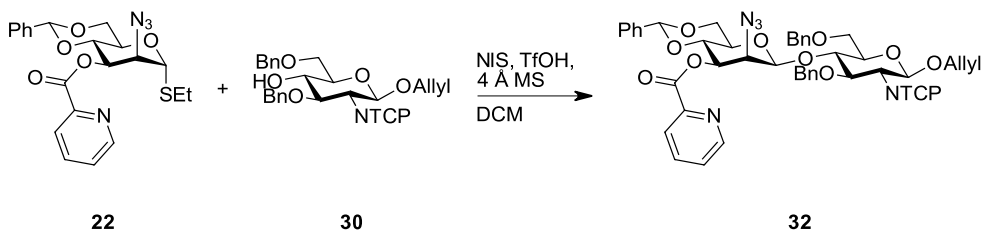

Scheme 22: Glycosylation of **22** and **30** with NIS/TfOH system

Purification *via* column chromatography revealed pre-dominantly the isolation of starting materials, accompanied by some derivative of the donor (not further characterized) and, according to coarse NMR analysis, presumably disaccharide in low quantities. The analysis indicated that the conditions are not reactive enough for the glycosylation. The temperature range might be too low for the unreactive 4-OH position of the glucosamine derivative **30** (Chapter 3.3) and/or the 3-*O*-benzyl group is a potential steric hindrance during the reaction.

Figure 18: TLC monitoring of inital glycosylation experiment

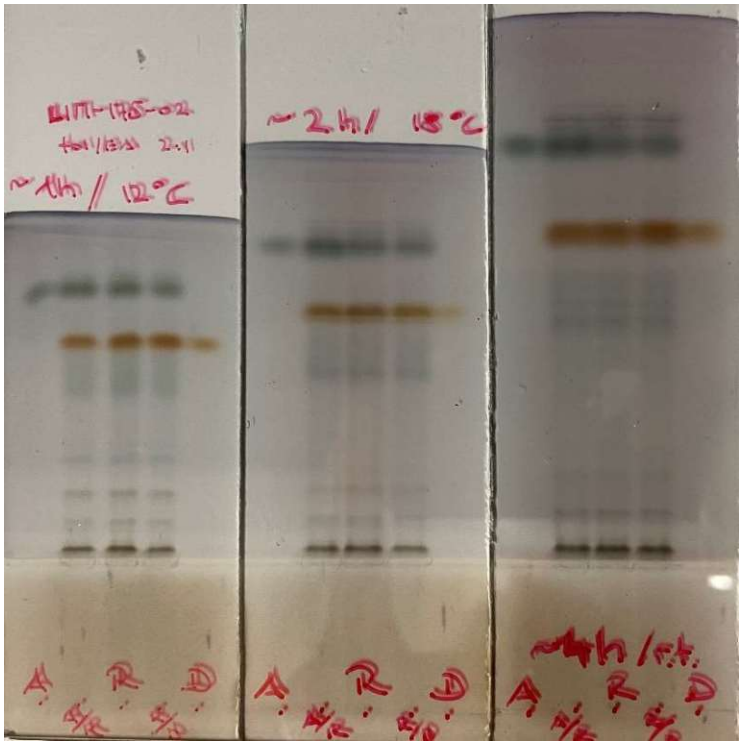

Figure 19: Glycosylation starting at 0 °C to ambient temperature (1.7 equiv. NIS and 1.2 equiv. of TfOH); (A = Acceptor, R = Reaction, D = Donor)

The repetition of the initial experiment (starting temperature of 0 °C with 1.2 equiv. of triflic acid added as 1 M solution in acetonitrile) indicated the formation of various byproducts and a very intensive baseline spot (hydrolyzed donor?). (Figure 19) The spots intensified upon warming up to ambient temperature and prolonged reaction time (4 hours). Purification *via* column chromatography revealed predominantly donor (36%) and acceptor (27%). A small quantity of donor without a 3-*O*-picoloyl group was isolated (< 1 mg) and clearly indicates the instability of the donor at these conditions. In addition to 3-*O*-picoloyl cleavage, the acetal might also cleave at these acidic conditions and result in ´self-polymerization´ of the donor to yield various kinds of byproducts (baseline spot). The LC-MS analysis (column: C_4, profile: 5% → 100%) of the presumed product fractions indicated the desired mass.

The glycosylation at ambient temperature instantly yielded a purple discoloration and product formation was indicated *via* TLC after 30 minutes. (Figure 20) The donor was almost consumed, but acceptor was still present. The reaction was quenched after 1.5 hours when a faint baseline spot started to form. Acceptor and residual donor were still present. The crude LC-MS analysis (column: C_4, profile: 5% → 100) confirmed almost full consumption of the donor. (Figure 21) Purification *via* column chromatography afforded roughly 25% (3 mg) of the presumed product.

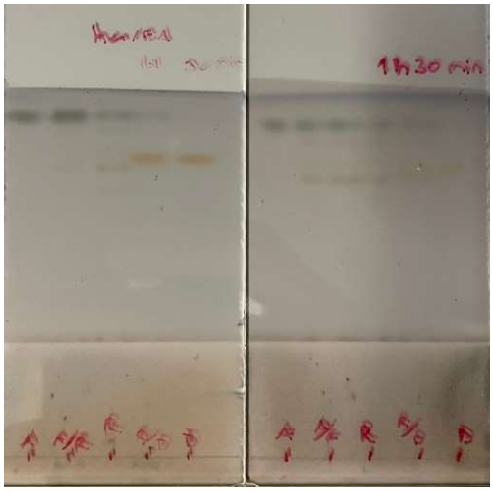

Figure 20: **22** (1.4 equiv.), **30** (7.5 mg, 1.0 equiv.), 5 mM in DCM, NIS (1.5 equiv.), TfOH (0.4 equiv., 0.23 M in ACN), rt (left) 30 min (right) 1.5 h

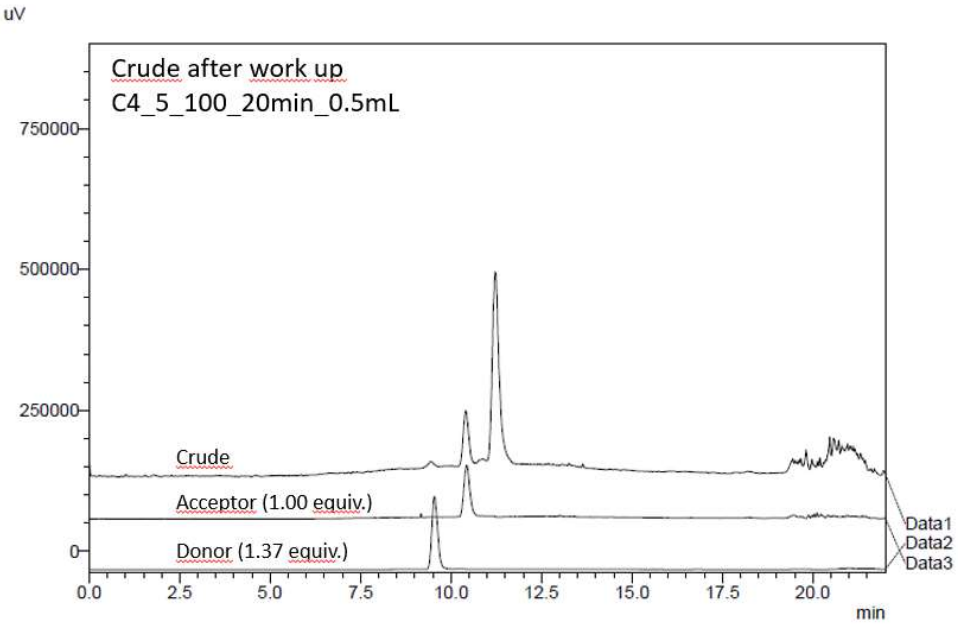

Figure 21: LC-MS of crude material indicates almost full consumption of donor **22**

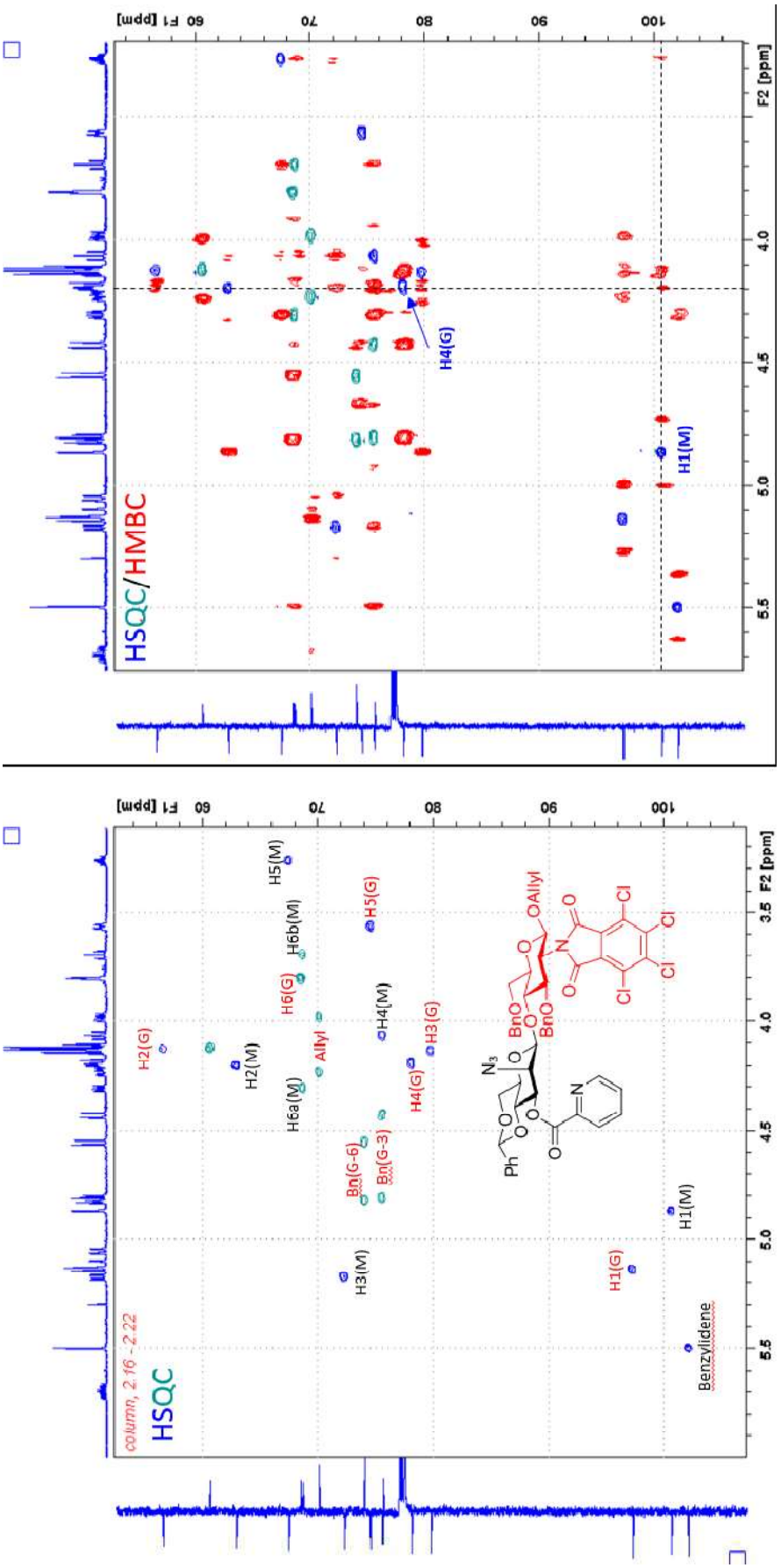

Figure 22: (left) HSQC (right) HSQC-HMBC overlap of isolated β-disaccharide **32**

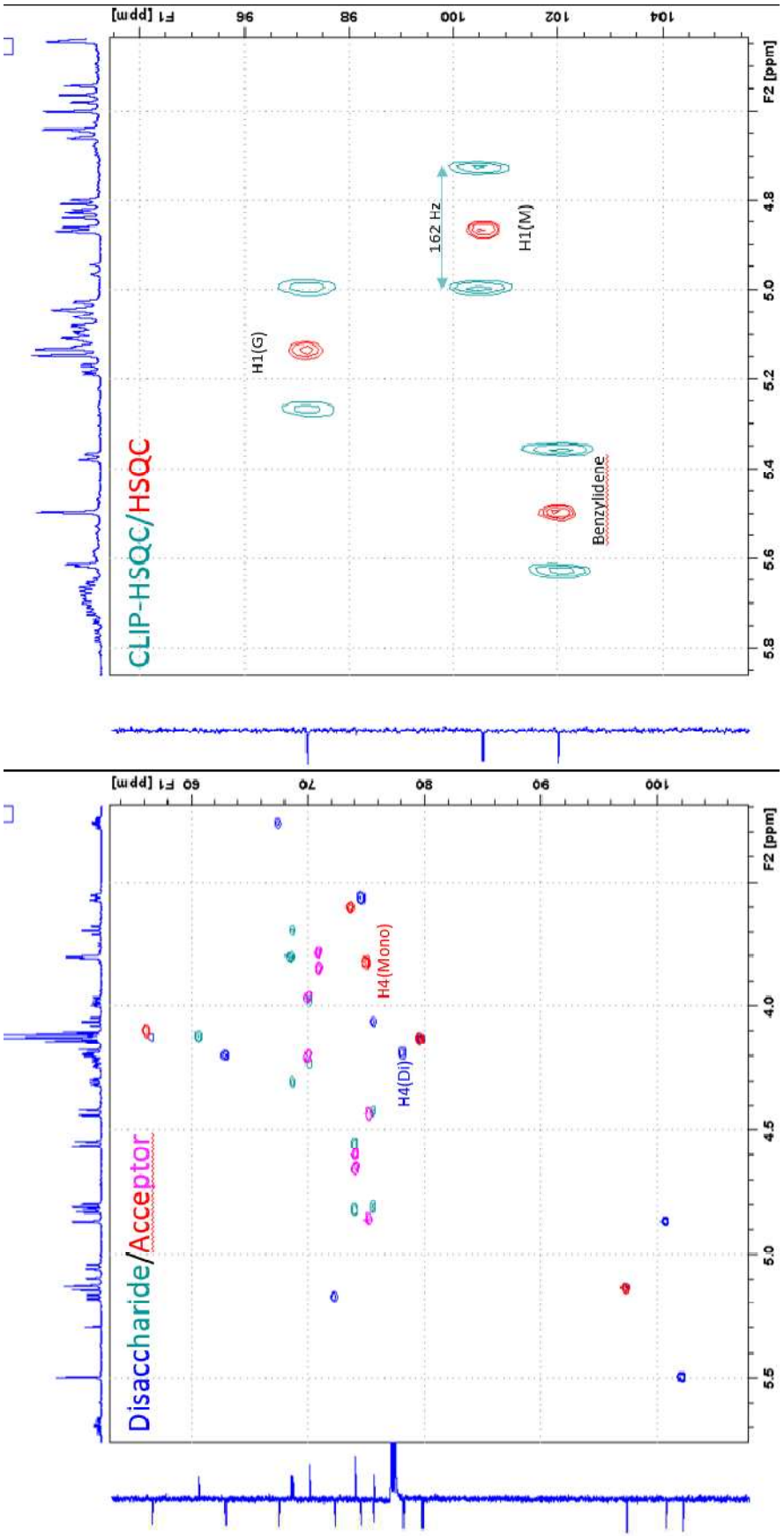

Figure 23: (left) HSQC overlaps of disaccharide **32** and acceptor **30** (right) CLIP-HSQC and HSQC overlap of **32**

The NMR analysis of **32** confirmed the β-(1→4) linkage *via* H_{1A}-C_{4B} bond correlation in the HMBC (Figure 22) and the heteronuclear coupling constant of $^{1}J_{C1A,H1A}$ = 162 Hz in the CLIP-HSQC (Figure 23).[175]

Further experiments using the same conditions gave varying results, but the donor (in excess) was always faster consumed than the acceptor. The intensive baseline spot was repeatedly obtained, indicating side reactions of the donor.

3.4.4.2 Activation with dimethyl disulfide and triflic anhydride

The 3-*O*-picoloyl group of **22** is a base that could potentially quench any acidic promoter. In addition, experiments showed cleavage of the picoloyl group under NIS/TfOH conditions and also acetal cleavage might occur during the glycosylation.

In analogy to dimethyl(methylthio)sulfonium triflate (DMTST)[176,185], the group of Fügedi[186] developed dimethyl disulfide – triflic anhydride (Me_2S_2-Tf_2O) as a powerful promoter for thioglycosides that releases triflic acid after the glycoside has been formed. (Scheme 24) Among others, a per-*O*-benzoylated thiodonor and 4-OH glucosamine acceptor were efficiently glycosylated at -40 °C/10 min to yield 79% of the disaccharide. (Scheme 23A)

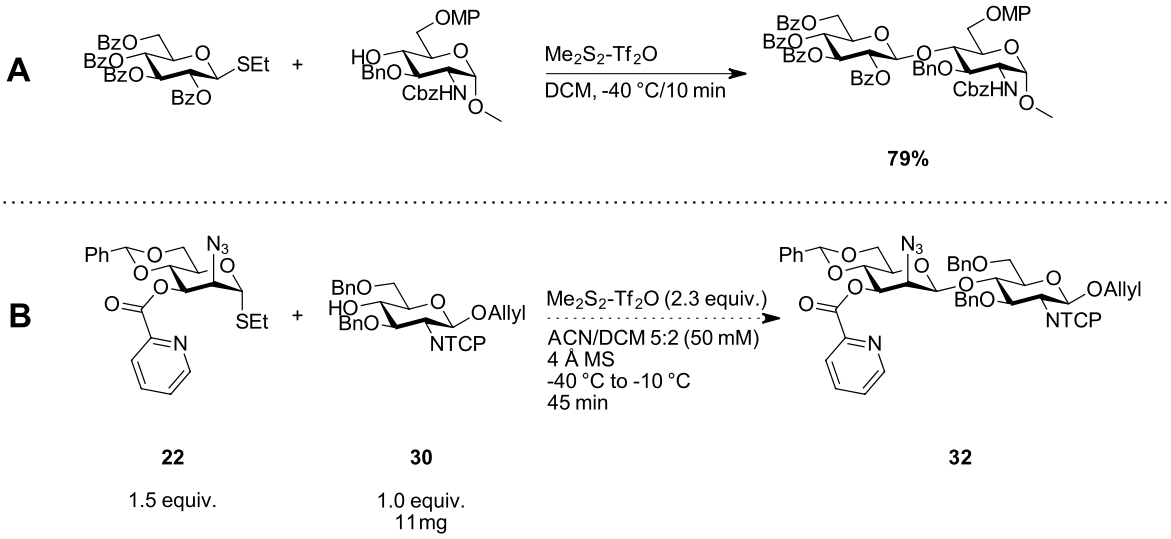

Scheme 23: Me_2S_2-Tf_2O as promoter for thioglycosides[186]

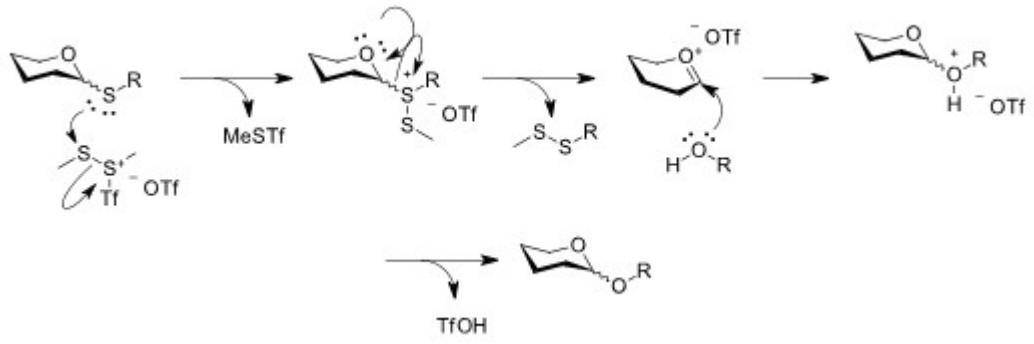

Scheme 24: Mechanism for thiodonor activation with dimethyl disulfide-triflic anhydride[186]

According to a literature procedure[186], to a solution of trifluoromethanesulfonic anhydride (1 M in dichloromethane, 1.00 equiv.) was added dimethyl disulfide (1.10 equiv.) at 0 °C to yield a 1 M solution of Me_2S_2-Tf_2O promoter. The solution was stored at -80 °C with argon overpressure.

The promoter solution (2.3 equiv.) was added at -40 °C to the donor/acceptor mixture. The temperature was slowly raised to -10 °C in 45 minutes. The monitoring *via* HPTLC showed full consumption of the acceptor and donor (1.5 equiv.). (Figure 24) Several byproducts were obtained, but the desired product was not present. A very intensive baseline spot indicated once more decomposition of the donor.

The crude NMR analysis showed the absence of any allyl signal, indicating again electrophilic addition byproducts. Similar results were obtained in a repetition experiment and thus no further investigations into dimethyl disulfide – triflic anhydride activation were made.

Figure 24: Activation with Me_2S_2-Tf_2O (A = Acceptor, X = Co-Spots of adjacent spots, R = Reaction, D = Donor)

3.4.4.3 Activation *via* trichloroacetimidate

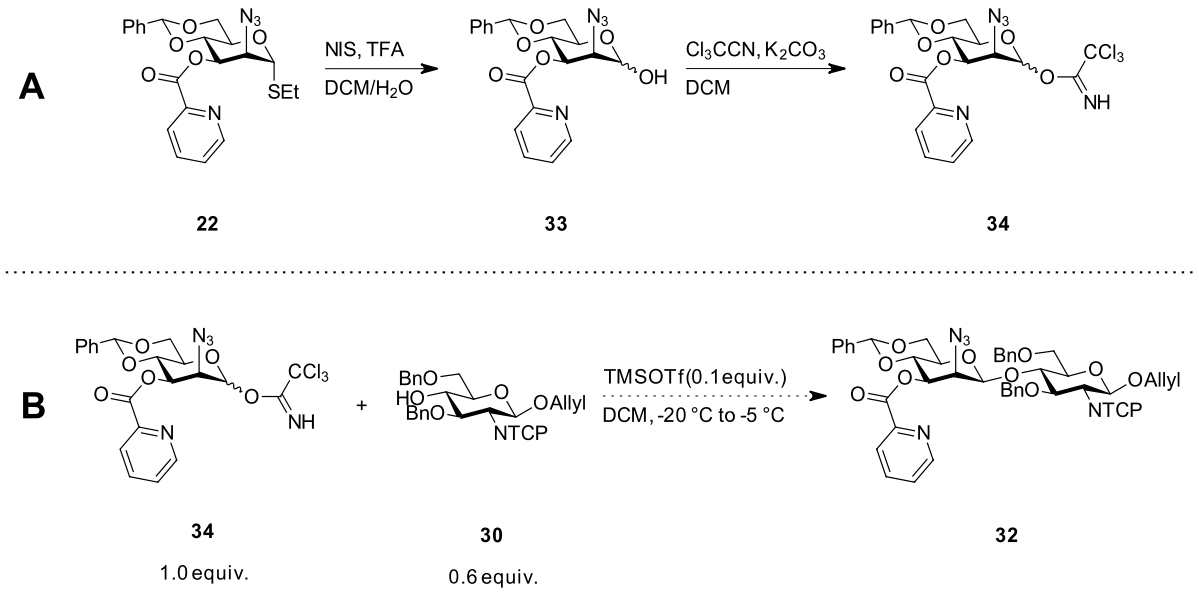

Scheme 25: Effort in glycosylation *via* imidate donor

For the synthesis of the trichloroacetimidate donor **34**, the thioglycoside **22** (22.1 mg, 0.05 mmol) was hydrolyzed using *N*-iodosuccinimide/trifluoroacetic acid in dichloromethane/water.[187] (Scheme 25A) The monitoring *via* TLC indicated incomplete consumption, even after further addition of reagents.

The reaction was quenched after roughly 50% consumption (indicated *via* TLC) and coarse purification *via* column chromatography gave 50% of the hemiacetal **33**. The ^{1}H NMR analysis showed the absence of the thioethyl group. (Figure 25) The basic nature of the picoloyl group may quench the acid and prevent further progress of the hydrolysis.

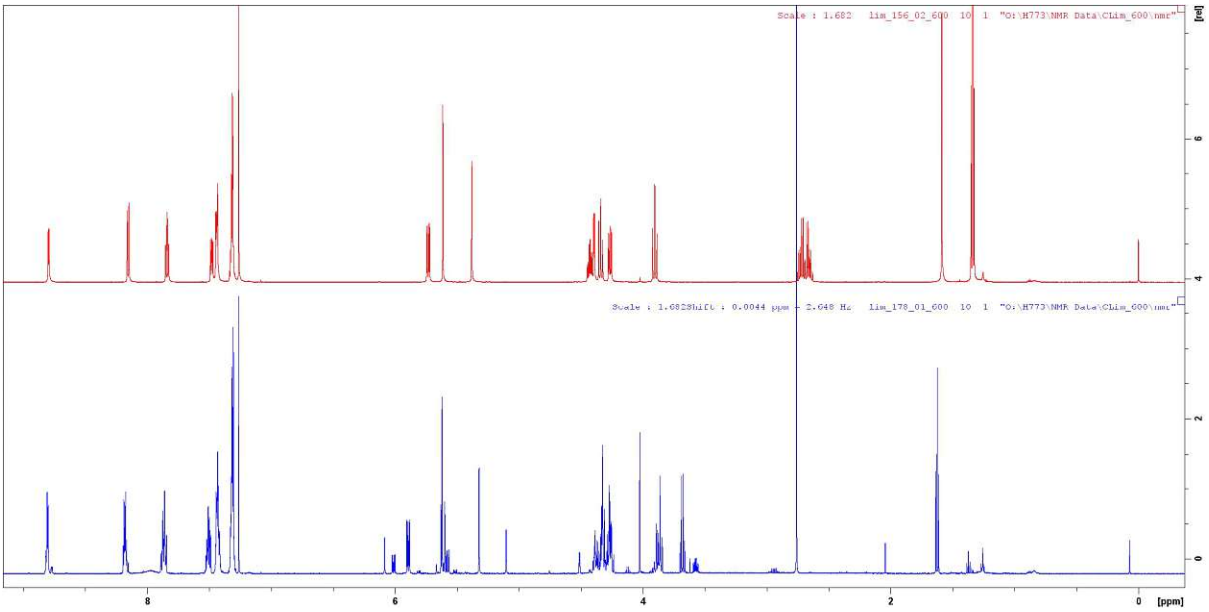

Figure 25: (red) ^{1}H NMR spectra of **22** (blue) and the corresponding hemiacetal **33**

The hemiacetal **33** was stirred with trichloroacetonitrile and potassium carbonate at ambient temperature for 19 hours. (Scheme 25A) (Figure 26) The solid materials were removed *via* filtration over Celite® and the crude **34** was used without further purification. (Scheme 25B)

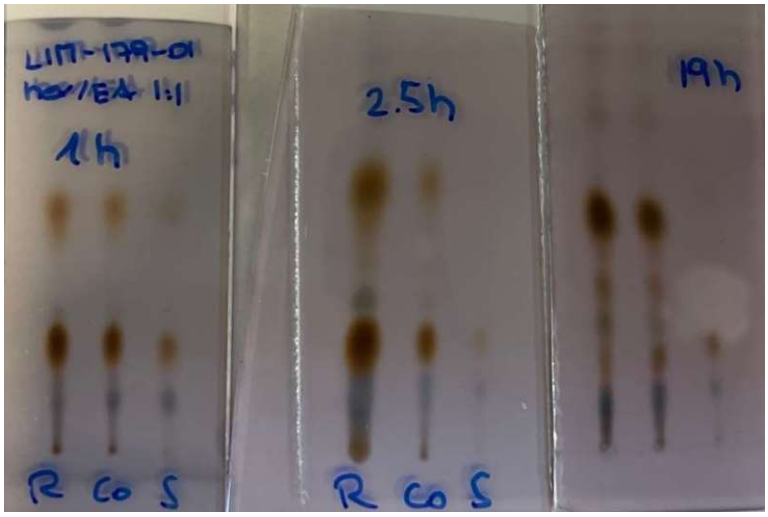

Figure 26: TLC monitoring of imidate formation **34**

To a solution of crude imidate donor **34** (7.1 mg, 13.1 µmol, 1.0 equiv.) and acceptor **30** (5.2 mg, 7.9 µmol, 0.6 equiv.) was added trimethylsilyl triflate (5.5 mM in dichloromethane, 0.24 ml, 1.3 µmol, 0.1 equiv.) at -20 °C. (Scheme 25B) The monitoring *via* TLC indicated no product formation at any time and warming up to

-5 °C, even after further addition of promoter. The reaction was quenched after 2h30min.

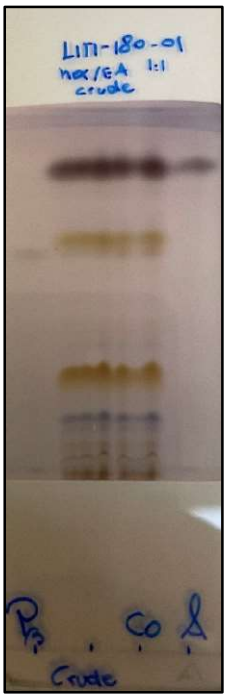

Figure 27: Crude material after work up (P = Product Reference, X = Co-Spots of adjacent spots, R = Reaction, A = Acceptor)

The crude TLC after work up indicated traces of the product and hemiacetal as major compound. (Figure 27) A byproduct that elutes above the product was also observed as second most compound. No further efforts were invested.

3.4.4.4 Activation *via* DBDMH

The group of Li has published the synthesis of challenging β-D-fructofuranosides *via* hydrogen-bond mediated aglycon delivery utilizing 1,3-dibromo-5,5-dimethylhydantoin (DBDMH) as promoter.[188] DBDMH is a non-toxic, stable and inexpensive bromine-containing reagent and gave very good β-selectivity (α/β < 1:20).[188] According to the proposed mechanism, the method is an acid-free activation.[188] (Scheme 26)

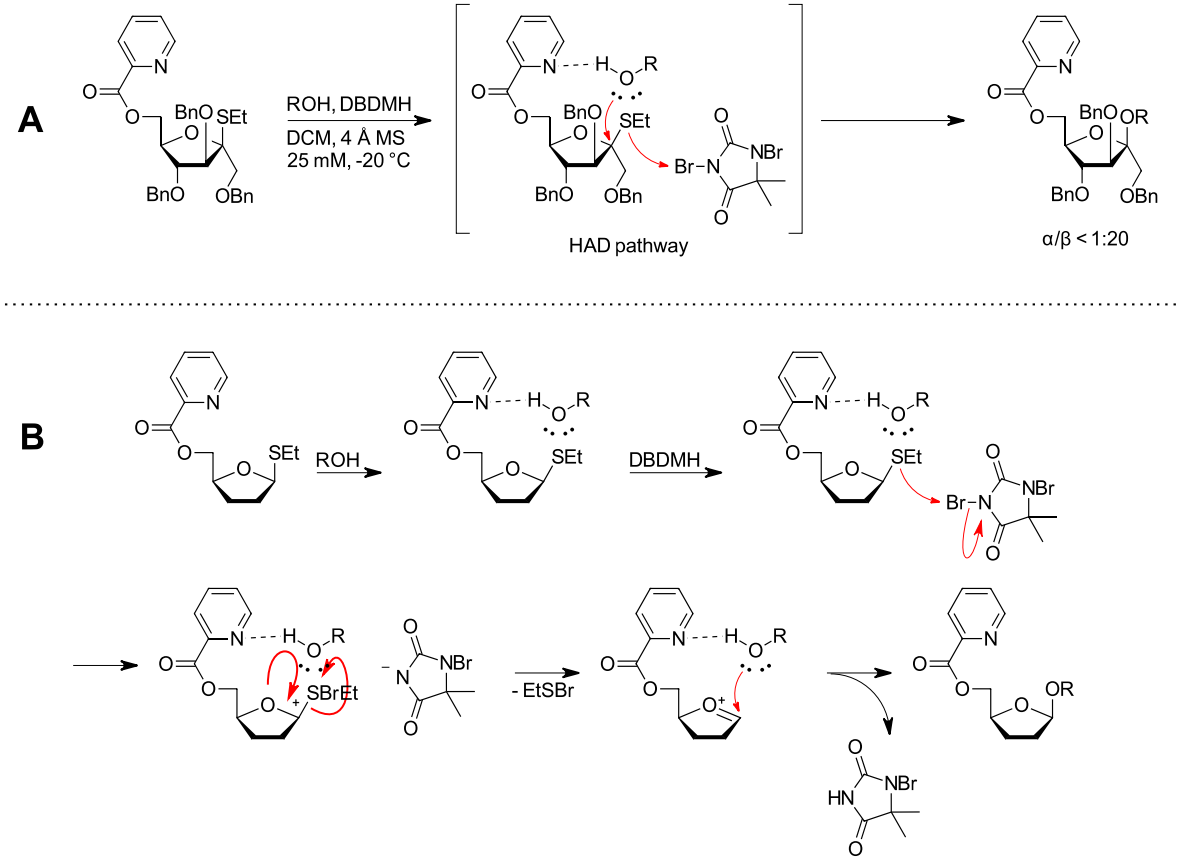

Scheme 26: (A) β-Fructofuranosides *via* DBDMH-promoted HAD pathway (B) Proposed mechanism[188]

Starting materials **22** and **30** were pre-stirred with 4 Å molecular sieves for 1 hour, before DBDMH was added at -20 °C. (Scheme 27) Monitoring *via* TLC did not indicate any consumption after 1 hour at -20 °C. The temperature was raised to ambient temperature within 2 hours, but **32** was not detected according to TLC. Donor decomposition was observed on the baseline. The reaction was quenched and the acceptor was recovered from the crude material. No further efforts were invested.

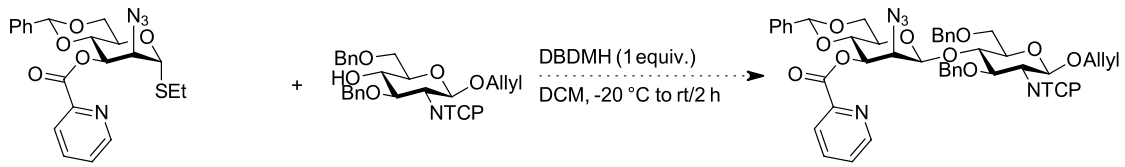

22

1.0 equiv.

30

0.84 equiv.

32

Scheme 27: DBDMH-promoted glycosylation of **22** and **30**

3.4.4.5 Activation *via* silver triflate and *N*-iodosuccinimide

The silver triflate/*N*-iodosuccinimide promoter system should not release any triflic acid according to the mechanism and thus prevents donor decomposition.[189] (Scheme 28)

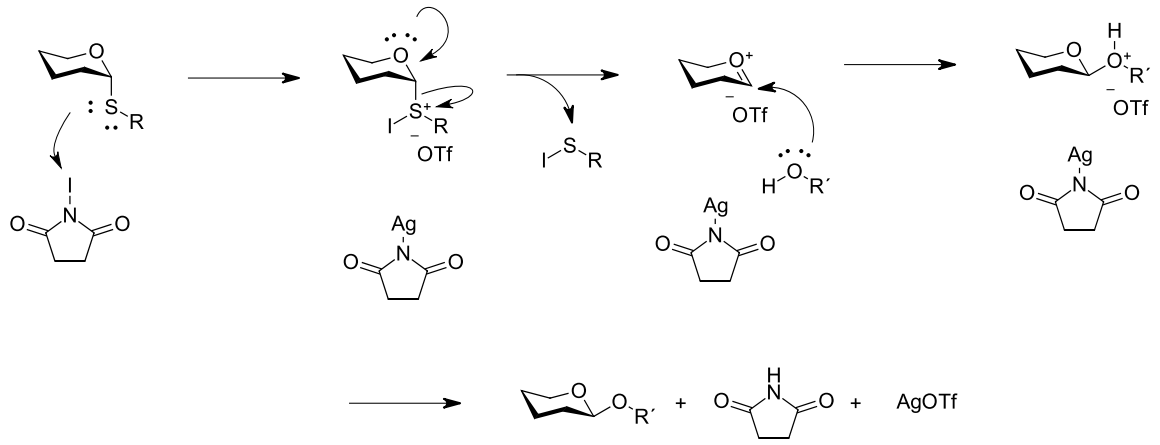

Scheme 28: Mechanism for AgOTf/NIS promoted glycosylation[189]

Initial experiments with *N*-iodosuccinimde (1.2 equiv.) and silver triflate (0.4 equiv.) did not give any or low conversion to the product at temperatures ranging from -10 °C to ambient temperature in dichloromethane as solvent. Donor decomposition was indicated according to TLC in almost all reactions. Product formation was finally observed at 50 °C and 0.6 equivalents of silver triflate. When the promoter silver triflate was added as a fresh solution in toluene, stored over silver oxide, donor decomposition could be prevented. To our surprise, this did not lead to any relevant yield increase after purification *via* column chromatography. The silver oxide prevents or slows down the formation of triflic acid, but promoter solutions gave donor decomposition according to TLC after few weeks of storage. (Figure 28)

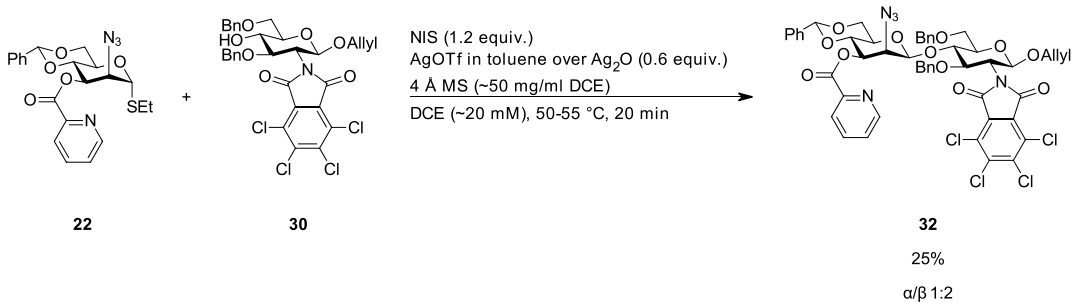

Scheme 29: Conditions used for the synthesis of **32**

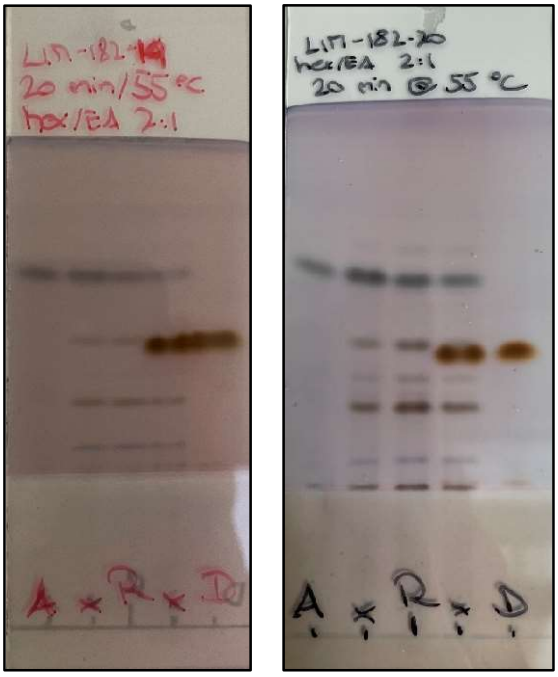

Figure 28: (left) Fresh AgOTf solution (right) Old AgOTf solution

The conditions shown in Scheme 29 were initially found to give clean reactions according to TLC. Decomposition of **22** was still observed with an excess of **30**, highlighting both the instability of the donor and the low reactivity of the 4-OH group in glucosamine derivatives. The decomposition of **22** takes place faster than the glycosylation, as significant amounts of **30** were recovered during the purifications. The acceptor **30** was stable under these conditions. The glycosylation gave an α/β ratio of 1:2 for α-byproduct **32a** (12%) and the desired β-ManNAc **32** (25%).

3.4.4.6 Summary

Table 4: Screening of activation conditions for 1+1 glycosylation

Entry	Conditions	Byproducts	Product
1	NIS/TfOH (1.7 eq & 0.6 eq) **22** (1.4 eq) **30** (1.0 eq) 5 mM DCM 30 min/1.5 h	Activation only at ≥ rt, s Several byproducts, complete donor consumption →decomposition	β (25%)
2	Me_2S_2-Tf_2O (2.3 eq) **22** (1.5 eq) **30** (1.0 eq) 50 mM ACN/DCM (5:2) -40 °C to -10 °C	Several byproducts, decomposition (TLC), electrophilic addition byproduct	-
3	TMSOTf (0.1 eq) **34** (1.0 eq) **30** (0.6 eq) DCM, -20 °C to -5 °C	Hemiacetal and two other byproducts (not characterized)	-
4	DBDMH (1 eq) **22** (1.0 eq) **30** (0.84 eq) DCM, -20 °C to rt, 2 h	Donor decomposition at rt	-
5	AgOTf soln. (0.6 eq) NIS (1.2 eq) **22** (1.0 eq) **30** (1.2 eq) DCE (~20 mM) 50-55 °C, 20 min	Donor decomposition with old AgOTf soln. (TLC)	α (12%) β (25%) α/β 1:2

3.4.5 Synthesis towards disaccharide donor **42** and acceptor **37**

Allyl deprotection of key intermediate **32** to hemiacetal **35** with hydrogen-activated $[Ir(cod)(PPh_2Me)_2]PF_6$ in tetrahydrofuran gave only traces of the corresponding propenyl ether as evidenced by the slightly higher R_f value on the TLC.[190] (Scheme 30) Further addition of iridium catalyst solution did not increase consumption. The basic nature of the picoloyl group may complex the catalyst and prevent further reaction.

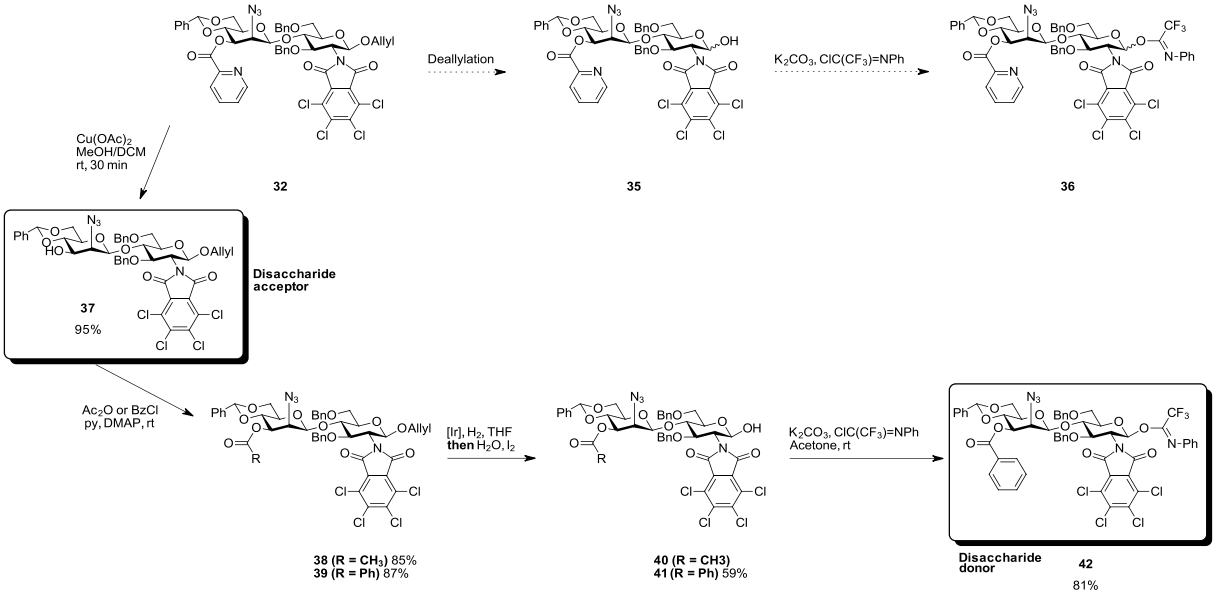

Scheme 30: Synthesis towards disaccharide building blocks from key intermediate **32**

Anomeric deprotection of **32** by employing tetrakis(triphenylphosphine) palladium in acetic acid resulted in the formation of several byproducts.[191] Among others, desired **35** and corresponding acetal-cleaved byproduct were observed in trace amounts. The literature reported that 4,6-*O*-benzylidene protected glucose derivatives are stable under these conditions, as the decalin system provides high scaffold stability.[191] The allyl isomerization of **32** *via* palladium on charcoal (10%) in methanol at 70 °C gave full consumption after 1 hour.[192] Purification and NMR analysis however revealed 3-*O*-picoloyl cleavage. The isomerization with palladium(II) chloride under buffered conditions with sodium acetate/acetic acid at pH 5 only gave traces of **35**.[193,194]

The efforts in allyl deprotection indicated that the picoloyl group quenches any (Lewis-)acid or transition metal *via* coordination. As circumvention, the picoloyl group was exchanged to a benzoyl ester protective group.

The picoloyl deprotection of key intermediate **32** with copper(II) sulfate in methanol/dichloromethane gave disaccharide acceptor **37** within 30 minutes.[195] For test purpose, **37** was acetylated to **38**. The allyl isomerization with hydrogen-activated $[Ir(cod)(PPh_2Me)_2]PF_6$ in tetrahydrofuran yielded the propenyl ether according to TLC and subsequent hydrolysis gave the desired hemiacetal **40**, as indicated *via* TLC and confirmed by LC-MS analysis (column: C_4, profile: 5% → 100% in 20 min).[190]

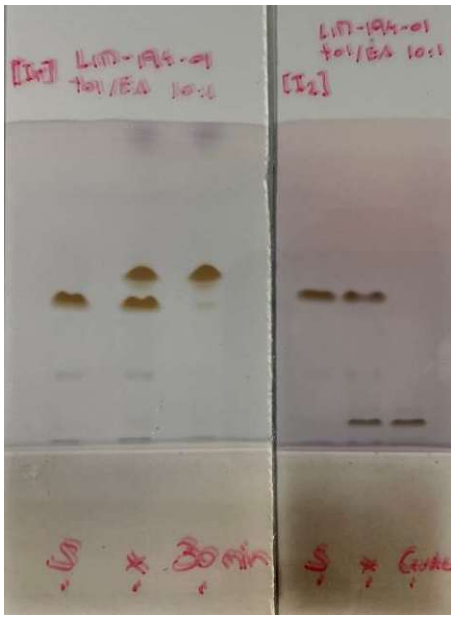

Figure 29: (left) Allyl isomerization of **39** with hydrogen-activated $[Ir(cod)(PPh_2Me)_2]PF_6$ (right) Subsequent hydrolysis with iodine/water[190]

In analogy to the test reaction, the disaccharide acceptor **37** was benzoylated to give **39** and allyl deprotection gave exclusively the β-hemiacetal **41**. (Figure 29) The benzoyl group was chosen over the acetyl group due to its stability against migration. Final imidate formation with 2,2,2-trifluoro-*N*-phenylacetimidoyl chloride and potassium carbonate in acetone gave donor **42**.[196] A drop of water was added to improve solubility of the base. The imidate was isolated *via* flash column chromatography using 0.1% pyridine. No (further) characterization of **42** was done.

3.4.6 Efforts towards tetrasaccharide target compounds

3.4.6.1 2+2 glycosylation

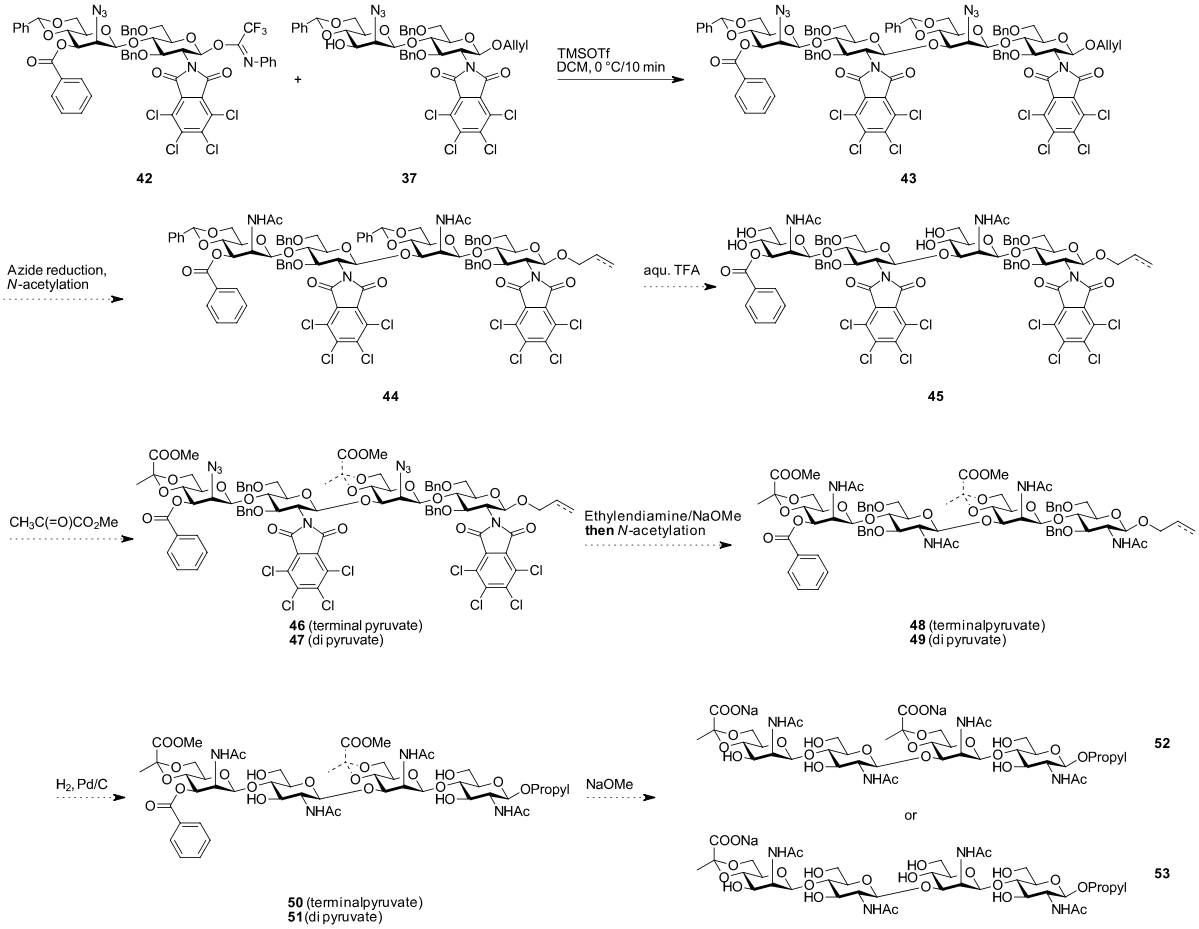

Scheme 31: Planned forward synthesis towards targets **52** and **53**

The glycosylation of **42** (1.0 equiv.) and **37** (1.5 equiv.), promoted by trimethylsilyl triflate (0.1 equiv.), gave the key tetrasaccharide **43** with 61% yield and surprisingly, was accompanied by 21% of side product **43a**. (Scheme 32)

The NMR analysis of **43** confirmed the β-(1→4) linkage *via* H_{1B}-C_{4C} bond correlation in the HMBC and the heteronuclear coupling constant of $^{1}J_{C1B,H1B}$ = 160 Hz in the CLIP-HSQC (Appendix 9.17.4).[175]

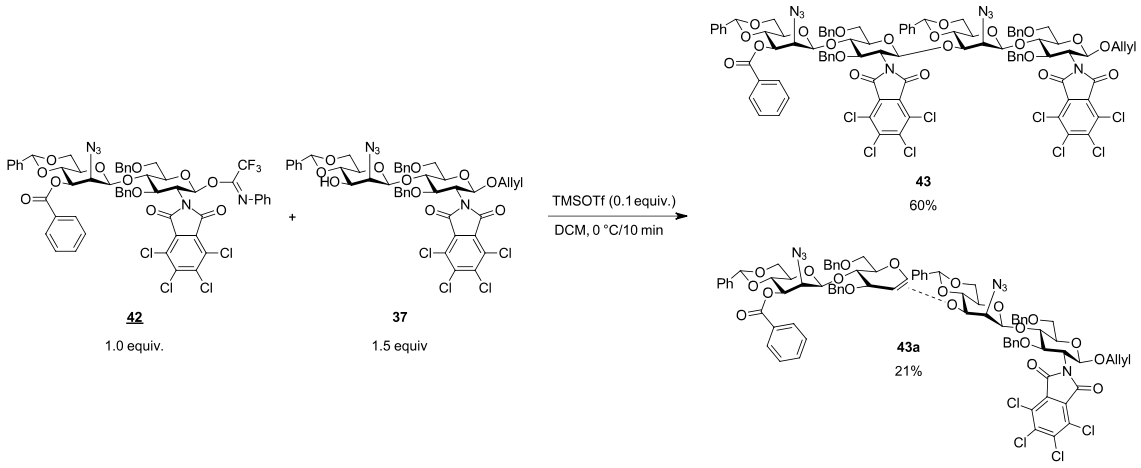

Scheme 32: Glycosylation gives tetrasaccharides **43** and **43a**

Glycosylations are substitution reactions that compete against elimination to form C_2-substituted glycals.[197] The glycosylation can be facilitated with an excess of donor, while elimination is generally supported at elevated temperatures and/or unreactive acceptors.[197,198] The elimination has been reported for many types of glycosyl donors and among them, 2-deoxy-2-phthalimido-D-glucopyranosyl imidate donors.[199–205] (Scheme 33)

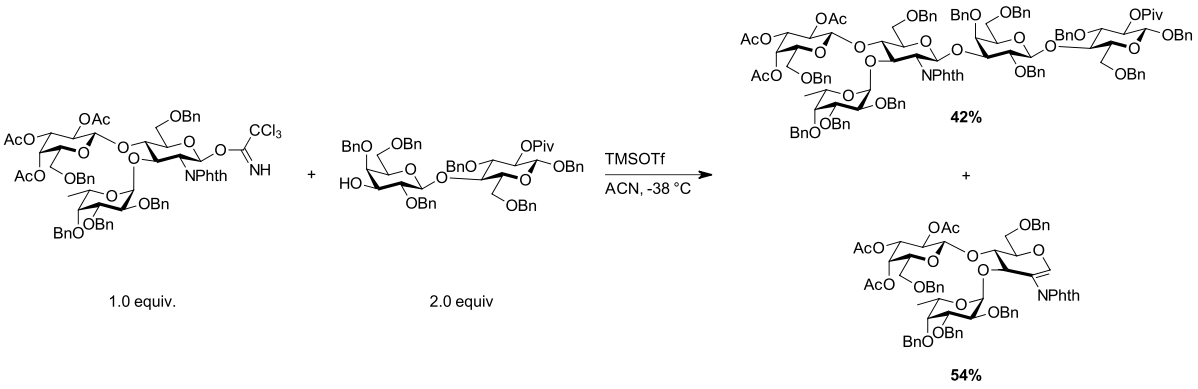

Scheme 33: Selected example of glycal formation observed with 2-deoxy-2-phthalimido glucopyranosyl imidate[205]

The formation of tetrasaccharide **43a** through elimination of the 2-tetrachlorophthalimido group was quite surprising, as (to the best of my knowledge) literature only reports β-elimination of the donor leaving group.[197] (Scheme 33) The 2-tetrachlorophthalimido glycal and the α-isomer of **43** were not observed. The NMR characterization of the byproduct **43a** is not conclusive on the linkage regioselectivity, but the proposed mechanism suggests a 2-*O*-linkage. The proposed mechanism (Scheme 34) includes an intramolecular attack of the TCP group to the oxocarbenium ion to form an oxazoline cation. The oxazoline cation rearranges to the 1-imidate while

the glycosyl acceptor attacks the C_2-carbo cation. Subsequent β-elimination of the imidate gives the 2-*O*-linked tetrasaccharide. The basic nature of the molecular sieves may facilitate the decisive proton abstraction in the last step.

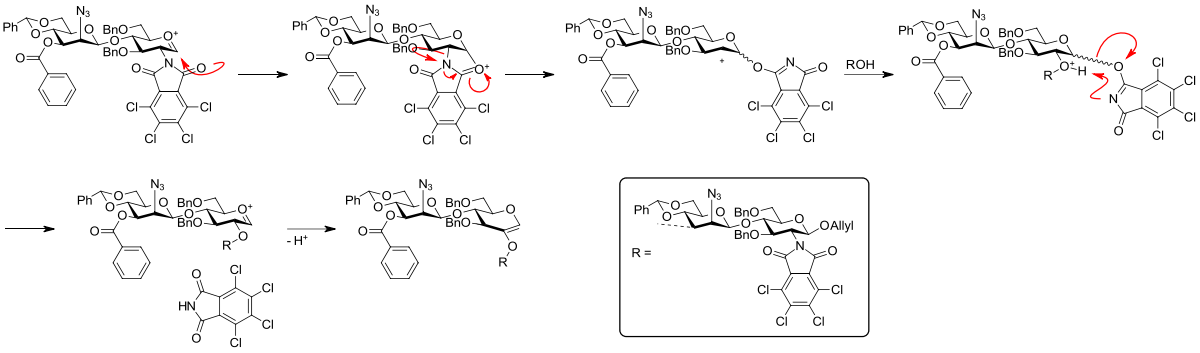

Scheme 34: Proposed mechanism for the glycal formation

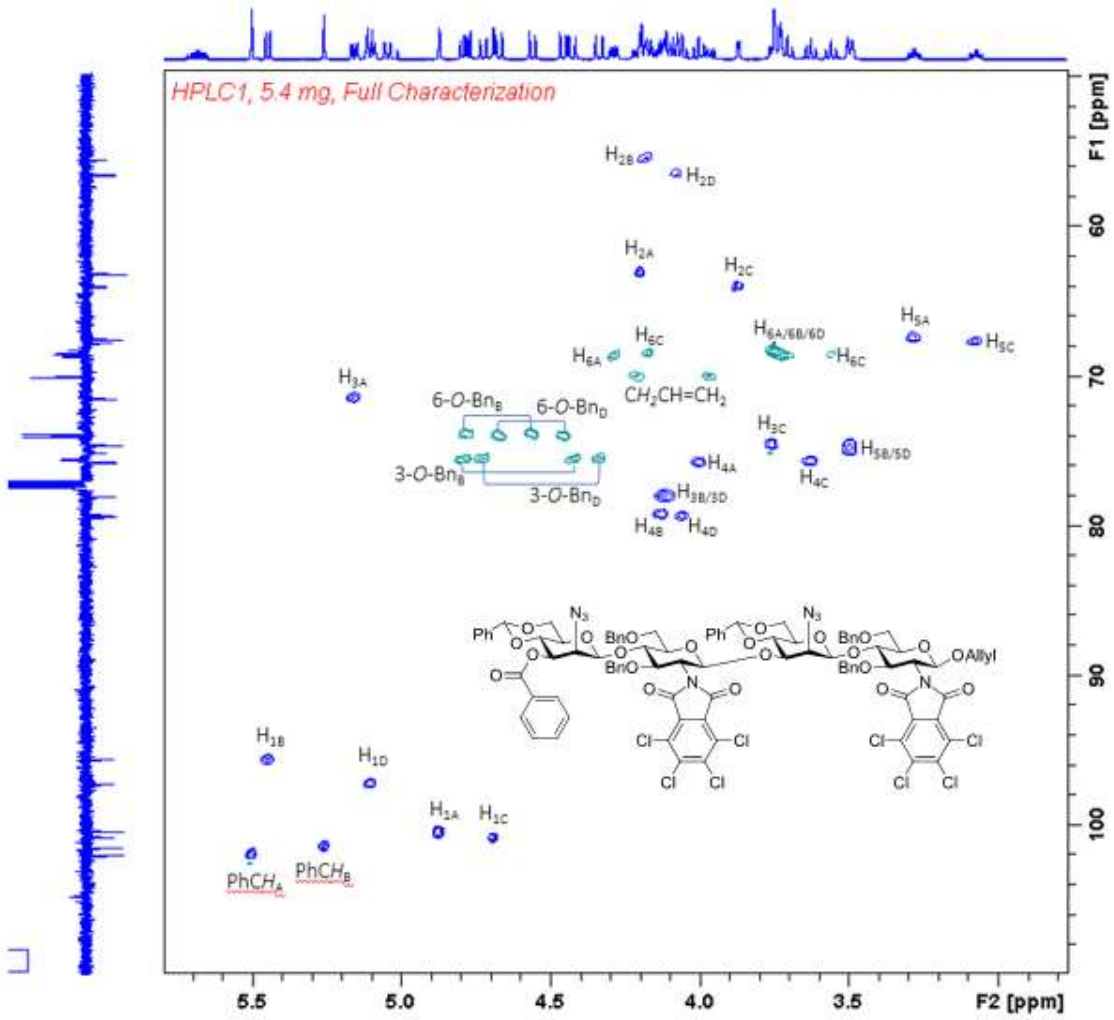

Figure 30: HSQC of **43** (rings are labeled with capital Latin letters starting with A from the non-reducing end to the reducing end)

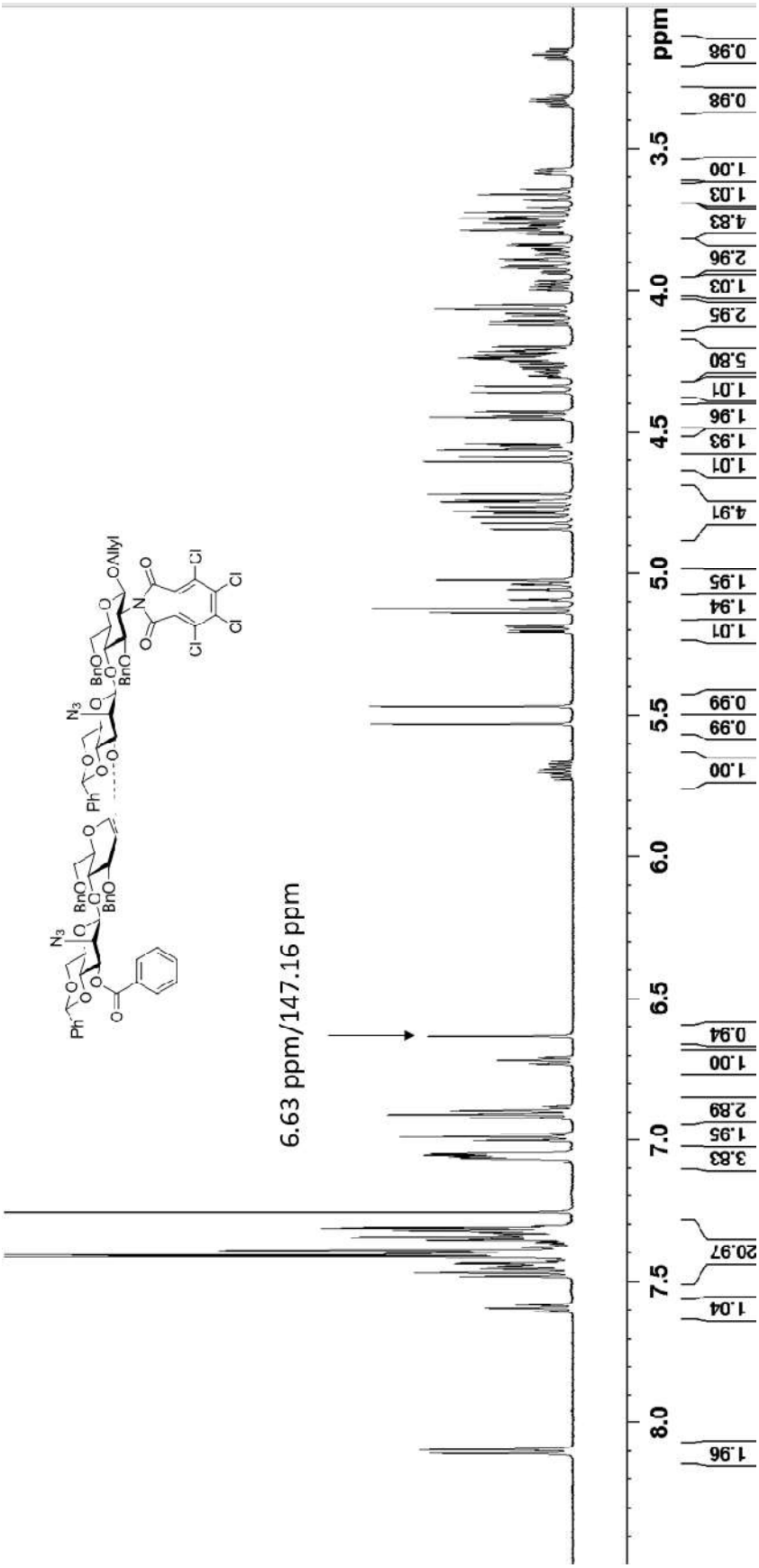

Figure 31: ^{1}H spectrum of **43a** (vinylic proton of glycal is indicated)

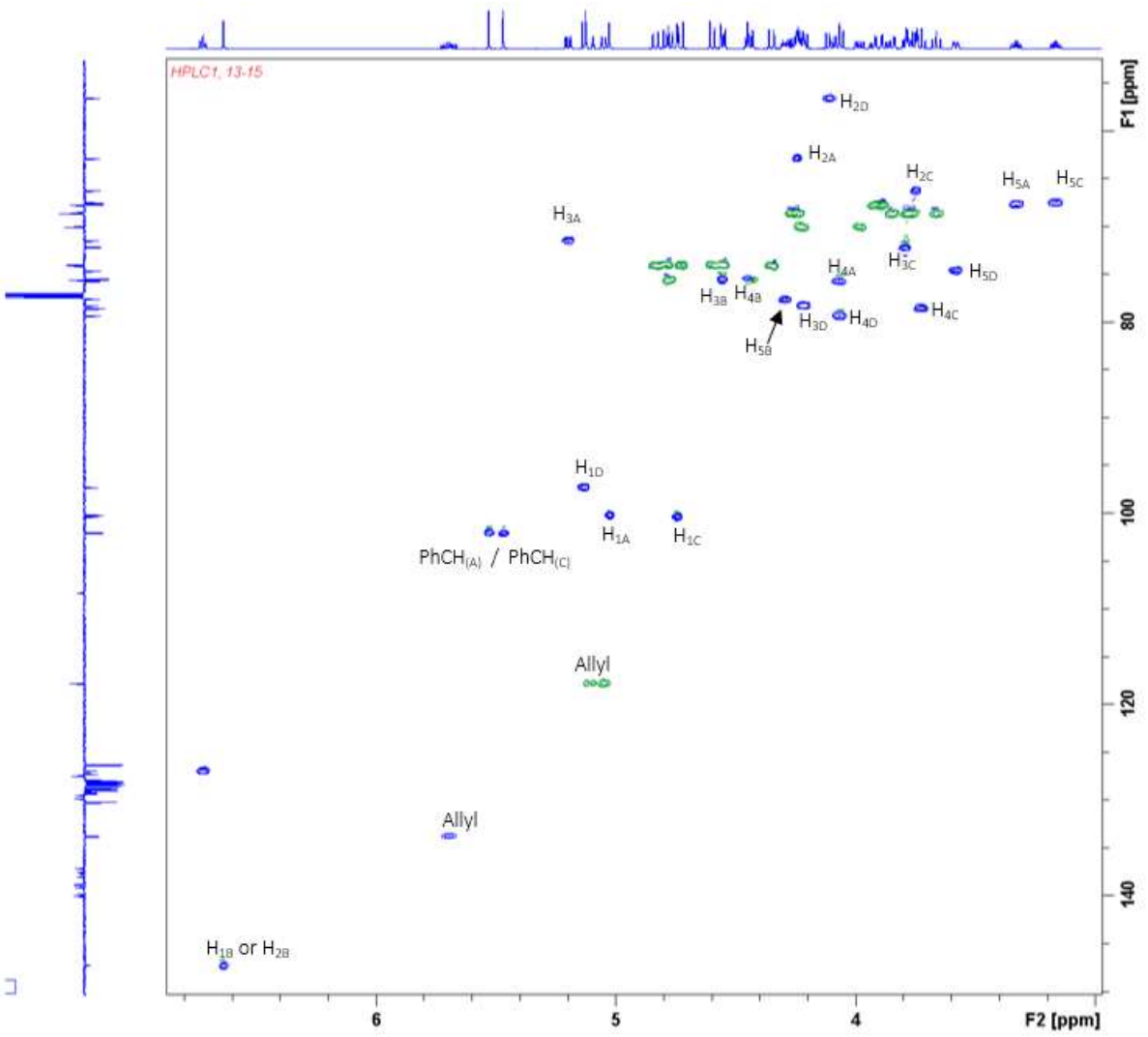

Figure 32: HSQC of **43a**

The ^{1}H NMR spectrum shows the characteristic vinylic signal at 6.63 ppm and 147.16 ppm in the ^{13}C NMR spectrum. (Figure 31) The corresponding HSQC spectrum shows three anomeric signals and the typical shift of the repetitive units are changed. (Figure 30 vs Figure 32) As expected, the HMBC spectrum shows a correlation of the vinylic signal to H_{4B} and H_{5B} (Figure 33), while the NOESY spectrum shows a strong correlation to the H_{3B} and a faint correlation to H_{5B}. (Figure 34)

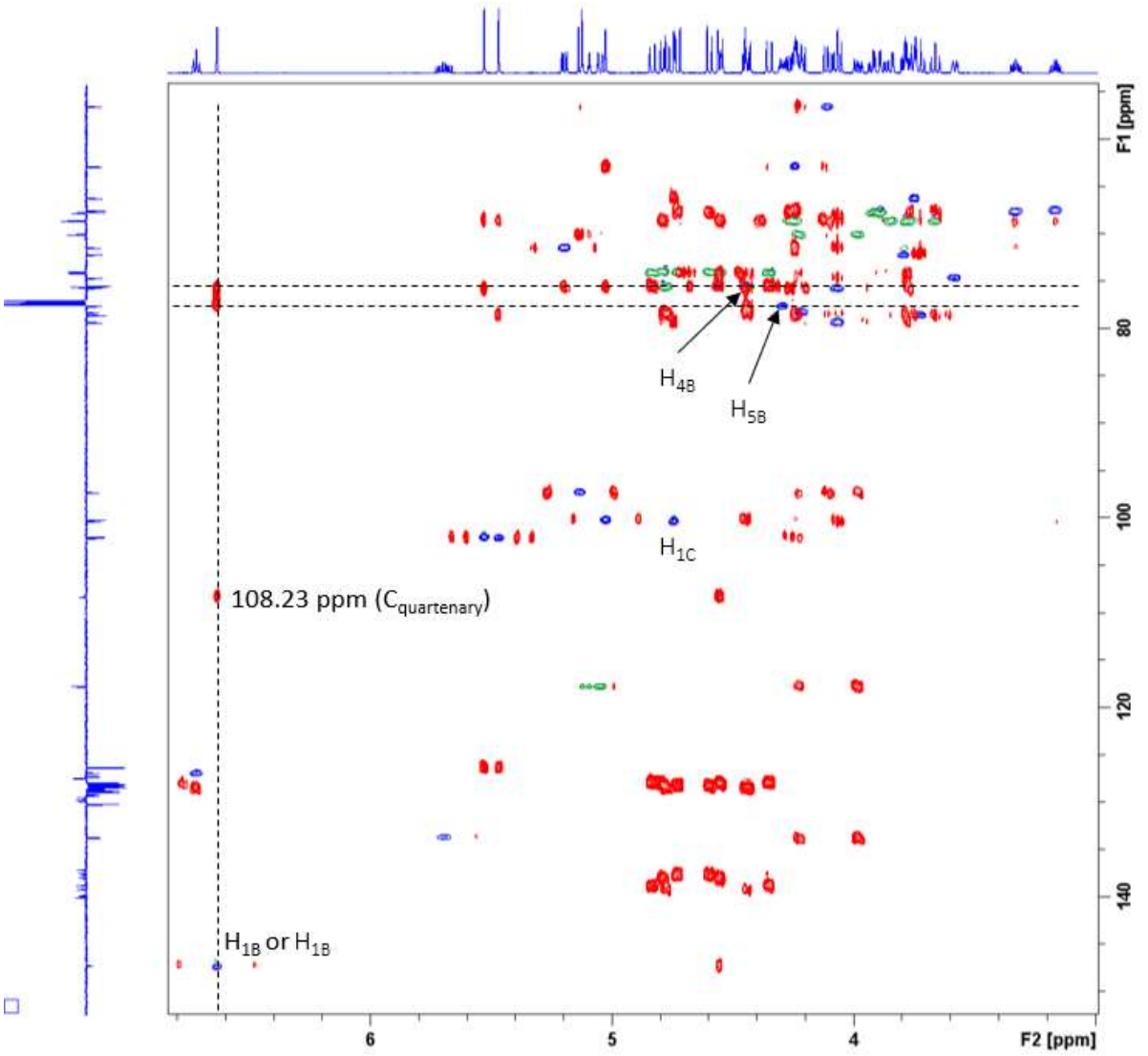

Figure 33: HSQC/HMBC overlap of **43a**

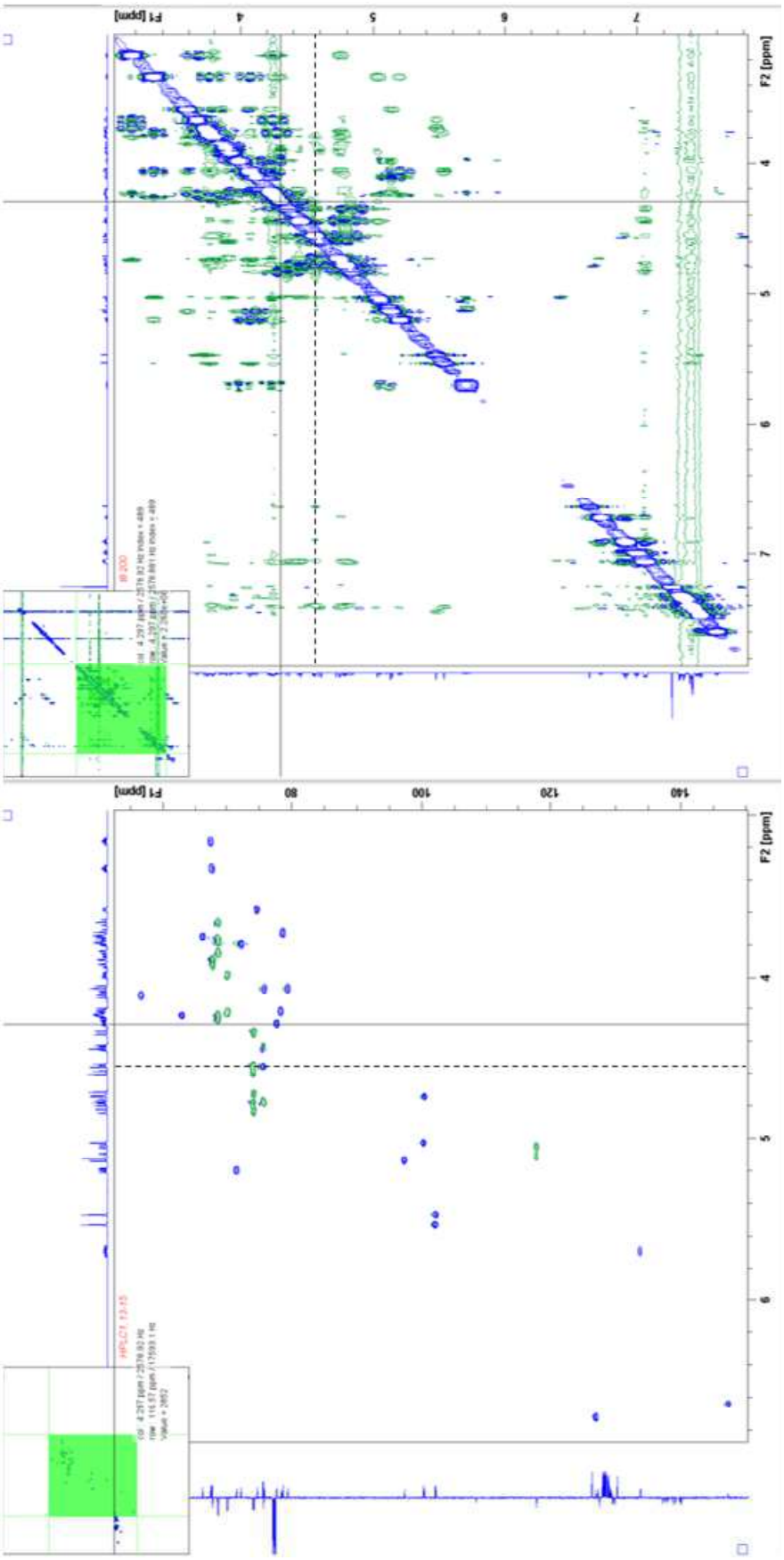

Figure 34: (bottom) HSQC (top) NOESY of **43a** (dashed line H_{3B}, non-dashed line H_{5B})

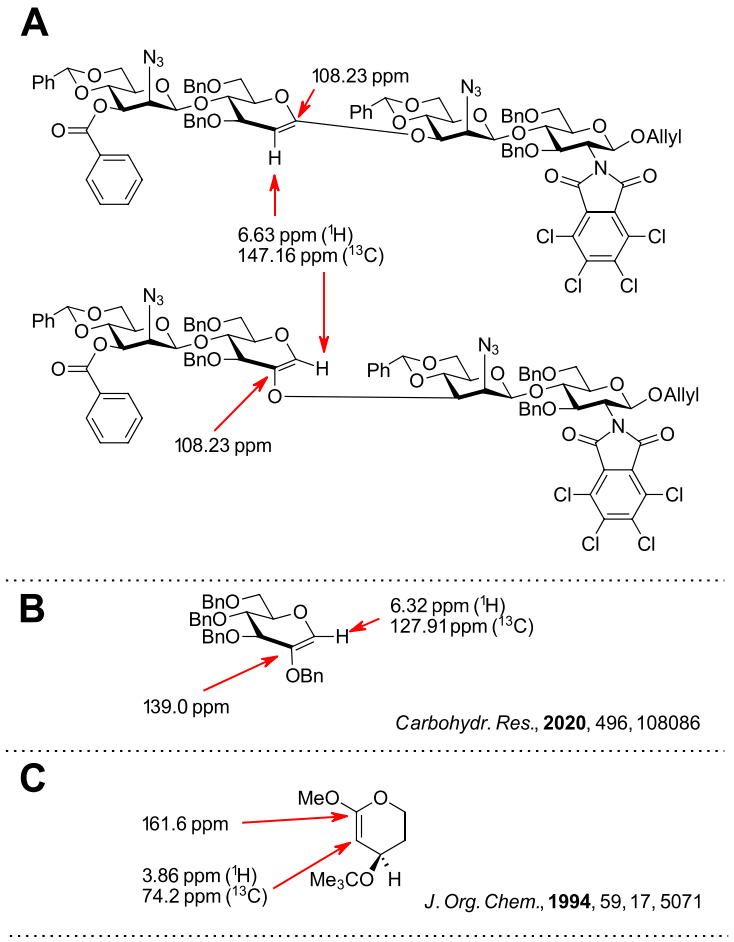

Scheme 35: Comparison of **43a** with selected vinylic (glycal) signals from the literature[206,207]

The comparison of the vinylic signals of **43a** with selected literature examples indicates the 2-*O*-glycal structure, as the carbon-shift of the mono-substituted vinylic position resembles structure B more than C. (Scheme 35)

3.4.6.2 Azide reduction

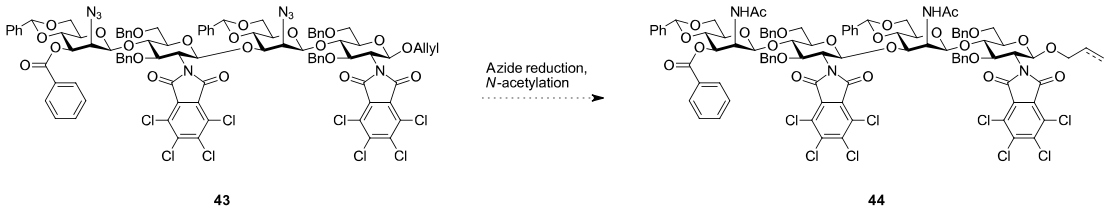

Scheme 36: Azide reduction and subsequent *N*-acetylation of key tetrasaccharide **43**

According to preliminary results on methyl 3-*O*-acetyl-2-azido-4,6-*O*-benzylidene-2-deoxy-β-D-mannopyranoside in our research group, the sequence order of azide reduction, *N*-acetylation, acetal-cleavage and pyruvate installation proved to be the best.[208]

The azide reduction of **43** with polymer-bound triphenylphosphine in dichloromethane indicated full consumption after 3 days at 40 °C and subsequent hydrolysis with water in tetrahydrofuran. The following crude *N*-acetylation and purification did not yield desired **44**.[208]

The Staudinger reduction of **43** with trimethylphosphine in tetrahydrofuran at -78 °C indicated no consumption within 2 hours.[209,210] Full consumption was obtained at ambient temperature and several byproducts were observed according to TLC. The crude *N*-acetylation and purification gave no *N*-acetyl compounds.

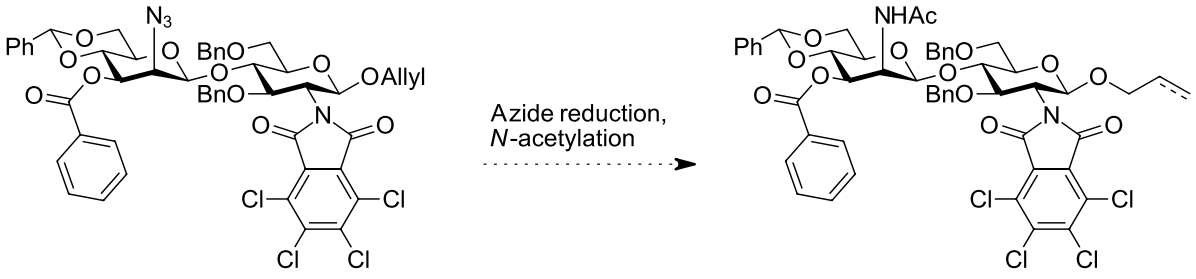

39 **54**

Scheme 37: Test reaction with disaccharide **39**

To avoid further waste of tetrasaccharide **43** and ease of monitoring, the disaccharide **39** was used for test reactions with various procedures. (Scheme 37)

The hydrogenation of **39** with an old batch of Lindlar catalyst at 1 atm and ambient temperature gave a mix of varying amounts of 1-propyl and 1-allyl *N*-acetylated compounds.[211] A fresh batch of Lindlar catalyst additionally yielded benzyl- and acetal-cleaved byproducts.

The hydrogenation of tetrasaccharide **43** with the “old batch” of Lindlar catalyst at 1 atm and ambient temperature yielded several compounds according to TLC after three days, but none matched the expected polarity of free amino groups.[211]

The azide reduction of **39** with propane-1,3-dithiol and triethylamine in methanol resulted predominantly in electrophilic addition towards the 1-*O*-allyl group.[211,212] The reduction towards an amino group was indicated according to TLC, but could have been a mix of desired **54** and the corresponding addition byproduct.

The reduction of **39** *via* thioacetic acid and 2,6-lutidine in chloroform showed no consumption at all according to TLC.[213]

To a solution of tin(ii) chloride and *p*-thiocresol in dichloromethane was added triethylamine to form the reducing agent $[Et_3NH][Sn(STol)_3]$.[214,215] The reduction of disaccharide **39** with the reducing agent gave full consumption and following *N*-acetylation yielded several compounds after purification *via* column chromatography. The *N*-acetyl group was observed in the ^{1}H NMR spectrum that showed the same signal pattern with minimal shifts for all compounds. In some cases, the STol signal was present, indicating presumably adduct formation with the agent. In addition, the 3-*O*-benzyl was cleaved in all compounds. The compounds were dissolved in chloroform and stirred against aqueous ethylendiaminetetraacetic acid (EDTA) to scavenge any (tin) adduct impurities, but no changes were observed according to TLC.

The reaction of **39** with zinc-copper-couple in glacial acetic acid went to full consumption and the formation of several compounds was observed.[129] Purification yielded predominantly two compounds, one with a cleaved 3-*O*-benzyl group and no NH signal. The other compound was *N*-acetylated on both the axial and equatorial amino functionalities. The TCP group was partially opened. As the zinc-copper-couple procedure proved to be the best, the tetrasaccharide **43** was reduced with latter method. The reaction gave several byproducts according to TLC and prolonged reaction time did not facilitate the formation of one single compound. The crude material was submitted to *N*-acetylation, but the desired product mass was not found with LC-MS analysis.

The global hydrogenolysis/hydrogenation of tetrasaccharide **43** with palladium on charcoal (unreduced, 10%) in *tert*-butanol/acetic acid (4:1) at roughly 8 bar and ambient temperature gave several compounds near the baseline after 4 days that stained with ninhydrin, indicating the presence of any amino group.[216] The crude material was submitted to peracetylation and coarse flash filtration. Predominantly one compound was obtained and according to ^{1}H NMR analysis, two *N*-acetyl and several *O*-acetyl signals were observed. All aromatic signals were gone (benzyl, benzoyl), but the corresponding product mass was not observed *via* LC-MS.

3.4.6.3 Summary

Table 5: Summary of used protocols for azide reduction

Entry	Substrate	Method	Result
1	**43**	PPh_3-polymer bound, rt to 40 °C, 4 days **then** N-acetylation	No *N*-acetylated compounds isolated
2	**43**	PMe_3 in THF, -78 °C to rt **then** N-acetylation	No *N*-acetylated compounds isolated
3	**39**	Hydrogenation, Lindlar (´old batch´), 1 atm, rt	Mix of *N*-acetyl 1-allyl and 1-propyl compounds
4	**39**	Hydrogenation, Lindlar (´new batch´), 1 atm, rt	As **Entry 3**, but additionally Bn- and acetal-cleavage byproducts
5	**43**	Hydrogenation, Lindlar (´old batch´), 1 atm, rt	Several compounds, but no amino group detected (TLC)
6	**39**	Propane-1,3-dithiol	Electrophilic addition to 1-allyl group
7	**39**	Thioacetic acid, 2,6-lutidine	No consumption
8	**39**	$[Et_3NH][Sn(STol)_3]$ then *N*-acetylation	*N*-Acetylation isolated, 3-O-Bn cleavage, several adduct formations with reagent that were not separable
9	**39**	zinc-copper-couple	Axial and equatorial *N*-acetylation, partial *N*-TCP opening, 3-*O*-Bn cleavage with no NH signal as byproduct
10	**43**	zinc-copper-couple	Several byproducts formed
11	**43**	Hydrogenation, Pd/C (unreduced, 10%), ^{t}BuOH/AcOH 4:1	Per-*O*- and per-*N*-acetylation observed, no aromatic signals (Bn, Bz)

3.5 Re-synthesis of UDP-ManNAc

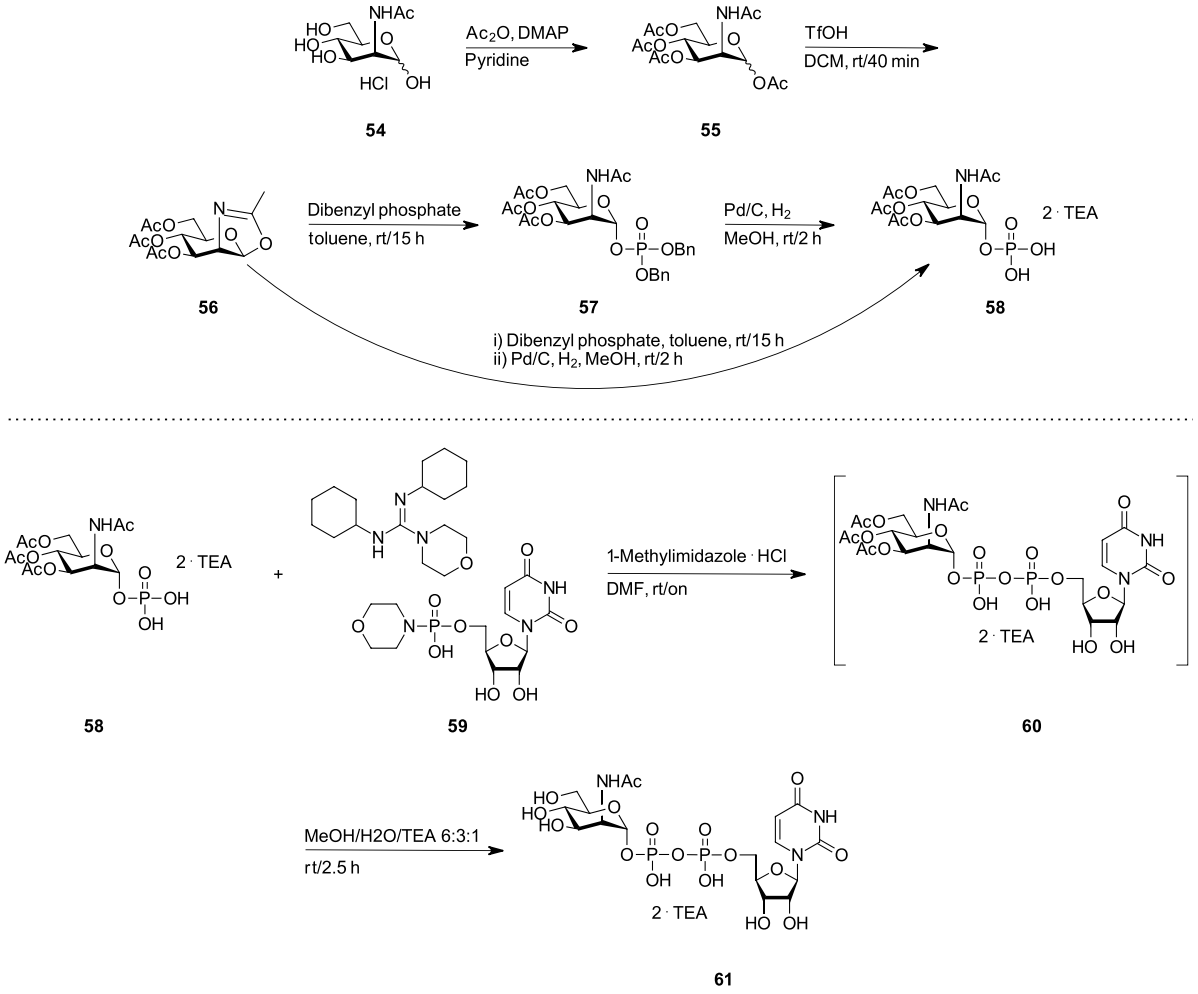

Scheme 38: Synthesis towards UDP-ManNAc [130,217–221]

The re-synthesis of NDP-sugar donor **61** for TagA and CsaB studies (Chapter 2.5) followed published procedures.[130,217–221]

N-Acetyl-D-mannosamine hydrochloride **54** was per-acetylated to give **55**.[130] The treatment of **55** with triflic acid yielded the corresponding oxazoline **56**.[218] As phosphotriester **57** was labile towards hydrolysis during isolation *via* column chromatography, the one-pot procedure of phosphorylation and subsequent hydrogenolysis afforded directly the phosphate **58** as triethylamine salt.[217,219] The coupling of **58** with UMP-morpholidate **59** with 1-methylimidazolium hydrochloride in dimethylformamide yielded protected pyrophosphate **60** that was coarsely purified *via* C_{18} flash column chromatography.[217,220,221] Final deprotection in a mixture of methanol/water/triethylamine (6:3:1) afforded UDP-ManNAc **61**.[217] In total, 43 mg of UDP-ManNAc were synthesized for TagA and CsaB studies.

3.6 Summary and outlook

Within this thesis, a synthetic route towards a fully orthogonally protected tetrasaccharide was developed and synthesized that serves as key intermediate for the synthesis of pyruvylated SpaA ligands (target compounds I) and pyrophosphate-linked substrates (target compounds II).

The 3-*O*-benzylation of 4,6-benzylidene-β-D-GlcNClAc-1-OAllyl monosaccharide acceptor was not feasible with various protocols due to the free, inhibiting N-H bond. The bidentate *N*-TCP group was finally compatible with a non-basic benzylation protocol. In total, two monosaccharide acceptors were obtained, 3,6-di-*O*-Bn-GlcNTCP-1-OAllyl and 6-*O*-Bn-GlcNTCP-1-OAllyl.

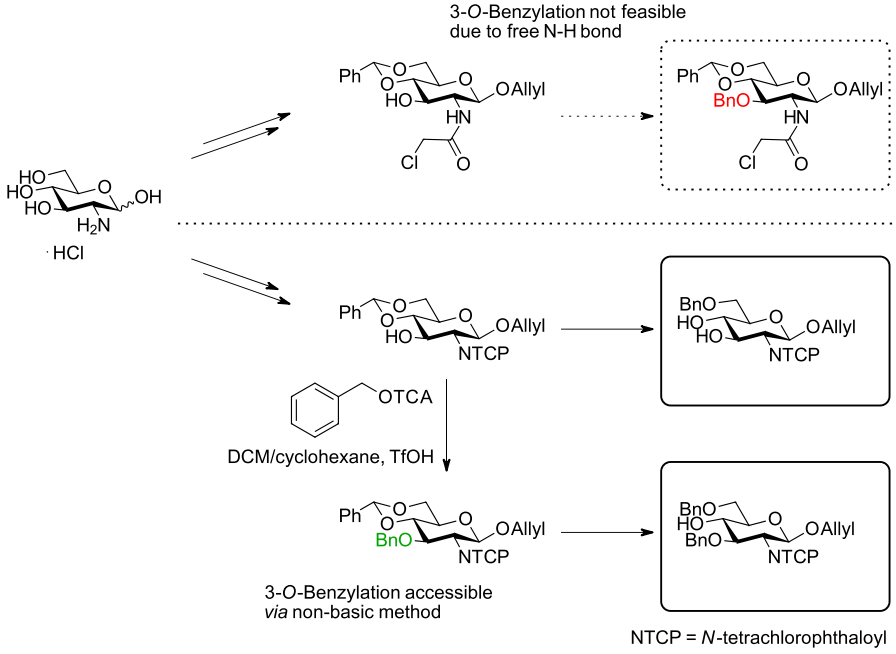

The glycosylation of literature-known 4,6-benzylidene-3-pico-α-D-ManN_3-1-SEt donor with 6-*O*-Bn-GlcNTCP-1-OAllyl acceptor *via* hydrogen-bond mediated aglycon delivery (HAD) pathway surprisingly gave the β-(1→3) regioisomer and not the desired β-(1→4) product – even in presence of the sterically bulky *N*-TCP group.

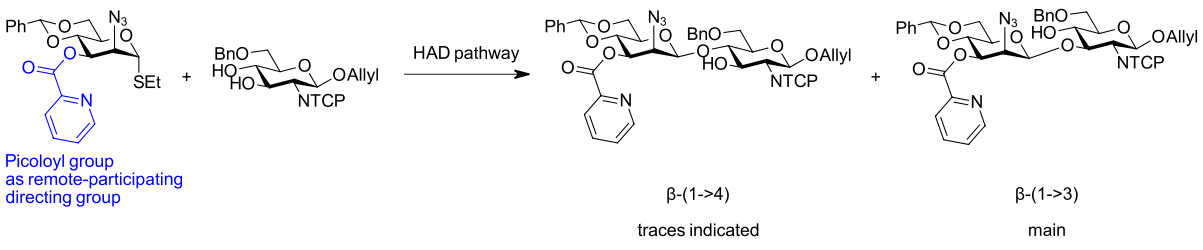

The glycosylation of 4,6-benzylidene-3-pico-α-D-ManN$_3$-1-SEt donor with 3,6-di-*O*-Bn-GlcNTCP-1-OAllyl acceptor *via* HAD pathway gave 25% yield of the desired β-linked disaccharide (α/β 1:2). To the best of my knowledge, this is the first diastereoselective approach *via* HAD pathway to construct the challenging β-D-ManNAc-(1→4)-GlcNAc glycosidic bond.

The basic nature of the donors picoloyl group and the low 4-OH group nucleophilicity of the 3,6-di-*O*-Bn-GlcNTCP-1-OAllyl acceptor complicated the reaction. An acid-free silver triflate promoter solution in toluene (stored over silver oxide) and very high glycosylation temperatures of 50-55 °C afforded the disaccharide. The use of novel charged thiourea hydrogen-bond-donor catalysts may provide a circumvention under mild conditions against the acid-quenching nature of the picoloyl group (*Chem. Sci.*, 2022, **13**, 1600 – 1607).

Due to incompatibility of anomeric allyl group deprotection with any transition metal-based protocol, the picoloyl group of the disaccharide was replaced by a benzoyl group. This allowed allyl group deprotection and synthesis of the *N*-phenyl trifluoroacetimidate disaccharide donor, conveniently starting from the disaccharide acceptor.

The 2+2 glycosylation of disaccharide donor and acceptor gave 61% yield of the desired β-linked tetrasaccharide as key intermediate. The corresponding α-linked glycoside was not observed. Surprisingly, an unusual glycal tetrasaccharide as elimination side product was obtained with 21% yield. The NMR data revealed β-elimination of the *N*-TCP group and nucleophilic attack of the acceptor to form either a 1-*O*- or 2-*O*-glycal, but the data is not conclusive on the anhydro regioisomery.

Azide group deprotection of the key intermediate *via* reduction and *N*-acetylation gave irreproducible results and significant byproduct formation with various procedures. The best result was obtained *via* hydrogenation/hydrogenolysis with excess of unreduced palladium (8 bar/4 days) and subsequent peracetylation. According to ^{1}H NMR analysis, pre-dominantly one compound was isolated *via* flash column chromatography, and two *N*-acetyl- and several *O*-acetyl-signals were observed in the spectrum. The aromatic signals were all gone (Bn, Bz) and the allyl group was reduced to the propyl group.

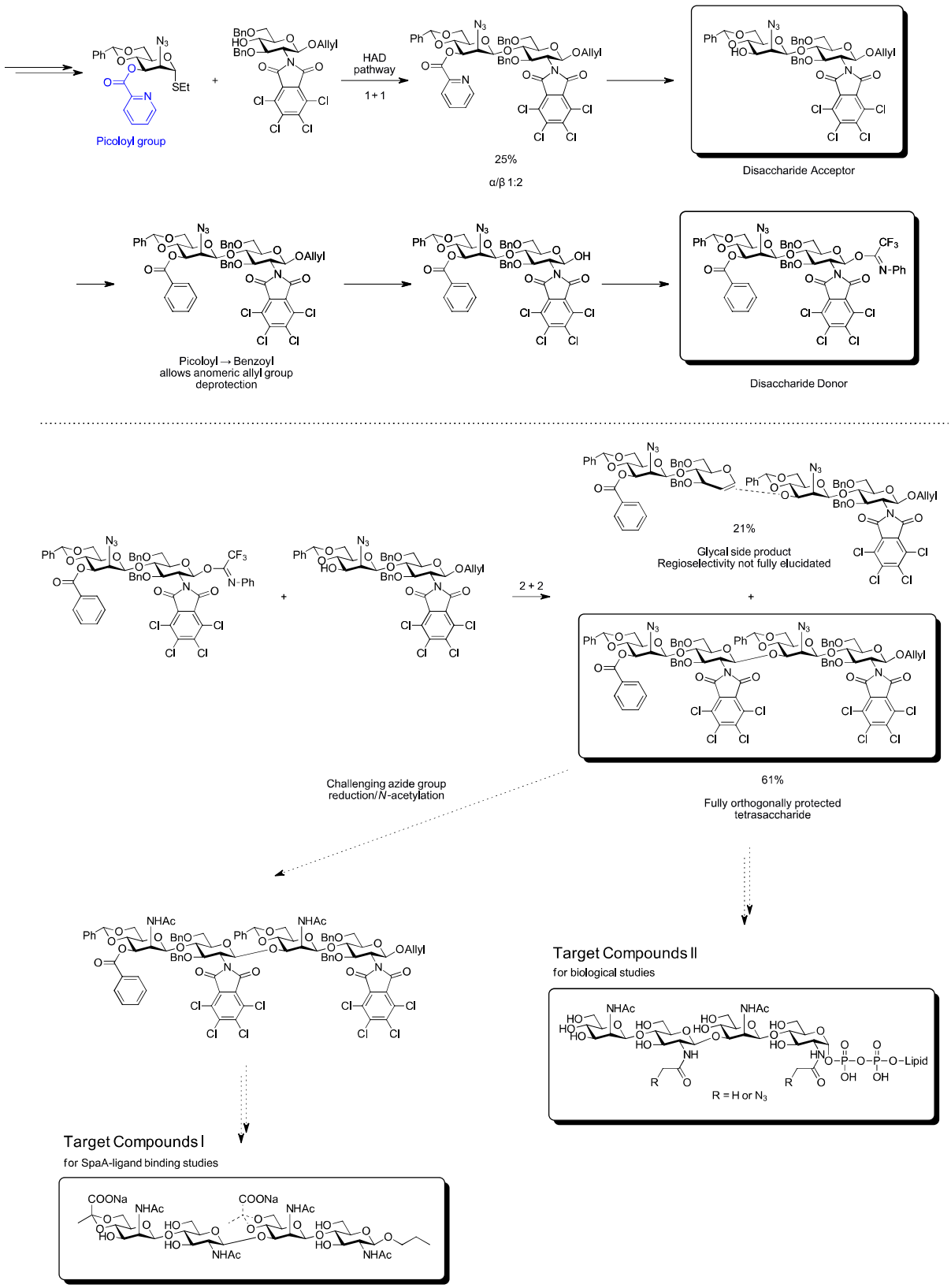

Deprotection and pyruvate installation

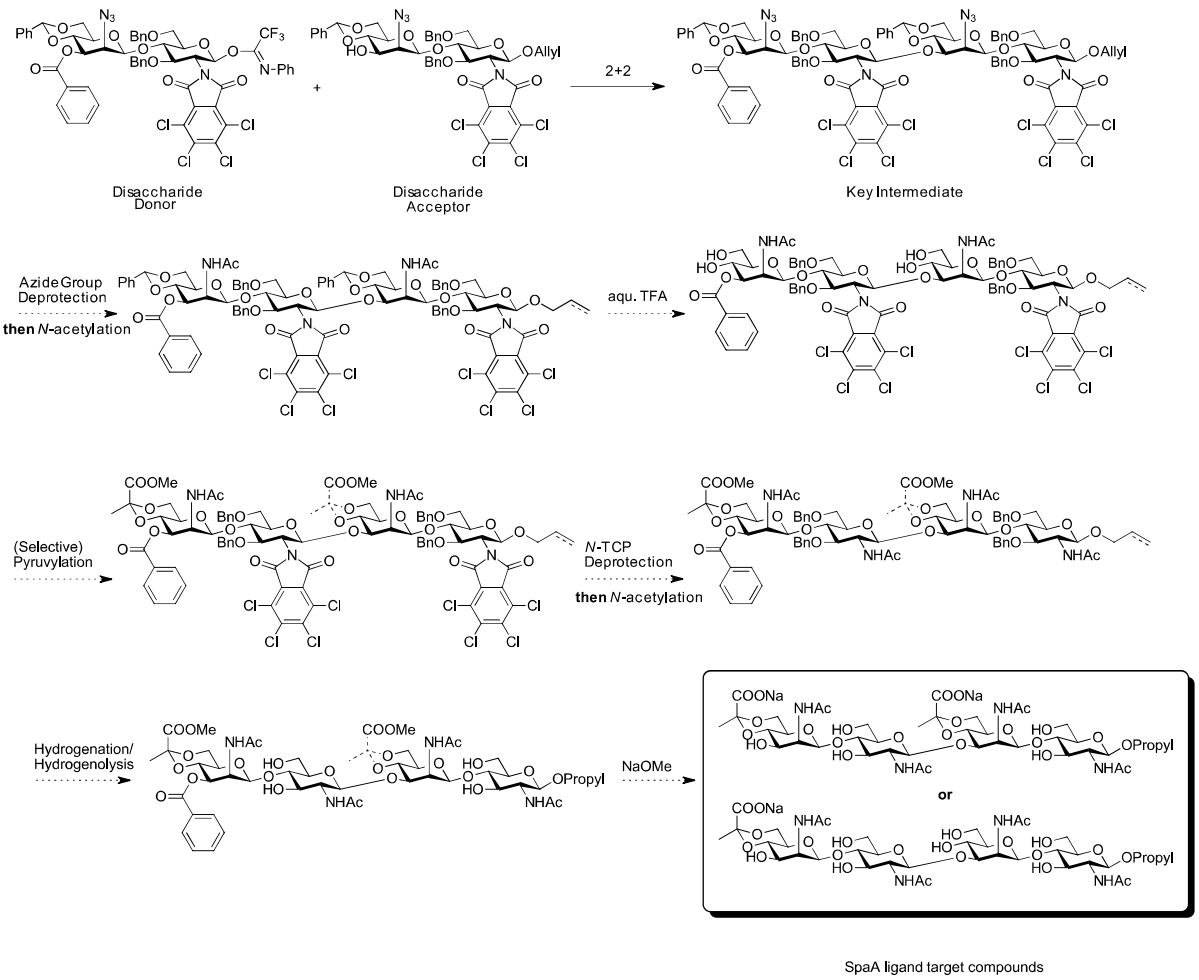

The planned deprotection of the key intermediate towards the SpaA ligand target compounds includes azide group deprotection, followed by *N*-acetylation. Preliminary test reactions on azide group deprotection have been conducted as described. Depending on the chosen protocol, the allyl group will be reduced to the propyl group in case of hydrogenolysis/hydrogenation. The benzylidene groups will be cleaved *via* acidic treatment. The selective pyruvylation, tuned *via* stoichiometry, might give access to the terminal and full pyruvylated compounds. *N*-TCP group deprotection and *N*-acetylation affords the equatorial *N*-acetyl groups. Final deprotections *via* hydrogenation/hydrogenolysis and Zemplen deacylation gives the target compounds.

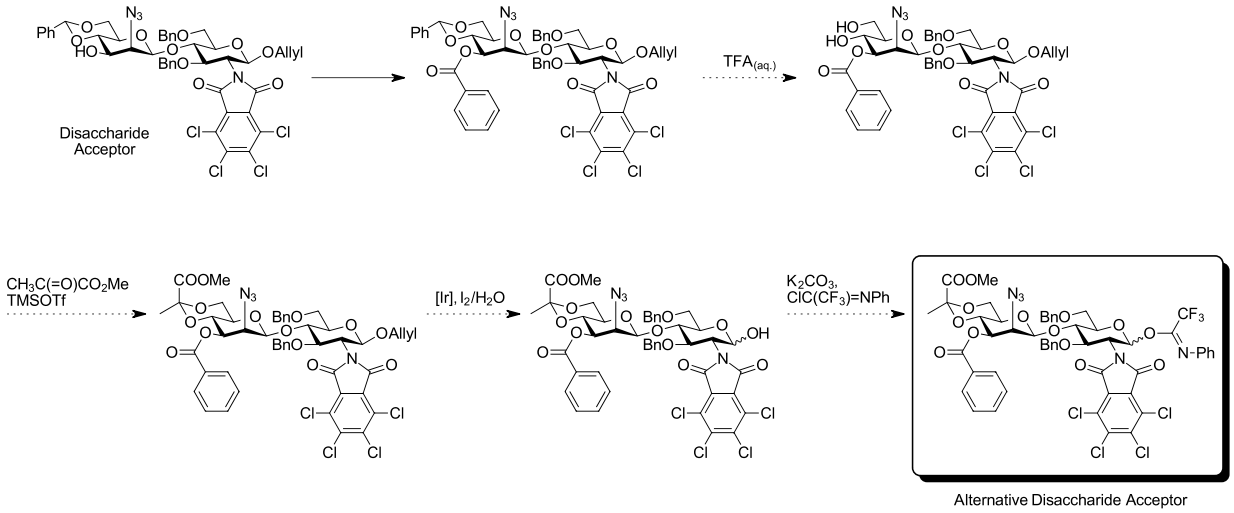

In case that the selective terminal pyruvylation is not feasible, an alternative disaccharide donor, already equipped with a protected pyruvate, might serve as circumvention.

UDP-ManNAc (43 mg) was re-synthesized for biological studies. The elaborated combination of flash reverse-phase column chromatography, anion-exchange chromatography, HILIC prep-HPLC and size-exclusion chromatography was necessary to afford the NDP-sugar donor with high purity. The pyrophosphate coupling mediated by 1-methylimidazolium hydrochloride in dimethylformamide vastly decreased the reaction time from several days to 15 hours as opposed to stirring solely in pyridine in absence of any Lewis/Brønsedt acid.

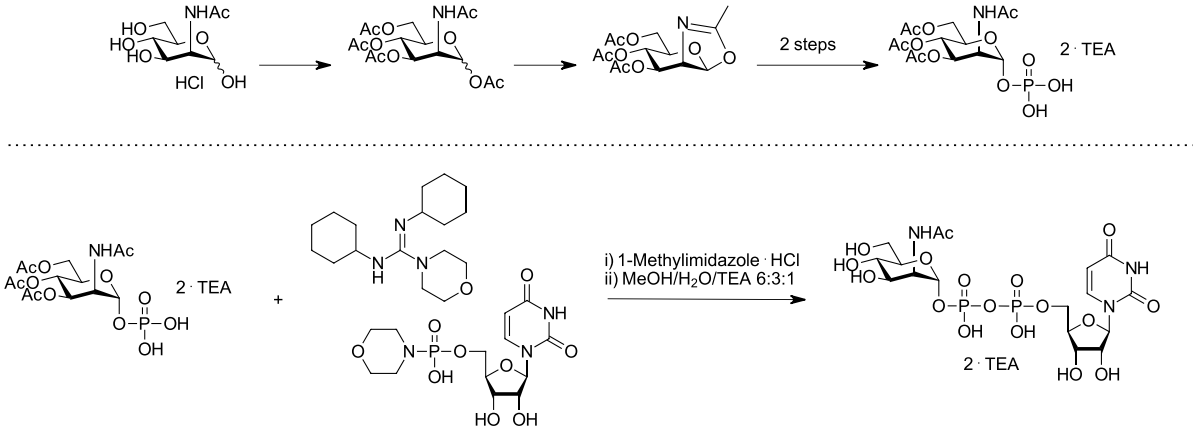

UDP-ManNAc was used as a donor substrate with synthetic GlcNAc-PP-UndPh as acceptor in a one-pot reaction sequence with TagA and CsaB to afford a pyruvylated disaccharide monomer precursor.

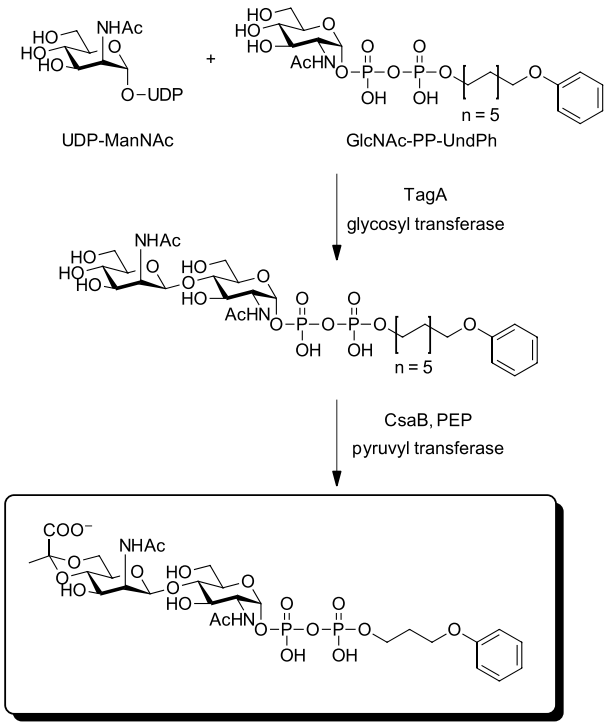

One-pot reaction sequence utilizing TagA and CsaB to yield a pyruvylated pyrophosphate-linked disaccharide repeat unit precursor

4 General schemes

4.1 Synthesis towards monosaccharide donor **4**

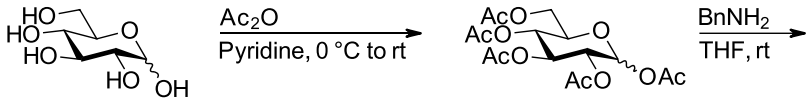

1 **2**

94%

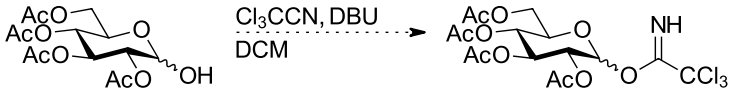

3 **4**

69%

4.2 Synthesis towards monosaccharide acceptor **15**

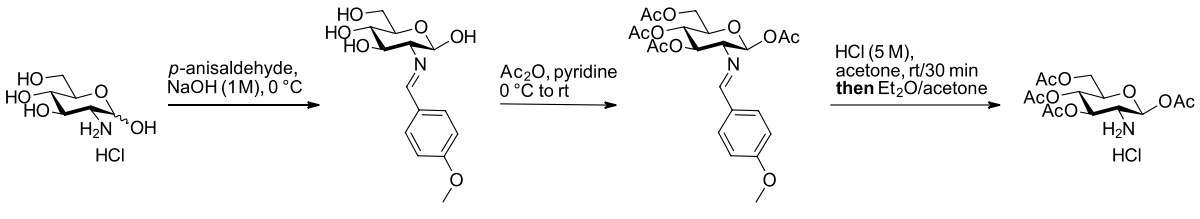

5 **6** **7** **8**

79% 90% 91%

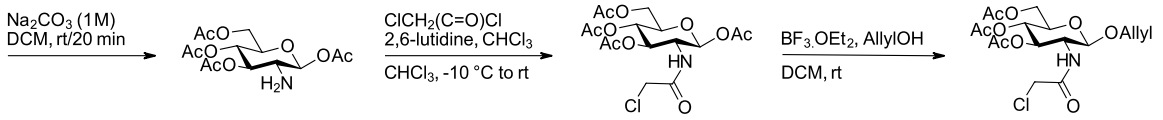

9 **10** **11**

84% 93% 48%

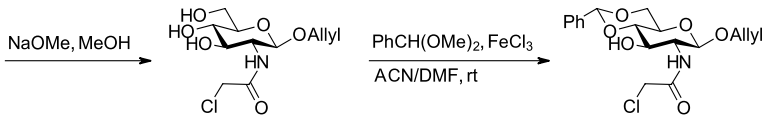

12 **13**

99% 82%

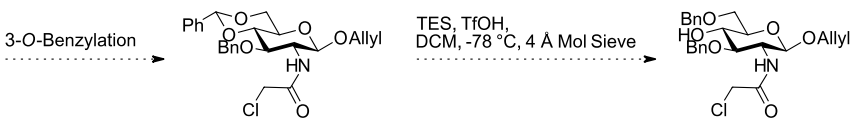

14 **15**

4.3 Synthesis of monosaccharide donor **22**

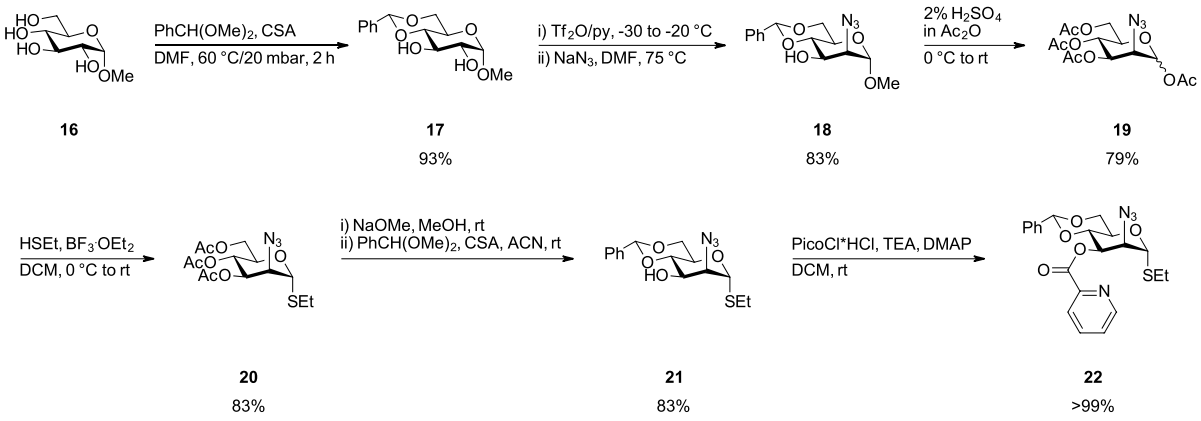

16 → **17** 93% → **18** 83% → **19** 79%

20 83% → **21** 83% → **22** >99%

4.4 Synthesis of monosaccharide acceptors **28** and **30**

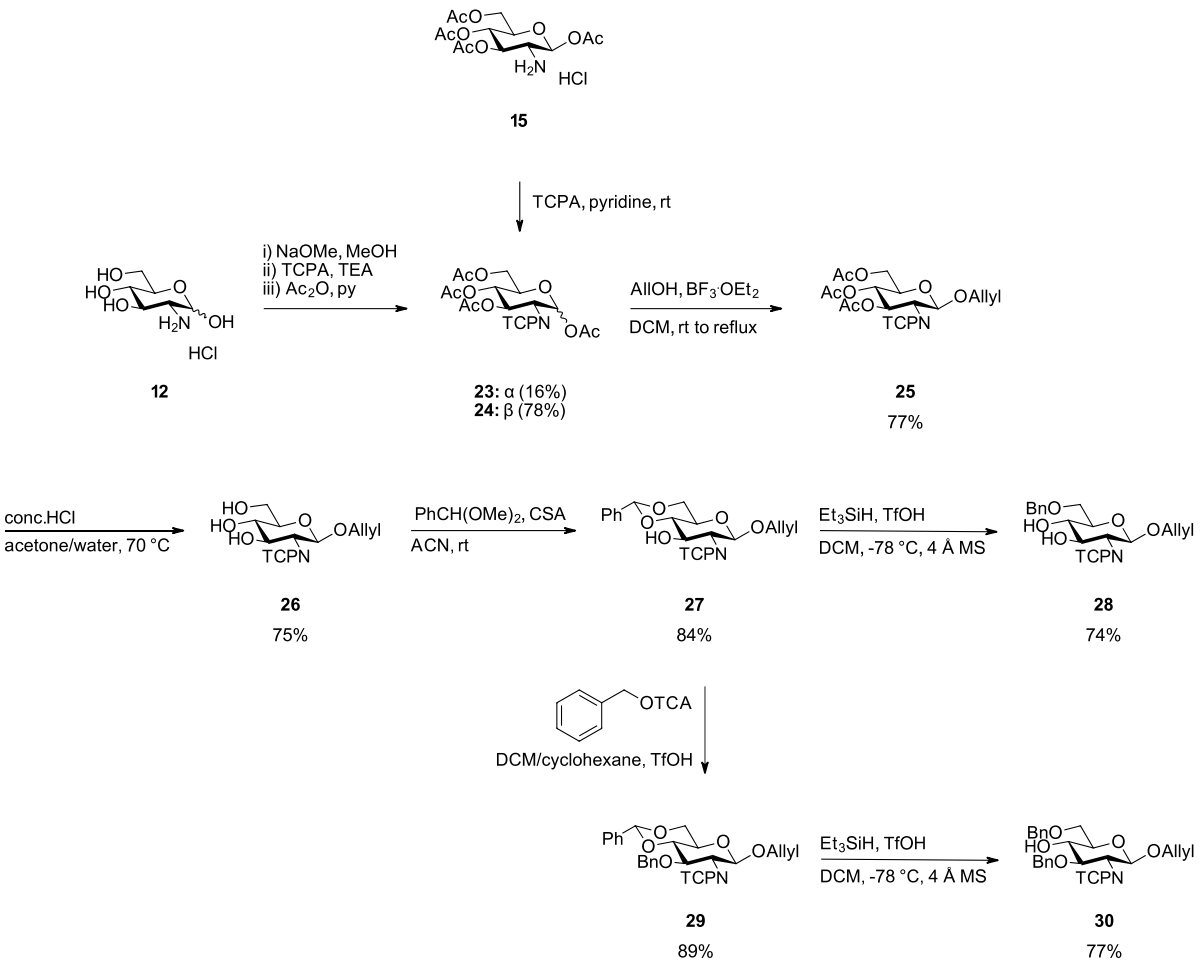

15 → **12** → **23:** α (16%), **24:** β (78%) → **25** 77%

26 75% → **27** 84% → **28** 74%

29 89% → **30** 77%

4.5 1+1 Glycosylation to disaccharide **31a**

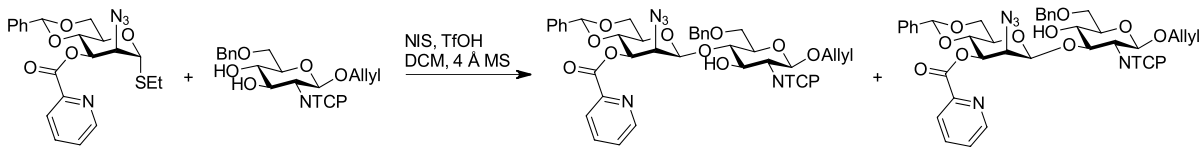

22 **28** **31** traces inidcated *via* LC-MS **31a** 40%

4.6 1+1 Glycosylation to disaccharide **32**

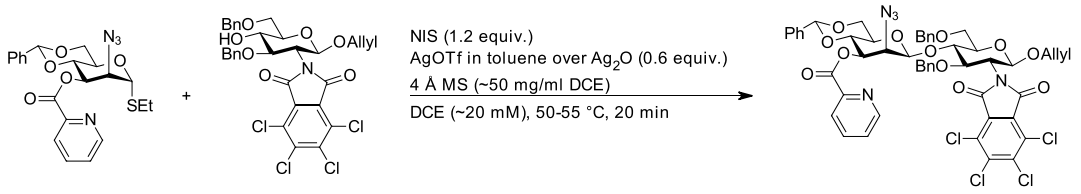

22 **30** **32** 25% α/β 1:2

4.7 Synthesis of disaccharide donor **37** and acceptor **42**

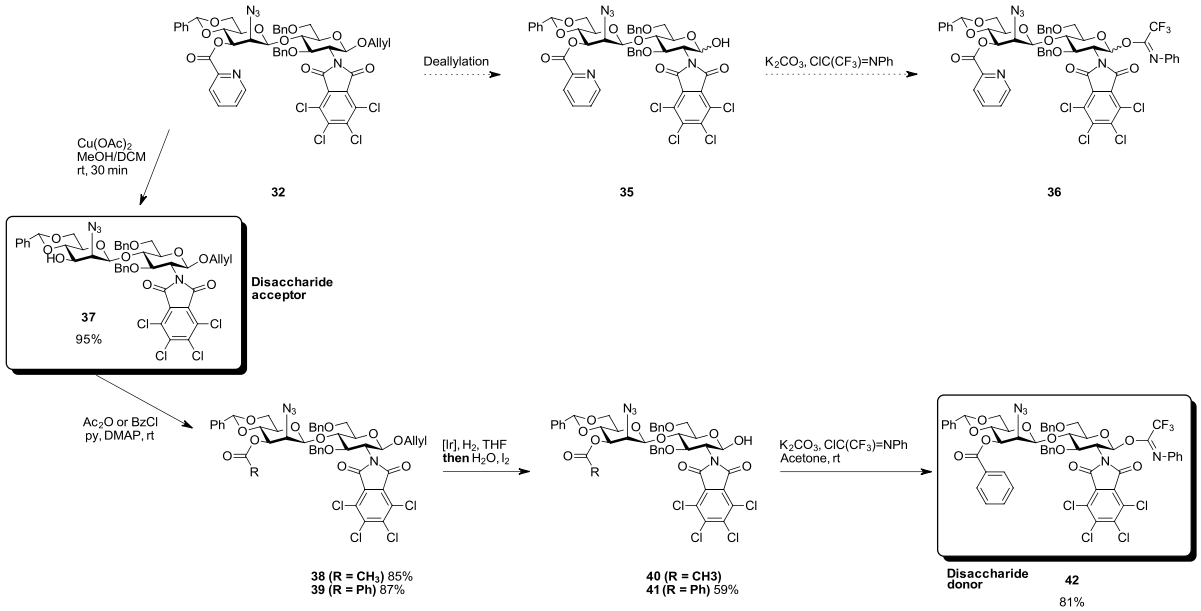

4.8 2+2 Glycosylation to **43**

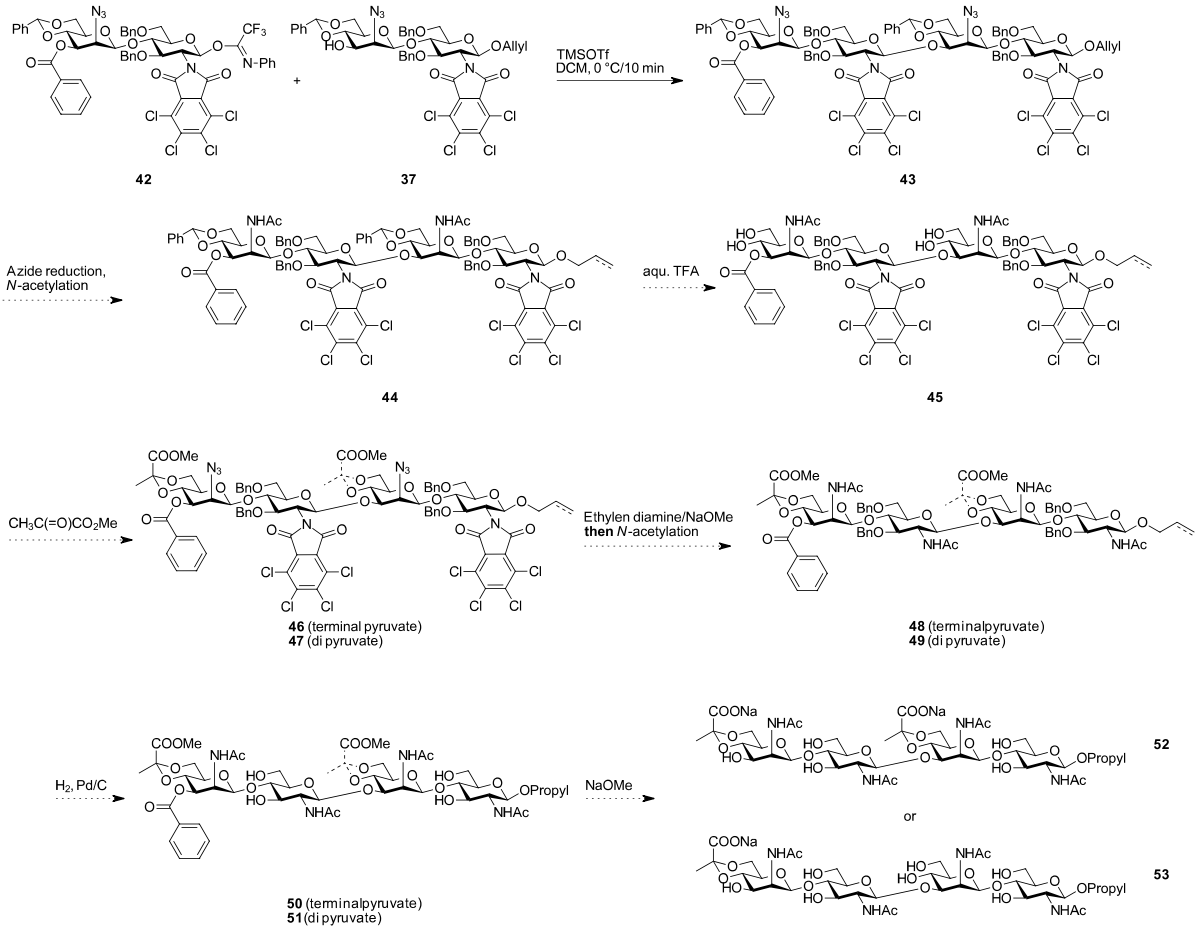

42 **37** **43**

44 **45**

46 (terminal pyruvate)
47 (di pyruvate)

48 (terminalpyruvate)
49 (di pyruvate)

50 (terminalpyruvate)
51 (di pyruvate)

52

53

4.9 Re-synthesis of UDP-ManNAc

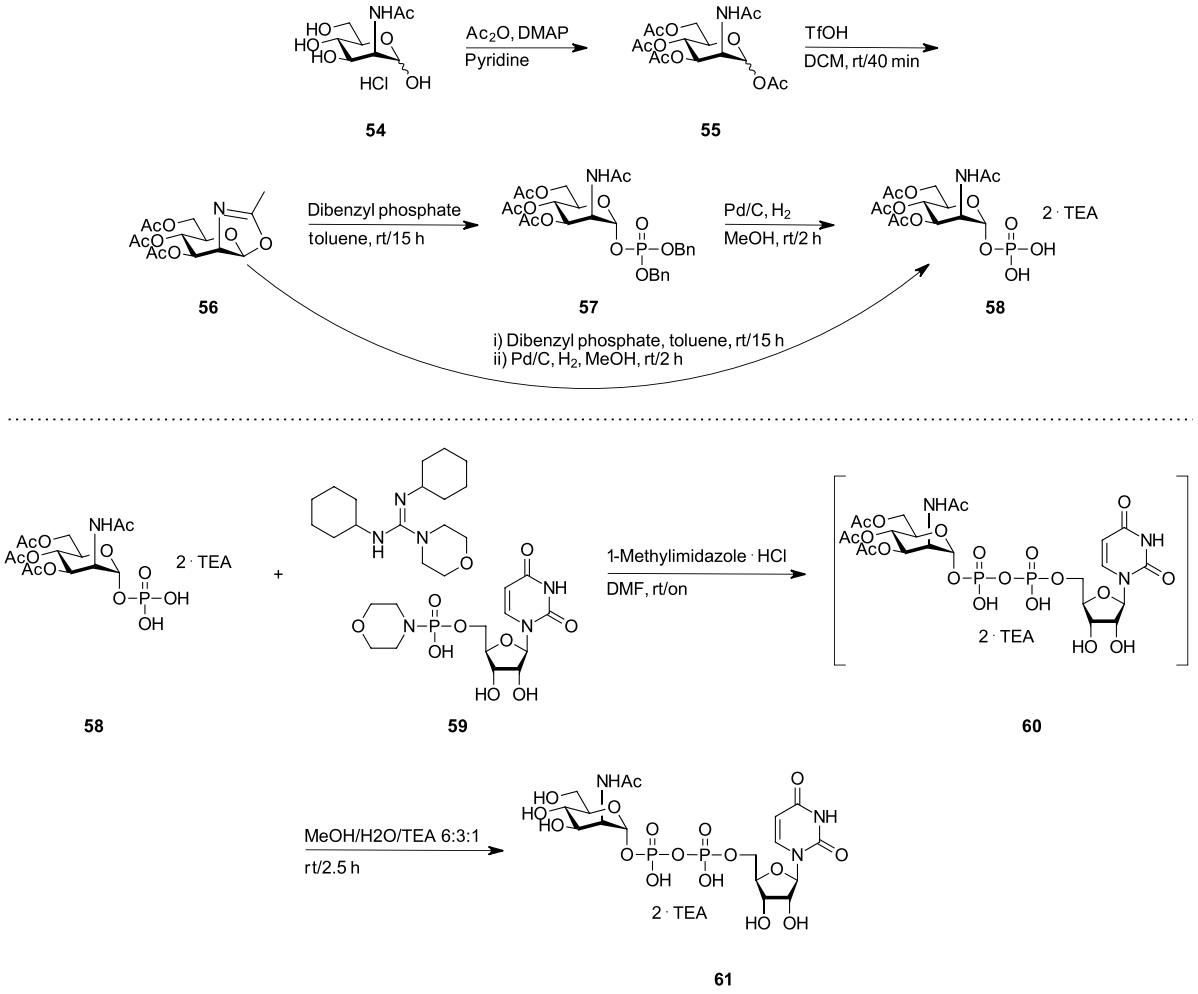

4.10 Biological studies with TagA and CsaB

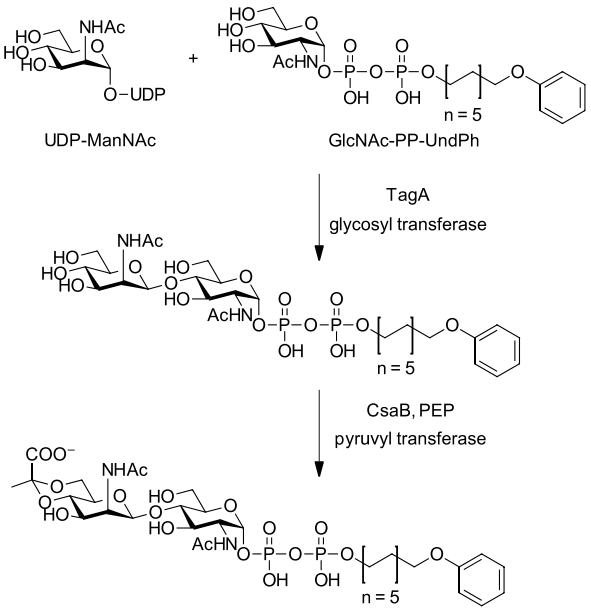

5 Experimental Part

5.1 General remarks

Chemicals were purchased from commercial suppliers and used without further purification, unless noted otherwise. Solvents were dried over 4 Å molecular sieves (3 Å for methanol) or were purchased in dry form. The water content was analyzed *via* Karl Fischer titration using a Mitsubishi Moisture Meter CA-21.

Molecular sieves (3 or 4 Å, spherical or powdered) for dry solvents and reactions were activated at 300 °C/0.002 mbar in a Kugelrohr apparatus (Büchi Glass Oven B-580) for at least 2 hours or were heated up to 500 °C at least twice at <0.5 mbar with a heat gun.

The resin DOWEX 50WX8 (hydrogen form) was washed and regenerated prior to use *via* treatment with hydrochloric acid (3 M), water and dry methanol.

Organic solvents were removed in *vacuo* at 40 °C using rotary evaporators. Aqueous solutions were removed *via* vacuum concentration (LABCONCO® Refrigerated CentriVap® Concentrator) and freeze drying (CHRIST A 2-4 LSCbasic).

NMR spectra were recorded at 297 K in the solvent indicated, with Bruker Avance III 600 (600.22 MHz for ^{1}H, 150.93 MHz for ^{13}C) and Bruker AVIII-HD (300 MHz) instruments employing standard software provided by the manufacturer. ^{1}H- and ^{13}C-NMR spectra in $CDCl_3$ were referenced to tetramethylsilane (TMS, $\delta = 0$ ppm). Spectra in CD_2Cl_2 and MeOD-d4 were referenced to TMS by calibration with the residual organic solvent signal. ^{1}H spectra in D_2O were referenced *via* external calibration to sodium 3-(trimethylsilyl)propane-1-sulfonate in dioxane or phosphoric acid in D_2O. ^{13}C-spectra in D_2O were referenced to dioxane.[222] Assignments were supported by ^{1}H-^{1}H-COSY, ^{1}H-^{13}C-HSQC, ^{1}H-^{13}C-HMBC, CLIP-HSQC[175] and NOESY data. The carbohydrate rings in polysaccharides were labeled with capital letters starting with A from the non-reducing end to the reducing end.

LC-MS analysis was performed on HILIC (SeQuant™ ZIC®-HILIC 150x4.6 mm, 3.5 µm, 100 Å), C_4 (Jupiter 5u C18 300 A) and C_{18} (ZORBAX Eclipse XDB-C18, 4.6x150 mm, 5 µm) columns using a Shimadzu LC10 system with Shimadzu 2020 mass spectrometer and Alltech ELSD 3300 (drift tube temperature: 60°C, receiver gain: 2).

Thin-layer chromatography was performed on pre-coated TLC-plates SIL G-25/UV_{254} with glass support from Macherey-Nagel. High-performance thin-layer chromatography was performed on HPTLC Silica gel 60 F254 with concentrating zone with glass support from Merck. The spots were visualized *via* UV-fluorescence and/or standard staining reagents (anisaldehyde, ninhydrin, vanillin, potassium permanganate) at 250 °C on a heating plate.

Automated column chromatography was performed on Büchi (MPLC), Interchim PuriFlash® 4/25 (Flash and preparative HPLC system) and Amersham Pharmacia Biotech ÄKTA explorer P-900 systems (FPLC). Normal-phase flash chromatography was performed on silica gel PuriFlash IR-50SI (40-60 µm) and pre-packed Interchim SI-S-2G/6 and SI-S-500/6. Normal-phase preparative HPLC was performed on YMC-Pack SIL-06 (250x10.0 mml.D. S-5 µm, 6 nm) with a preceding YMC Guard Cartridge (SIL, 10x10 mml.D., SI-5 µm, 6 nm). HILIC preparative HPLC was performed on a SeQuant® ZIC®-HILIC (5 µm, 200 Å, 250x10 mm). Size-exclusion chromatography was performed on Bio-Gel® P-2 material. Anion-exchange chromatography was performed on Dowex® 1X8 HCO_3^- form material (manual) or BIO-RAD Bio-Scale™ Mini Macro-Prep® High Q Cartridge (FPLC).

Optical rotation was determined in the solvent indicated and measured on an Anton Paar MCP 100 polarimeter.

ESI-HRMS data was obtained on an Agilent Technologies 6230 LC TOF MS instrument.

5.2 Synthetic procedures

5.2.1 Penta-*O*-acetyl-α-D-glucopyranose (**2**)

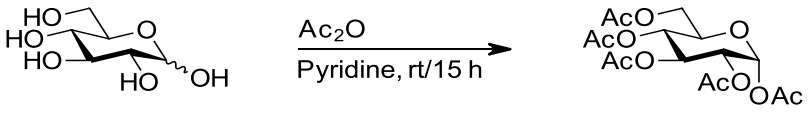

$C_6H_{12}O_6$
180.156 amu

1

$C_{16}H_{22}O_{11}$
390.338 amu

2

To a solution of D-glucose **1** (8.00 g, 44.4 mmol, 1.00 equiv.) in pyridine (dry, 100 ml) was added acetic anhydride (40.72 ml, 430.74 mmol, 9.70 equiv.) at ambient temperature. Monitoring *via* TLC (toluene/ethyl acetate 3:1) indicated full consumption of the starting material after 15 h at ambient temperature. The reaction was quenched by an excess of methanol, followed by addition of saturated aqueous sodium bicarbonate at 0 °C. The crude material was isolated *via* extraction with ethyl acetate (3x). The combined organic layers were washed with aqueous copper(II) sulfate (10 vol%), water and brine. Drying over magnesium sulfate and removal of the volatiles in *vacuo* afforded 19.75 g of a greenish crude oil. Purification *via* automated column chromatography using silica gel (Büchi MPLC, 800 g of silica gel, liquid loading with dichloromethane, applying a gradient of ethyl acetate in toluene from 25% to 50%) afforded 94% (16.37 g) of **2** as a colorless powder.

The analytical data is in accordance to the literature.[130,223]

5.2.2 2,3,4,6-Tetra-*O*-acetyl-D-glucopyranose (**3**)

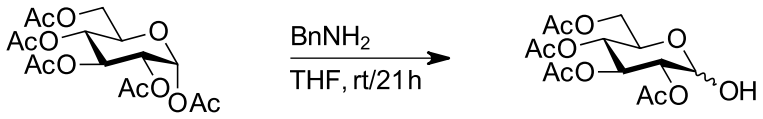

$C_{16}H_{22}O_{11}$
390.338 amu

2

$C_{14}H_{20}O_{10}$
348.302 amu

3

To a solution of **2** (5.00 g, 12.81 mmol, 1.00 equiv.) in tetrahydrofuran (dry, 50 ml) was added benzyl amine (2.09 ml, 19.21 mmol, 1.50 equiv.) at ambient temperature. Monitoring *via* TLC (toluene/ethyl acetate 1:1) indicated full consumption after 21 hours. The reaction was quenched by addition of water/ethyl acetate 5:1. The layers were separated and the aqueous phase was re-extracted with ethyl acetate (3x). The combined organic layers were washed with aqueous sodium bisulfate (2 M) and brine. Drying over magnesium sulfate and removal of the volatiles in *vacuo* afforded 6.62 g of a dark oil. Purification *via* automated column chromatography using silica gel (Büchi MPLC, 320 g of silica gel, liquid loading with dichloromethane, isocratic elution with toluene/ethyl acetate 1:1) afforded 69% (2.94 g) of **3**.

The analytical data is in accordance to the literature.[130]

5.2.3 2-Deoxy-2-[[(4-methoxyphenyl)methylene]amino]-β-D-glucose (**6**)

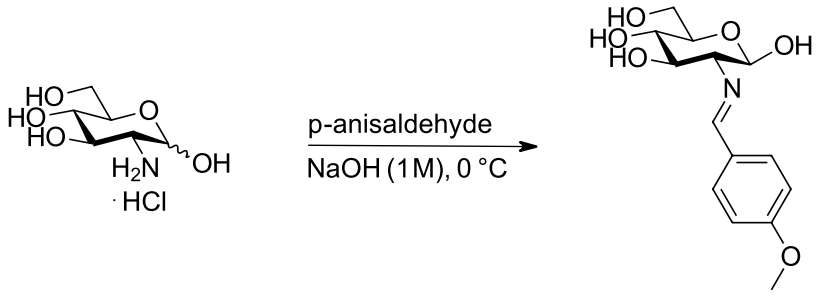

$C_6H_{14}ClNO_5$
215.631 amu

5

$C_{14}H_{19}NO_6$
297.303 amu

6

To a solution of **5** (15.00 g, 69.56 mmol, 1.00 equiv.) in aqueous sodium hydroxide (1 M, 75 ml, 1.08 equiv.) was slowly added *p*-anisaldehyde (8.79 ml, 72.35 mmol, 1.04 equiv.) at 0 °C. The reaction was stirred for 1 hour at 0 °C to yield a colorless precipitate. The precipitate was collected *via* filtration and was washed with cold water, cold ethanol and diethyl ether. Drying in *vacuo* afforded 79% (16.40 g) of **6** as a colorless powder.

The analytical data is in accordance to the literature.[131,133]

5.2.4 1,3,4,6-Tetra-*O*-acetyl-2-deoxy-2-[[(4-methoxyphenyl)methylene]amino]-β-D-glucopyranose (**7**)

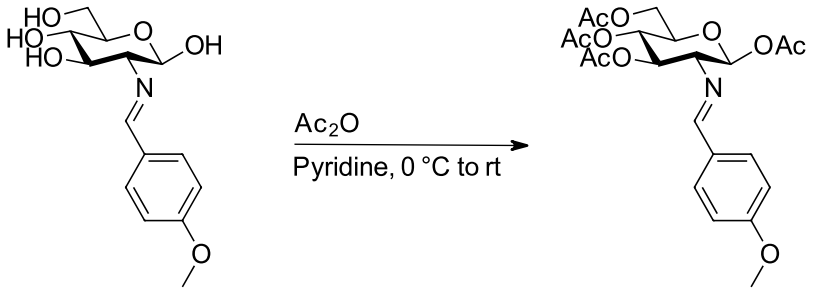

$C_{14}H_{19}NO_6$
297.303 amu

6

$C_{22}H_{27}NO_{10}$
465.449 amu

7

To a suspension of **6** (13.15 g, 44.23 mmol, 1.00 equiv.) in pyridine (anhydrous, 50 ml) was slowly added acetic anhydride (33.45 ml, 0.35 mol, 8.00 equiv.) at 0 °C. The suspension was slowly warmed to ambient temperature. Monitoring *via* TLC (dichloromethane/methanol 10:1 + 1 drop of triethylamine) indicated full consumption of the starting material after 15 hours. The reaction was quenched by slow addition of methanol (15 ml, > 8 equiv.) at 0 °C, followed by addition of saturated aqueous sodium bicarbonate after 10 minutes. The crude material was isolated *via* extraction with ethyl acetate (3x). The combined organic layers were washed with water and brine. Drying over magnesium sulfate and removal of the volatiles in *vacuo* afforded 90% (18.43 g) of **7**.

The analytical data is in accordance to the literature.[131]

5.2.5 1,3,4,6-Tetra-*O*-acetyl-2-amino-2-deoxy-β-D-glucopyranose hydrochloride (**8**)

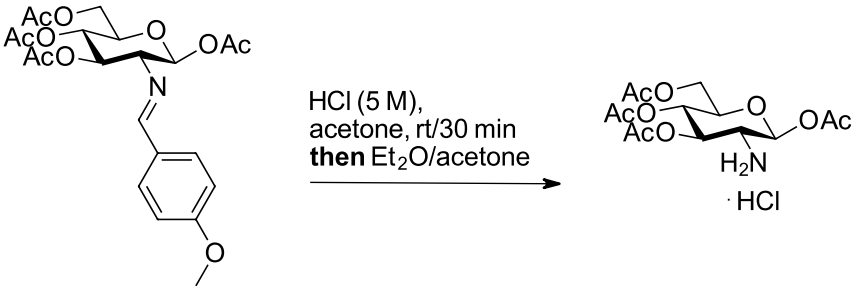

$C_{22}H_{27}NO_{10}$
465.449 amu

7

$C_{14}H_{22}ClNO_9$
383.777 amu

8

To a solution of **7** (4.68 g, 10.06 mmol, 1.00 equiv.) in acetone (60 ml) was added HCl (5 M in water, 2.33 ml, 11.67 mmol, 1.16 equiv.) to afford an off-white precipitate. Addition of diethyl ether yielded an even dispersion. The suspension was stirred for roughly 1 hour at ambient temperature. The solid material was isolated *via* filtration and the filtration residue was washed with cold diethyl ether. Removal of the volatiles in *vacuo* afforded 91% (3.5 g) of **8** as a colorless powder.

The analytical data is in accordance to the literature.[132]

5.2.6 1,3,4,6-Tetra-*O*-acetyl-2-amino-2-deoxy-β-D-glucopyranose (**9**)

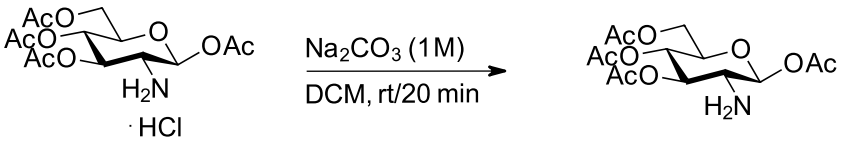

$C_{14}H_{22}ClNO_9$
383.777 amu

8

$C_{14}H_{21}NO_9$
347.317 amu

9

To a suspension of **8** (300 mg, 0.78 mmol, 1.00 equiv.) in dichloromethane (5 ml) was added sodium carbonate (1 M in water, 5 ml, 5 mmol, 6.41 equiv.) at ambient temperature. The reaction was stirred for 1 hour at ambient temperature to afford a clear biphasic system. The layers were separated, and the aqueous phase was re-extracted with dichloromethane (3x). The combined organic layers were washed with water. Drying over magnesium sulfate and removal of the volatiles in *vacuo* afforded 84% (229 mg) of **9** as a colorless powder.

The analytical data is in accordance to the literature.[132]

5.2.7 1,3,4,6-Tetra-*O*-acetyl-2-chloroacetamido-2-deoxy-β-D-glucopyranose (**10**)

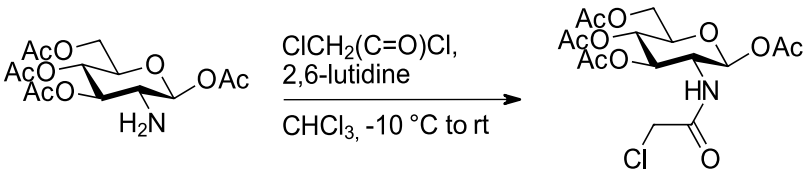

$C_{14}H_{21}NO_9$
347.317 amu

9

$C_{16}H_{22}ClNO_{10}$
423.798 amu

10

To a solution of **9** (700 mg, 2.02 mmol, 1.00 equiv.) and 2,6-lutidine (0.39 ml, 3.33 mmol, 1.65 equiv.) in chloroform (dry, 4 ml) was added chloroacetyl chloride (0.18 ml, 2.26 mmol, 1.12 equiv.) at -10 °C. The reaction was slowly warmed to 0 °C. Monitoring *via* TLC (toluene/ethyl acetate 2:1 and dichloromethane/methanol 5:1) indicated full consumption of the starting material after 2 hours. The reaction was quenched by addition of water. The layers were separated, and the aqueous phase was re-extracted with dichloromethane (3x). The combined organic layers were washed with saturated aqueous sodium bicarbonate and water. Drying over magnesium sulfate and removal of the volatiles in *vacuo* afforded 1.14 g of a crude solid material. Purification *via* manual column chromatography using silica gel (40 g of silica gel, liquid loading with dichloromethane, isocratic elution with toluene/ethyl acetate 2:1) afforded 93% (795 mg) of **10** as a colorless powder.

The analytical data is in accordance to the literature.[133]

5.2.8 Allyl 3,4,6-tri-*O*-acetyl-2-chloroacetamido-2-deoxy-β-D-glucopyranoside (**11**)

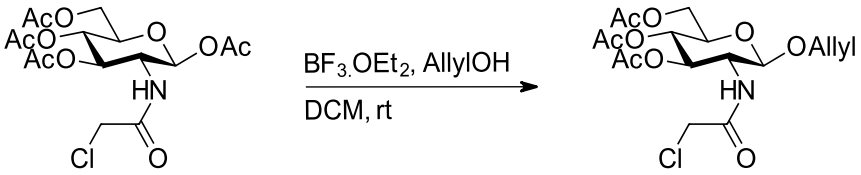

$C_{16}H_{22}ClNO_{10}$
423.798 amu

10

$C_{17}H_{24}ClNO_9$
421.825 amu

11

To a solution of **10** (986 mg, 2.33 mmol, 1.00 equiv.) in dichloromethane (dry, 5.5 ml) was added molecular sieves (3 Å) at ambient temperature. The suspension was stirred for 5 min at ambient temperature. Allylic alcohol (0.79 ml, 11.63 mmol, 5.00 equiv.) was added at 5 °C, followed by dropwise-addition of boron trifluoride diethyl etherate (2.87 ml, 23.27 mmol, 10.00 equiv.). The reaction was stirred for 1 hour at 5 °C, before the reaction was slowly warmed to ambient temperature. Monitoring *via* TLC (HPTLC, toluene/ethyl acetate 1:1) indicated full consumption of the starting material after 21 hours. The reaction was quenched by addition of water (4 ml) at 0 °C. The organic phase was diluted with dichloromethane and the layers were separated. The aqueous phase was re-extracted with dichloromethane (3x). The combined organic layers were washed with water (2x), saturated aqueous sodium bicarbonate (2x) and brine. Drying over magnesium sulfate and removal of the volatiles in *vacuo* afforded 86% (845 mg) of a crude material as an off-white solid. Purification *via* automated column chromatography using silica gel (Interchim PuriFlash® 4/25, liquid loading with 1.5 ml of dichloromethane, column: F040, 9 ml/fraction, collection *via* threshold: 5 mV, applying a gradient of ethyl acetate in toluene from 50% to 70% in 10 CV) afforded 48% (472 mg) of **11** as a colorless solid.

The analytical data is in accordance to the literature.[134]

5.2.9 Allyl 2-chloroacetamido-2-deoxy-β-D-glucopyranoside (**12**)

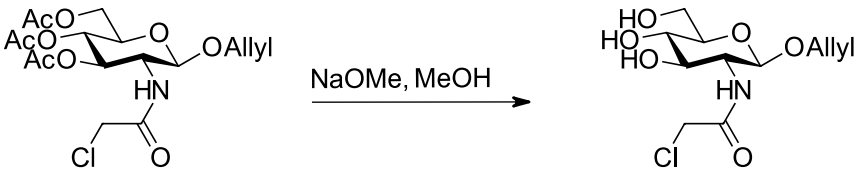

$C_{17}H_{24}ClNO_9$
421.825 amu

11

$C_{11}H_{18}ClNO_6$
295.715 amu

12

To a solution of **11** (640 mg, 1.52 mmol, 1.00 equiv.) in methanol (anhydrous, 3 ml) was added sodium methoxide (0.1 M in methanol, 10.00 ml, 1.00 mmol, 0.66 equiv.). The reaction was stirred at ambient temperature for 1 hour and then at 5 °C for 20 hours. Monitoring *via* TLC (dichloromethane/methanol 6:1) indicated full consumption of the starting material. The reaction was quenched by addition of Dowex® 50WX8 until pH 7. The solid material was removed *via* filtration over Celite® with methanol. Removal of the volatiles in *vacuo* afforded 505 mg of a crude material as an off-colorless solid. Coarse purification *via* flash filtration using silica gel (chloroform/methanol 10:1) afforded 99% (443 mg) of **12** as a colorless solid.

The analytical data is in accordance to the literature.[224]

5.2.10 Allyl 2-chloroacetamido-4,6-*O*-benzylidene-2-deoxy-β-D-glucopyranoside (**13**)

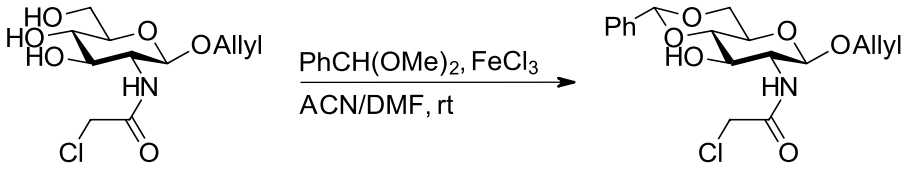

$C_{11}H_{18}ClNO_6$
295.715 amu

12

$C_{18}H_{22}ClNO_6$
383.821 amu

13

To a suspension of molecular sieves (powdered, 4 Å) in acetonitrile (dry, 1.5 ml) was added **12** (100 mg, 0.34 mmol, 1.00 equiv.) at ambient temperature, followed by benzaldehyde dimethyl acetal (76 µl, 0.51 mmol, 1.50 equiv.) and ferric(III) chloride (anhydrous, catalytic amount) after 5 minutes. To the yellow suspension was added dimethylformamide (anhydrous, 0.9 ml) after 30 minutes. Additional benzaldehyde dimethyl acetal (51 µl, 0.34 mmol, 1.00 equiv.) was added after 15 hours. Monitoring *via* TLC (chloroform/methanol 6:1) indicated full consumption after 20 hours at ambient temperature. The reaction was quenched by addition of saturated aqueous sodium bicarbonate and ethyl acetate. The solid material was removed *via* filtration over Celite® with ethyl acetate. The layers were separated and the aqueous phase was re-extracted with ethyl acetate (3x). The combined organic layers were washed with water and brine. Drying over magnesium sulfate and removal of the solvent in *vacuo* afforded 64% (83 mg) of **13** as a colorless solid that was used as obtained. Further extraction of the filtration residue with dichloromethane yielded additional 38% (49 mg) of crude material. Purification *via* manual column chromatography using silica gel (2.7 g of silica gel, dry loading with silica gel, isocratic elution with toluene/ethyl acetate 2:1 and dichloromethane/methanol 4:1) afforded another 18% (23 mg) of **13** as a colorless solid (combined yield of 82%).[225]

R_f = 0.57 in dichloromethane/methanol 9:1

^{1}H NMR (600 MHz, $CDCl_3$): δ = 7.50 – 7.48 (m, 2 H, Ar), 7.39 – 7.35 (m, 3 H, Ar), 6.78 (d, *J* = 5.7 Hz, 1 H, 3-OH), 5.93 – 5.86 (m, 1 H, CH_2CH=CH_2), 5.56 (s, 1 H, PhC*H*), 5.34 – 5.24 (m, 2 H, CH_2CH=CH_2), 4.77 (d, $J_{1,2}$ = 8.3 Hz, 1 H, H_1), 4.39 – 4.35 (m, 2 H, H_6, CH_2CH=CH_2), 4.22 – 4.18 (m, 1 H, H_3), 4.13 – 4.09 (m, 3 H, CH_2CH=CH_2,

ClC*H*$_2$(C=O)), 3.81 (t, *J* = 10.3 Hz, 1 H, H$_{6'}$), 3.61 – 3.57 (m, 2 H, H$_2$, H$_4$), 3.53 – 3.49 (m, 1 H, H$_5$) ppm

^{13}C-APT NMR (150 MHz, CDCl$_3$): δ = 133.35 (CH$_2$*C*H=CH$_2$), 129.41, 128.46, 126.44, 118.61 (CH$_2$CH=*C*H$_2$), 102.15 (Ph*C*H), 99.66 (C$_1$), 81.65 (C$_4$), 70.95 (C$_3$), 70.51 (*C*H$_2$CH=CH$_2$), 68.72 (C$_6$), 66.46 (C$_5$), 59.15 (C$_2$), 42.80 (Cl*C*H$_2$(C=O)) ppm

ESI-TOF-MS: calc.: [M+H]$^+$ = 384.1208 m/z; measured.: [M+H]$^+$ = 384.1215 m/z; Δ = -1.74

5.2.11 Methyl 4,6-*O*-benzylidene-α-D-glucopyranoside (**17**)

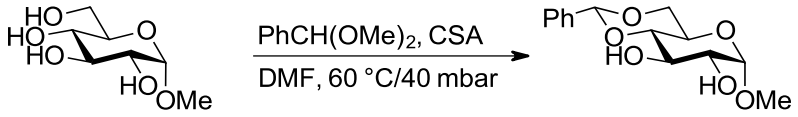

$C_7H_{14}O_6$
194.182 amu

16

$C_{14}H_{18}O_6$
282.288 amu

17

To a suspension of **16** (9.70 g, 49.95 mmol, 1.00 equiv.) in dimethylformamide (anhydrous, 40 ml) was added benzaldehyde dimethyl acetal (7.50 ml, 49.95 mmol, 1.00 equiv.) and DL-camphorsulfonic acid (104 mg, 0.45 mmol, 0.01 equiv.) at ambient temperature. The reaction was performed on a rotary evaporator at 60 °C/20 mbar to afford a homogeneous mixture. Monitoring *via* TLC (dichloromethane/methanol 10:1) indicated full consumption of the starting material after 2 hours. The reaction was quenched by addition of triethylamine. Removal of the volatiles in *vacuo* afforded a colorless oil. The residual dimethylformamide was removed *via* repeated azeotropic distillation with *n*-heptane, followed by extraction between chloroform and water. The organic layer was dried with magnesium sulfate and removal of the volatiles in *vacuo* afforded 93% (13.09 g) of **17** as a colorless powder.

The analytical data is in accordance to the literature.[153,154]

5.2.12 Methyl 2-azido-4,6-*O*-benzylidene-2-deoxy-α-D-mannopyranoside (**18**)

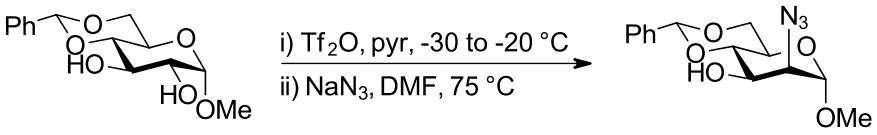

$C_{14}H_{18}O_6$
282.288 amu

17

$C_{14}H_{17}N_3O_5$
307.301 amu

18

To a solution of **17** (7.30 g, 25.87 mmol, 1.00 equiv.) and pyridine (4.17 ml, 51.73 mmol, 2.00 equiv.) in dichloromethane (anhydrous, 86 ml) was added trifluoromethanesulfonic anhydride (27.16 ml, 27.16 mmol, 1.05 equiv.) at -30 °C. The reaction was stirred at -30 °C for 1.5 hours and then 1 hour at -20 °C. Monitoring *via* TLC (*n*-hexane/ethyl acetate 1:1) indicated full consumption of **17** after 2.5 hours. The reaction was quenched by addition of water at ambient temperature. The layers were separated and the aqueous phase was re-extracted with dichloromethane (3x). Drying over magnesium sulfate and removal of the volatiles in *vacuo* afforded a red crude oil. The crude material was dried in *vacuo*.

To a solution of crude triflate in dimethylformamide (anhydrous, 100 ml) was added sodium azide (8.42 g, 0.13 mol, 5.00 equiv.) at ambient temperature. The mixture was stirred at 75 °C. Monitoring *via* TLC (*n*-hexane/ethyl acetate 5:1) indicated full consumption of the triflate after 15 hours. The volatiles were removed in *vacuo* and the residue was dissolved in dichloromethane/water. The layers were separated and the aqueous phase was re-extracted with dichloromethane (3x). The combined organic layers were dried over magnesium sulfate and removal of the volatiles in *vacuo* afforded 10.1 g of a crude dark oil. Purification *via* automated column chromatography using silica gel (Interchim PuriFlash® 4/25, dry loading with silica gel in F080, column: F080, 30 ml/fraction, 40 ml/min, applying a gradient of ethyl acetate in toluene from 0% to 10% in 9 CV) afforded 83% (6.6 g) of **18** as an off-colorless oil.

The analytical data is in accordance to the literature.[157,158]

5.2.13 1,3,4,6-Tetra-*O*-acetyl-2-azido-2-deoxy-D-mannopyranose (**19**)

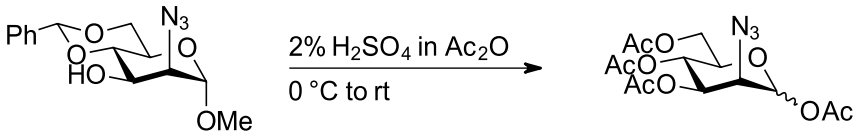

$C_{14}H_{17}N_3O_5$
307.301 amu

18

$C_{14}H_{19}N_3O_9$
373.315 amu

19

To a solution of **18** (1.74 g, 5.66 mmol, 1.00 equiv.) in acetic anhydride (74 ml, 170 mmol, 30 equiv.) was added sulfuric acid (0.60 ml, 10.76 mmol, 1.90 equiv.) at 0 °C. The reaction was warmed up to ambient temperature. Monitoring *via* TLC (toluene/ethyl acetate 3:1) indicated full consumption of the starting material after 3 hours. The reaction was reverse-quenched by slow addition of the reaction mixture into a mixture of saturated aqueous sodium bicarbonate/ethyl acetate. The layers were separated and the aqueous phase was re-extracted with ethyl acetate (3x). Drying over magnesium sulfate and removal of the volatiles in *vacuo* afforded roughly 5 g of a crude orange oil. Purification *via* automated column chromatography using silica gel (Interchim PuriFlash® 4/25, dry loading with 10 g silica gel in F040, column: F080, 12 ml/fraction, 34 ml/min, applying a gradient of ethyl acetate in toluene from 0% to 30% in 8 CV then isocratic) afforded 79% (1.54 g) of **19**.

The analytical data is in accordance to the literature.[158]

5.2.14 Ethyl 3,4,6-tri-*O*-acetyl-2-azido-2-deoxy-1-thio-α-D-mannopyranoside (**20**)

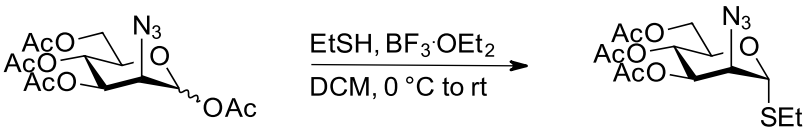

$C_{14}H_{19}N_3O_9$
373.315 amu

19

$C_{14}H_{21}N_3O_7S$
375.400 amu

20

To a solution of **19** (5.52 g, 14.78 mmol, 1.00 equiv.) and ethane thiol (2.19 ml, 29.56 mmol, 2.00 equiv.) in dichloromethane (dry, 110 ml) was added boron trifluoride etherate (7.80 ml, 62.07 mmol, 4.20 equiv.) at 0 °C. The reaction was slowly warmed to ambient temperature overnight. Monitoring *via* TLC (HPTLC, toluene/ethyl acetate 5:1) indicated full consumption of the starting material after 15 hours. The reaction was quenched by addition of pyridine and the crude reaction mixture was washed with water. The volatiles were removed in *vacuo*. Purification *via* manual column chromatography using silica gel (250 g of silica gel, liquid loading in toluene/ethyl acetate 5:1, 10-30 ml/fraction, isocratic elution with toluene/ethyl acetate 5:1) afforded 83% (4.63 g) of **20** (α/β 6:1).

The analytical data is in accordance to the literature.[158]

5.2.15 Ethyl 2-azido-4,6-*O*-benzylidene-2-deoxy-1-thio-α-D-mannopyranoside (**21**)

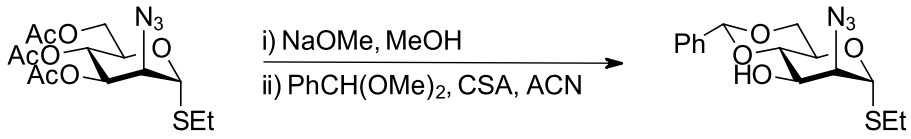

$C_{14}H_{21}N_3O_7S$
375.400 amu

20

$C_{15}H_{19}N_3O_4S$
337.397 amu

21

To a solution of **20** (4.63 g, 12.33 mmol, 1.00 equiv.) in methanol (SeccoSolv®, 50 ml) was added sodium methoxide (commercial, 0.5 M in methanol, 2.10 ml, 1.05 mmol, 0.09 equiv.). Monitoring *via* TLC (dichloromethane/methanol 10:1) indicated full consumption of the starting material after 21 hours. The reaction was acidified by addition of Dowex® 50WX8 H^+ form to pH ~6. The solid material was removed *via* filtration over Celite® with methanol. Removal of the volatiles and drying in *vacuo* afforded an off-colorless solid crude material.

To a suspension of the crude material in acetonitrile (dry, 100 ml) were added benzaldehyde dimethyl acetal (3.71 ml, 24.66 mmol, 2.00 equiv.) and DL-camphorsulfonic acid (286 mg, 1.23 mmol, 0.10 mmol) at ambient temperature to yield a homogenous solution. Monitoring *via* TLC (dichloromethane/methanol 10:1) indicated full consumption of the intermediate after 15 hours. The reaction was quenched by addition of triethylamine. Removal of the solvent in *vacuo* afforded 6 g of a crude oil. Purification *via* automated column chromatography using silica gel (Interchim PuriFlash® 4/25, dry loading with 21 g of silica gel in F080, column: F200, 30 ml/fraction, 60 ml/min, collect *via* threshold: 10 mV, applying a gradient of ethyl acetate in toluene from 0% to 10% within 10 CV) afforded 83% (3.46 g) of **21**.

The analytical data is in accordance to the literature.[123]

5.2.16 Ethyl 2-azido-4,6-*O*-benzylidene-2-deoxy-3-*O*-picoloyl-1-thio-α-D-mannopyranoside (**22**)

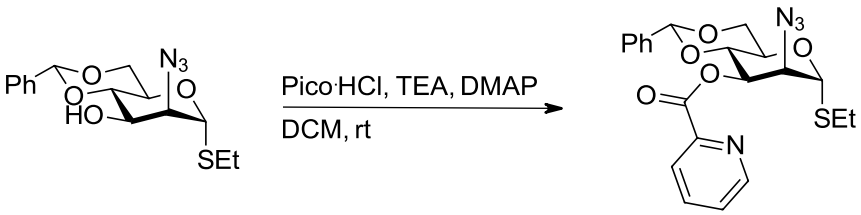

$C_{15}H_{19}N_3O_4S$
337.397 amu

21

$C_{21}H_{22}N_4O_5S$
442.490 amu

22

To a solution of **21** (3.46 g, 10.26 mmol, 1.00 equiv.) in dichloromethane (dry, 150 ml) were added triethylamine (dry, 14.31 ml, 0.10 mol, 10.00 equiv.), 4-dimethylaminopyridine (cat.) and 2-pyridine carbonyl choride hydrochloride (3.84 g, 21.55 mmol, 2.10 equiv.) at ambient temperature. Monitoring *via* TLC (toluene/ethyl acetate 4:1) indicated full consumption of the starting material after 15 hours at ambient temperature. The reaction was quenched by addition of water and after 30 minutes, the layers were separated. The aqueous phase was re-extracted with dichloromethane (3x) and the combined organic layers were dried over magnesium sulfate. Removal of the volatiles in *vacuo* afforded 7 g of a crude material. Purification *via* manual column chromatography using silica gel (210 g of silica gel, liquid loading with dichloromethane, ~15-30 ml/fraction, applying a slow gradient of ethyl acetate in *n*-hexane from 25% to 33%) afforded >99% (4.89 g) of **22** as a pale-yellow wax.

The analytical data is in accordance to the literature.[123]

5.2.17 1,3,4,6-Tetra-*O*-acetyl-2-deoxy-2-(tetrachlorophthalimido)-α-D-glucopyranose (**23**)

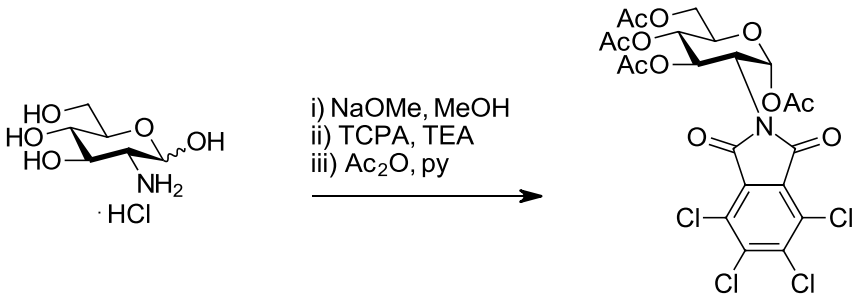

$C_6H_{14}ClNO_5$
215.631amu

5

$C_{22}H_{19}Cl_4NO_{11}$
615.193amu

23

A suspension of **5** (5.00 g, 23.19 mmol, 1.00 equiv.) in sodium methoxide (1 M in methanol, 23.19 ml, 23.19 mmol, 1.00 equiv.) was stirred for 2 hours at ambient temperature. To the suspension was added tetrachloro phthalic acid anhydride (3.46 g + 3.98 g, 26.03 mmol, 1.12 equiv.) in two portions at an interval of 45 minutes. Monitoring *via* LC-MS (column: HILIC, profile: 95%→40% in 17 min) indicated full consumption of the starting material after 22 hours at ambient temperature. The solid material was removed *via* filtration and the volatiles was removed in *vacuo* to yield a crude brownish foam. To a solution of the crude material in pyridine (anhydrous, 50 ml) was slowly added acetic anhydride (32.88 ml, 0.35 mol, 15.00 equiv.) at 0 °C. The reaction was slowly warmed to ambient temperature. Monitoring *via* LC-MS (column: HILIC, profile: 95%→40% in 17 min) indicated full consumption of the intermediate and conversion to the product. The excess of acetic anhydride was quenched by slow addition of methanol (15.95 ml, 0.39 mol, 17.00 equiv.) at 0 °C. The crude reaction was reverse-quenched with saturated aqueous sodium bicarbonate and dichloromethane. The layers were separated and the aqueous phase was re-extracted with dichloromethane (3x). The combined organic layers were washed with water. Drying over magnesium sulfate and removal of the volatiles in *vacuo* afforded 18 g of a crude material. Purification *via* recrystallization from ethanol (abs.) afforded 16% (2.31 g) of **23** as a colorless powder.

The analytical data is in accordance to the literature.[160]

5.2.18 1,3,4,6-Tetra-*O*-acetyl-2-deoxy-2-(tetrachlorophthalimido)-β-D-glucopyranose (**24**)

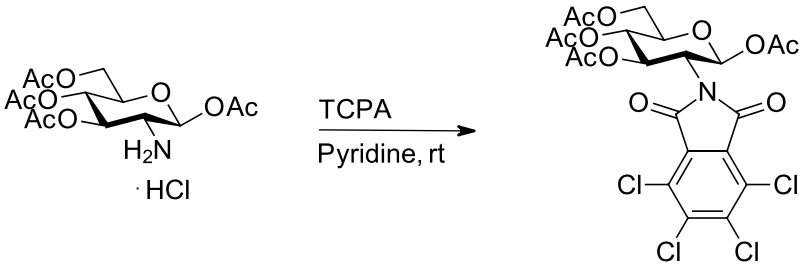

$C_{14}H_{22}ClNO_9$
383.777 amu

8

$C_{22}H_{19}Cl_4NO_{11}$
615.193 amu

24

To a suspension of **8** (468 mg, 1.22 mmol, 1.00 equiv.) in pyridine (dry, 10 ml) was added tetrachlorophthalic anhydride (418 mg, 1.46 mmol, 1.20 equiv.) at ambient temperature. Monitoring *via* LC-MS (column: C_4, profile: 5%→100% in 35min) indicated full consumption of the starting material and conversion to the product after 15 hours. The reaction was quenched by addition of acetic anhydride (0.3 ml) at 0 °C. Removal of the volatiles in *vacuo* afforded an off-colorless crude solid material. Purification *via* dispersion in methanol and filtration afforded 78% (584 mg) of **24** as a colorless powder.

The analytical data is in accordance to the literature.[143]

5.2.19 Allyl 3,4,6-tri-*O*-acetyl-2-deoxy-2-(tetrachlorophthalimido)-β-D-glucopyranoside (**25**)

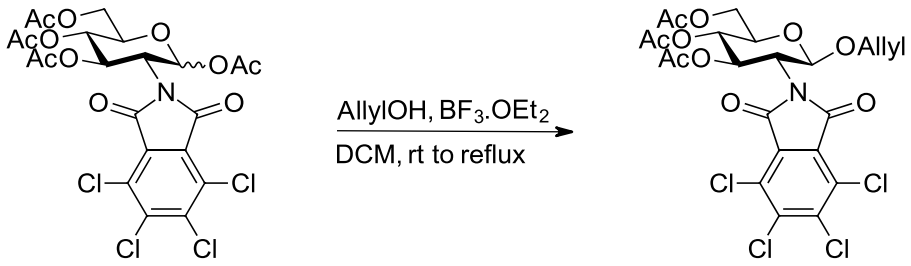

$C_{22}H_{19}Cl_4NO_{11}$
615.193 amu

23 or 24

$C_{23}H_{21}Cl_4NO_{10}$
613.220 amu

25

To a solution of **23** or **24** (5.47 g, 8.89 mmol, 1.00 equiv.) and allylic alcohol (1.82 ml, 26.67 mmol, 3.00 equiv.) in dichloromethane (dry, 50 ml) was slowly added boron trifluoride etherate (6.58 ml, 53.34 mmol, 6.00 equiv.) at 0 °C. The reaction was slowly warmed to ambient temperature. Monitoring *via* TLC (HPTLC, toluene/ethyl acetate 10:1) indicated roughly 50% consumption of the starting material after 15 hours at ambient temperature. Further stirring for 3 hours at reflux temperature gave full consumption. The reaction was quenched by slow addition of pyridine (~15 ml, >20.00 equiv.) at ambient temperature to give a precipitate. The precipitate was removed *via* extraction between water and dichloromethane. Removal of the volatiles in *vacuo* afforded an off-colorless solid crude material. Purification *via* crystallization from methanol afforded 77% (4.20 g) of **25** as a colorless solid material.[226]

R_f = 0.27 in toluene/ethyl acetate 10:1

^{lim}_139_02_600 60-64

^{13}C-APT NMR (150 MHz, $CDCl_3$): δ = 170.80, 170.72, 169.50, 140.77, 133.30 ($CH_2CH=CH_2$), 130.18, 127.16, 118.39 ($CH_2CH=CH_2$), 96.96 (C_1), 72.08 (C_5), 71.15 (C_3), 70.45 ($CH_2CH=CH_2$), 68.92 (C_4), 62.14 (C_6), 55.57 (C_2), 20.90 (CH_3), 20.74 (CH_3), 20.64 (CH_3) ppm

ESI-TOF-MS: calc.: $[M+NH_4]^+$ = 629.0258 m/z; measured.: $[M+NH_4]^+$ = 629.0275 m/z; Δ = -2.66 ppm

$[\alpha]_D^{20}$=+28.4 (*c* 0.7, $CHCl_3$)

5.2.20 Allyl 2-deoxy-2-(tetrachlorophthalimido)-β-D-glucopyranoside (**26**)

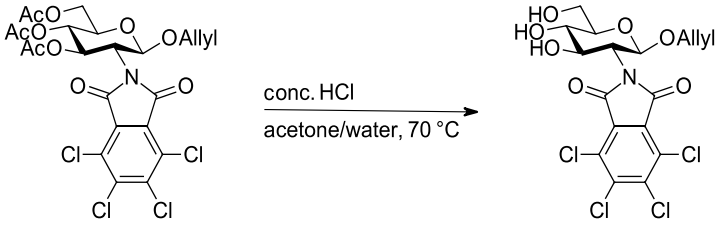

$C_{23}H_{21}Cl_4NO_{10}$
613.220 amu

25

$C_{17}H_{15}Cl_4NO_7$
487.110 amu

26

To a suspension of **25** (6.94 g, 11.32 mmol, 1.00 equiv.) in acetone (150 ml) and water (50 ml) was added hydrochloric acid (37%, 13.59 ml, 0.16 mol, 14.50 equiv.) at ambient temperature. The reaction was stirred at 70 °C to yield a homogeneous reaction mixture. Monitoring *via* TLC (toluene/ethyl acetate 10:1 and dichloromethane/methanol 10:1) indicated full consumption of the starting material after 15 hours. The reaction was roughly concentrated in *vacuo* and the crude material was extracted between saturated aqueous sodium bicarbonate and ethyl acetate. The combined organic layers were dried over magnesium sulfate and removal of the volatiles in *vacuo* afforded a crude brown oil. Purification *via* crystallization from ethyl acetate/*n*-hexane afforded 75% (4.17 g) of **26** as an off-colorless powder.[169]

R_f = 0.33 in toluene/ethyl acetate 10:1

^{1}H NMR (600 MHz, CD_2Cl_2): δ = 5.77 – 5.70 (m, 1 H, CH_2CH=CH_2), 5.20 (d, $J_{1,2}$ = 8.4 Hz, 1 H, H_1), 5.15 – 5.11 (m, 1 H, CH_2CH=CH_2), 5.08 – 5.06 (m, 1 H, CH_2CH=CH_2), 4.32 – 4.23 (m, 2 H, H_3, CH_2CH=CH_2), 4.07 – 4.01 (m, 2 H, H_2, CH_2CH=CH_2), 3.92 – 3.87 (m, 2 H, H_6, $H_{6'}$), 3.68 – 3.65 (m, 2 H, H_4, OH), 3.51 – 3.48 (m, 2 H, H_5, OH), 2.67 (br, 1 H, OH) ppm

^{13}C-APT NMR (150 MHz, CD_2Cl_2): δ = 163.63 (C=O), 140.25, 133.78 (CH_2CH=CH_2), 129.82, 127.43, 117.46 (CH_2CH=CH_2), 97.37 (C_1), 75.46 (C_5), 71.96 (C_4), 71.27 (C_3), 70.25 (CH_2CH=CH_2), 62.07 (C_6), 57.21 (C_2) ppm

ESI-TOF-MS: calc.: $[M+NH_4]^+$ = 502.9941 m/z; measured.: $[M+NH_4]^+$ = 502.9946 m/z; Δ = -1.02 ppm

$[\alpha]_D^{20}$ = -8.3 (*c* 0.2, $CHCl_3$)

5.2.21 Allyl 4,6-*O*-benzylidene-2-deoxy-2-(tetrachlorophthalimido)-β-D-glucopyranoside (**27**)

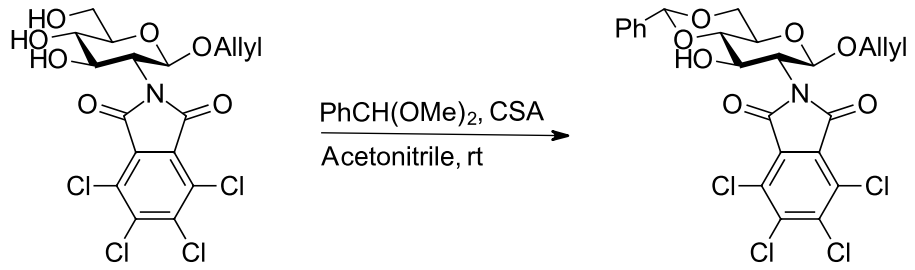

$C_{17}H_{15}Cl_4NO_7$
487.110 amu

26

$C_{24}H_{19}Cl_4NO_7$
575.216 amu

27

To a suspension of **26** (2.14 g, 4.39 mmol, 1.00 equiv.) in acetonitrile (anhydrous, 25 ml) were added benzaldehyde dimethyl acetal (1.32 ml, 8.79 mmol, 2.00 equiv.) and DL-camphorsulfonic acid (catalytic amount) at ambient temperature to yield a homogeneous reaction mixture. Monitoring *via* TLC (toluene/ethyl acetate 20:1 and dichloromethane/methanol 10:1) indicated full consumption of the starting material after 15 hours at ambient temperature. The reaction was quenched by addition of pyridine (0.2 ml). Removal of the volatiles in *vacuo* afforded 4 g of a crude orange oil. Purification *via* automated column chromatography using silica gel (Interchim PuriFlash® 4/25, dry loading with 8 g silica gel in F040, column: F080, 34 ml/min, 10 ml/fraction, collect *via* threshold: 5 mV, applying a gradient of ethyl acetate in *n*-hexane from 0% to 25% in 11 CV) afforded 84% (2.13 g) of **27** as a colorless foam.[227]

R_f = 0.26 in n-hexane/ethyl acetate 4:1

^{1}H NMR (600 MHz, CD_2Cl_2): δ = 7.49 – 7.47 (m, 2 H, Ar), 7.38 – 7.37 (m, 3 H, Ar), 5.78 – 5.71 (CH_2CH=CH_2), 5.58 (s, 1 H, PhC*H*), 5.26 (d, $J_{1,2}$ = 8.5 Hz, 1 H, H_1), 5.18 – 5.14 (m, 1 H, CH_2CH=CH_2), 5.10 – 5.08 (m, 1 H, CH_2CH=C$H_{2'}$), 4.61 – 4.57 (m, 1 H, H_3), 4.39 – 4.36 (m, 1 H, H_6), 4.29 – 4.25 (m, 1 H, CH_2CH=CH_2), 4.21 – 4.17 (dd, $J_{1,2}$ = 8.5 Hz, $J_{2,3}$ = 10.4 Hz, 1 H, H_2), 4.06 – 4.02 (m, 1 H, CH_2CH=CH_2), 3.86 – 3.81 (m, 1 H, $H_{6'}$), 3.64 – 3.59 (m, 2 H, H_4, H_5), 2.56 (d, *J* = 3.5 Hz, 1 H, OH) ppm

^{13}C-APT NMR (150 MHz, CD_2Cl_2): δ = 140.29, 137.34, 133.60 ($CH_2CH=CH_2$), 129.32, 128.32, 127.38, 126.36, 117.60 ($CH_2CH=CH_2$), 101.95 (PhCH), 97.79 (C_1), 82.17 (C_4), 70.28 ($CH_2CH=CH_2$), 68.68 (C_6), 68.41 (C_3), 66.29 (C_5), 57.31 (C_2) ppm

ESI-TOF-MS: calc.: $[M+H]^+$ = 573.9988 m/z; measured.: $[M+H]^+$ = 573.9988 m/z; Δ = 0.01 ppm

$[\alpha]_D^{20}$ = -11.9 (*c* 1.0, $CHCl_3$)

5.2.22 Allyl 6-*O*-benzyl-2-deoxy-2-(tetrachlorophthalimido)-β-D-glucopyranoside (**28**)

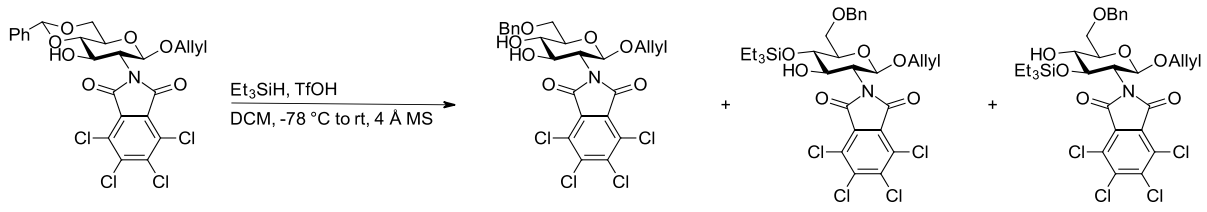

$C_{24}H_{19}Cl_4NO_7$
575.216 amu

27

$C_{24}H_{21}Cl_4NO_7$
577.232 amu

28

$C_{30}H_{35}Cl_4NO_7Si$
691.493amu

28a

$C_{30}H_{35}Cl_4NO_7Si$
691.493amu

28b

A suspension of molecular sieves (powdered, 4 Å, 230 mg) and **27** (47 mg, 0.08 mmol, 1.00 equiv.) in dichloromethane (1 ml) was stirred for 1 hour at ambient temperature. To the suspension were added triethylsilane (39 µl, 0.25 mmol, 3.00 equiv.) and triflic acid (25 µl, 0.28 mmol, 3.40 equiv.) at -70 °C. Monitoring *via* TLC (toluene/ethyl acetate 5:1) indicated full consumption of the starting material after 1 hour between -75 °C and -70 °C. The reaction was quenched by addition of triethylamine (100 µl) and methanol (0.4 ml) at -70 °C, before warming up to ambient temperature. The solid material was removed *via* filtration over Celite® with dichloromethane and ethyl acetate. The filtrate was concentrated in *vacuo* to afford 100 mg of a crude material. The crude residue was dissolved in ethyl acetate and washed with saturated aqueous sodium bicarbonate and brine. Drying over magnesium sulfate and removal of the volatiles in *vacuo* afforded a colorless crude solid material. Coarse purification *via* flash filtration using silica gel (pre-packed Interchim® SI-S-500MG/6 ml, isocratic elution with dichloromethane/methanol 50:1) afforded 74% (35 mg) of **28**.[170]

Mixtures of **28**, **28a** and **28b** were separated *via* automated column chromatography using silica gel (Interchim PuriFlash® 4/25, dry loading with 2 g of silica gel directly into column, column: F080, 36 ml/min, 5 ml/fraction, collection *via* threshold: 5 mV, applying a gradient of acetone in isomers of hexane from 0% to 15% in 10 CV). The byproducts **28a** and **28b** were converted to desired **28** *via* a TBAF-mediated desilylation method published in the literature.[171]

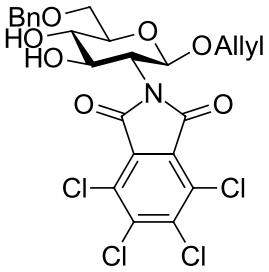

$C_{24}H_{21}Cl_4NO_7$
577.232 amu

28

R_f = 0.18 in toluene/ethyl acetate 4:1

^{1}H NMR (600 MHz, $CDCl_3$): δ = 7.39-7.31 (m, 5 H, Ar), 5.77-5.70 (m, 1 H, CH_2CH=CH_2), 5.22 (d, $J_{1,2}$ = 8.4 Hz, 1 H, H_1), 5.17-5.13 (m, 1 H, CH_2CH=CH_2), 5.10-5.08 (m, 1 H, CH_2CH=CH_2), 4.65 (d, J_{gem} = 11.9 Hz, 1 H, 6-*O*-Bn), 4.58 (d, J_{gem} = 11.9 Hz, 1 H, 6-*O*-Bn´), 4.31-4.24 (m, 2 H, H_3, CH_2CH=CH_2), 4.17 (dd, $J_{1,2}$ = 8.3 Hz, $J_{2,3}$ = 11.0 Hz, 1 H, H_2), 4.04-4.00 (m, 1 H, CH_2CH=CH_2), 3.85 (dd, J_{vic} = 4.6 Hz, J_{gem} = 10.0 Hz, 1 H, H_6)3.77 (dd, J_{vic} = 5.5 Hz, J_{gem} = 10.1 Hz, 1 H, $H_{6'}$), 3.66-3.63 (m, 1 H, H_4), 3.61-3.58 (m, 1 H, H_5), 3.13 (d, J_{vic} = Hz, 1 H, 4-OH), 2.52 (br, 1 H, 3-OH) ppm

^{13}C-APT NMR (150 MHz, $CDCl_3$): δ = 140.43, 137.48, 133.60 (CH_2*C*H=CH_2), 128.73, 128.21, 127.98, 127.39, 117.84, 97.21 (C_1), 74.63 (C_4), 73.98 (6-*O*-Bn), 73.37 (C_5), 71.38 (C_3), 70.71 (C_6), 70.04 (*C*H_2CH=CH_2), 56.71 (C_2) ppm

ESI-TOF-MS: calc.: $[M+ NH_4]^+$ = 593.0410 m/z; measured.: $[M+NH_4]^+$ = 593.0417 m/z; Δ = -1.16 ppm

$[\alpha]_D^{20}$ = -9.6 (*c* 0.6, $CHCl_3$)

5.2.23 Allyl 6-*O*-benzyl-4-*O*-(triethylsilyl)-2-deoxy-2-(tetrachlorophthalimido)-β-D-glucopyranoside (**28a**)

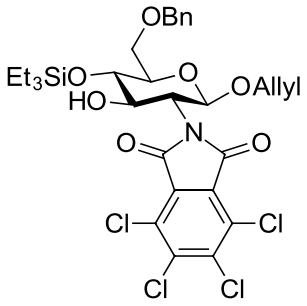

$C_{30}H_{35}Cl_4NO_7Si$
691.493 amu

28a

R_f = 0.37 in toluene/ethyl acetate 5:1

^{1}H NMR (600 MHz, $CDCl_3$): δ = 7.38 – 7.28 (m, 5 H, Ar), 5.80 – 5.74 (m, 1 H, CH_2CH=CH_2), 5.21 (d, $J_{1,2}$ = 7.9 Hz, 1 H, H_1), 5.18 – 5.15 (m, 1 H, CH_2CH=CH_2), 5.10 – 5.08 (m, 1 H, CH_2CH=C$H_{2'}$), 4.66 (d, J_{gem} = 12.4 Hz, 1 H, 6-*O*-Bn), 4.59 (d, J_{gem} = 12.4 Hz, 1 H, 6-*O*-Bn´), 4.31 – 4.28 (m, 1 H, CH_2CH=CH_2), 4.22 – 4.15 (m, 2 H, H_3, H_2), 4.07 – 4.03 (m, 1 H, CH_2CH=CH_2), 3.78 – 3.76 (m, 1 H, H_6), 3.69 – 3.67 (m, 1 H, $H_{6'}$), 3.64 – 3.61 (m, 1 H, H_4), 3.55 – 3.52 (m, 1 H, H_5), 1.97 (d, *J* = 5.3 Hz, 1 H, OH), 0.91 (t, *J* = 8.0 Hz, 9 H, CH_3CH_2), 0.62 – 0.57 (m, 6 H, CH_3CH_2) ppm

^{13}C NMR (150 MHz, $CDCl_3$): δ = 140.4, 138.3, 133.8 (CH_2*C*H=CH_2), 128.5, 127.8, 127.7, 127.4, 117.7 (CH_2CH=*C*H_2), 97.1 (C_1), 76.4 (C_5), 73.6 (6-*O*-Bn), 73.5 (C_4), 72.7 (C_3), 69.9 (*C*H_2CH=CH_2), 69.1 (C_6), 57.2 (C_2), 7.0 (*C*H_3CH_2Si), 5.3 (CH_3*C*H_2Si) ppm

ESI-TOF-MS: calc.: $[M+ NH_4]^+$ = 707.1275 m/z; measured.: $[M+NH_4]^+$ = 707.1287 m/z; Δ = -1.67 ppm

5.2.24 Allyl 6-*O*-benzyl-3-*O*-(triethylsilyl)-2-deoxy-2-(tetrachlorophthalimido)-β-D-glucopyranoside (**28b**)

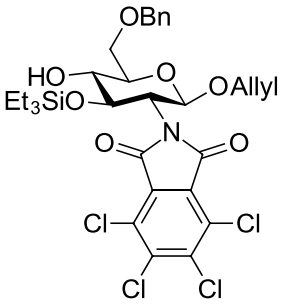

$C_{30}H_{35}Cl_4NO_7Si$
691.493 amu

28b

R_f = 0.29 in toluene/ethyl acetate 5:1

^{1}H NMR (600 MHz, $CDCl_3$): δ = 7.39 – 7.30 (m, 5 H, Ar), 5.75 – 5.68 (m, 1 H, CH_2CH=CH_2), 5.16 – 5.06 (m, 3 H, H_1, CH_2CH=CH_2), 4.67 (d, *J* = 12.0 Hz, 1 H, 6-*O*-Bn), 4.57 (d, *J* = 12.0 Hz, 1 H, 6-*O*-Bn´), 4.33 (dd, $J_{3,4}$ = 8.0 Hz, $J_{2,3}$ = 10.6 Hz, 1 H, H_3), 4.25 – 4.22 (m, 1 H, CH_2CH=CH_2), 4.15 (dd, $J_{1,2}$ = 8.5 Hz, $J_{2,3}$ = 10.6 Hz, 1 H, H_2), 4.02 – 3.99 (m, 1 H, CH_2CH=CH_2), 3.83 – 3.75 (m, 2 H, H_6), 3.62 – 3.53 (m, 2 H, H_4, H_5), 2.65 (d, *J* = 2.9 Hz, 1 H, 4-OH), 0.78 (t, *J* = 8.0 Hz, 9 H, CH_3CH_2Si), 0.52 – 0.34 (m, 6 H, CH_3CH_2Si) ppm

^{13}C-APT NMR (150 MHz, $CDCl_3$): δ = 137.74, 133.75 (CH_2CH=CH_2), 128.69, 128.11, 128.00, 117.69 (CH_2CH=CH_2), 97.09 (C_1), 74.67 (C_4), 73.90 (6-*O*-Bn), 73.74 (C_5), 72.68 (C_3), 70.70 (C_6), 69.89 (CH_2CH=CH_2), 57.90 (C_2), 6.77 (CH_3CH_2Si), 5.27 (CH_3CH_2Si) ppm

ESI-TOF-MS: calc.: $[M+NH_4]^+$ = 707.1275 m/z; measured.: $[M+NH_4]^+$ = 707.1280 m/z; Δ = -0.62 ppm

5.2.25 Allyl 3-*O*-benzyl-4,6-*O*-benzylidene-2-deoxy-2-(tetrachlorophthalimido)-β-D-glucopyranoside (**29**)

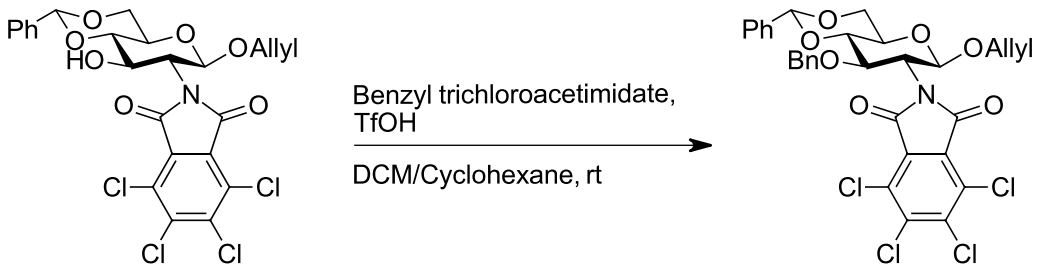

$C_{24}H_{19}Cl_4NO_7$
575.216 amu

27

$C_{31}H_{25}Cl_4NO_7$
665.339 amu

29

To a solution of **27** (300 mg, 0.52 mmol, 1.00 equiv.) in dichloromethane (anhydrous, 2.7 ml) and cyclohexane (dry, 1.6 ml) were added molecular sieves (powdered, 3 Å, 333 mg) and benzyl 2,2,2-trichloroacetimidate (0.40 ml, 2.14 mmol, 4.10 equiv.) at ambient temperature. The suspension was stirred at ambient temperature for 45 minutes. To the suspension was added triflic acid (2.76 µl, 31.29 µmol, 0.06 equiv.) at ambient temperature. Monitoring *via* TLC (*n*-hexane/ethyl acetate 5:1) indicated traces of starting material after 15 hours at ambient temperature. The reaction was quenched by addition of pyridine (0.1 ml) and dichloromethane. The solid material was removed *via* filtration over Celite®. The filtrate was washed with water and the aqueous phase was re-extracted with dichloromethane (3x). Drying over magnesium sulfate and removal of the solvent in *vacuo* afforded 1 g of a crude material. Purification *via* automated column chromatography using silica gel (Interchim PuriFlash® 4/25, dry loading with 1.5 g silica gel in F025, column: F040, 26 ml/min, 5 ml/fraction, collect *via* threshold: 5 mV, applying a gradient of ethyl acetate in *n*-hexane from 0% to 25% in 11 CV) afforded 89% (310 mg) of **29** as a wax.[172]

R_f = 0.53 in *n*-hexane/ethyl acetate 5:1

^{1}H NMR (600 MHz, $CDCl_3$): δ = 7.54-7.52 (m, 2 H, Ar), 7.42-7.37 (m, 3 H, Ar), 7.05-7.04 (m, 2 H, Ar), 6.94-6.91 (m, 2 H, Ar), 6.83-6.80 (m, 1 H, Ar), 5.71-5.65 (m, 1 H, CH_2CH=CH_2), 5.63 (s, 1 H, PhC*H*), 5.21 (d, $J_{1,2}$ = 8.5 Hz, 1 H, H_1), 5.14-5.11 (m, 1 H, CH_2CH=CH_2), 5.07-5.04 (m, 1 H, CH_2CH=C$H_{2'}$), 4.81 (d, *J* = 12.8 Hz, 1 H, 3-*O*-Bn),

4.41-4.39 (m, 2 H, 3-*O*-Bn´, H_6), 4.33 (dd, $J_{3,4}$ = 8.9 Hz, $J_{2,3}$ = 10.4 Hz, 1 H, H_3), 4.25-4.17 (m, 1 H, CH_2CH=CH_2), 4.18 (dd, $J_{1,2}$ = 8.5 Hz, $J_{2,3}$ = 10.4 Hz, 1 H, H_2), 4.00-3.96 (m, 1 H, CH_2CH=CH_2), 3.86 (t, J = 10.3 Hz, 1 H, $H_{6'}$), 3.79 (t, J = 9.3 Hz, 1 H, H_4), 3.62-3.57 (m, 1 H, H_5) ppm

^{13}C-APT NMR (150 MHz, $CDCl_3$): δ = 139.95, 138.38, 137.39, 133.37 ($CH_2CH=CH_2$), 129.21, 128.52, 128.44, 128.08, 127.25, 126.20, 117.96, 101.57 (PhCH), 97.75 (C_1), 82.91 (C_4), 75.29 (C_3), 74.62 (3-*O*-Bn), 70.25 ($CH_2CH=CH_2$), 68.84 (C_6), 66.30 (C_5), 56.61 (C_2) ppm

ESI-TOF-MS: calc.: $[M+H]^+$ = 664.0458 m/z; measured.: $[M+H]^+$ = 664.0450 m/z; Δ = +1.15 ppm

$[\alpha]_D^{20}$ = +60.6 (*c* 0.5, $CHCl_3$)

5.2.26 Allyl 3,6-di-*O*-benzyl-2-deoxy-2-(tetrachlorophthalimido)-β-D-glucopyranoside (**30**)

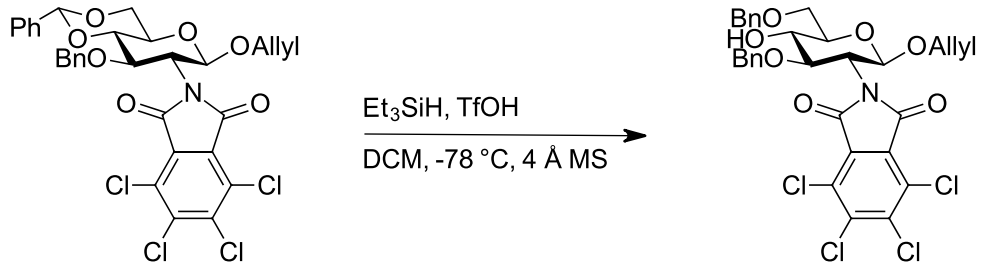

$C_{31}H_{25}Cl_4NO_7$
665.339 amu

29

$C_{31}H_{27}Cl_4NO_7$
667.355 amu

30

A suspension of **29** (2.06 g, 3.10 mmol, 1.00 equiv.) and molecular sieves (powdered, 4 Å, 2 g) in dichloromethane (dry, 36 ml) was stirred for 30 minutes at ambient temperature. To the suspension was added triethylsilane (0.21 ml, 1.31 mmol, 3.00 equiv.) at ambient temperature. After stirring for additional 30 minutes at ambient temperature, triflic acid (0.13 ml, 1.48 mmol, 3.40 equiv.) was added at -65 °C. Monitoring *via* TLC (*n*-hexane/ethyl acetate 5:1) indicated full consumption of the starting material after 30 minutes at -60 °C. The reaction was quenched by addition of pyridine (1.00 ml, 12.38 mmol, 4.00 equiv.) and methanol (2 ml) at -60 °C, before warming up to ambient temperature. The solid material was removed *via* filtration over Celite® with dichloromethane. The filtrate was washed with aqueous sodium bicarbonate and the aqueous phase was re-extracted with dichloromethane (3x). Drying over magnesium sulfate and removal of the volatiles in *vacuo* afforded 2.5 g of a crude oil. Purification *via* automated column chromatography using silica gel (Interchim PuriFlash® 4/25, dry loading with 4.1 g Celite® in F040, column: F080, 30 ml/min, 12 ml/fraction, collection *via* threshold: 5 mV, applying a gradient of ethyl acetate in *n*-hexane from 0% to 30% in 8 CV then 4 CV isocratic) afforded 77% (1.23 g) of **30** as a colorless foam.[170]

R_f = 0.15 in n-hexane/ethyl acetate 5:1

^{1}H NMR (600 MHz, $CDCl_3$): δ = 7.39-7.31 (m, 5 H, Ar), 7.07-7.06 (m, 2 H, Ar), 6.95-6.93 (m, 2 H, Ar), 6.79-6.76 (m, 1 H, Ar), 5.71-5.64 (CH_2CH=CH_2), 5.14 (d, $J_{1,2}$ = 8.2

Hz, 1 H, H_1), 5.11-5.08 (m, 1 H, $CH_2CH=CH_2$), 5.05-5.02 (m, 1 H, $CH_2CH=CH_{2'}$), 4.85 (d, J_{gem} = 12.7 Hz, 1 H, 3-*O*-Bn), 4.65 (d, J_{gem} = 12.0, 1 H, 6-*O*-Bn), 4.59 (d, J_{gem} = 11.8, 1 H, 6-*O*-Bn´), 4.43 (d, J_{gem} = 12.9, 1 H, 3-*O*-Bn´), 4.22-4.18 (m, 1 H, $CH_2CH=CH_2$), 4.15-4.08 (m, 2 H, H_3, H_2), 3.98-3.94 (m, 1 H, $CH_2CH=CH_2$), 3.86-3.77 (m, 3 H, H_6, $H_{6'}$, H_4), 3.62-3.58 (m, 1 H, H_5), 3.00 (d, *J* = 2.6 Hz, 1 H, 4-O*H*) ppm

^{13}C-APT NMR (150 MHz, $CDCl_3$): δ = 139.79, 138.81, 137.60, 133.64 ($CH_2CH=CH_2$), 128.70, 128.20, 128.14, 128.09, 127.98, 127.07, 117.71 ($CH_2CH=CH_2$), 97.16 (C_1), 79.52 (C_3), 75.12 (3-*O*-Bn), 75.03 (C_4), 74.00 (6-*O*-Bn), 73.46 (C_5), 70.88 (C_6), 69.94 ($CH_2CH=CH_2$), 56.11 (C_2) ppm

ESI-TOF-MS: calc.: $[M+NH_4]^+$ = 683.0880 m/z; measured.: $[M+NH_4]^+$ = 683.0891 m/z; Δ = -1.60 ppm

$[\alpha]_D^{20}$ = +23.5 (*c* 0.5, $CHCl_3$)

5.2.27 Allyl 2-azido-4,6-*O*-benzylidene-2-deoxy-3-*O*-picoloyl-β-D-mannopyranosyl-(1→3)-6-*O*-benzyl-2-deoxy-2-(tetrachlorophthalimido)-β-D-glucopyranoside (**31a**)

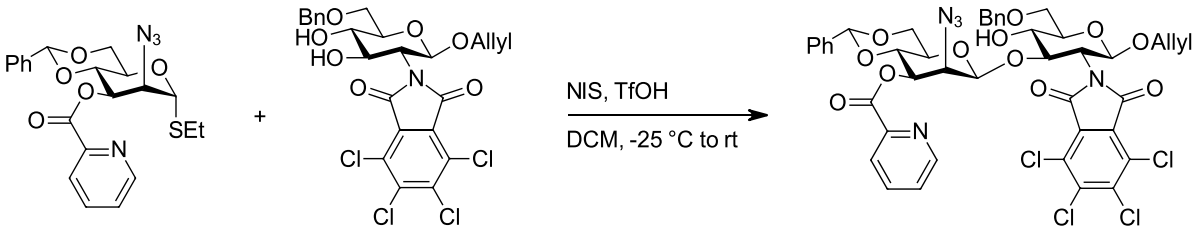

$C_{21}H_{22}N_4O_5S$	$C_{24}H_{21}Cl_4NO_7$	$C_{43}H_{37}Cl_4N_5O_{12}$
442.490amu	577.233amu	957.586amu
22	**28**	**31a**

To a solution of **22** (28.9 mg, 65.3 µmol, 1.3 equiv.) and **28** (29.0 mg, 50.2 µmol, 1.0 equiv.) in dichloromethane (dry, 1 ml) were added molecular sieves (powdered, 4 Å, 90 mg) at ambient temperature. The suspension was stirred for 30 min at ambient temperature. To the suspension were added *N*-iodosuccinimide (27.1 mg, 120.6 µmol, 2.4 equiv.) and triflic acid (1.8 µl, 20.1 µmol, 0.4 equiv.) at -25 °C. The reaction was warmed up to ambient temperature. A gradual discoloration towards purple between -7 °C and 0 °C indicated visually the start of the glycosylation. Monitoring *via* TLC (HPTLC, toluene/ethyl acetate 2:1) indicated traces of acceptor after 2.5 hours at ambient temperature. The reaction was quenched by addition of pyridine (0.1 ml) and aqueous sodium thiosulfate solution. The aqueous phase was separated and the solid material was removed *via* filtration over Celite®. The aqueous phase was re-extracted with dichloromethane (3x). The combined organic layers were washed with saturated aqueous sodium bicarbonate and water. Drying over magnesium sulfate and removal of the volatiles in *vacuo* afforded 62 mg of a crude brown material. Purification *via* manual column chromatography using silica gel (10 g of silica gel, dry loading with 120 mg silica gel, applying a gradient of ethyl acetate in toluene from 0% to 35%) afforded 40% (20 mg) of **31a** as an off-colorless solid material.[123]

R_f = 0.56 in toluene/ethyl acetate 2:1

^{1}H NMR (600 MHz, CD_2Cl_2): δ = 8.71 – 8.70 (m, 1 H, Ar), 8.07 – 8.06 (m, 1 H, Ar), 7.85 – 7.82 (m, 1 H, Ar), 7.49 – 7.47 (m, 1 H, Ar), 7.40 – 7.35 (m, 6 H, Ar), 7.32 – 7.29

(m, 4 H, Ar), 5.77 – 5.70 (m, 1 H, CH_2CH=CH_2), 5.56 (s, 1 H, $PhCH_A$), 5.26 (dd, $J_{2,3}$ = 3.9 Hz, $J_{3,4}$ = 10.1 Hz, 1 H, H_{3A}), 5.16 – 5.15 (m, 1 H, CH_2CH=CH_2), 5.10 (d, $J_{1,2}$ = 8.5 Hz, 1 H, H_{1B}), 5.09 – 5.07 (m, 1 H, CH_2CH=$CH_{2'}$), 4.85 (d, $^3J_{H1A,H2A}$ = 1.4 Hz, $^1J_{C1A,H1A}$ = 161.6 Hz, 1 H, H_{1A}), 4.65 – 4.60 (m, 2 H, 6-*O*-Bn_B), 4.56 (dd, J = 8.3 Hz, J = 10.8 Hz, 1 H, H_{3B}), 4.33 (dd, J_{vic} = 4.9 Hz, J_{gem} = 10.5 Hz, 1 H, H_{6A}), 4.29 – 4.25 (m, 2 H, CH_2CH=CH_2, H_{2B}), 4.11 (t, J = 9.7 Hz, 1 H, H_{4A}), 4.05 – 4.00 (m, 2 H, CH_2CH=CH_2, H_{2A}), 3.90 – 3.87 (m, 2 H, $H_{6A'}$, H_{6B}), 3.81 – 3.77 (m, 2 H, $H_{6B'}$, 4-OH), 3.75 – 3.72 (m, 1 H, H_{4B}), 3.64 – 3.61 (m, 1 H, H_{5B}), 3.60 – 3.56 (m, 1 H, H_{5A}) ppm

^{13}C-APT NMR (150 MHz, CD_2Cl_2): δ = 150.12, 147.05, 140.73, 138.56, 137.09, 136.93, 133.65 (CH_2CH=CH_2), 129.26, 128.41, 128.24, 127.71, 127.65, 127.44, 126.23, 125.60, 117.53 (CH_2CH=CH_2), 102.01 ($PhCH_A$), 100.59 (C_{1A}), 97.06 (C_{1B}), 82.36 (C_{3B}), 75.27 (C_{5B}), 74.98 (C_{4A}), 73.59 (Bn), 71.13 (C_{3A}), 70.34 (C_{4B}), 69.99 (CH_2CH=CH_2), 69.49 (C_{6B}), 67.97 (C_{6A}), 67.67 (C_{5A}), 62.87 (C_{2A}), 55.76 (C_{2B}) ppm

ESI-TOF-MS: calc.: $[M+Na]^+$ = 978.1085 m/z; measured.: $[M+Na]^+$ = 978.1085 m/z; Δ = -0.03 ppm

$[\alpha]_D^{20}$ = -9.2 (*c* 0.4, $CHCl_3$)

5.2.28 Allyl 2-azido-4,6-*O*-benzylidene-2-deoxy-3-*O*-picoloyl-β-D-mannopyranosyl-(1→4)-3,6-di-*O*-benzyl-2-deoxy-2-(tetrachlorophthalimido)-β-D-glucopyranoside (**32**)

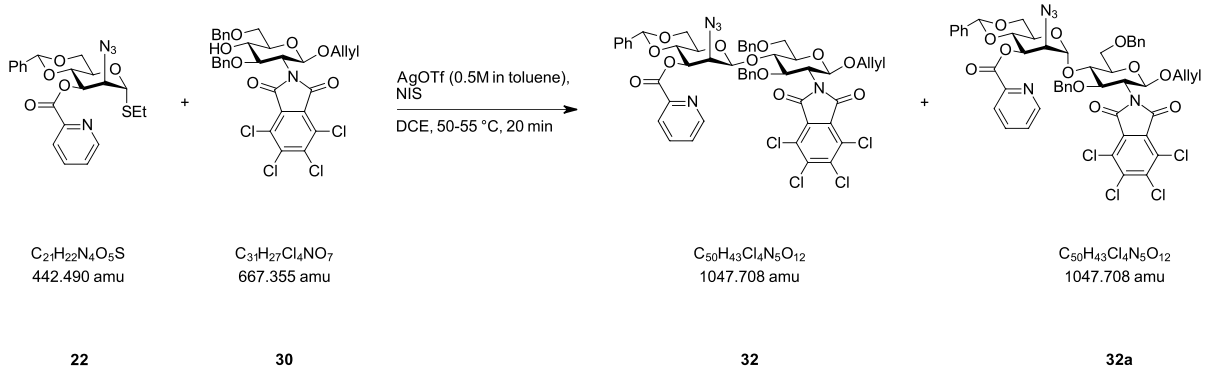

To a solution of **22** (128.7 mg, 290.9 µmol, 1.0 equiv.) and **30** (225.2 mg, 337.4 µmol, 1.2 equiv.) in 1,2-dichloroethane (anhydrous, 14.5 ml, ~20 mM) was added molecular sieves (powdered, 4 Å, 650 mg). The suspension was stirred at ambient temperature for 45 minutes. *N*-Iodosuccinimide (92.9 mg, 0.4 mmol, 1.4 equiv.) and silver triflate (0.338 M in toluene, stored over silver oxide, 430 µl, 145 µmol, 0.5 equiv.) were added at ambient temperature. The temperature was raised to 55 °C. Monitoring *via* TLC (HPTLC, *n*-hexane/ethyl acetate 2:1) indicated full consumption of the glycosyl donor after 10 minutes at 55 °C. The reaction was quenched by addition of pyridine (0.5 ml) and the solid material was removed *via* filtration over Celite® with dichloromethane. The crude reaction was washed with saturated aqueous sodium bicarbonate and saturated aqueous sodium thiosulfate (1:1). The aqueous phase was diluted with water and the layers were separated. The aqueous phase was re-extracted with dichloromethane (3x). Drying over magnesium sulfate and removal of the volatiles in *vacuo* afforded a dark crude material. Purification of *via* automated column chromatography using silica gel (Interchim PuriFlash® 4/25, dry loading with 4.8 g of silica gel in F012, column: F080, 30 ml/min, 15 ml/fraction, applying a gradient of ethyl acetate in *n*-hexane from 30% to 50% in 8 CV then isocratic) afforded 25% (76 mg) of **32** (α/β 1:2) as an off-colorless solid material.[123]

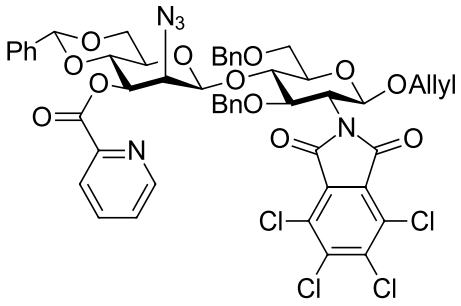

$C_{50}H_{43}Cl_4N_5O_{12}$
1047.708 amu

32

R_f = 0.39 in *n*-hexane/ethyl acetate 1.5:1

^{1}H NMR (600 MHz, $CDCl_3$): δ = 8.83 – 8.82 (m, 1 H, Ar), 8.15 – 8.14 (m, 1 H, Ar), 7.87 – 7.84 (m, 1 H, Ar), 7.51 – 7.49 (m, 1 H, Ar), 7.45 – 7.39 (m, 6 H, Ar), 7.35 – 7.31 (m, 4 H, Ar), 7.07 – 7.06 (m, 2 H, Ar), 6.93 – 6.90 (m, 2 H, Ar), 6.74 – 6.72 (m, 1 H, Ar), 5.73 – 5.66 (m, 1 H, CH_2CH=CH_2), 5.50 (s, 1 H, PhCH_A), 5.17 (dd, $J_{2,3}$ = 3.9 Hz, $J_{3,4}$ = 10.1 Hz, 1 H, H_{3A}), 5.14 – 5.10 (m, 2 H, H_{1B}, CH_2CH=CH_2), 5.06 – 5.04 (m, 1 H, CH_2CH=C$H_{2'}$), 4.87 (d, $^3J_{H1A,H2A}$ = 1.0 Hz, $^1J_{C1A,H1A}$ = 161.6 Hz, 1 H, H_{1A}), 4.83 – 4.80 (m, 2 H, 6-*O*-Bn_B, 3-*O*-Bn_B), 4.55 (d, J_{gem} = 12.0 Hz, 1 H, 6-*O*-$Bn_{B'}$), 4.43 (d, J_{gem} = 13.1 Hz, 1 H, 3-*O*-$Bn_{B'}$), 4.31 (dd, J_{vic} = 5.0 Hz, J_{gem} = 10.6 Hz, 1 H, H_{6A}), 4.25 – 4.17 (m, 3 H, CH_2CH=CH_2, H_{2A}, H_{3B}), 4.15 – 4.11 (m, 2 H, H_{2B}, H_{4B}), 4.06 (t, *J* = 9.7 Hz, 1 H, H_{4A}), 4.00 – 3.97 (m, 1 H, CH_2CH=CH_2), 3.83 – 3.78 (m, 2 H, H_{6B}, $H_{6B'}$), 3.69 (t, *J* = 10.3 Hz, 1 H, $H_{6A'}$), 3.58 – 3.55 (m, 1 H, H_{5B}), 3.28 – 3.24 (m, 1 H, H_{5A}) ppm

^{13}C-APT NMR (150 MHz, $CDCl_3$): δ = 164.14, 150.44, 147.32, 139.75, 139.02, 137.64, 137.14, 137.06, 133.65 (CH_2CH=CH_2), 129.24, 128.92, 128.46, 128.43, 128.35, 128.00, 127.35, 126.88, 126.30, 125.70, 117.77 (CH_2CH=CH_2), 101.96 (PhCH_A), 100.51 (C_{1A}), 97.15 (C_{1B}), 79.65 (C_{4B}), 77.98 (C_{3B}), 75.49 (3-*O*-Bn_B), 75.47 (C_{4A}), 74.42 (C_{5B}), 73.90 (6-*O*-Bn_B), 72.13 (C_{3A}), 69.97 (CH_2CH=CH_2), 68.55 (C_{6A}), 68.40 (C_{6B}), 67.35 (C_{5A}), 62.79 (C_{2A}), 56.46 (C_{2B}),ppm

ESI-TOF-MS: calc.: $[M+H]^+$ = 1046.1735 m/z; measured.: $[M+H]^+$ = 1046.1739 m/z; Δ = -0.42 ppm

$[\alpha]_D^{20}$ = -8.9 (*c* 0.8, $CHCl_3$)

5.2.29 Allyl 2-azido-4,6-*O*-benzylidene-2-deoxy-3-*O*-picoloyl-α-D-mannopyranosyl-(1→4)-3,6-di-*O*-benzyl-2-deoxy-2-(tetrachlorophthalimido)-α-D-glucopyranoside (**32a**)

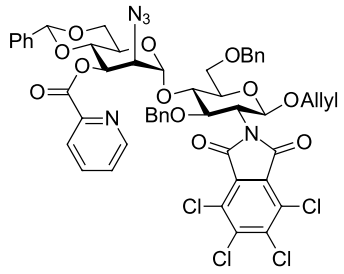

$C_{50}H_{43}Cl_4N_5O_{12}$
1047.708 amu

32a

R_f = 0.52 in n-hexane/ethyl acetate 1.5:1

^{1}H NMR (600 MHz, CD_2Cl_2): δ = 8.72 – 8.71 (m, 1 H, Ar), 8.12 – 8.11 (m, 1 H, Ar), 7.85 – 7.82 (m, 1 H, Ar), 7.49 – 7.47 (m, 1 H, Ar), 7.45 – 7.29 (m, 10 H, Ar), 7.09 – 7.08 (m, 2 H, Ar), 6.96 – 6.93 (m, 2 H, Ar), 6.72 – 6.69 (m, 1 H, Ar), 5.79 – 5.76 (dd, $J_{2,3}$ = Hz, $J_{3,4}$ = Hz, 1 H, H_{3A}), 5.75 – 5.68 (m, 1 H, CH_2CH=CH_2), 5.63 (s, 1 H, PhCH_A), 5.38 (d, $^3J_{H1A,H2A}$ = 1.5 Hz, 1 H, $^1J_{C1A,H1A}$ = 172.5 Hz, 1 H, H_{1A}), 5.12 – 5.09 (m, 2 H, H_{1B}, CH_2CH=CH_2), 5.06 – 5.04 (m, 1 H, CH_2CH=C$H_{2'}$), 4.96 (d, J = 12.9 Hz, 1 H, 3-*O*-Bn_B), 4.64 (s, 2 H, 6-*O*-Bn_B), 4.43 (dd, $J_{2,3}$ = 8.8 Hz, $J_{3,4}$ = 10.8 Hz, 1 H, H_{3A}), 4.39 (d, J = 12.9 Hz, 1 H, 3-*O*-Bn_B´), 4.35 (dd, $J_{2,3}$ = 1.6 Hz, $J_{1,2}$ = 3.6 Hz, 1 H, H_{2A}), 4.31 (t, J = 9.8 Hz, 1 H, H_{4A}), 4.24 – 4.19 (m, 2 H, CH_2CH=CH_2, H_{6A}), 4.16 – 4.04 (m, 3 H, H_{5A}, H_{2B}, H_{4B}), 4.01 – 3.94 (m, 2 H, CH_2CH=CH_2, H_{6B}), 3.87 – 3.82 (m, 2 H, $H_{6B'}$, $H_{6A'}$), 3.71 – 3.68 (m, 1 H, H_{5B}) ppm

^{13}C-APT NMR (150 MHz, CD_2Cl_2): δ = 150.13, 139.69, 138.57, 138.36, 137.36, 137.02, 133.77 (CH_2CH=CH_2), 129.18, 128.44, 128.26, 128.10, 127.76, 127.69, 127.56, 127.33, 126.95, 126.32, 125.61, 117.39 (CH_2CH=CH_2), 102.11 (PhCH_A), 101.08 (C_{1A}), 97.09 (C_{1B}), 81.40 (C_{3B}), 79.31 (C_{4B}), 75.95 (3-*O*-Bn),75.94 (C_{4A}), 74.44 (C_{5B}), 73.62 (6-*O*-Bn), 71.05 (C_{3A}), 70.03 (CH_2CH=CH_2), 68.88 (C_{6B}), 68.58 (C_{6A}), 65.31 (C_{5A}), 62.85 (C_{2A}), 56.49 (C_{2B}) ppm

ESI-TOF-MS: calc.: $[M+ Na]^+$ = 1068.1555 m/z; measured.: $[M+Na]^+$ = 1068.1560 m/z; Δ = -0.49 ppm

$[\alpha]_D^{20}$ = +31.7 (*c* 0.5, $CHCl_3$)

5.2.30 Allyl 2-azido-4,6-*O*-benzylidene-2-deoxy-β-D-mannopyranosyl-(1→4)-3,6-di-*O*-benzyl-2-deoxy-2-(tetrachlorophthalimido)-β-D-glucopyranoside (**37**)

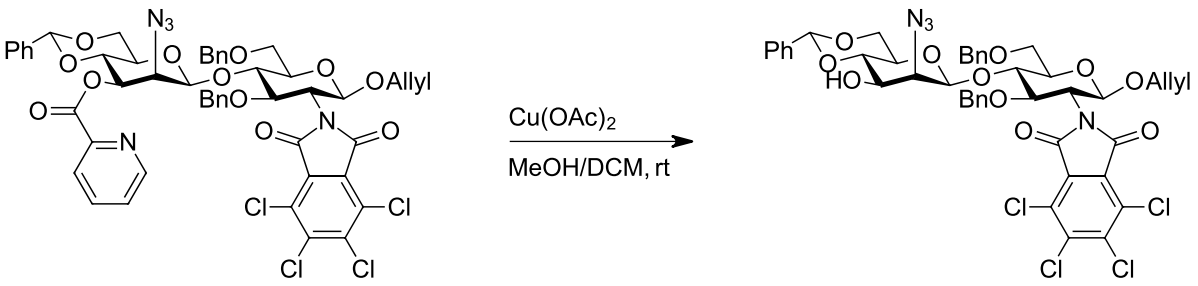

$C_{50}H_{43}Cl_4N_5O_{12}$
1047.708 amu

32

$C_{44}H_{40}Cl_4N_4O_{11}$
942.615 amu

37

To a solution of **32** (140.0 mg, 133.6 µmol, 1.0 equiv.) in methanol/dichloromethane (2 ml, 1:1) was added copper(II) acetate (catalytic amount) to yield a homogeneous blue solution. Monitoring *via* TLC (*n*-hexane/ethyl acetate 2:1) indicated full consumption of the starting material after 30 minutes. The reaction was quenched by addition of saturated aqueous sodium bicarbonate and dichloromethane. The layers were separated and the aqueous phase was re-extracted with dichloromethane (3x). Drying over magnesium sulfate and removal of the volatiles in *vacuo* afforded >99% of a crude material. Purification *via* automated column chromatography using silica gel (Interchim PuriFlash® 4/25, dry loading with 1.5 g of silica gel in F004, column: F012, 7.5 ml/min, 3 ml/fraction, collection *via* threshold: 5 mV, applying a gradient of ethyl acetate in *n*-hexane from 10% to 35% in 7 CV then isocratic with 35%) afforded 95% (120 mg) of **37** as a colorless solid material.[195]

R_f = 0.41 in n-hexane/ethyl acetate 2:1

^{1}H NMR (600 MHz, CD_2Cl_2): δ = 7.46 – 7.35 (m, 10 H, Ar), 7.06 – 7.04 (m, 2 H, Ar), 6.93 – 6.91 (m, 2 H, Ar), 6.79 – 6.76 (m, 1 H, Ar), 5.76 – 5.69 (m, 1 H, CH_2CH=CH_2), 5.48 (s, 1 H, PhCH_A), 5.14 – 5.10 (m, 2 H, H_{1B}, CH_2CH=CH_2), 5.07 – 5.05 (m, 1 H, CH_2CH=C$H_{2'}$), 4.81 – 4.76 (m, 3 H, H_{1A}, 6-*O*-Bn_B, 3-*O*-Bn_B), 4.53 (d, J_{gem} = 11.8 Hz, 1 H, 6-*O*-$Bn_{B'}$), 4.44 (d, J_{gem} = 12.8 Hz, 1 H, 3-*O*-$Bn_{B'}$), 4.29 (dd, J_{vic} = 5.0 Hz, J_{gem} = 10.3 Hz, 1 H, H_{6A}), 4.24 – 4.21 (m, 1 H, CH_2CH=CH_2), 4.18 – 4.15 (dd, $J_{3B,4B}$ = 8.6 Hz, *J* = 10.7 Hz, 1 H, H_{3B}), 4.11 – 4.08 (dd, $J_{4B,3B}$ = 8.7 Hz, *J* = 9.7 Hz, 1 H, H_{4B}), 4.02 –

3.97 (m, 2 H, H_{2B}, C*H*$_2$CH=CH$_2$), 3.87 – 3.86 (m, 1 H, H_{2A}), 3.83 – 3.77 (m, 2 H, H_{6B}, $H_{6B'}$), 3.69 – 3.59 (m, 4 H, H_{3A}, H_{4A}, $H_{6A'}$, H_{5B}), 3.19 – 3.15 (m, 1 H, H_{5A}), 2.41 (d, *J* = 5.8 Hz, 1 H, OH) ppm

^{13}C-APT NMR (150 MHz, CD_2Cl_2): δ = 140.0, 139.3, 138.3, 137.7, 134.1 (CH$_2$*C*H=CH$_2$), 129.8, 129.5, 129.0, 128.8, 128.6, 128.4, 128.2, 127.2, 126.6, 117.7 (CH$_2$CH=*C*H$_2$), 102.4 (Ph*C*H$_A$), 101.0 (C_{1A}), 97.4 (C_{1B}), 79.7 (C_{4B}), 78.8 (C_{4A}), 77.9 (C_{3B}), 75.6 (3-*O*-Bn$_B$), 74.6 (C_{5B}), 74.0 (6-*O*-Bn$_B$), 70.5 (C_{3A}), 70.3 (*C*H$_2$CH=CH$_2$), 68.8 (C_{6B}), 68.7 (C_{6A}), 67.4 (C_{5A}), 65.4 (C_{2A}), 56.8 (C_{2B}) ppm

ESI-TOF-MS: calc.: $[M]^+$ = 941.1520 m/z; measured.: $[M]^+$ = 941.1516 m/z; Δ = +0.43 ppm

$[\alpha]_D^{20}$ = +7.8 (*c* 0.6, $CHCl_3$)

5.2.31 Allyl 3-*O*-acetyl-2-azido-4,6-*O*-benzylidene-2-deoxy-β-D-mannopyranosyl-(1→4)-3,6-di-*O*-benzyl-2-deoxy-2-(tetrachlorophthalimido)-β-D-glucopyranoside (**38**)

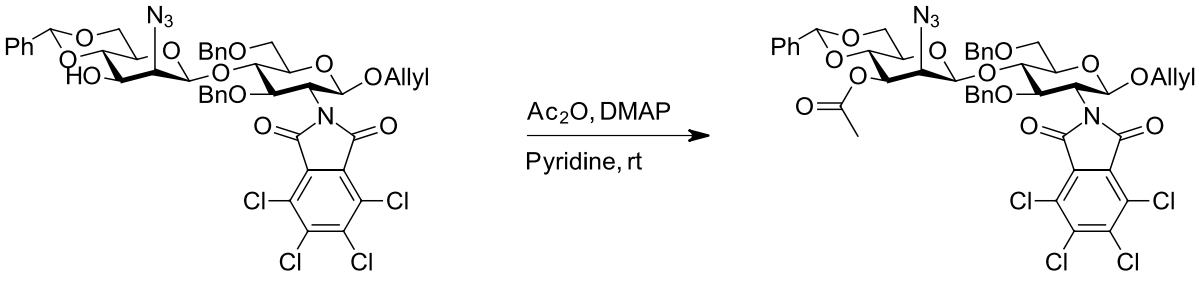

$C_{44}H_{40}Cl_4N_4O_{11}$
942.615 amu

$C_{46}H_{42}Cl_4N_4O_{12}$
984.651 amu

37 **38**

To a solution of **37** (5.6 mg, 5.9 µmol, 1.0 equiv.) in pyridine (dry, 0.5 ml) was added acetic anhydride (15 µl, 34.2 µmol, 5.8 equiv.) and 4-(dimethylamino)pyridine (catalytic amount) at ambient temperature. Monitoring *via* TLC (*n*-hexane/ethyl acetate 2:1) indicated full consumption of the starting material after 3 hours. The reaction was quenched by addition of methanol. The volatiles were removed in *vacuo* to afford a brown crude material. Purification *via* manual column chromatography using silica gel (column: pre-packed Isolute® SPE column 500 mg Flash Si 6 ml, liquid loading with toluene, isocratic with *n*-hexane/ethyl acetate 2:1) afforded 85% (5.0 mg) of **38** as a colorless material.[228]

R_f = 0.49 in *n*-hexane/ethyl acetate 2:1

^{1}H NMR (600 MHz, CD_2Cl_2): δ = 7.44 – 7.34 (m, 10 H, Ar), 7.06 – 7.05 (m, 2 H, Ar), 6.92 – 6.90 (m, 2 H, Ar), 6.74 – 6.72 (m, 1 H, Ar), 5.73 – 5.66 (m, 1 H, CH_2CH=CH_2), 5.46 (s, 1 H, PhCH_A), 5.14 – 5.04 (m, 3 H, H_{1B}, CH_2CH=CH_2), 4.88 (dd, $J_{3,2}$ = 3.8 Hz, $J_{3,4}$ = 10.2 Hz, 1 H, H_{3A}), 4.81 – 4.77 (m, 3 H, H_{1A}, 3-*O*-PhCH_B, 6-*O*-PhCH_B), 4.54 (6-*O*-PhC$H_{B'}$), 4.42 (3-*O*-PhC$H_{B'}$), 4.28 (dd, J_{gem} = 10.5 Hz, $J_{6,5}$ = 4.8 Hz, 1 H, H_{6A}), 4.24 – 4.21 (m, 1 H, CH_2CH=CH_2), 4.20 – 4.17 (dd, $J_{3,2}$ = 8.4 Hz, $J_{3,4}$ = 10.5 Hz, 1 H, H_{3B}), 4.12 – 4.08 (m, 3 H, H_{4B}, H_{2B}, H_{2A}), 4.00 – 3.96 (m, 1 H, CH_2CH=CH_2), 3.84 (t, *J* = 9.8 Hz, 1 H, H_{4A}), 3.78 – 3.77 (m, 2 H, H_{6B}, $H_{6B'}$), 3.66 (t, *J* = 10.3 Hz, 1 H, $H_{6A'}$), 3.56 – 3.54 (m, 1 H, H_{5B}), 3.23 – 3.19 (m, 1 H, H_{5A}), 2.15 (CH_3) ppm

^{13}C-APT NMR (150 MHz, CD_2Cl_2): δ = 170.3, 139.8, 139.0, 137.7, 137.1, 133.7 ($CH_2CH=CH_2$), 129.3, 128.8, 128.5, 128.4, 128.3, 128.2, 128.0, 126.9, 126.3, 117.8 ($CH_2CH=CH_2$), 102.0 ($PhCH_A$), 100.2 (C_{1A}), 97.2 (C_{1B}), 79.5 (C_{4B}), 77.9 (C_{3B}), 75.5 (C_{4A}), 75.4 (3-*O*-Bn_B), 74.5 (C_{5B}), 73.9 (6-*O*-Bn_B), 71.2 (C_{3A}), 70.0 ($CH_2CH=CH_2$), 68.5 (C_{6A}), 68.4 (C_{6B}), 67.3 (C_{5A}), 62.8 (C_{2A}), 56.5 (C_{2B}), 20.9 (CH_3) ppm

ESI-TOF-MS: calc.: $[M+H]^+$ = 983.1626 m/z; measured.: $[M+H]^+$ = 983.1622 m/z; Δ = +0.46 ppm

$[\alpha]_D^{20}$ = +0.2 (*c* 0.4, $CHCl_3$)

5.2.32 Allyl 2-azido-3-*O*-benzoyl-4,6-*O*-benzylidene-2-deoxy-β-D-mannopyranosyl-(1→4)-3,6-di-*O*-benzyl-2-deoxy-2-(tetrachlorophthalimido)-β-D-glucopyranoside (**39**)

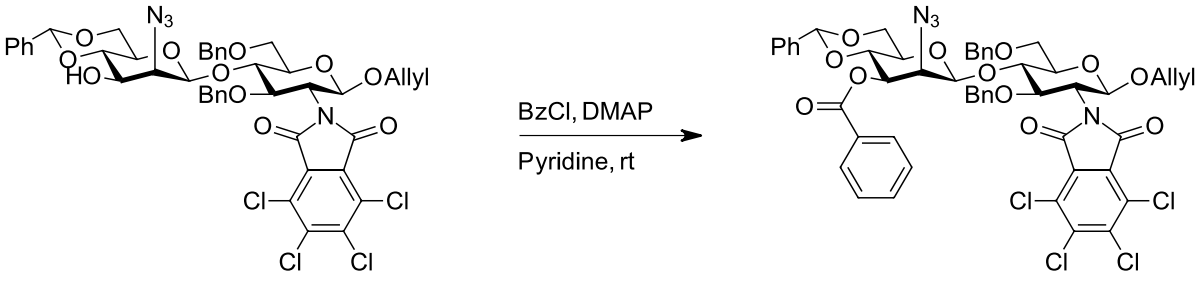

$C_{44}H_{40}Cl_4N_4O_{11}$
942.615 amu

37

$C_{51}H_{44}Cl_4N_4O_{12}$
1046.720 amu

39

To a solution of **37** (60 mg, 64 µmol, 1.0 equiv.) and 4-(dimethylamino)pyridine (catalytic amount) in pyridine (dry, 2 ml) was added benzoyl chloride (0.5 ml, 4.1 mmol, 67 equiv.) at ambient temperature. Monitoring *via* TLC (toluene/ethyl acetate 2:1) indicated full consumption of the starting material after 16 hours at ambient temperature. The reaction was quenched by slow addition of methanol (1 ml) and was concentrated in *vacuo*. The crude material was isolated *via* extraction between saturated aqueous sodium bicarbonate and ethyl acetate. The combined organic layers were dried over magnesium sulfate. Removal of the volatiles in *vacuo* afforded a crude green liquid. Purification *via* automated column chromatography using silica gel (Interchim PuriFlash® 4/25, liquid loading with toluene, column: F025, 15 ml/min, 4 ml/fraction, collect *via* threshold: 5 mV, applying a gradient of ethyl acetate in toluene from 0% to 10% in 9 CV then isocratic with 10% ethyl acetate) afforded 87% (58 mg) of **39** as a colorless solid material.[229]

R_f = 0.50 in *n*-hexane/ethyl acetate 2:1

^{1}H NMR (600 MHz, $CDCl_3$): δ = 8.11 – 8.09 (m, 2 H, Ar), 7.61 – 7.58 (m, 1 H, Ar), 7.49 – 7.40 (m, 8 H, Ar), 7.34 – 7.30 (m, 4 H, Ar), 7.08 – 7.06 (m, 2 H, Ar), 6.93 – 6.90 (m, 2 H, Ar), 6.74 – 6.71 (m, 1 H, Ar), 5.73 – 5.66 (m, 1 H, CH_2CH=CH_2), 5.50 (s, 1 H, PhCH_A), 5.16 – 5.09 (m, 3 H, H_{3A}, H_{1B}, CH_2CH=CH_2), 5.07 – 5.04 (m, 1 H, CH_2CH=C$H_{2'}$), 4.87 (d, $J_{1,2}$ = 1.2 Hz, 1 H, H_{1A}), 4.82 – 4.80 (m, 2 H, 6-*O*-Bn_B, 3-*O*-

Bn_B), 4.56 (d, J_{gem} = 12.1 Hz, 1 H, 6-*O*-$Bn_{B'}$), 4.44 (d, J_{gem} = 13.1 Hz, 1 H, 3-*O*-$Bn_{B'}$), 4.32 (dd, J_{gem} = 5.0 Hz, J_{vic} = 10.6 Hz, 1 H, H_{6A}), 4.25 – 4.17 (m, 3 H, CH_2CH=CH_2, H_{3B}, H_{2A}), 4.14 – 4.10 (m, 2 H, H_{4B}, H_{2B}), 4.02 – 3.96 (m, 2 H, H_{4A}, CH_2CH=CH_2), 3.82 – 3.78 (m, 2 H, H_{6B}, $H_{6B'}$), 3.71 (t, J = 10.3 Hz, 1 H, $H_{6A'}$), 3.57 – 3.55 (m, 1 H, H_{5B}), 3.30 – 3.26 (m, 1 H, H_{5A}) ppm

^{13}C-APT NMR (150 MHz, $CDCl_3$): δ = 165.77, 139.74, 139.00, 137.65, 137.09, 133.64 (CH_2*C*H=CH_2), 133.62, 130.09, 129.43, 129.19, 128.87, 128.62, 128.45, 128.40, 128.34, 128.28, 127.99, 126.88, 126.23, 117.76 (CH_2CH=*C*H_2), 101.88 (Ph*C*H_A), 100.38 (C_{1A}), 97.14 (C_{1B}), 79.51 (C_{4B}), 77.96 (C_{3B}), 75.70 (C_{4A}), 75.48 (3-*O*-Bn_B), 74.44 (C_{5B}), 73.89 (6-*O*-Bn_B), 71.45 (C_{3A}), 69.96 (*C*H_2CH=CH_2), 68.56 (C_{6A}), 68.38 (C_{6B}), 67.36 (C_{5A}), 63.08 (C_{2A}), 56.45 (C_{2B}) ppm

ESI-TOF-MS: calc.: $[M+ NH_4]^+$ = 1062.2048 m/z; measured.: $[M+NH_4]^+$ = 1062.2046 m/z; Δ = +0.24 ppm

$[\alpha]_D^{20}$ = -7.6 (*c* 0.9, $CHCl_3$)

5.2.33 2-Azido-3-*O*-benzoyl-4,6-*O*-benzylidene-2-deoxy-β-D-mannopyranosyl-(1→4)-3,6-di-*O*-benzyl-2-deoxy-2-(tetrachlorophthalimido)-β-D-glucopyranose (**41**)

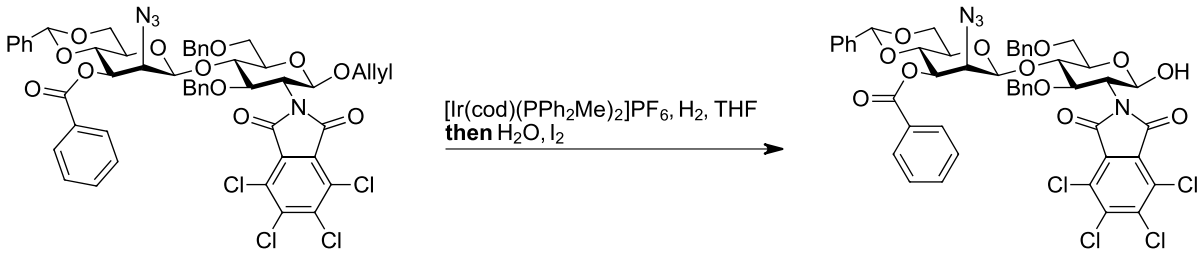

$C_{51}H_{44}Cl_4N_4O_{12}$
1046.720 amu

39

$C_{48}H_{40}Cl_4N_4O_{12}$
1006.657 amu

41

A suspension of [Ir(cod)(PPh2Me)2]PF_6 (1.9 mg, 2.2 µmol, 0.1 equiv.) in tetrahydrofuran (dry, 2 ml) was stirred under hydrogen atmosphere for roughly 5 minutes at ambient temperature to yield a homogeneous, yellowish catalyst solution.

To a solution of **39** (35.5 mg, 33.9 µmol, 1.0 equiv.) in tetrahydrofuran (dry, 2 ml) was added all of the catalyst solution. Monitoring *via* TLC (HPTLC, toluene/ethyl acetate 10:1) indicated incomplete conversion of the starting material to the propenyl ether after 1h 30min. Additional catalyst solution (2.0 mg in 1 ml tetrahydrofuran, 2.3 µmol, 0.1 equiv.) was added. Monitoring *via* TLC (HPTLC, toluene/ethyl acetate 10:1) indicated full conversion of the starting material to the vinyl ether after 2 hours. To the reaction was added water (2 ml) and iodine (43 mg, 170 µmol, 5 equiv.) and the mixture was stirred for additional 20 minutes. The reaction was quenched by addition of saturated aqueous sodium thiosulfate. The crude material was isolated *via* extraction with ethyl acetate (3x). Drying over magnesium sulfate and removal of the volatiles in *vacuo* afforded a brownish crude material. The crude material was submitted to coarse flash filtration (column: pre-packed Interchim® 2g/6 ml, liquid loading with toluene/ethyl acetate 5:1, isocratic elution with toluene/ethyl acetate 5:1). Further purification *via* preparative HPLC using silica gel (Interchim PuriFlash® 4/25, liquid loading with toluene: 2x 0.5 ml, guard column: YMC SIL 10x10 mmI.D., column: YMC-Pack SIL/S-5µm/6nm 250x10x0 mmI.D., 5 ml/min, 10 ml/fraction until 3 CV then 2 ml/fraction, collect all, applying a gradient of ethyl acetate in toluene from 0% to 30%

in 6 CV then isocratic with 30% ethyl acetate) afforded 59% (20 mg) of **41** as an off-colorless solid material.[190]

R_f = 0.10 in toluene/ethyl acetate 10:1

^{1}H NMR (600 MHz, $CDCl_3$): δ = 8.11 – 8.09 (m, 2 H, Ar), 7.61 – 7.58 (m, 1 H, Ar), 7.49 – 7.46 (m, 2 H, Ar), 7.44 – 7.40 (m, 6 H, Ar), 7.34 – 7.30 (m, 4 H, Ar), 7.08 – 7.07 (m, 2 H, Ar), 6.94 – 6.91 (m, 2 H, Ar), 6.76 – 6.73 (m, 1 H, Ar), 5.50 (s, 1 H, PhCH_A), 5.34 (t, J = 8.0 Hz, 1 H, H_{1B}), 5.14 (dd, $J_{2,3}$ = 3.9 Hz, $J_{3,4}$ = 10.2 Hz, 1 H, H_{3A}), 4.84 – 4.78 (m, 3 H, H_{1B}, 6-*O*-Bn_B, 3-*O*-Bn_B), 4.54 (d, J_{gem} = 11.9 Hz, 1 H, 6-*O*-$Bn_{B'}$), 4.44 (d, J_{gem} = 13.0 Hz, 1 H 3-*O*-$Bn_{B'}$), 4.32 – 4.25 (m, 2 H, H_{6A}, H_{3B}), 4.14 – 4.11 (m, 2 H, H_{2A}, H_{4B}), 4.03 – 3.99 (m, 2 H, H_{2B}, H_{4A}), 3.82 – 3.77 (m, 2 H, H_{6B}, $H_{6B'}$), 3.71 (t, J = 10.2 Hz, 1 H, $H_{6A'}$), 3.65 – 3.62 (m, 1 H, H_{5B}), 3.30 – 3.26 (m, 1 H, H_{5A}), 2.94 (d, J = 7.8 Hz, 1 H, OH) ppm

^{13}C-APT NMR (150 MHz, $CDCl_3$): δ = 165.77, 139.85, 139.03, 137.47, 137.08, 133.65, 130.10, 129.42, 129.21, 128.96, 128.64, 128.55, 128.40, 128.36, 128.03, 126.94, 126.24, 101.91 (Ph*C*H_A), 100.35 (C_{1A}), 92.67 (C_{1B}), 79.21 (C_{4B}), 77.71 (C_{3B}), 75.70 (C_{4a}), 75.47 (4-O-Bn_B), 74.61 (C_{5B}), 74.01 (6-*O*-Bn_B), 71.44 (C_{3A}), 68.55 (C_{6A}), 68.30 (C_{6B}), 67.41 (C_{5A}), 63.10 (C_{2A}), 58.25 (C_{2B}) ppm

ESI-TOF-MS: calc.: $[M+NH_4]^+$ = 1022.1735 m/z; measured.: $[M+NH_4]^+$ = 1022.1724 m/z; Δ = +1.11 ppm

$[\alpha]_D^{20}$ = -3.4 (*c* 1.3, $CHCl_3$)

5.2.34 Allyl 2-azido-3-*O*-benzoyl-4,6-*O*-benzylidene-2-deoxy-β-D-mannopyranosyl-(1→4)-3,6-di-*O*-benzyl-2-deoxy-2-(tetrachlorophthalimido)-β-D-glucopyranosyl-(1→3)-2-azido-4,6-*O*-benzylidene-2-deoxy-β-D-mannopyranosyl-(1→4)-3,6-di-*O*-benzyl-2-deoxy-2-(tetrachlorophthalimido)-β-D-glucopyranoside (**43**)

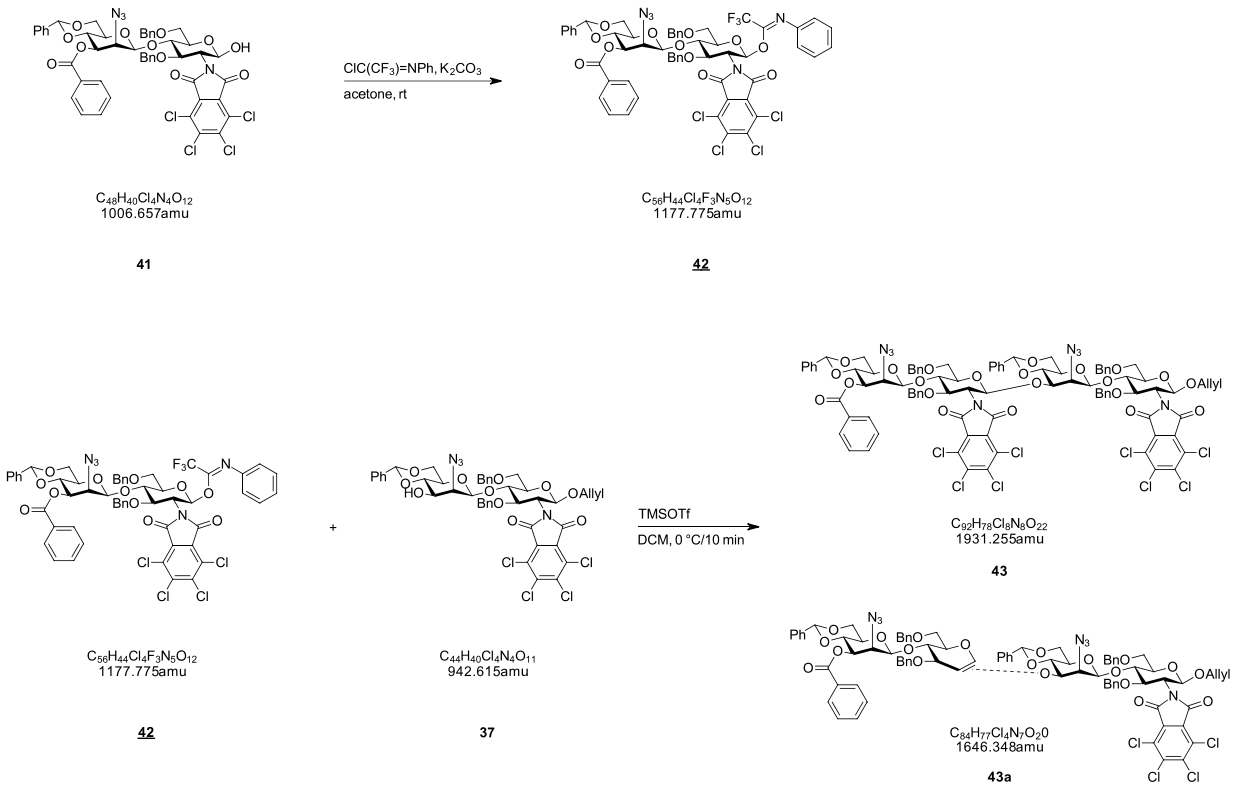

To a solution of **41** (64.0 mg, 63.6 µmol, 1.0 equiv.) in acetone (HPLC grade, 2 ml) were added 2,2,2-trifluoro-*N*-phenylacetimidoyl chloride (100 µl, 623 µmol, 2.3 equiv.) and potassium carbonate (23.7 mg, 0.17 mmol, 3.0 equiv.). To the reaction was added one drop of water to enhance solubility of the base. Monitoring *via* TLC (HPTLC, toluene/ethyl acetate 10:1) indicated full consumption of the starting material after 2 hours at ambient temperature. The reaction mixture was diluted with ethyl acetate to precipitate the base. The solid material was removed *via* filtration over Celite® with ethyl acetate. Removal of the volatiles in *vacuo* afforded a brownish crude liquid. Purification *via* manual column chromatography using silica gel (column: pre-packed Isolute® 2 g Flash SI/6 ml, liquid loading with toluene + 0.1% pyridine, applying a gradient of ethyl acetate in toluene with 0.1% pyridine from 0.5% to 1%) afforded 81% (61 mg) of donor **42**. The intermediate was stored at -20 °C.

To a suspension of glycosyl donor **42** (65.7 mg, 55.8 µmol, 1.0 equiv.), glycosyl acceptor **37** (78.9 mg, 83.7 µmol, 1.5 equiv.) and molecular sieves (4 Å, powdered, 390 mg) in dichloromethane (anhydrous, 9.0 ml) was added trimethylsilyl triflate (83 µM in dichloromethane, 168 µl, 14.0 nmol, 0.02 mol%) at 0 °C. Monitoring *via* TLC (HPTLC, toluene/ethyl acetate 10:1) indicated full consumption of **37** after 10 minutes at 0 °C. The reaction was quenched by addition of pyridine (0.2 ml) at 0 °C. The solid material was removed *via* filtration over Celite® with dichloromethane. Removal of the volatiles in *vacuo* afforded roughly a yellowish crude material. Purification *via* automated column chromatography using silica gel (Interchim PuriFlash® 4/25, liquid loading: 3x 0.5 ml toluene, column: F025, 20 ml/min, 5 ml/fraction, collection *via* threshold: 5 mV, applying a gradient of ethyl acetate in toluene from 0% to 15% in 7 CV then isocratic for 5 CV) afforded 61% (77 mg) of **43** and 21% (23 mg) of **43a** as colorless solid materials.[139]

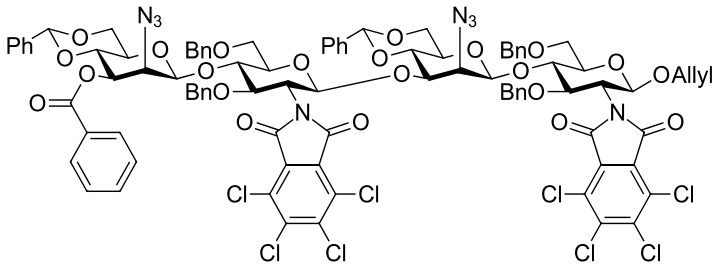

$C_{92}H_{78}Cl_8N_8O_{22}$
1931.255 amu

43

R_f = 0.27 in toluene/ethyl acetate 10:1

^{1}H NMR (600 MHz, $CDCl_3$): δ = 8.10 – 8.09 (m, 2 H, Ar), 7.61 – 7.58 (m, 1 H, Ar), 7.43 – 7.30 (m, 16 H, Ar), 7.23 – 7.13 (m, 6 H, Ar), 7.03 – 7.00 (m, 4 H, Ar), 6.90 – 6.86 (m, 4 H, Ar), 6.73 – 6.69 (m, 2 H, Ar), 5.72 – 5.65 (m, 1 H, CH_2CH=CH_2), 5.50 (s, 1 H, PhCH_A), 5.45 (d, $^3J_{1,2}$ = 8.7 Hz, $^1J_{C1B,H1B}$ = 160.8 Hz, 1 H, H_{1B}), 5.26 (s, 1 H, PhCH_C), 5.16 (dd, $J_{2,3}$ = 3.8 Hz, $J_{3,4}$ = 9.9 Hz, 1 H, H_{3A}), 5.12 – 5.09 (m, 2 H, H_{1D}, CH_2CH=CH_2), 5.06 – 5.04 (m, 1 H, CH_2CH=C$H_{2'}$), 4.87 (d, $J_{1,2}$ = 1 Hz, 1 H, H_{1A}), 4.80 – 4.77 (m, 2 H, 3-*O*-Bn_B, 6-*O*-Bn_B), 4.73 (d, J_{gem} = 13.1 Hz, 1 H, 3-*O*-Bn_D), 4.69 – 4.66 (m, 2 H, H_{1C}, 6-*O*-Bn_D), 4.56 (d, J_{gem} = 12.1 Hz, 1 H, 6-*O*-$Bn_{B'}$), 4.47 – 4.42 (m, 2 H, 6-*O*-$Bn_{D'}$, 3-*O*-$Bn_{B'}$), 4.34 (d, J_{gem} = 13.1 Hz, 1 H, 3-*O*-$Bn_{D'}$), 4.29 (dd, J_{gem} = 10.5 Hz, J_{vic} = 4.8 Hz, 1 H, H_{6A}), 4.23 – 3.95 (m, 11 H, CH_2CH=CH_2, H_{2A}, H_{2B}, H_{2D}, H_{6C}, H_{3B}, H_{3D}, H_{4A}, H_{4B}, H_{4D}), 3.88 – 3.87 (m, 1 H, H_{2C}), 3.77 – 3.69 (m, 6 H, H_{3C}, $H_{6A'}$, H_{6B}, $H_{6B'}$, H_{6D}, $H_{6D'}$), 3.63 (t, *J* = 9.6 Hz, 1 H, H_{4C}), 3.56 (t, *J* = 10.3 Hz, 1 H, $H_{6C'}$), 3.51 – 3.49 (m, 2 H, H_{5B}, H_{5D}), 3.30 – 3.26 (m, 1 H, H_{5A}), 3.09 – 3.05 (m, 1 H, H_{5C}) ppm

^{13}C-APT NMR (150 MHz, $CDCl_3$): δ = 165.79, 139.74, 138.96, 138.75, 137.86, 137.64, 137.07, 137.01, 133.67 (CH_2CH=CH_2), 130.10, 129.41, 129.22, 128.88, 128.81, 128.73, 128.64, 128.44, 128.40, 128.36, 128.30, 128.04, 127.97, 127.91, 126.98, 126.84, 126.23, 125.84, 117.73 (CH_2CH=CH_2), 101.90 (PhCH_A), 101.38 (PhCH_C), 100.68 (C_{1C}), 100.32 (C_{1A}), 97.14 (C_{1D}), 95.50 (C_{1B}). 79.31 (C_{4D}), 79.18 (C_{4B}), 77.95 (C_{3B}, C_{3D}), 75.69 (C_{4A}), 75.62 (C_{4C}), 75.50 (3-*O*-Bn_B), 75.45 (3-*O*-Bn_D), 75.00 (C_{5B}, C_{5D}), 74.53 (C_{3C}), 73.94 (6-*O*-Bn_D), 73.77 (6-*O*-Bn_B), 71.44 (C_{3A}), 69.94 (CH_2CH=CH_2), 68.56 (C_{6A}), 68.37 (C_{6C}), 68.15 (C_{6B}, C_{6D}), 67.62 (C_{5C}), 67.43 (C_{5A}), 63.91 (C_{2C}), 63.05 (C_{2A}), 56.44 (C_{2D}), 55.42 (C_{2B}) ppm

ESI-TOF-MS: calc.: $[M+ NH_4]^+$ = 1944.3077 m/z; measured.: $[M+NH_4]^+$ = 1944.3059 m/z; Δ = +0.91 ppm

$[\alpha]_D^{20}$ = -7.8 (*c* 0.2, $CHCl_3$)

5.2.35 Byproduct **43a**

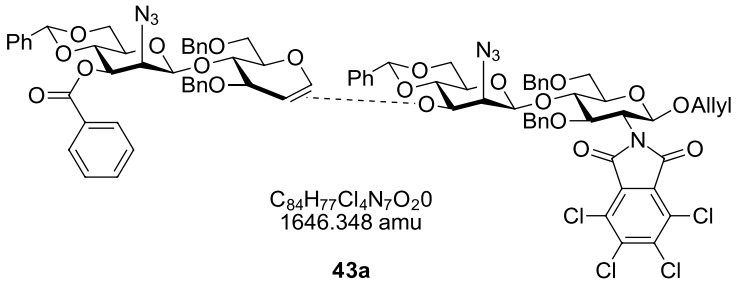

$C_{84}H_{77}Cl_4N_7O_{20}$
1646.348 amu

43a

R_f = 0.56 in toluene/ethyl acetate 10:1

^{1}H NMR (600 MHz, $CDCl_3$): δ = 8.11 – 8.09 (m, 2 H, Ar), 7.61 – 7.58 (m, 1 H, Ar), 7.48 – 7.31 (m, 21 H, Ar), 7.07 – 7.05 (m, 4 H, Ar), 7.00 – 6.98 (m, 2 H, Ar), 6.92 – 6.88 (m, 3 H, Ar), 6.73 – 6.71 (m, 1 H, Ar), 6.63 (d, *J* = 1.4 Hz, 1 H, H_{1B} or H_{2B}), 5.73 – 5.66 (m, 1 H, CH_2CH=CH_2), 5.33 (s, 1 H, $PhCH_A$), 5.47 (s, 1 H, $PhCH_C$), 5.20 (dd, $J_{2,3}$ = 3.8 Hz, $J_{3,4}$ = 10.1 Hz, 1 H, H_{3A}), 5.14 – 5.09 (m, 2 H, H_{1D}, CH_2CH=CH_2), 5.06 – 5.02 (m, 2 H, CH_2CH=CH_2, H_{1A}), 4.84 – 4.72 (m, 5 H, 4x Bn, H_{1C}), 4.60 (d, *J* = 11.8 Hz, 1 H, Bn), 4.56 – 4.54 (m, 2 H, Bn, H_{3B}), 4.46 – 4.43 (m, 2 H, Bn, H_{4B}), 4.35 (d, *J* = 12.5 Hz, 1 H, Bn), 4.31 – 4.20 (m, 6 H, H_{5B}, H_6*, H_6*, H_{2A}, CH_2CH=CH_2, H_{3D}), 4.12 – 4.05 (m, 3 H, H_{2D}, H_{4A}, H_{4D}), 4.00 – 3.96 (m, 1 H, CH_2CH=CH_2), 3.94 – 3.83 (m, 3 H, H_{6B}, $H_{6B'}$, H_6*), 3.80 – 3.71 (m, 5 H, H_{3C}, H_6*, H_6*, H_{2C}, H_{4C}), 3.66 (t, *J* = 10.3 Hz, 1 H, H_6*), 3.59 – 3.57 (m, 1 H, H_{5D}), 3.35 – 3.31 (m, 1 H, H_{5A}), 3.18 – 3.14 (m, 1 H, H_{5C}) ppm

^{13}C NMR (150 MHz, $CDCl_3$): δ = 165.84, 162.88, 147.16 (C_{1B} or C_{2B}), 139.92, 139.74, 139.06, 138.73, 137.90, 137.60, 137.40, 137.04, 133.69 (CH_2CH=CH_2), 133.63, 130.10, 129.74, 129.42, 129.21, 129.07, 128.83, 128.73, 128.62, 128.40, 128.34, 128.25, 128.20, 128.14, 128.08, 127.98, 127.84, 127.37, 127.18, 126.84, 126.26, 126.22, 117.68 (CH_2CH=CH_2), 108.22, 102.00 ($PhCH_C$), 101.90 ($PhCH_A$), 100.26 (C_{1C}), 100.09 (C_{1A}), 97.22 (C_{1D}), 79.25 (C_{4D}), 78.50 (C_{4C}), 78.22 (C_{3D}), 77.53 (C_{5B}), 75.62 (C_{4A}), 75.48 (3-*O*-Bn_D), 75.43 (C_{3B}), 74.56 (C_{5D}), 74.02 (3-*O*-Bn_B), 73.97 (Bn), 73.90 (Bn), 72.08 (C_{3C}), 71.39 (C_{3A}), 69.95 (CH_2CH=CH_2), 68.54 (C_6*, C_6*), 68.45 (C_6*), 67.67 (C_6*), 67.59 (C_{5A}), 67.44 (C_{5C}),66.15 (C_{2C}),62.82 (C_{2A}), 56.49 (C_{2D}), 0.40 ppm

$[\alpha]_D^{20}$ = -0.7 (*c* 1.7, $CHCl_3$)

5.2.36 2-Acetamido-2-deoxy-1,3,4,6-tetra-*O*-acetyl-D-mannopyranose (**55**)

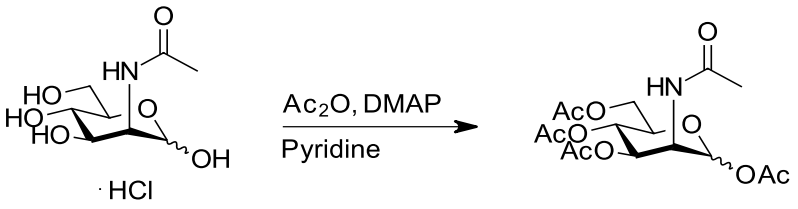

$C_8H_{14}ClNO_6$
255.652 amu

$C_{16}H_{23}NO_{10}$
389.354 amu

54 **55**

To a solution of **54** (4.00 g, 15.52 mmol, 1.00 equiv.) in pyridine (dry, 40 ml) were added acetic anhydride (18.34 ml, 0.19 mol, 12.50 equiv.) and 4-(dimethylamino)pyridine (catalytic amount) at 0 °C. The reaction was slowly warmed to ambient temperature. Monitoring *via* TLC (toluene/ethyl acetate 1:1) indicated full consumption of the starting material after 18 hours. The reaction was quenched by addition of ethanol (15 ml, > 12,5 equiv.) at 0 °C, followed by saturated aqueous sodium bicarbonate after 10 minutes. The crude material was isolated *via* extraction with ethyl acetate (3x). The combined organic layers were washed with water and brine. Drying over magnesium sulfate and removal of the volatiles in *vacuo* *via* azeotropic distillation with toluene afforded >99% (6.30 g) of a crude material. The residue was re-dissolved in ethyl acetate, washed with saturated aqueous sodium bicarbonate, 2 M sodium bisulfate and brine. The solvent was removed in *vacuo* to afford 77% (4.63 g) of **55** as a colorless powder.

The analytical data is in accordance to the literature.[130]

5.2.37 2-Methyl-4,5-dihydro-(3,4,6-tri-*O*-acetyl-2-deoxy-β-D-mannopyranoso)[2,1-d]-1,3-oxazoline (**56**)

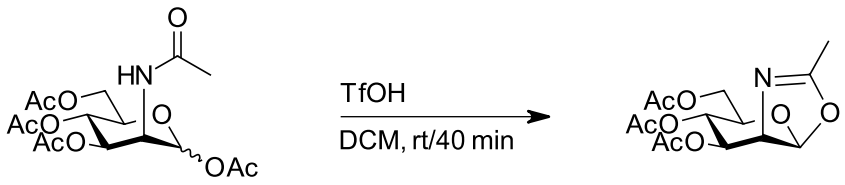

$C_{16}H_{23}NO_{10}$
389.354 amu

55

$C_{14}H_{19}NO_8$
329.302 amu

56

To a solution of **55** (1.50 g, 3.85 mmol, 1.00 equiv.) in dichloromethane (dry, 6 ml) was added triflic acid (1.01 ml, 11.55 mmol, 3.00 equiv.) at 0 °C. The reaction was slowly warmed to ambient temperature. Monitoring *via* TLC (ethyl acetate) indicated full consumption of the starting material after 2 hours. The reaction was quenched by slow addition of triethylamine (2.15 ml, 15.40 mmol, 4.00 equiv.) at 0 °C. The reaction was diluted with dichloromethane and water. The layers were separated and the aqueous phase was re-extracted with dichloromethane (3x). The combined organic layers were washed with water, aqueous phosphate buffer (1 M, pH 6.5) and water. Drying over magnesium sulfate and removal of the volatiles in *vacuo* afforded 95% (1.21 g) of **56** as an orange solid.

The analytical data is in accordance to the literature.[218]

5.2.38 2-Acetamido-3,4,6-tri-*O*-acetyl-2-deoxy-α-D-mannopyranosyl phosphate (**58**)

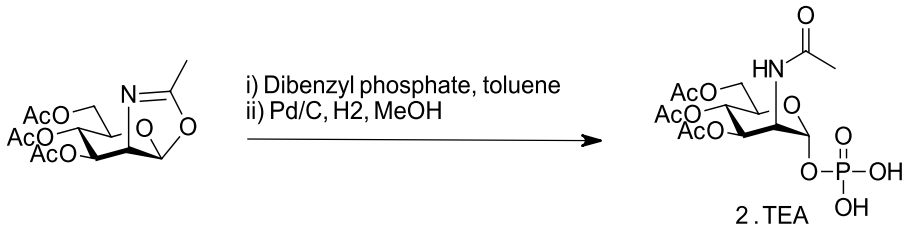

$C_{14}H_{19}NO_8$
329.302 amu

56

$C_{26}H_{56}N_3O_{12}P$
633.709amu

58

To a mixture of **56** (300 mg, 0.91 mmol, 1.00 equiv.) and dibenzyl phosphate (406 mg, 1.46 mmol, 1.60 equiv.) was added toluene (dry, 8.5 ml) at ambient temperature under argon atmosphere. Monitoring *via* LC-MS (column: C_{18}, profile: 5%→100% in 15 min) indicated pre-dominantly the phosphotriester after 15 hours. To the crude reaction was added methanol (anhydrous, 8.5 ml) and palladium on charcoal (10%, catalytic amount). The atmosphere was changed to hydrogen. Monitoring *via* LC-MS (column: C_{18}, profile: 5%→100% in 15 min) after 7 hours at ambient temperature indicated pre-dominantly **58**, accompanied by phosphodiester intermediate (phosphomonoester/phosphodiester 6.4:1) and traces of hemiacetal. The solid material was removed *via* centrifugation and removal of the volatiles in *vacuo* afforded a crude yellow oil. To the crude yellow oil was added water (Milli Q, < 1ml) and an even emulsion was obtained after using a Vortex mixer. Neutralization by addition of triethylamine yielded a yellow solution. Purification *via* anion-exchange chromatography using Dowex® 1X8 HCO_3^- form (column: F012/half packed, flow: gravitation, 4 ml/fraction, 2 fraction/CV, ~ 8 ml/CV, applying a step-wise gradient of aqueous triethylammonium bicarbonate with pH 8, profile: 2 CV → 0 M, 2 CV → 0.05 M, 2 CV → 0.15 M, 12 CV → 0.25 M) afforded 781 mg of **58** as an off-colorless powder that was accompanied by an excess of salt. Desalting *via* size-exclusion chromatography using Bio-Gel® P-2 Media (eluent: 10 mM NaCl and 0.02% NaN_3 in H_2O/EtOH 95:5 – degassed *via* ultra-sonic, bed: ~3 g dry gel/9 ml hydrated, column: 30 x 1 cm, loading: 200 mg in 0.7 ml buffer = 8 vol%, 38 s/drop, 1 ml/fraction, 15 min/fraction, Pharmacia LKB FRAC-100) afforded 21% (122 mg) of **58** as triethylammonium species.

The analytical data is in accordance to the literature.[217,219]

5.2.39 UDP-Man*N*Ac (**61**)

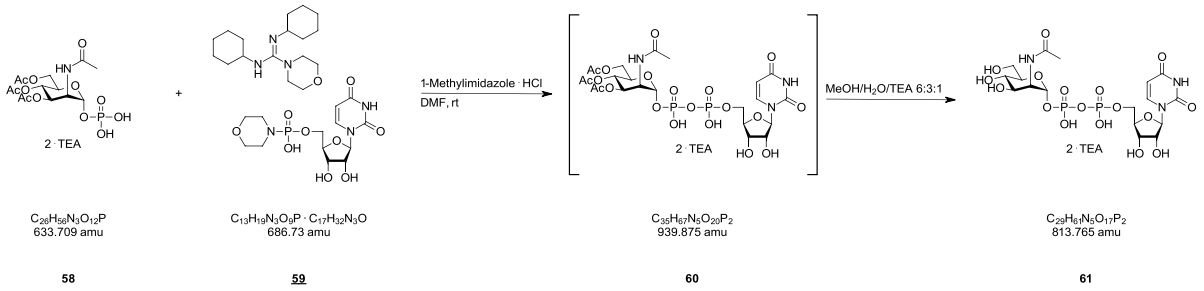

To a suspension of 1-methylimidazolium chloride (85 mg, 0.72 mmol, 5.80 equiv.) in dimethylformamide (anhydrous, 0.5 ml) were added **59** (136 mg, 0.20 mmol, 1.60 equiv.) in dimethylformamide (anhydrous, 1 ml) and **58** (78 mg, 0.12 mmol, 1.00 equiv.) in dimethylformamide (anhydrous, 1.0 ml) to yield a homogenous mixture at ambient temperature. The reaction was stirred at ambient temperature. Monitoring *via* LC-MS (column: C_4, profile: 5%→90% in 20 min) indicated full consumption of the starting material after 23 hours. The reaction was quenched by addition of methanol (0.1 ml). Removal of the volatiles in *vacuo* afforded over 300 mg of a crude brown residue. Coarse purification *via* manual reverse-phase column chromatography using C_{18} material (Interchim PuriFlash® 4/25, liquid loading in starting conc., column: 4 g C18/~6.5 ml in F006, 3 ml/min, 1 ml/fraction, applying a gradient of methanol in aqueous 13 mM NH_4OAc, profile: 5% in 3 CV, 5% to 90% in 4 CV, 90% in 5 CV) afforded 91 mg of **60** as a brownish foam.

A solution of **60** (91 mg) in a methanol/water/triethylamine (7 ml, 6:3:1) was stirred at ambient temperature. Monitoring *via* TLC (chloroform/methanol/ammonium acetate (1 N) 10:10:1) and LC-MS (column: C_4, profile: 5%→90% in 20 min) indicated full consumption of **60** and the presence of **61** after 3 hours. The reaction was diluted with water (Milli Q) and methanol was removed in *vacuo* with a rotary evaporator. Removal of the aqueous volatiles *via* lyophilization afforded 103 mg of a crude material. Purification *via* FPLC (ÄKTA purifier P-900 system, column: BIO-RAD Bio-Scale™ Mini Macro-Prep® High Q Cartridge, loading: ~2.5 ml in starting conc., 5 ml/fraction, 2.5 ml/min, eluent: aqueous triethylammonium bicarbonate pH 8.78, profile: 0.05 M for 7 CV, 0.05 M to 0.25 M in 30 CV, 0.25 M for 4 CV) afforded 20% (20.5 mg) of **61**.

The analytical data is in accordance to the literature.[217,220,221]

6 References

1. Dörr, T., Moynihan, P. J. & Mayer, C. Editorial: Bacterial Cell Wall Structure and Dynamics. *Front Microbiol* **10**, (2019).

2. Madigan Michael. *Brock Biology of Microorganisms, Global Edition*. (Pearson, 2021).

3. Vollmer, W., Blanot, D. & De Pedro, M. A. Peptidoglycan structure and architecture. *FEMS Microbiol Rev* **32**, 149–167 (2008).

4. Silhavy, T. J., Kahne, D. & Walker, S. The Bacterial Cell Envelope. *Cold Spring Harb Perspect Biol* **2**, a000414–a000414 (2010).

5. Glauert, A. M. & Thornley, M. J. The Topography Of The Bacterial Cell Wall. *Annu Rev Microbiol* **23**, 159–198 (1969).

6. Archibald, A. R., Hancock, I. C. & Harwood, C. R. Cell Wall Structure, Synthesis, and Turnover. in *Bacillus subtilis and Other Gram-Positive Bacteria* 379–410 (ASM Press, 2014). doi:10.1128/9781555818388.ch27.

7. Pooley, H. M. & Karamata, D. Chapter 9 Teichoic acid synthesis in Bacillus subtilis: genetic organization and biological roles. in *New Comprehensive Biochemistry* vol. 27 187–198 (1994).

8. Schäffer, C. & Messner, P. The structure of secondary cell wall polymers: how Gram-positive bacteria stick their cell walls together. *Microbiology (N Y)* **151**, 643–651 (2005).

9. Blackler, R. J. *et al.* Structural basis of cell wall anchoring by SLH domains in *Paenibacillus* alvei. *Nat Commun* **9**, 1–11 (2018).

10. Sleytr, U. B. *et al.* S-layers as a tool kit for nanobiotechnological applications. *FEMS Microbiol Lett* **267**, 131–144 (2007).

11. Messner, P., Schäffer, C. & Kosma, P. Bacterial cell-envelope glycoconjugates. in *Advances in Carbohydrate Chemistry and Biochemistry* vol. 69 209–272 (2013).

12. Sára, M. & Sleytr, U. B. S-Layer Proteins. *J Bacteriol* **182**, 859–868 (2000).

13. Messner, P., Schäffer, C., Egelseer, E. M. & Sleytr, U. B. Occurrence, structure, chemistry, genetics, morphogenesis, and functions of S-layers. in *Prokaryotic Cell Wall Compounds: Structure and Biochemistry* 53–109 (Springer Berlin Heidelberg, 2010). doi:10.1007/978-3-642-05062-6_2.

14. Baranova, E. *et al.* SbsB structure and lattice reconstruction unveil Ca^{2+} triggered S-layer assembly. *Nature* **487**, 119–122 (2012).

15. Arbing, M. A. *et al.* Structure of the surface layer of the methanogenic archaean *Methanosarcina acetivorans*. *PNAS* **109**, 11812–11817 (2012).

16. Chung, S., Shin, S.-H., Bertozzi, C. R. & De Yoreo, J. J. Self-catalyzed growth of S layers via an amorphous-to-crystalline transition limited by folding kinetics. *PNAS* **107**, 16536–16541 (2010).

17. Pum, D., Toca-Herrera, J. & Sleytr, U. S-Layer Protein Self-Assembly. *Int J Mol Sci* **14**, 2484–2501 (2013).

18. Altman, E., Brisson, J.-R., Messner, P. & Sleytr, U. B. Structure of the glycan chain from the surface layer glycoprotein of *Bacillus alvei* CCM 2051. *Biochem Cell Biol* **69**, 72–78 (1991).

19. Zarschler, K., Janesch, B., Zayni, S., Schäffer, C. & Messner, P. Construction of a Gene Knockout System for Application in *Paenibacillus alvei* CCM 2051 ^{T}, Exemplified by the S-Layer Glycan Biosynthesis Initiation Enzyme WsfP. *Appl Environ Microbiol* **75**, 3077–3085 (2009).

20. Sara, M., Moser-Thier, K., Kainz, U. & Sleytr, U. B. Characterization of S-layers from mesophilic bacillaceae and studies on their protective role towards muramidases. *Arch Microbiol* **153**, 209–214 (1990).

21. A.L. Houwink & J.B. Le Poole. Eine Struktur in der Zellmembran einer Bakterie. *Physikalische Verhandlungen* **3**, 98 (1952).

22. Engelhardt, H. Are S-layers exoskeletons? The basic function of protein surface layers revisited. *J Struct Biol* **160**, 115–124 (2007).

23. Beveridge, T. J. *et al.* V. Functions of S-layers. *FEMS Microbiol Rev* **20**, 99–149 (1997).

24. Legg, M. S. G. *et al.* The S-layer homology domains of *Paenibacillus alvei* surface protein SpaA bind to cell wall polysaccharide through the terminal monosaccharide residue. *J Biol Chem* **298**, 101745 (2022).

25. Messner, P., Steiner, K., Zarschler, K. & Schäffer, C. S-layer nanoglycobiology of bacteria. *Carbohydr Res* **343**, 1934–1951 (2008).

26. Zarschler, K. *et al.* Protein tyrosine *O*-glycosylation -- A rather unexplored prokaryotic glycosylation system. *Glycobiology* **20**, 787–798 (2010).

27. Pleschberger, M. *et al.* An S-Layer Heavy Chain Camel Antibody Fusion Protein for Generation of a Nanopatterned Sensing Layer To Detect the Prostate-Specific Antigen by Surface Plasmon Resonance Technology. *Bioconjug Chem* **15**, 664–671 (2004).

28. Sekot, G. *et al.* Potential of the *Tannerella forsythia* S-layer to Delay the Immune Response. *J Dent Res* **90**, 109–114 (2011).

29. Settem, R. P., Honma, K. & Sharma, A. Neutrophil Mobilization by Surface-Glycan Altered Th17-Skewing Bacteria Mitigates Periodontal Pathogen Persistence and Associated Alveolar Bone Loss. *PLoS One* **9**, e108030 (2014).

30. Konstantinov, S. R. *et al.* S layer protein A of *Lactobacillus acidophilus* NCFM regulates immature dendritic cell and T cell functions. *PNAS* **105**, 19474–19479 (2008).

31. Sleytr, U. B., Schuster, B., Egelseer, E.-M. & Pum, D. S-layers: principles and applications. *FEMS Microbiol Rev* **38**, 823–864 (2014).

32. Hynönen, U. & Palva, A. Lactobacillus surface layer proteins: structure, function and applications. *Appl Microbiol Biotechnol* **97**, 5225–5243 (2013).

33. Fagan, R. P. & Fairweather, N. F. Biogenesis and functions of bacterial S-layers. *Nat Rev Microbiol* **12**, 211–222 (2014).

34. Gerbino, E., Carasi, P., Mobili, P., Serradell, M. A. & Gómez-Zavaglia, A. Role of S-layer proteins in bacteria. *World J Microbiol Biotechnol* **31**, 1877–1887 (2015).

35. Schäffer, C. & Messner, P. Emerging facets of prokaryotic glycosylation. *FEMS Microbiol Rev* **41**, 49–91 (2017).

36. Ferner-Ortner, J., Mader, C., Ilk, N., Sleytr, U. B. & Egelseer, E. M. High-Affinity Interaction between the S-Layer Protein SbsC and the Secondary Cell Wall Polymer of *Geobacillus stearothermophilus* ATCC 12980 Determined by Surface Plasmon Resonance Technology. *J Bacteriol* **189**, 7154–7158 (2007).

37. Huber, C. *et al.* Heterotetramers Formed by an S-Layer-Streptavidin Fusion Protein and Core-Streptavidin as a Nanoarrayed Template for Biochip Development. *Small* **2**, 142–150 (2006).

38. Schäffer, C. & Messner, P. Surface-layer glycoproteins: an example for the diversity of bacterial glycosylation with promising impacts on nanobiotechnology. *Glycobiology* **14**, 31R-42R (2004).

39. Schäffer, C. *et al.* Novel Biocatalysts Based on S-Layer Self-Assembly of *Geobacillus Stearothermophilus* NRS 2004/3a: A Nanobiotechnological Approach. *Small* **3**, 1549–1559 (2007).

40. Steiner, K. *et al.* Recombinant Glycans on an S-Layer Self-Assembly Protein: A New Dimension for Nanopatterned Biomaterials. *Small* **4**, 1728–1740 (2008).

41. Völlenkle, C. *et al.* Construction of a functional S-layer fusion protein comprising an immunoglobulin G-binding domain for development of specific adsorbents for extracorporeal blood purification. *Appl. Environ. Microbiol.* **70**, 1514–1521 (2004).

42. Moll, D. *et al.* S-layer-streptavidin fusion proteins as template for nanopatterned molecular arrays. *PNAS* **99**, 14646–14651 (2002).

43. Archibald, A. R., Baddiley, J. & Blumsom, N. L. The Teichoic Acids. in *Advances in Enzymology - and Related Areas of Molecular Biology* 223–253 (2006). doi:10.1002/9780470122754.ch5.

44. Hancock, I. C. & Baddiley, J. Biosynthesis of the Bacterial Envelope Polymers Teichoic Acid and Teichuronic Acid. in *The Enzymes of Biological Membranes* 279–307 (Springer US, 1985). doi:10.1007/978-1-4613-2355-6_8.

45. Martonosi, A. N. Membrane Structure and Dynamics. in *The Enzymes of Biological Membranes* (ed. Martonosi, A. N.) vol. 1 (Springer US, 1985).

46. Ward, J. B. Teichoic and teichuronic acids: biosynthesis, assembly, and location. *Microbiol Rev* **45**, 211–243 (1981).

47. Araki, Y. & Ito, E. Linkage Units in Cell Walls of Gram-Positive Bacteria. *Crit Rev Microbiol* **17**, 121–135 (1989).

48. Naumova, I. B. & Shashkov, A. S. Anionic polymers in cell walls of gram-positive bacteria. *Biochemistry (Mosc)* **62**, 809–40 (1997).

49. Naumova, I. B. *et al.* Cell wall teichoic acids: structural diversity, species specificity in the genus *Nocardiopsis* , and chemotaxonomic perspective. *FEMS Microbiol Rev* **25**, 269–283 (2001).

50. Kojima, N., Araki, Y. & Ito, E. Structure of the linkage units between ribitol teichoic acids and peptidoglycan. *J Bacteriol* **161**, 299–306 (1985).

51. Neuhaus, F. C. & Baddiley, J. A continuum of anionic charge: structures and functions of D-alanyl-teichoic acids in gram-positive bacteria. *Microbiol Mol Biol Rev* **67**, 686–723 (2003).

52. Brown, S., Santa Maria, J. P. & Walker, S. Wall Teichoic Acids of Gram-Positive Bacteria. *Annu Rev Microbiol* **67**, 313–336 (2013).

53. Endl, J., Seidl, H. P., Fiedler, F. & Schleider, K. H. Chemical composition and structure of cell wall teichoic acids of staphylococci. *Arch Microbiol* **135**, 215–223 (1983).

54. Endl, J., Seidl, P. H., Fiedler, F. & Schleifer, K. H. Determination of cell wall teichoic acid structure of staphylococci by rapid chemical and serological screening methods. *Arch Microbiol* **137**, 272–280 (1984).

55. Messner, P. & Schäffer, C. Prokaryotic Glycoproteins. in *Progress in the Chemistry of Organic Natural Products* vol. 85 51–124 (2003).

56. Novotny, R., Pfoestl, A., Messner, P. & Schäffer, C. Genetic organization of chromosomal S-layer glycan biosynthesis loci of Bacillaceae. *Glycoconj J* **20**, 435–447 (2003).

57. Johnson, S. D., Lacher, K. P. & Anderson, J. S. Carbon-13 NMR spectroscopic study of teichuronic acid from *Micrococcus luteus* cell walls. Comparison of the polysaccharide isolated from cells with that synthesized in vitro. *Biochemistry* **20**, 4781–4785 (1981).

58. Hase, S. & Matsushima, Y. Structural Studies on a Glucose-containing Polysaccharide Obtained from Cell Walls of *Micrococcus lysodeikticus*. *J Biochem* **72**, 1117–1128 (1972).

59. Deng, L. L., Alexander, A. A., Lei, S. & Anderson, J. S. The Cell Wall Teichuronic Acid Synthetase (TUAS) Is an Enzyme Complex Located in the Cytoplasmic Membrane of *Micrococcus luteus*. *Biochem Res Int* **2010**, 1–8 (2010).

60. Schäffer, C., Graninger, M. & Messner, P. Prokaryotic glycosylation. *Proteomics* **1**, 248–261 (2001).

61. Altman, E., Brisson, J.-R., Messner, P. & Sleytr, U. B. Chemical characterization of the regularly arranged surface layer glycoprotein of *Clostridium thermosaccharolyticum* D120-70. *Eur J Biochem* **188**, 73–82 (1990).

62. Messner, P., Sleytr, U. B., Christian, R., Schulz, G. & Unger, F. M. Isolation and structure determination of a diacetamidodideoxyuronic acid-containing glycan chain from the S-layer glycoprotein of *Bacillus stearothermophilus* NRS 2004/3a. *Carbohydr Res* **168**, 211–218 (1987).

63. Schäffer, C. *et al.* The diacetamidodideoxyuronic-acid-containing glycan chain of *Bacillus stearothermophilus* NRS 2004/3a represents the secondary cell-wall polymer of wild-type *B. stearothermophilus* strains. *Microbiology (N Y)* **145**, 1575–1583 (1999).

64. Schäffer, C. *et al.* A pyrophosphate bridge links the pyruvate-containing secondary cell wall polymer of *Paenibacillus alvei* CCM 2051 to muramic acid. *Glycoconj J* **17**, 681–690 (2000).

65. Steindl, C. *et al.* The first biantennary bacterial secondary cell wall polymer and its influence on S-layer glycoprotein assembly. *Biochem J* **368**, 483–494 (2002).

66. Mesnage, S. Bacterial SLH domain proteins are non-covalently anchored to the cell surface via a conserved mechanism involving wall polysaccharide pyruvylation. *EMBO J* **19**, 4473–4484 (2000).

67. Altman, E., Schäffer, C., Brisson, J.-R. & Messner, P. Isolation and characterization of an amino sugar-rich glycopeptide from the surface layer glycoprotein of *Thermoanaerobacterium thermosaccharolyticum* E207-71. *Carbohydr Res* **295**, 245–253 (1996).

68. Steindl, C., Schäffer, C., Smrečki, V., Messner, P. & Müller, N. The secondary cell wall polymer of *Geobacillus tepidamans* GS5-97T: structure of different glycoforms. *Carbohydr Res* **340**, 2290–2296 (2005).

69. Steiner, K. *et al.* Molecular Basis of S-layer Glycoprotein Glycan Biosynthesis in *Geobacillus stearothermophilus*. *J Biol Chem* **283**, 21120–21133 (2008).

70. Kählig, H. *et al. N*-Acetylmuramic Acid as Capping Element of α-D-Fucose-containing S-layer Glycoprotein Glycans from *Geobacillus tepidamans* GS5–97T. *J Biol Chem* **280**, 20292–20299 (2005).

71. Kosma, P., Wugeditsch, T., Christian, R., Zayni, S. & Messner, P. Glycan structure of a heptose-containing S-layer glycoprotein of *Bacillus thermoaerophillus*. *Glycobiology* **6**, 5–5 (1996).

72. Petersen, B. O. *et al.* Corrigendum to “Structural characterization of the acid-degraded secondary cell wall polymer of *Geobacillus stearothermophilus* PV72/p2” [Carbohydr. Res. 343 (2008) 1346–1358]. *Carbohydr Res* **373**, 52 (2013).

73. Petersen, B. O. *et al.* Structural characterization of the acid-degraded secondary cell wall polymer of *Geobacillus stearothermophilus* PV72/p2. *Carbohydr Res* **343**, 1346–1358 (2008).

74. Ellwood, D. C. & Tempest, D. W. Influence of growth environment on the cell wall anionic polymers in some Gram-positive bacteria. *J Gen Microbiol* **57**, xv (1969).

75. Rogers, H. J., Perkins, H. R. & Ward, J. B. *Microbial Cell Walls and Membranes*. (Springer Netherlands, 1980). doi:10.1007/978-94-011-6014-8.

76. Baddiley, J. Teichoic acids in cell walls and membranes of bacteria. *Essays Biochem* **8**, 35–77 (1972).

77. Fischer, W. Chapter 10 Lipoteichoic acids and lipoglycans. in *New Comprehensive Biochemistry* vol. 27 199–215 (1994).

78. Munson, R. S. & Glaser, L. Teichoic acid and peptidoglycan assembly in Gram-positive organisms. in *Biology of carbohydrates* (eds. Ginsburg, V. & Robbins P) vol. 1 91–122 (Wiley New York, 1981).

79. Navarre, W. W. & Schneewind, O. Surface Proteins of Gram-Positive Bacteria and Mechanisms of Their Targeting to the Cell Wall Envelope. *Microbiol Mol Biol Rev* **63**, 174–229 (1999).

80. Albers, S.-V. & Meyer, B. H. The archaeal cell envelope. *Nat Rev Microbiol* **9**, 414–426 (2011).

81. Kandiba, L. & Eichler, J. Archaeal S-layer glycoproteins: post-translational modification in the face of extremes. *Front Microbiol* **5**, (2014).

82. Janesch, B., Messner, P. & Schäffer, C. Are the Surface Layer Homology Domains Essential for Cell Surface Display and Glycosylation of the S-Layer Protein from *Paenibacillus alvei* CCM 2051T? *J Bacteriol* **195**, 565–575 (2013).

83. Griffiths, S. G. & Lynch, W. H. Characterization of *Aeromonas salmonicida* variants with altered cell surfaces and their use in studying surface protein assembly. *Arch Microbiol* **154**, 308–312 (1990).

84. Thomas, S. R. & Trust, T. J. Tyrosine Phosphorylation of the Tetragonal Paracrystalline Array of *Aeromonas hydrophila*: Molecular Cloning and High-level Expression of the S-layer Protein Gene. *J Mol Biol* **245**, 568–581 (1995).

85. Engelhardt, H. & Peters, J. Structural Research on Surface Layers: A Focus on Stability, Surface Layer Homology Domains, and Surface Layer–Cell Wall Interactions. *J Struct Biol* **124**, 276–302 (1998).

86. Xu, Q. *et al.* Dramatic performance of *Clostridium thermocellum* explained by its wide range of cellulase modalities. *Sci Adv* **2**, (2016).

87. Usenik, A. *et al.* The CWB2 Cell Wall-Anchoring Module Is Revealed by the Crystal Structures of the Clostridium difficile Cell Wall Proteins Cwp8 and Cwp6. *Structure* **25**, 514–521 (2017).

88. Cava, F., De Pedro, M. A., Schwarz, H., Henne, A. & Berenguer, J. Binding to pyruvylated compounds as an ancestral mechanism to anchor the outer envelope in primitive bacteria. *Mol Microbiol* **52**, 677–690 (2004).

89. Finn, R. D. *et al.* The Pfam protein families database: towards a more sustainable future. *Nucleic Acids Res* **44**, D279–D285 (2016).

90. Messner, P., Christian, R., Neuninger, C. & Schulz, G. Similarity of 'core' structures in two different glycans of tyrosine-linked eubacterial S-layer glycoproteins. *J Bacteriol* **177**, 2188–2193 (1995).

91. Zarschler, K. *et al.* Cell surface display of chimeric glycoproteins via the S-layer of *Paenibacillus alvei*. *Carbohydr Res* **345**, 1422–1431 (2010).

92. May, A., Pusztahelyi, T., Hoffmann, N., Fischer, R.-J. & Bahl, H. Mutagenesis of conserved charged amino acids in SLH domains of *Thermoanaerobacterium thermosulfurigenes* EM1 affects attachment to cell wall sacculi. *Arch Microbiol* **185**, 263–269 (2006).

93. Bhavsar, A. P., Truant, R. & Brown, E. D. The TagB Protein in *Bacillus subtilis* 168 Is an Intracellular Peripheral Membrane Protein That Can Incorporate Glycerol Phosphate onto a Membrane-bound Acceptor in Vitro. *J Biol Chem* **280**, 36691–36700 (2005).

94. Formstone, A., Carballido-López, R., Noirot, P., Errington, J. & Scheffers, D.-J. Localization and Interactions of Teichoic Acid Synthetic Enzymes in *Bacillus subtilis*. *J Bacteriol* **190**, 1812–1821 (2008).

95. Hager, F. F. *et al.* Functional Characterization of Enzymatic Steps Involved in Pyruvylation of Bacterial Secondary Cell Wall Polymer Fragments. *Front Microbiol* **9**, (2018).

96. Montoya-Peleaz, P. J. *et al.* Identification of a UDP-Gal: GlcNAc-R galactosyltransferase activity in *Escherichia coli* VW187. *Bioorg Med Chem Lett* **15**, 1205–1211 (2005).

97. Morgan, P. M., Sala, R. F. & Tanner, M. E. Eliminations in the Reactions Catalyzed by UDP-*N*-Acetylglucosamine 2-Epimerase. *J Am Chem Soc* **119**, 10269–10277 (1997).

98. Murkin, A. S., Chou, W. K., Wakarchuk, W. W. & Tanner, M. E. Identification and Mechanism of a Bacterial Hydrolyzing UDP-*N*-Acetylglucosamine 2-Epimerase. *Biochemistry* **43**, 14290–14298 (2004).

99. Mann, P. A. *et al.* Chemical Genetic Analysis and Functional Characterization of Staphylococcal Wall Teichoic Acid 2-Epimerases Reveals Unconventional Antibiotic Drug Targets. *PLoS Pathog* **12**, e1005585 (2016).

100. Missiakas, D. & Schneewind, O. Assembly and Function of the *Bacillus anthracis* S-Layer. *Annu Rev Microbiol* **71**, 79–98 (2017).

101. Choudhury, B. *et al.* The Structure of the Major Cell Wall Polysaccharide of *Bacillus anthracis* Is Species-specific. *J Biol Chem* **281**, 27932–27941 (2006).

102. Oh, S.-Y., Lunderberg, J. M., Chateau, A., Schneewind, O. & Missiakas, D. Genes Required for *Bacillus anthracis* Secondary Cell Wall Polysaccharide Synthesis. *J Bacteriol* **199**, (2017).

103. Chateau, A. *et al.* Galactosylation of the Secondary Cell Wall Polysaccharide of *Bacillus anthracis* and Its Contribution to Anthrax Pathogenesis. *J Bacteriol* **200**, (2018).

104. Liszewski Zilla, M., Chan, Y. G. Y., Lunderberg, J. M., Schneewind, O. & Missiakas, D. LytR-CpsA-Psr Enzymes as Determinants of *Bacillus anthracis* Secondary Cell Wall Polysaccharide Assembly. *J Bacteriol* **197**, 343–353 (2015).

105. Chateau, A. *et al.* Distinct Pathways Carry Out α and β Galactosylation of Secondary Cell Wall Polysaccharide in *Bacillus anthracis*. *J Bacteriol* **202**, (2020).

106. Rismondo, J., Gillis, A. & Gründling, A. Modifications of cell wall polymers in Gram-positive bacteria by multi-component transmembrane glycosylation systems. *Curr Opin Microbiol* **60**, 24–33 (2021).

107. Lazarevic, V. & Karamata, D. The tagGH operon of *Bacillus subtilis* 168 encodes a two-component ABC transporter involved in the metabolism of two wall teichoic acids. *Mol Microbiol* **16**, 345–355 (1995).

108. Schirner, K., Stone, L. K. & Walker, S. ABC Transporters Required for Export of Wall Teichoic Acids Do Not Discriminate between Different Main Chain Polymers. *ACS Chem Biol* **6**, 407–412 (2011).

109. Stefanović, C., Hager, F. F. & Schäffer, C. LytR-CpsA-Psr Glycopolymer Transferases: Essential Bricks in Gram-Positive Bacterial Cell Wall Assembly. *Int J Mol Sci* **22**, 908 (2021).

110. Hübscher, J., Lüthy, L., Berger-Bächi, B. & Stutzmann Meier, P. Phylogenetic distribution and membrane topology of the LytR-CpsA-Psr protein family. *BMC Genomics* **9**, 617 (2008).

111. Forsgren, E. European foulbrood in honey bees. *J Invertebr Pathol* **103**, S5–S9 (2010).

112. Janesch, B. *et al.* Flagellin glycosylation in *Paenibacillus alvei* CCM 2051 ^{T}. *Glycobiology* cwv087 (2015) doi:10.1093/glycob/cwv087.

113. Hager-Mair, F. F. *et al.* Assaying *Paenibacillus alvei* CsaB-Catalysed Ketalpyruvyltransfer to Saccharides by Measurement of Phosphate Release. *Biomolecules* **11**, 1732 (2021).

114. Krauter, S., Schäffer, C. & Kosma, P. Synthesis of a pyruvylated *N*-acetyl-β-D-mannosamine containing disaccharide repeating unit of a cell wall glycopolymer from *Paenibacillus alvei*. *Arkivoc* **2021**, 137–151 (2020).

115. Alex, C. & Demchenko, A. V. Recent Advances in Stereocontrolled Mannosylation: Focus on Glycans Comprising Acidic and/or Amino Sugars. *Chem Rec* **21**, 3278–3294 (2021).

116. Nigudkar, S. S. & Demchenko, A. V. Stereocontrolled 1,2-*cis* glycosylation as the driving force of progress in synthetic carbohydrate chemistry. *Chem Sci* **6**, 2687–2704 (2015).

117. El Ashry, E., Rashed, N. & Ibrahim, E. Strategies of Synthetic Methodologies for Constructing β-Mannosidic Linkage. *Curr Org Synth* **2**, 175–213 (2005).

118. Leng, W.-L., Yao, H., He, J.-X. & Liu, X.-W. Venturing beyond Donor-Controlled Glycosylation: New Perspectives toward Anomeric Selectivity. *Acc Chem Res* **51**, 628–639 (2018).

119. Paulsen, H. & Lockhoff, O. Bausteine von Oligosacchariden, XXX. Neue effektive β-Glycosidsynthese für Mannose-Glycoside Synthesen von Mannose-haltigen Oligosacchariden. *Chem Ber* **114**, 3102–3114 (1981).

120. Van Boeckel, C. A. A., Beetz, T. & Van Aelst, S. F. Substituent effects on carbohydrate coupling reactions promoted by insoluble silver salts. *Tetrahedron* **40**, 4097–4107 (1984).

121. Crich, D. & Chandrasekera, N. S. Mechanism of 4,6-*O*-Benzylidene-Directed β-Mannosylation as Determined by α-Deuterium Kinetic Isotope Effects. *Angew Chem Int Ed* **43**, 5386–5389 (2004).

122. Pravdic, N. & Fletcher, H. G. Behavior of 2-acetamido-2-deoxy-D-mannose with isopropenyl acetate in the presence of *p*-toluenesulfonic acid. I. Isolation and identification of derivatives of 2-amino-D-glucal (2-amino-1,2-dideoxy-D-arabino-hex-1-enopyranose) and of other products. *J Org Chem* **32**, 1806–1810 (1967).

123. Alex, C., Visansirikul, S. & Demchenko, A. V. A versatile approach to the synthesis of mannosamine glycosides. *Org Biomol Chem* **18**, 6682–6695 (2020).

124. Xu, H. *et al.* Stereoselective β-Mannosylation with 2,6-Lactone-bridged Thiomannosyl Donor by Remote Acyl Group Participation. *Chem Asian J* **14**, 1424–1428 (2019).

125. Adhikari, S., Li, X. & Zhu, J. Studies of *S*-But-3-ynyl and *gem*-Dimethyl *S*-But-3-ynyl Thioglycoside Donors in Gold-Catalyzed Glycosylations. *J Carbohydr Chem* **32**, 336–359 (2013).

126. Teodorović, P., Slättegård, R. & Oscarson, S. Improved synthesis of 1,3,4,6-tetra-*O*-acetyl-2-azido-2-deoxy-α-D-mannopyranose. *Carbohydr Res* **340**, 2675–2676 (2005).

127. Angata, T. & Varki, A. Chemical Diversity in the Sialic Acids and Related α-Keto Acids: An Evolutionary Perspective. *Chem Rev* **102**, 439–470 (2002).

128. Banoub, J., Boullanger, P. & Lafont, D. Synthesis of oligosaccharides of 2-amino-2-deoxy sugars. *Chem Rev* **92**, 1167–1195 (1992).

129. Chapman, R. N., Liu, L. & Boons, G.-J. 4,6-*O*-Pyruvyl Ketal Modified *N*-Acetylmannosamine of the Secondary Cell Wall Polysaccharide of *Bacillus anthracis* Is the Anchoring Residue for Its Surface Layer Proteins. *J Am Chem Soc* **140**, 17079–17085 (2018).

130. Manzo, E., Ciavatta, M. L., Pagano, D. & Fontana, A. An efficient and versatile chemical synthesis of bioactive glyco-glycerolipids. *Tetrahedron Lett* **53**, 879–881 (2012).

131. Dąbrowa, K., Niedbała, P. & Jurczak, J. Engineering Light-Mediated Bistable Azobenzene Switches Bearing Urea D-Aminoglucose Units for Chiral Discrimination of Carboxylates. *J Org Chem* **81**, 3576–3584 (2016).

132. Biswas, N. N. *et al.* Synthesis of antimicrobial glucosamides as bacterial quorum sensing mechanism inhibitors. *Bioorg Med Chem* **25**, 1183–1194 (2017).

133. Wu, B., Yang, X. & Yan, M. Synthesis and Structure–Activity Relationship Study of Antimicrobial Auranofin against ESKAPE Pathogens. *J Med Chem* **62**, 7751–7768 (2019).

134. Kosma, P., Strobl, M., Allmaier, G., Schmid, E. & Brade, H. Synthesis of pentasaccharide core structures corresponding to the genus-specific lipopolysaccharide epitope of Chlamydia. *Carbohydr Res* **254**, 105–132 (1994).

135. Wang, C.-C., Kulkarni, S. S., Lee, J.-C., Luo, S.-Y. & Hung, S.-C. Regioselective one-pot protection of glucose. *Nat Protoc* **3**, 97–113 (2008).

136. Iversen, T. & Bundle, D. R. Benzyl trichloroacetimidate, a versatile reagent for acid-catalysed benzylation of hydroxy-groups. *J Chem Soc Chem Commun* 1240 (1981) doi:10.1039/c39810001240.

137. Eckenberg, P., Groth, U., Huhn, T., Richter, N. & Schmeck, C. A useful application of benzyl trichloroacetimidate for the benzylation of alcohols. *Tetrahedron* **49**, 1619–1624 (1993).

138. Okada, Y., Ohtsu, M., Bando, M. & Yamada, H. Benzyl *N*-Phenyl-2,2,2-trifluoroacetimidate: A New and Stable Reagent for *O*-Benzylation. *Chem Lett* **36**, 992–993 (2007).

139. Yu, B. & Tao, H. Glycosyl trifluoroacetimidates. Part 1: Preparation and application as new glycosyl donors. *Tetrahedron Lett* **42**, 2405–2407 (2001).

140. Mukherjee, C., Liu, L. & Pohl, N. L. B. Regioselective Benzylation of 2-Deoxy-2-aminosugars using Crown Ethers: Application to a Shortened Synthesis of Hyaluronic Acid Oligomers. *Adv Synth Catal* **356**, 2247–2256 (2014).

141. Xia, J., Alderfer, J. L., Locke, R. D., Piskorz, C. F. & Matta, K. L. Complex Oligosaccharide Investigations: Synthesis of an Octasaccharide Incorporating the Dimeric Le^x Structure of PSGL-1. *J Org Chem* **68**, 2752–2759 (2003).

142. Zhang, Z., Niikura, K., Huang, X.-F. & Wong, C.-H. A strategy for the one-pot synthesis of sialylated oligosaccharides. *Can J Chem* **80**, 1051–1054 (2002).

143. Ellervik, U. & Magnusson, G. A High Yielding Chemical Synthesis of Sialyl Lewis x Tetrasaccharide and Lewis x Trisaccharide; Examples of Regio- and Stereodifferentiated Glycosylations. *J Org Chem* **63**, 9314–9322 (1998).

144. Nikrad, P. V., Kashem, M. A., Wlasichuk, K. B., Alton, G. & Venot, A. P. Use of human-milk fucosyltransferase in the chemoenzymic synthesis of analogues of the sialyl Lewis and sialyl Lewis tetrasaccharides modified at the C-2 position of the reducing unit. *Carbohydr Res* **250**, 145–160 (1993).

145. Toepfer, A. & Schmidt, R. R. An Efficient Synthesis of the Lewis A (Le ^{a}) Antigen Pentasaccharide Moiety. *J Carbohydr Chem* **12**, 809–822 (1993).

146. Kameyama, A., Ishida, H., Kiso, M. & Hasegawa, A. Synthetic Studies on Sialoglycoconjugates 59: Total Synthesis of Tumor-Associated Ganglioside, Sialyl Le. *J Carbohydr Chem* **13**, 641–654 (1994).

147. Osborn, H. M. I., Brome, V. A., Harwood, L. M. & Suthers, W. G. Regioselective C-3-*O*-acylation and *O*-methylation of 4,6-*O*-benzylidene-β-D-gluco- and galactopyranosides displaying a range of anomeric substituents. *Carbohydr Res* **332**, 157–166 (2001).

148. Szeja, W., Fokt, I. & Grynkiewicz, G. Benzylation of sugar polyols by means of the PTC method. *Recl Trav Chim Pays-Bas* **108**, 224–226 (2010).

149. Crich, D. & Dudkin, V. Why Are the Hydroxy Groups of Partially Protected *N*-Acetylglucosamine Derivatives Such Poor Glycosyl Acceptors, and What Can Be Done about It? A Comparative Study of the Reactivity of *N*-Acetyl-, *N*-Phthalimido-, and 2-Azido-2-deoxy-glucosamine Derivatives in Glycosylation. 2-Picolinyl Ethers as Reactivity-Enhancing Replacements for Benzyl Ethers. *J Am Chem Soc* **123**, 6819–6825 (2001).

150. Roychoudhury, R. & Pohl, N. L. B. Light Fluorous-Tag-Assisted Synthesis of Oligosaccharides. in *Modern Synthetic Methods in Carbohydrate Chemistry* 221–239 (Wiley-VCH Verlag GmbH & Co. KGaA, 2013). doi:10.1002/9783527658947.ch8.

151. Pistorio, S. G., Yasomanee, J. P. & Demchenko, A. V. Hydrogen-Bond-Mediated Aglycone Delivery: Focus on β-Mannosylation. *Org Lett* **16**, 716–719 (2014).

152. Debenham, J. S., Debenham, S. D. & Fraser-Reid, B. *N*-tetrachlorophthaloyl (TCP) for ready protection/deprotection of amino sugar glycosides. *Bioorg Med Chem* **4**, 1909–1918 (1996).

153. Evans, M. E. Methyl 4,6-*O*-benzylidene-α- and -β-D-glucosides. *Carbohydr Res* **21**, 473–475 (1972).

154. Meng, S., Zhong, W., Yao, W. & Li, Z. Stereoselective Phenylselenoglycosylation of Glycals Bearing a Fused Carbonate Moiety toward the Synthesis of 2-Deoxy-β-galactosides and β-Mannosides. *Org Lett* **22**, 2981–2986 (2020).

155. Veselý, J. *et al.* Preparation of Ethyl 2-Azido-2-deoxy-1-thio-β-D-mannopyranosides, and their Rearrangement to 2-*S*-Ethyl-2-thio-β-D-mannopyranosylamines. *Synthesis (Stuttg)* **2006**, 699–705 (2006).

156. Henderson, A. S., Bower, J. F. & Galan, M. C. Carbohydrate-based *N*-heterocyclic carbenes for enantioselective catalysis. *Org. Biomol. Chem.* **12**, 9180–9183 (2014).

157. Knapp, S., Kukkola, P. J., Sharma, S., Dhar, T. G. M. & Naughton, A. B. J. Amino alcohol and amino sugar synthesis by benzoylcarbamate cyclization. *J Org Chem* **55**, 5700–5710 (1990).

158. Alex, C. *et al.* Synthesis of 2-azido-2-deoxy- and 2-acetamido-2-deoxy-D-manno derivatives as versatile building blocks. *Carbohydr Res* **488**, 107900 (2020).

159. Myszka, H., Bednarczyk, D., Najder, M. & Kaca, W. Synthesis and induction of apoptosis in B cell chronic leukemia by diosgenyl 2-amino-2-deoxy-β-D-glucopyranoside hydrochloride and its derivatives. *Carbohydr Res* **338**, 133–141 (2003).

160. Reintjens, N. R. M. *et al.* Synthesis of *C*-Glycosyl Amino Acid Building Blocks Suitable for the Solid-Phase Synthesis of Multivalent Glycopeptide Mimics. *Eur J Org Chem* **2020**, 5126–5139 (2020).

161. Debenham, J. S., Madsen, R., Roberts, C. & Fraser-Reid, B. Two New Orthogonal Amine-Protecting Groups that can be Cleaved under Mild or Neutral Conditions. *J Am Chem Soc* **117**, 3302–3303 (1995).

162. Debenham, J. S. & Fraser-Reid, B. Tetrachlorophthaloyl as a Versatile Amine Protecting Group. *J Org Chem* **61**, 432–433 (1996).

163. Castro-Palomino, J. C. & Schmidt, R. R. *N*-Tetrachlorophthaloyl-protected trichloroacetimidate of glucosamine as glycosyl donor in oligosaccharide synthesis. *Tetrahedron Lett* **36**, 5343–5346 (1995).

164. Kiso, M. & Anderson, L. Protected glycosides and disaccharides of 2-amino-2-deoxy-D-glucopyranose by ferric chloride-catalyzed coupling. *Carbohydr Res* **136**, 309–323 (1985).

165. Singh, A. K., Tiwari, V., Mishra, K. B., Gupta, S. & Kandasamy, J. Urea–hydrogen peroxide prompted the selective and controlled oxidation of thioglycosides into sulfoxides and sulfones. *Beilstein J Org Chem* **13**, 1139–1144 (2017).

166. Yao-Chang, X., Bizuneh, A. & Walker, C. Selective deprotection of alkyl esters using magnesium methoxide. *Tetrahedron Lett* **37**, 455–458 (1996).

167. Xu, Y.-C., Bizuneh, A. & Walker, C. A Reagent for Selective Deprotection of Alkyl Acetates. *J Org Chem* **61**, 9086–9089 (1996).

168. Morley, T. J. & Withers, S. G. Chemoenzymatic Synthesis and Enzymatic Analysis of 8-Modified Cytidine Monophosphate-Sialic Acid and Sialyl Lactose Derivatives. *J Am Chem Soc* **132**, 9430–9437 (2010).

169. Khiar, N. *et al.* Highly Diastereoselective Oxidation of 2-Amino-2-deoxy-1-thio-β-D-glucopyranosides: Synthesis of Imino Sulfinylglycosides. *J Org Chem* **68**, 1433–1442 (2003).

170. Sakagami, M. & Hamana, H. A selective ring opening reaction of 4,6-*O*-benzylidene acetals in carbohydrates using trialkylsilane derivatives. *Tetrahedron Lett* **41**, 5547–5551 (2000).

171. Kaburagi, Y. & Kishi, Y. Operationally Simple and Efficient Workup Procedure for TBAF-Mediated Desilylation: Application to Halichondrin Synthesis. *Org Lett* **9**, 723–726 (2007).

172. Rodebaugh, R., Debenham, J. S. & Fraser-Reid, B. TCP Building Blocks for Oligosaccharide Synthesis: Progress Towards the Synthesis of Nodulation Factors. *J Carbohydr Chem* **16**, 1407–1432 (1997).

173. Chang, K.-L., Zulueta, M. M. L., Lu, X.-A., Zhong, Y.-Q. & Hung, S.-C. Regioselective One-Pot Protection of D-Glucosamine. *J Org Chem* **75**, 7424–7427 (2010).

174. Despras, G., Urban, D., Vauzeilles, B. & Beau, J.-M. One-pot synthesis of D-glucosamine and chitobiosyl building blocks catalyzed by triflic acid on molecular sieves. *Chem. Commun.* **50**, 1067–1069 (2014).

175. Bock, K., Lundt, I. & Pedersen, C. Assignment of anomeric structure to carbohydrates through geminal ^{13}C-H coupling constants. *Tetrahedron Lett* **14**, 1037–1040 (1973).

176. Fügedi, P. & Garegg, P. J. A novel promoter for the efficient construction of 1,2-*trans* linkages in glycoside synthesis, using thioglycosides as glycosyl donors. *Carbohydr Res* **149**, C9–C12 (1986).

177. Dasgupta, F. & Garegg, P. J. Alkyl sulfenyl triflate as activator in the thioglycoside-mediated formation of β-glycosidic linkages during oligosaccharide synthesis. *Carbohydr Res* **177**, c13–c17 (1988).

178. Martichonok, V. & Whitesides, G. M. Stereoselective α-Sialylation with Sialyl Xanthate and Phenylsulfenyl Triflate as a Promotor. *J Org Chem* **61**, 1702–1706 (1996).

179. Crich, D. & Sun, S. Direct chemical synthesis of β-mannopyranosides and other glycosides via glycosyl triflates. *Tetrahedron* **54**, 8321–8348 (1998).

180. Huang, X., Huang, L., Wang, H. & Ye, X.-S. Iterative One-Pot Synthesis of Oligosaccharides. *Angew Chem Int Ed* **43**, 5221–5224 (2004).

181. Aoki, S. *et al.* Synthesis of Disaccharide Nucleosides by the *O*-Glycosylation of Natural Nucleosides with Thioglycoside Donors. *Chem Asian J* **10**, 740–751 (2015).

182. Steinkopf, W., Herold, J. & Stöhr, J. Über das Thiodiglykolchlorid und einige Abkömmlinge desselben. *Ber Dtsch Chem Ges (A and B Series)* **53**, 1007–1012 (1920).

183. Heidary, F. *et al.* Alteration in serum levels of ICAM-1 and P-, E- and L-selectins in seriously eye-injured long-term following sulfur-mustard exposure. *Int Immunopharmacol* **76**, 105820 (2019).

184. Crich, D., Cai, F. & Yang, F. A stable, commercially available sulfenyl chloride for the activation of thioglycosides in conjunction with silver trifluoromethanesulfonate. *Carbohydr Res* **343**, 1858–1862 (2008).

185. Andersson, F., Fúgedi, P., Garegg, P. J. & Nashed, M. Synthesis of 1,2-*cis*-linked glycosides using dimethyl(methylthio) sulfonium triplate as promoter and thioglycosides as glycosyl donors. *Tetrahedron Lett* **27**, 3919–3922 (1986).

186. Tatai, J. & Fügedi, P. A New, Powerful Glycosylation Method: Activation of Thioglycosides with Dimethyl Disulfide−Triflic Anhydride. *Org Lett* **9**, 4647–4650 (2007).

187. Dinkelaar, J., Witte, M. D., van den Bos, L. J., Overkleeft, H. S. & van der Marel, G. A. NIS/TFA: a general method for hydrolyzing thioglycosides. *Carbohydr Res* **341**, 1723–1729 (2006).

188. Wang, P. *et al.* Hydrogen-Bond-Mediated Aglycone Delivery: Synthesis of β-D-Fructofuranosides. *Org Lett* **22**, 2967–2971 (2020).

189. Ranade, S. C. & Demchenko, A. V. Mechanism of Chemical Glycosylation: Focus on the Mode of Activation and Departure of Anomeric Leaving Groups. *J Carbohydr Chem* **32**, 1–43 (2013).

190. Nagasaki, M. *et al.* Chemical Synthesis of a Complex-Type *N*-Glycan Containing a Core Fucose. *J Org Chem* **81**, 10600–10616 (2016).

191. Nakayama, K., Uoto, K., Higashi, K., Soga, T. & Kusama, T. A Useful Method for Deprotection of the Protective Allyl Group at the Anomeric Oxygen of Carbohydrate Moieties Using Tetrakis(triphenylphosphine)palladium. *Chem Pharm Bull (Tokyo)* **40**, 1718–1720 (1992).

192. Smith, A. B., Fukui, M., Vaccaro, H. A. & Empfield, J. R. Phyllanthoside-phyllanthostatin synthetic studies. 7. Total synthesis of (+)-phyllanthocin and (+)-phyllanthocindiol. *J Am Chem Soc* **113**, 2071–2092 (1991).

193. Barbier, M., Grand, E. & Kovensky, J. Allyl deprotection of galacturonic acid derivatives: mechanistic aspects of mercuric-catalyzed prop-1-enyl acetal cleavage. *Carbohydr Res* **342**, 2635–2640 (2007).

194. Lohman, G. J. S. & Seeberger, P. H. A Stereochemical Surprise at the Late Stage of the Synthesis of Fully *N*-Differentiated Heparin Oligosaccharides Containing Amino, Acetamido, and *N*-Sulfonate Groups. *J Org Chem* **69**, 4081–4093 (2004).

195. Geringer, S. A., Mannino, M. P., Bandara, M. D. & Demchenko, A. V. Picoloyl protecting group in synthesis: focus on a highly chemoselective catalytic removal. *Org Biomol Chem* **18**, 4863–4871 (2020).

196. Yu, B. & Sun, J. Glycosylation with glycosyl *N*-phenyltrifluoroacetimidates (PTFAI) and a perspective of the future development of new glycosylation methods. *Chem Comm* **46**, 4668 (2010).

197. Christensen, H. M., Oscarson, S. & Jensen, H. H. Common side reactions of the glycosyl donor in chemical glycosylation. *Carbohydr Res* **408**, 51–95 (2015).

198. Zhang, Z. & Yu, B. Total Synthesis of the Antiallergic Naphtho-α-pyrone Tetraglucoside, Cassiaside C_2 , Isolated from Cassia Seeds. *J Org Chem* **68**, 6309–6313 (2003).

199. Zhang, Y.-M., Brodzky, A., Sinaÿ, P., Saint-Marcoux, G. & Perly, B. Synthesis of a nonasaccharide with two lewis x trisaccharides anchored onto a branched trimannoside. *Tetrahedron Asymmetry* **6**, 1195–1216 (1995).

200. Huang, L., Wang, Z., Li, X., Ye, X. & Huang, X. Iterative one-pot syntheses of chitotetroses. *Carbohydr Res* **341**, 1669–1679 (2006).

201. Ogawa, T., Nakabayashi, S. & Sasajima, K. Synthesis of phenyl 6-*O*-acyl-3-*O*-benzyl-2-deoxy-2-phthalimido-1-thio-β-D-glucopyranoside. *Carbohydr Res* **95**, 308–312 (1981).

202. Lönn, H. Synthesis of a tetra- and a nona-saccharide which contain α-L-fucopyranosyl groups and are part of the complex type of carbohydrate moiety of glycoproteins. *Carbohydr Res* **139**, 115–121 (1985).

203. Maranduba, A. & Veyrières, A. Glycosylation of lactose: synthesis of branched oligosaccharides involved in the biosynthesis of glycolipids having blood-group I activity. *Carbohydr Res* **151**, 105–119 (1986).

204. Sato, S., Ito, Y. & Ogawa, T. A total synthesis of dimeric Lex^x antigen, $III_3V_3Fuc_2nLc_6Cer$: Pivaloyl auxiliary for stereocontrolled glycosylation. *Tetrahedron Lett* **29**, 5267–5270 (1988).

205. Numomura, S., Iida, M., Numata, M., Sugimoto, M. & Ogawa, T. Total synthesis of sulfated Le pentaosyl ceramide. *Carbohydr Res* **263**, C1–C6 (1994).

206. Choutka, J., Kratochvíl, M., Zýka, J., Pohl, R. & Parkan, K. Straightforward synthesis of protected 2-hydroxyglycals by chlorination-dehydrochlorination of carbohydrate hemiacetals. *Carbohydr Res* **496**, 108086 (2020).

207. Kassam, K. & Warkentin, J. Thermolysis of 2-(3-Butyn-1-oxy)-2-methoxy-5,5-dimethyl-.DELTA.3-1,3,4-oxadiazoline in Solution. A remarkable Cascade of Carbene and Other Reactions. *J Org Chem* **59**, 5071–5075 (1994).

208. Martinz, G. Synthesis of mono- and disaccharide ligands related to the secondary cell wall polymer of *Paenibacillus alvei* containing pyruvate-substituted β-D-mannosamine residues. (University of Vienna, 2015).

209. Greenberg, W. A. *et al.* Design and Synthesis of New Aminoglycoside Antibiotics Containing Neamine as an Optimal Core Structure: Correlation of Antibiotic Activity with in Vitro Inhibition of Translation. *J Am Chem Soc* **121**, 6527–6541 (1999).

210. Nyffeler, P. T., Liang, C.-H., Koeller, K. M. & Wong, C.-H. The Chemistry of Amine−Azide Interconversion: Catalytic Diazotransfer and Regioselective Azide Reduction. *J Am Chem Soc* **124**, 10773–10778 (2002).

211. Reddy, P. G., Pratap, T. V., Kumar, G. D. K., Mohanty, S. K. & Baskaran, S. The Lindlar Catalyst Revitalized: A Highly Chemoselective Method for the Direct Conversion of Azides to *N*-(*tert*-Butoxycarbonyl)amines. *Eur J Org Chem* **2002**, 3740–3743 (2002).

212. Gao, C., Fisher, Z. B. & Edgar, K. J. Azide reduction by DTT or thioacetic acid provides access to amino and amido polysaccharides. *Cellulose* **26**, 445–462 (2019).

213. Shangguan, N., Katukojvala, S., Greenberg, R. & Williams, L. J. The Reaction of Thio Acids with Azides: A New Mechanism and New Synthetic Applications. *J Am Chem Soc* **125**, 7754–7755 (2003).

214. Bartra, M., Romea, P., Urpí, F. & Vilarrasa, J. A fast procedure for the reduction of azides and nitro compounds based on the reducing ability of $Sn(SR)_3$-species. *Tetrahedron* **46**, 587–594 (1990).

215. Baum, D., Kosma, P. & Zamyatina, A. Synthesis of Zwitterionic 1,1′-Glycosylphosphodiester: A Partial Structure of Galactosamine-Modified *Francisella* Lipid A. *Org Lett* **16**, 3772–3775 (2014).

216. Nishimura, S. *Handbook of Heterogeneous Catalytic Hydrogenation for Organic Synthesis*. (Wiley, 2001).

217. Kronsteiner, M. Chemische und enzymatische Synthese von UDP *N*-Acetylmannosaminuronsäure als Substrat für die Aminotransferase WbpE aus

Pseudomonas aeruginosa. (University of Natural Resources and Life Sciences, 2002).

218. Freese, S. J. & Vann, W. F. Synthesis of 2-acetamido-3-*O*-acetyl-2-deoxy-D-mannose phosphoramidites. *Carbohydr Res* **281**, 313–319 (1996).

219. Yamazaki, T., Warren, C. D., Herscovics, A. & Jeanloz, R. W. The synthesis of uridine diphosphate *N*-acetylhexosamines and uridine 5′-(2-acetamido-2-deoxy-α-D-mannopyranosyluronic acid diphosphate). *Can J Chem* **59**, 2247–2252 (1981).

220. Muthana, M. M. *et al.* Efficient one-pot multienzyme synthesis of UDP-sugars using a promiscuous UDP-sugar pyrophosphorylase from Bifidobacterium longum (BLUSP). *Chem Commun* **48**, 2728 (2012).

221. Tsukamoto, H. & Kahne, D. *N*-Methylimidazolium chloride-catalyzed pyrophosphate formation: Application to the synthesis of Lipid I and NDP-sugar donors. *Bioorg Med Chem Lett* **21**, 5050–5053 (2011).

222. Fulmer, G. R. *et al.* NMR Chemical Shifts of Trace Impurities: Common Laboratory Solvents, Organics, and Gases in Deuterated Solvents Relevant to the Organometallic Chemist. *Organometallics* **29**, 2176–2179 (2010).

223. Chen, C.-T. *et al.* Nucleophilic Acyl Substitutions of Anhydrides with Protic Nucleophiles Catalyzed by Amphoteric, Oxomolybdenum Species. *J Org Chem* **70**, 1188–1197 (2005).

224. Qin, C. *et al.* Total Synthesis of a Densely Functionalized *Plesiomonas shigelloides* Serotype 51 Aminoglycoside Trisaccharide Antigen. *J Am Chem Soc* **140**, 3120–3127 (2018).

225. Basu, N., Maity, S. K., Roy, S., Singha, S. & Ghosh, R. $FeCl_3$ mediated arylidenation of carbohydrates. *Carbohydr Res* **346**, 534–539 (2011).

226. Lin, Y. A., Chalker, J. M., Floyd, N., Bernardes, G. J. L. & Davis, B. G. Allyl Sulfides Are Privileged Substrates in Aqueous Cross-Metathesis: Application to Site-Selective Protein Modification. *J Am Chem Soc* **130**, 9642–9643 (2008).

227. Kurfiřt, M. *et al.* Selectively Deoxyfluorinated *N*-Acetyllactosamine Analogues as ^{19}F NMR Probes to Study Carbohydrate-Galectin Interactions. *Chem Eur J* **27**, 13040–13051 (2021).

228. Weber, H. & Khorana, H. G. CIV. Total synthesis of the structural gene for an alanine transfer ribonucleic acid from yeast. Chemical synthesis of an icosadeoxynucleotide corresponding to the nucleotide sequence 21 to 40. *J Mol Biol* **72**, 219–249 (1972).

229. F. Batey, J., Bullock, C., O'Brien, E. & Williams, J. M. The selective benzoylation of monosaccharides. *Carbohydr Res* **43**, 43–50 (1975).

7 Publications resulting from this thesis

7.1 Conference

- Lim, C; Krauter, S; Legg, M.S; Hager-Mair, F; Blaukopf, M; Evans, S.V; Schäffer, C.; Kosma, P..(2023): Synthesis and binding interactions of Secondary Cell Wall Polysaccharide Fragments of *Paenibacillus Alvei*; 21st European Carbohydrate Symposium, Paris, 09.07-13.07.2023; In: Bonnaffé, D. (ED.), Abstract Book, OL117

7.2 Journal Articles

- Legg, MSG; Hager-Mair, FF; Krauter, S; Gagnon, SML; Lopez-Guzman, A; Lim, C; Blaukopf, M; Kosma, P; Schaeffer, C; Evans, SV. (2022): The S-layer homology domains of *Paenibacillus alvei* surface protein SpaA bind to cell wall polysaccharide through the terminal monosaccharide residue. *J. Bio. Chem.* **2022**; 298(4), 101745
- Hager-Mair, FF; Stefanovic, C; Lim, C; Webhofer, K; Krauter, S; Blaukopf, M; Ludwig, R; Kosma, P; Schaffer, C. (2021): Assaying *Paenibacillus alvei* CsaB-Catalysed Ketalpyruvyltransfer to Saccharides by Measurement of Phosphate Release. *Biomolecules* **2021**; 11(11), 1732

8 Curriculum Vitae

CHARLIE LIM, MSc

*25th. April 1991, Los Angeles

EDUCATION

TU Wien *since Jul 2019*
Doctoral Programme in Engineering Sciences
Thesis: ´Synthesis of Secondary Cell Wall Polysaccharide Fragments of *Paenibacillus Alvei*´
Work conducted at **Universität für Bodenkultur Wien (BOKU)**
Supervisors: Prof. Paul Kosma (BOKU)
Prof. Michael Schnürch (TU Wien)

TU Wien *Nov 2016 - June 2019*
Master Programme in Technical Chemistry *with distinction*
Focus: ´Applied Synthetic Chemistry´
Thesis: ´Chiral Cyclooctadiene Ligands for Rhodium Catalysis´
Supervisor: Prof. Michael Schnürch, Institute of Applied Synthetic Chemistry

TU Wien *Oct 2012 - Nov 2016*
Bachelor Programme in Technical Chemistry
Thesis: ´Synthesis of Photoswitchable MAT-ligands´
Supervisor: Prof. Marko D. Mihovilovic, Institute of Applied Synthetic Chemistry

PROFESSIONAL EXPERIENCE

Research Fellow, Universität für Bodenkultur Wien *Nov 2019 - Oct 2023*
Insitute of Organic Chemistry
Vienna, Austria

Short-Term Scientific Mission, Sanofi-Aventis GmbH *Aug 2019 - Sep 2019*
Frankfurt am Main, Germany
Visiting scientist from TU Wien working on late-stage radioisotope-labeling of drugs *via* C-H activation

Lab Technician, Sanochemia Pharmazeutika AG *Sep 2016 - April 2018*
Neufeld an der Leitha, Austria
Quality Control (Pharm. Eur./USP), cGMP

Research Internships, TU Wien
Institute of Applied Synthetic Chemistry
Research group of Prof. Johannes Fröhlich *Nov 2017 - Jan 2018*
Research group of Prof. Marko D. Mihovilovic *May 2017 - Jul 2017*

Internships, Sanochemia Pharmazeutika AG *Jul 2016 - Aug 2016*
Neufeld an der Leitha, Austria *Jul 2015 - Aug 2015*
Quality Control (Pharm. Eur./USP), cGMP

Software Developer, at-visions Informationstechnologie GmbH — *April 2012 - Aug 2012*
Wolfau, Austria
Backend Development (PHP) for Digital Signage solutions

TEACHING EXPERIENCE AS TUTOR

Universität für Bodenkultur Wien — *March 2020 - Oct 2022*

TU Wien — *March 2018 - June 2019*

Sigmund Freud - Privatuniversität Wien — *Sep 2017 - Sep 2018*

SCIENTIFIC PRESENTATIONS

Synthesis and binding interactions of Secondary Cell Wall Polysaccharide Fragments of *Paenibacillus Alvei*
Lim, C; Krauter, S; Legg, M.S; Hager-Mair, F; Blaukopf, M; Evans, S.V; Schäffer, C.; Kosma, P.
21st European Carbohydrate Symposium, Paris, 09.07-13.07.2023
In: Bonnaffé, D. (ED.), Abstract Book, OL117

Chiral Cyclooctadiene Ligands for Rhodium Catalysis
Lim, C; Spettel, M; Pollice, R; Schnürch, M.
VIENNA young SCIENTISTS SYMPOSIUM, Vienna, 13.06-14.06.2019
In: VSS 2019, Abstract Book, CAT.14

PUBLICATIONS

Stefanović, C., Hager-Mair, F.F., Breslmayr, E., López-Guzmán, A., Lim, C., Blaukopf, M., Kosma, P., Oostenbrink, C., Ludwig, R. & Schäffer, C.
Sci Rep **13**, 13394 (2023)
Molecular modelling and site-directed mutagenesis provide insight into saccharide pyruvylation by the *Paenibacillus alvei* CsaB enzyme
DOI: https://doi.org/10.1038/s41598-023-40072-1

Legg, MSG; Hager-Mair, FF; Krauter, S; Gagnon, SML; Lopez-Guzman, A; Lim, C; Blaukopf, M; Kosma, P; Schäffer, C; Evans, SV.
J Biol Chem 2022, **298**(4), 101745
The S-layer homology domains of *Paenibacillus alvei* surface protein SpaA bind to cell wall polysaccharide through the terminal monosaccharide residue
DOI: https://doi.org/10.1016/j.jbc.2022.101745

Hager-Mair, FF; Stefanovic, C; Lim, C; Webhofer, K; Krauter, S; Blaukopf, M; Ludwig, R; Kosma, P; Schäffer, C.
Biomolecules 2021, **11**(11), 1732
Assaying *Paenibacillus alvei* CsaB-Catalysed Ketalpyruvyltransfer to Saccharides by Measurement of Phosphate Release
DOI: https://doi.org/10.3390/biom11111732

9 Appendix

9.1 Compound **13**

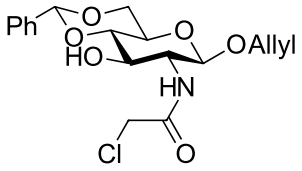

$C_{18}H_{22}ClNO_6$
383.821 amu

13

9.1.1 ^{1}H NMR

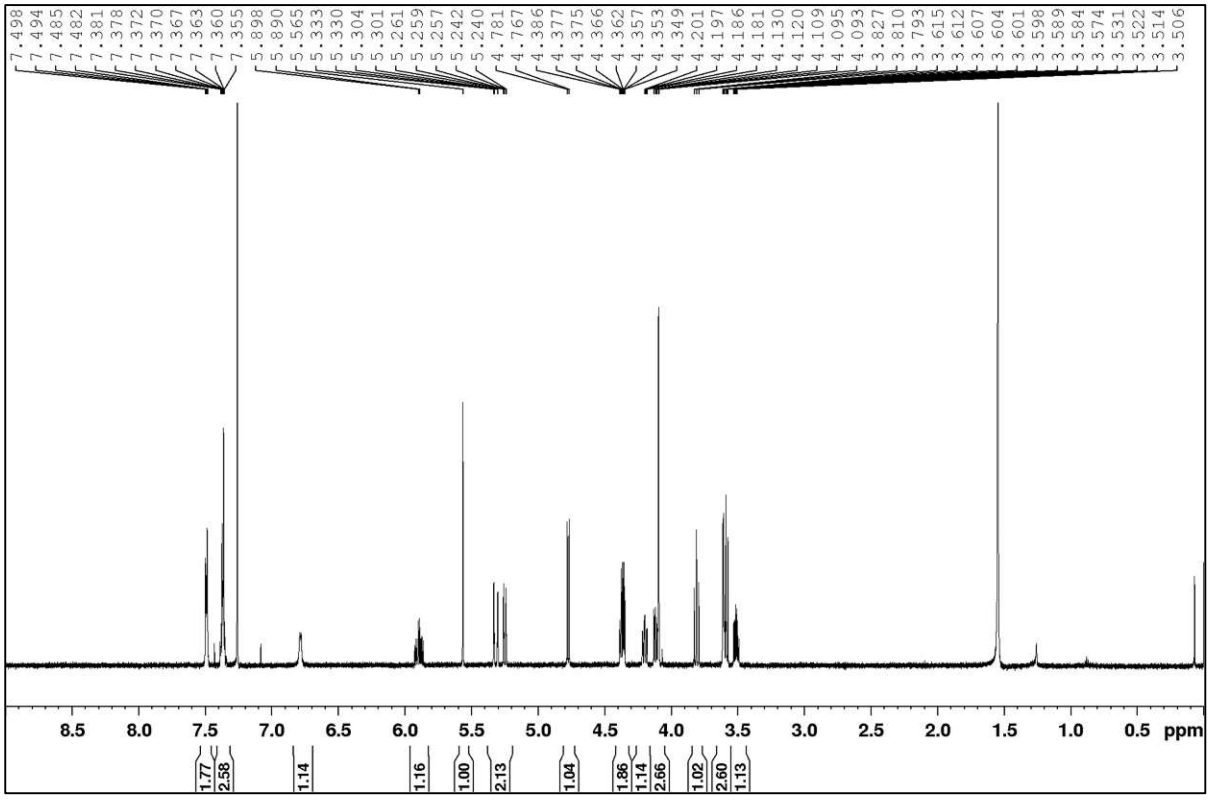

9.1.2 ^{13}C NMR

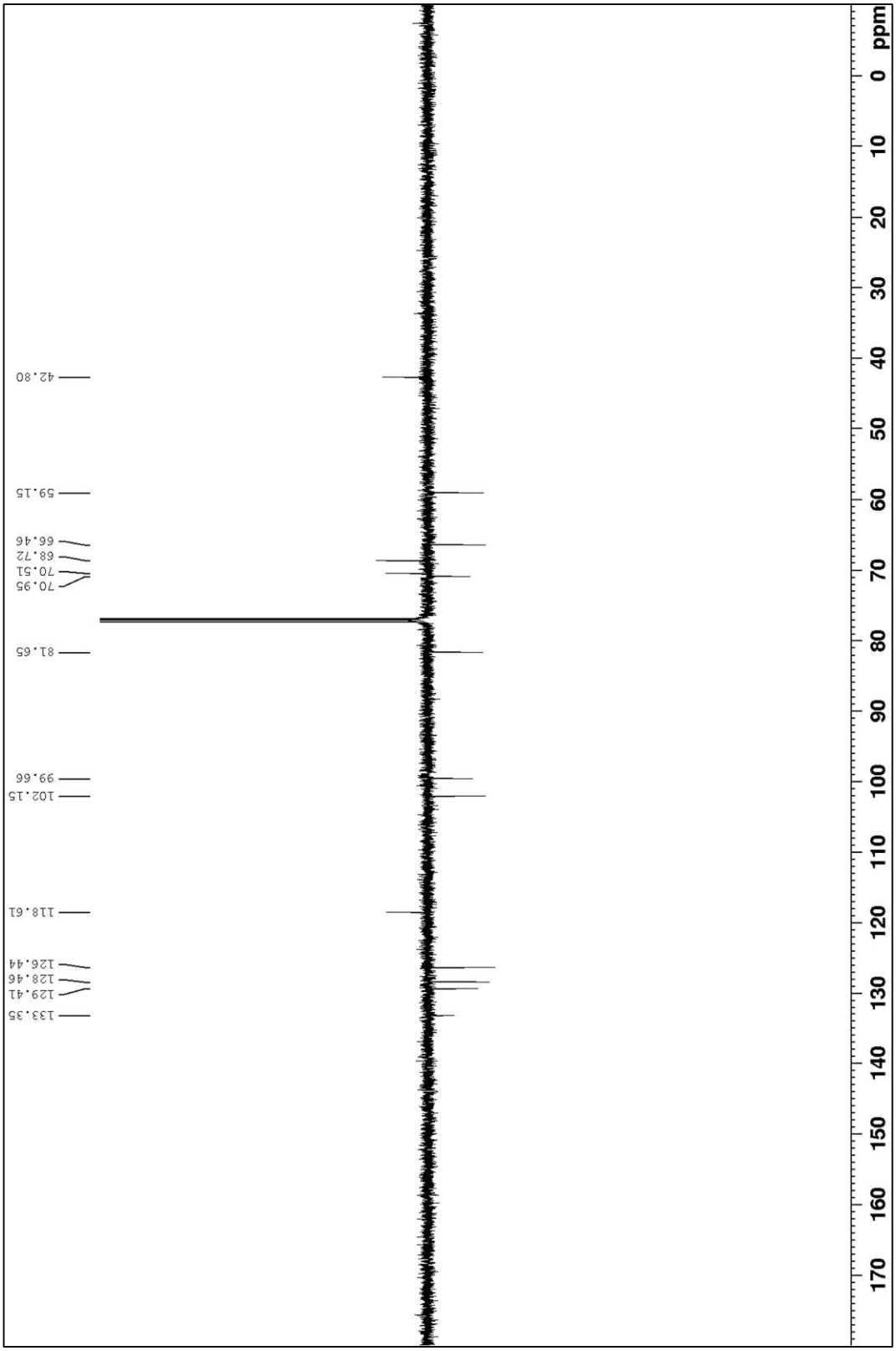

9.1.3 ^{1}H-^{13}C-HSQC

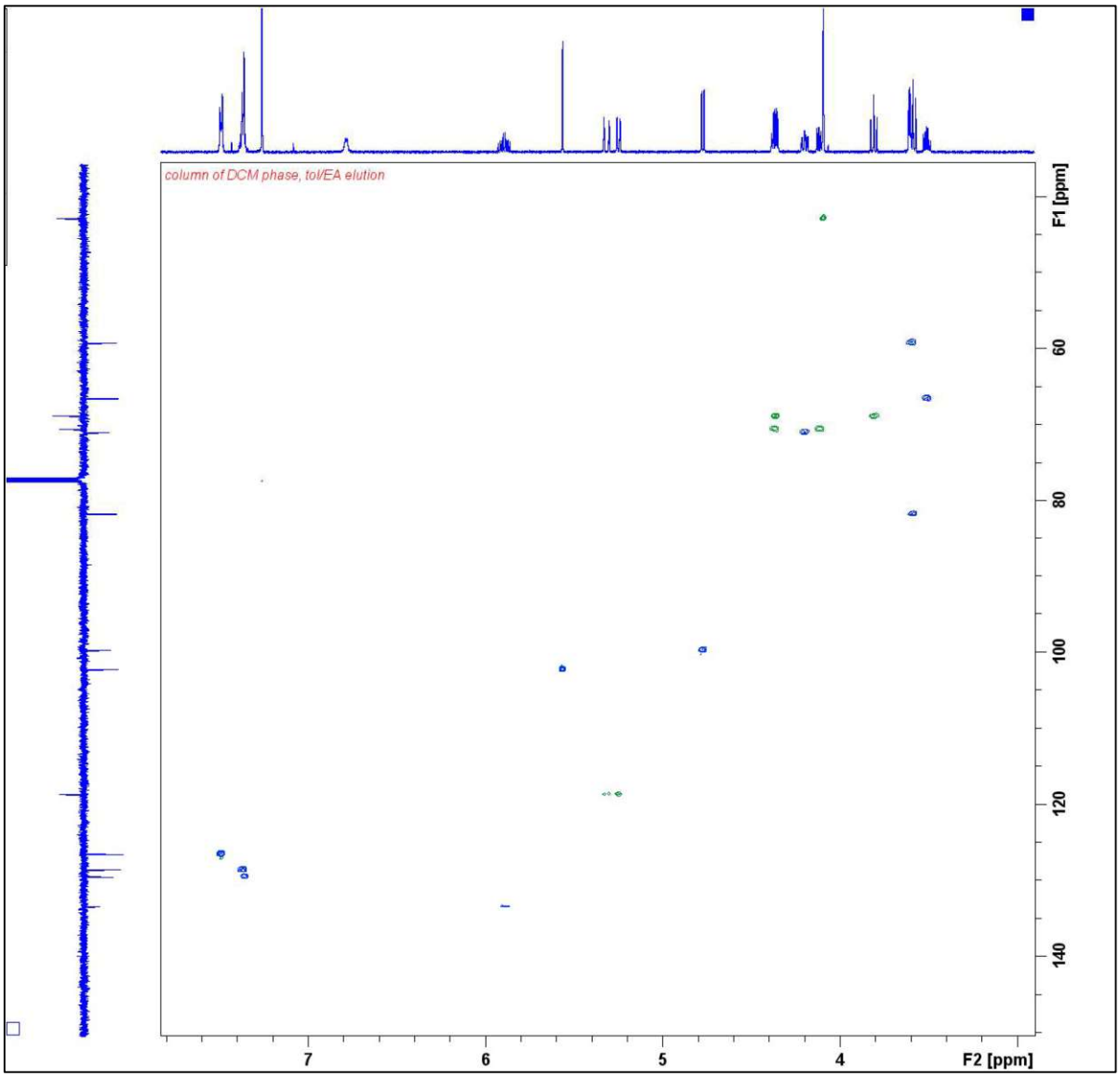

9.2 Compound **25**

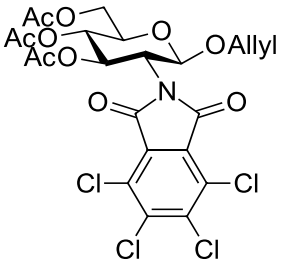

$C_{23}H_{21}Cl_4NO_{10}$
613.220 amu

25

9.2.1 ^{1}H NMR

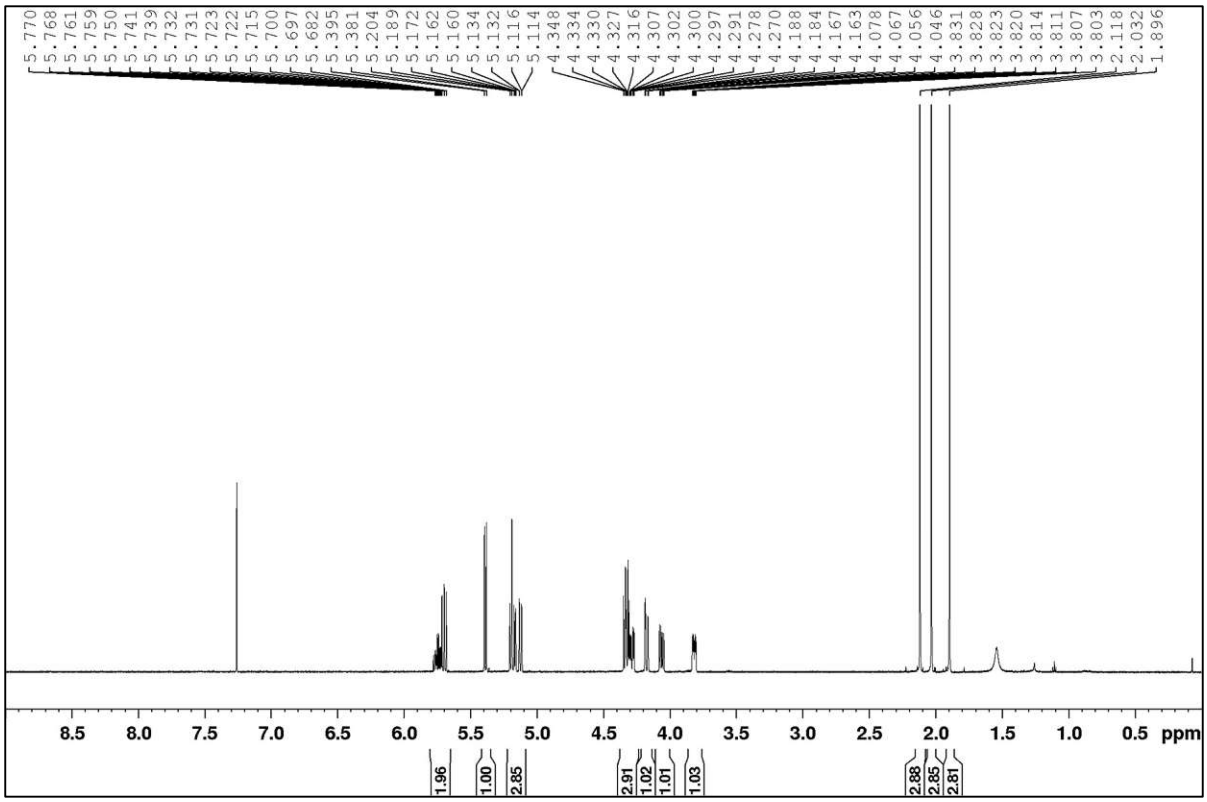

9.2.2 ^{13}C NMR

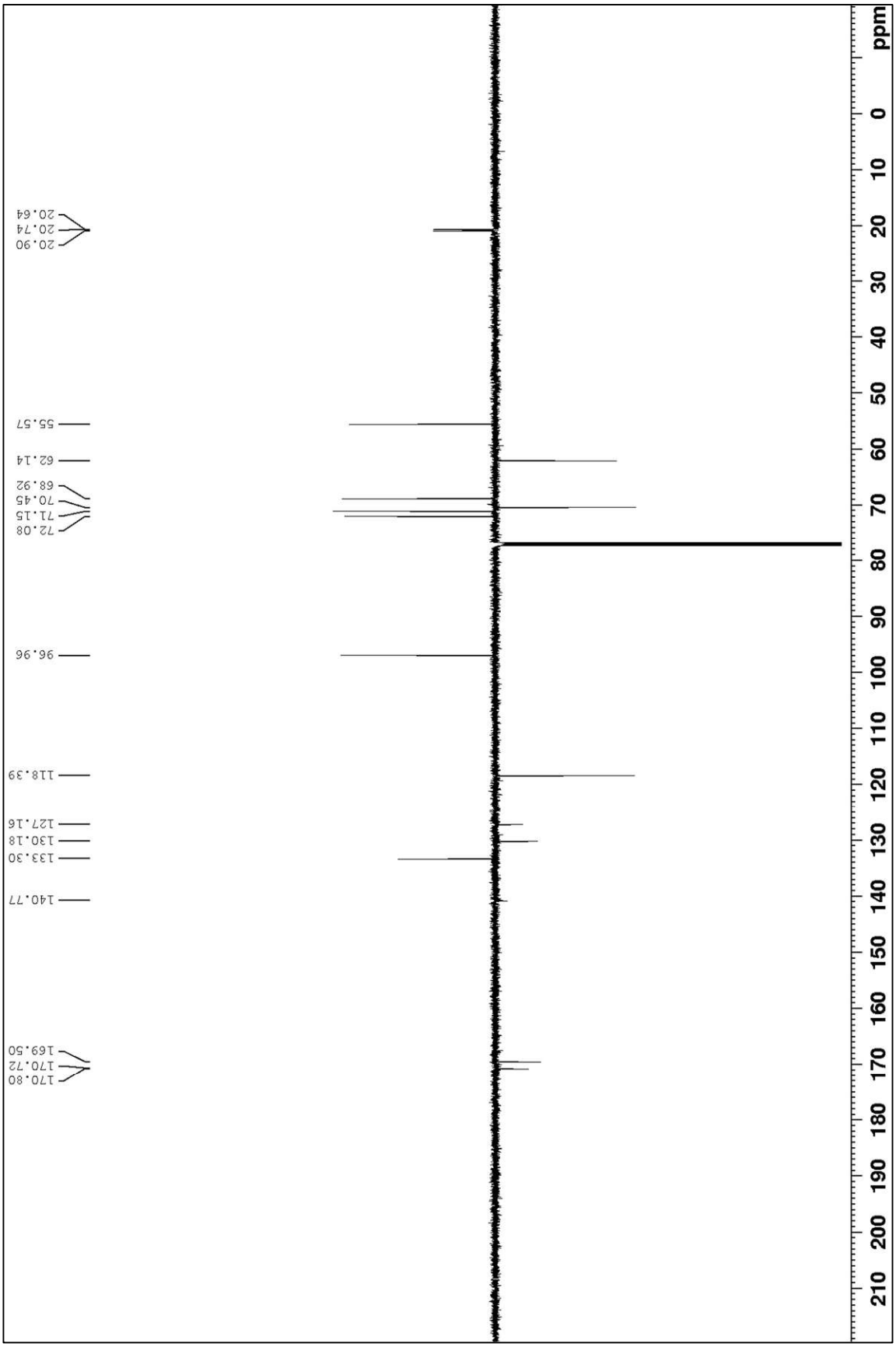

9.2.3 ^{1}H-^{13}C-HSQC

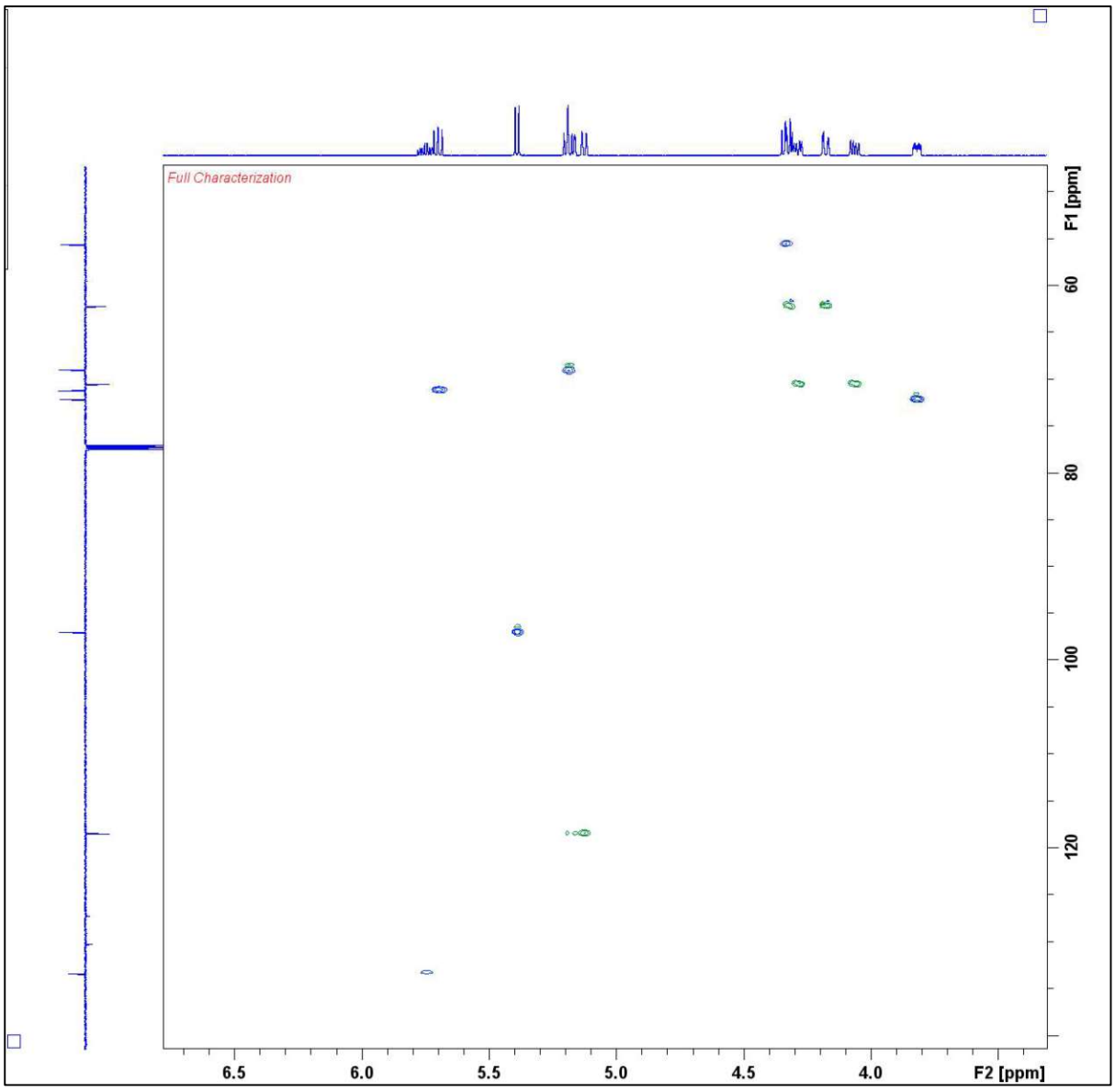

9.3 Compound **26**

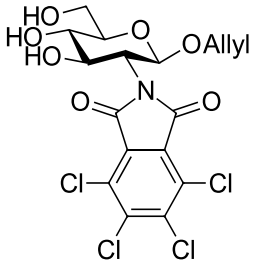

$C_{17}H_{15}Cl_4NO_7$
487.110 amu

26

9.3.1 ^{1}H NMR

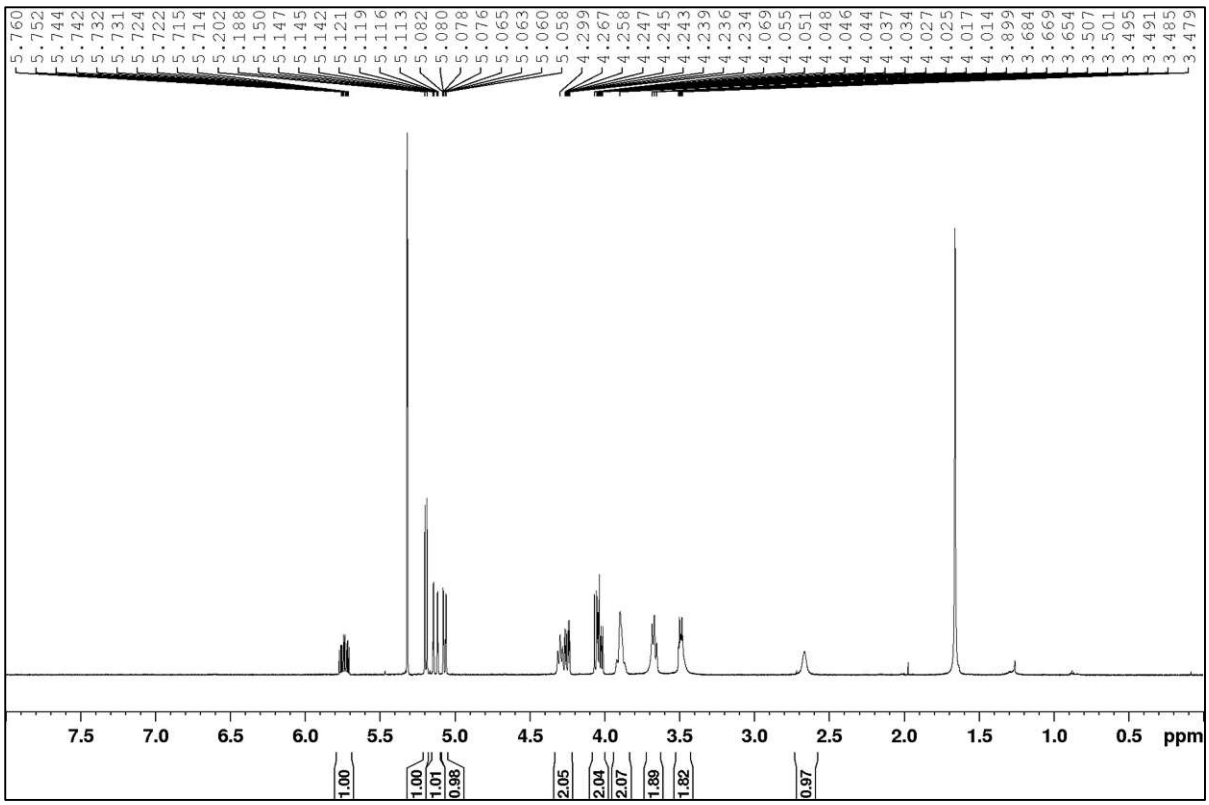

9.3.2 ^{13}C NMR

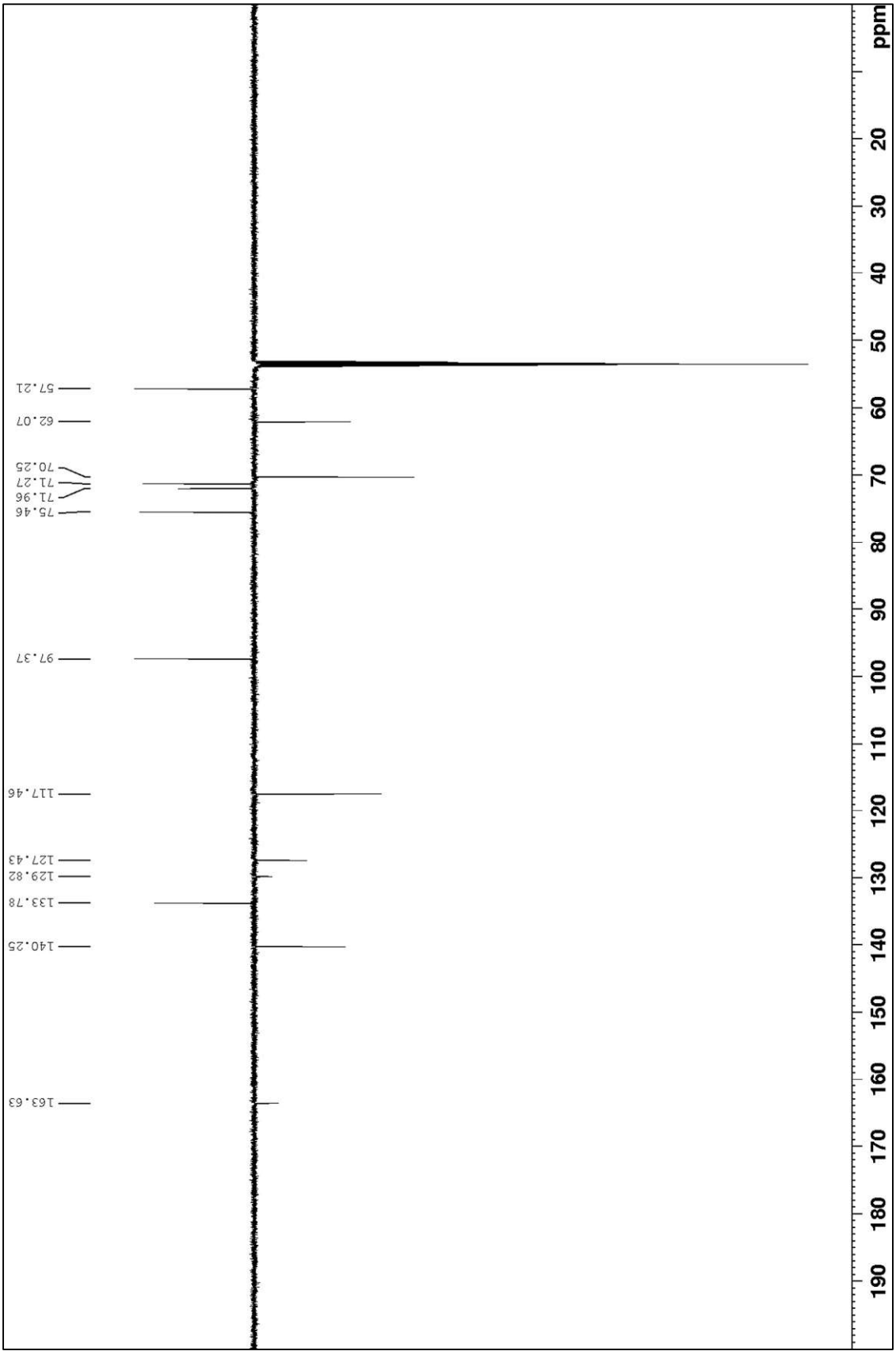

9.3.3 ^{1}H-^{13}C-HSQC

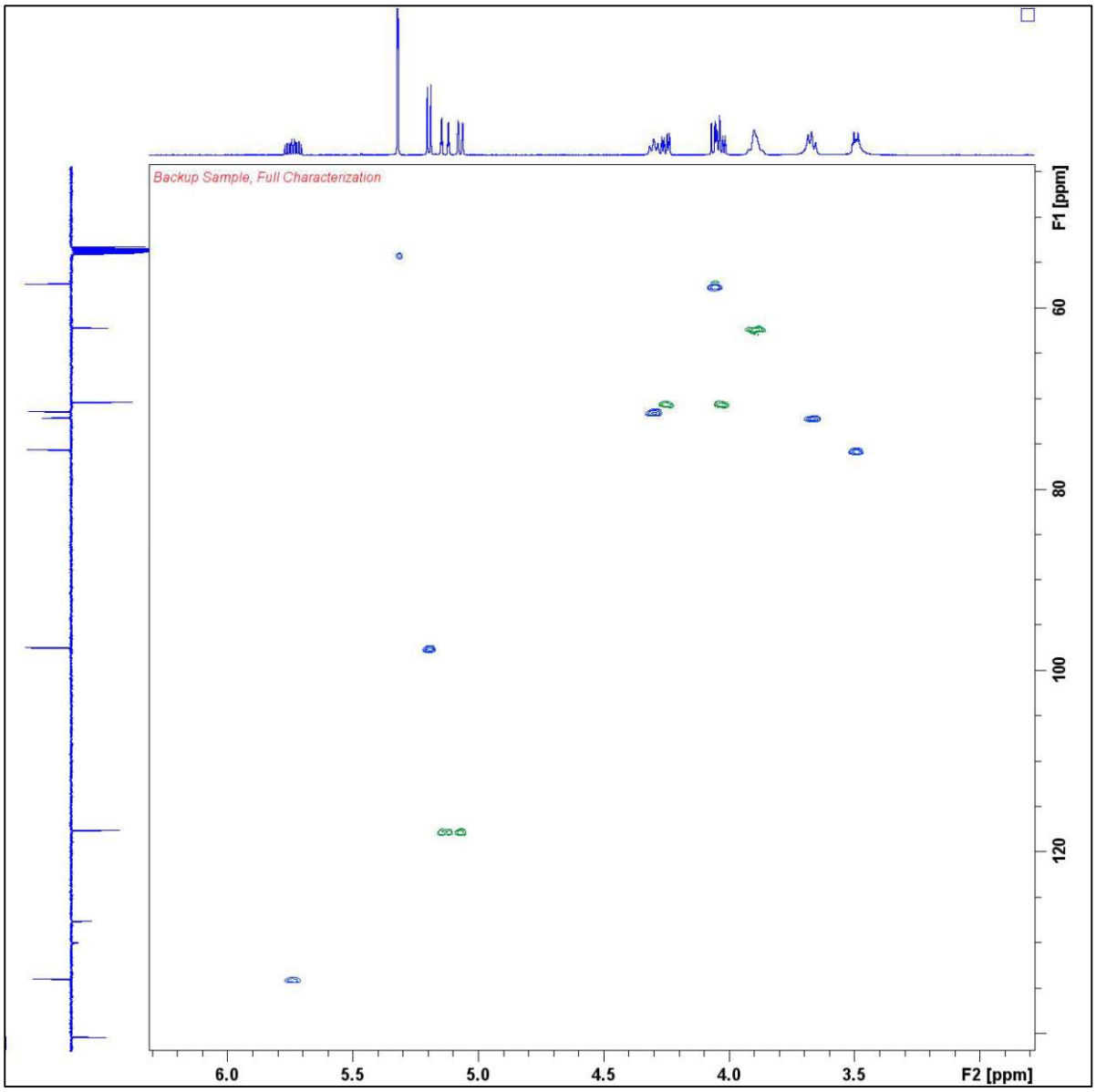

9.4 Compound **27**

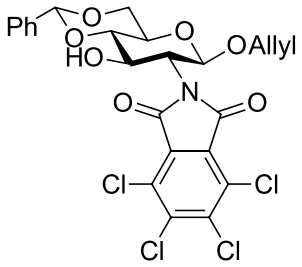

$C_{24}H_{19}Cl_4NO_7$
575.216 amu

27

9.4.1 ^{1}H NMR

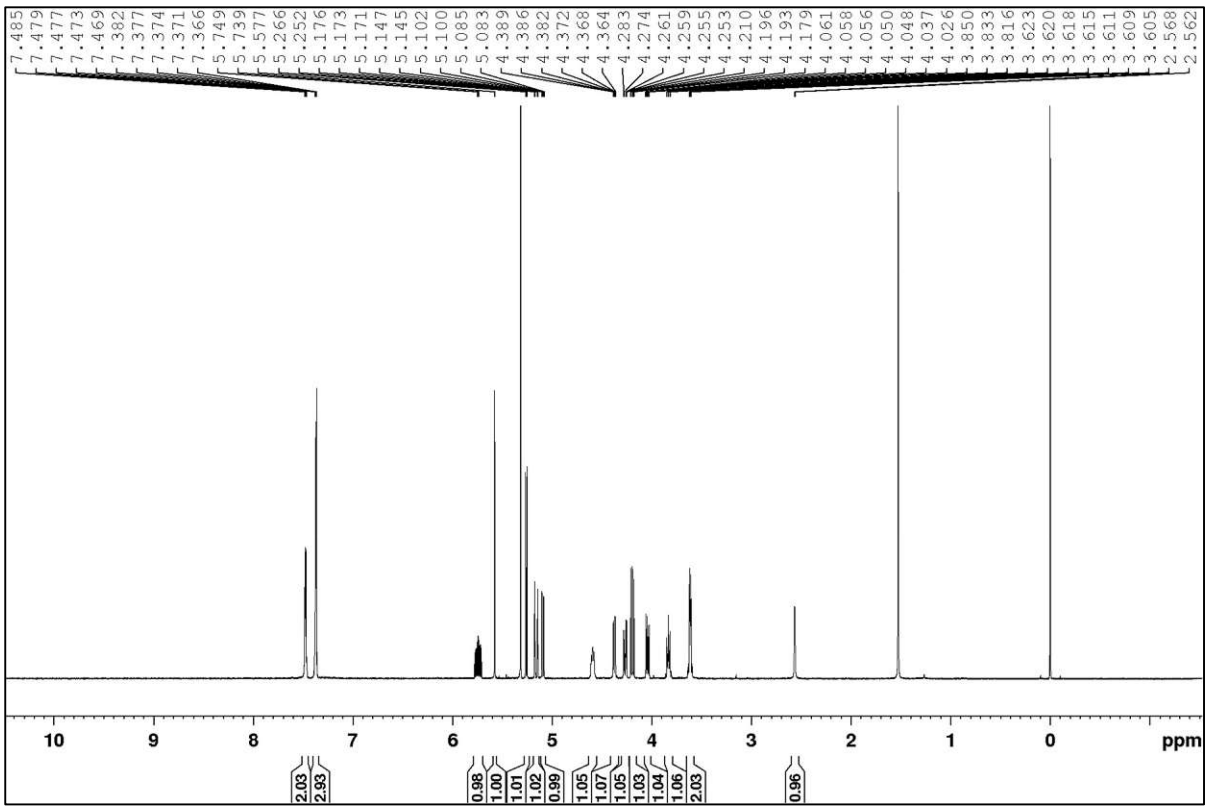

9.4.2 ^{13}C NMR

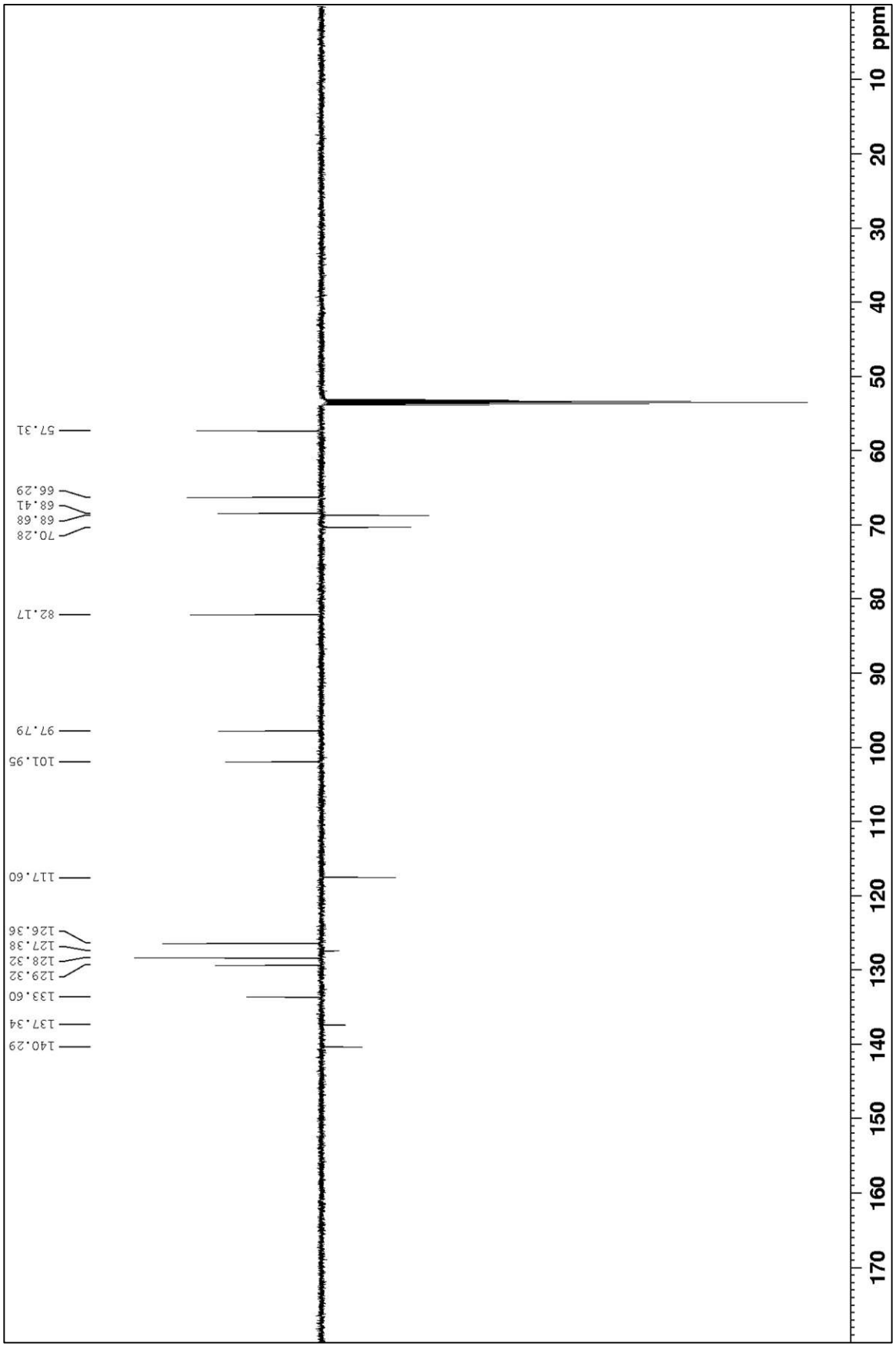

9.4.3 ^{1}H-^{13}C-HSQC

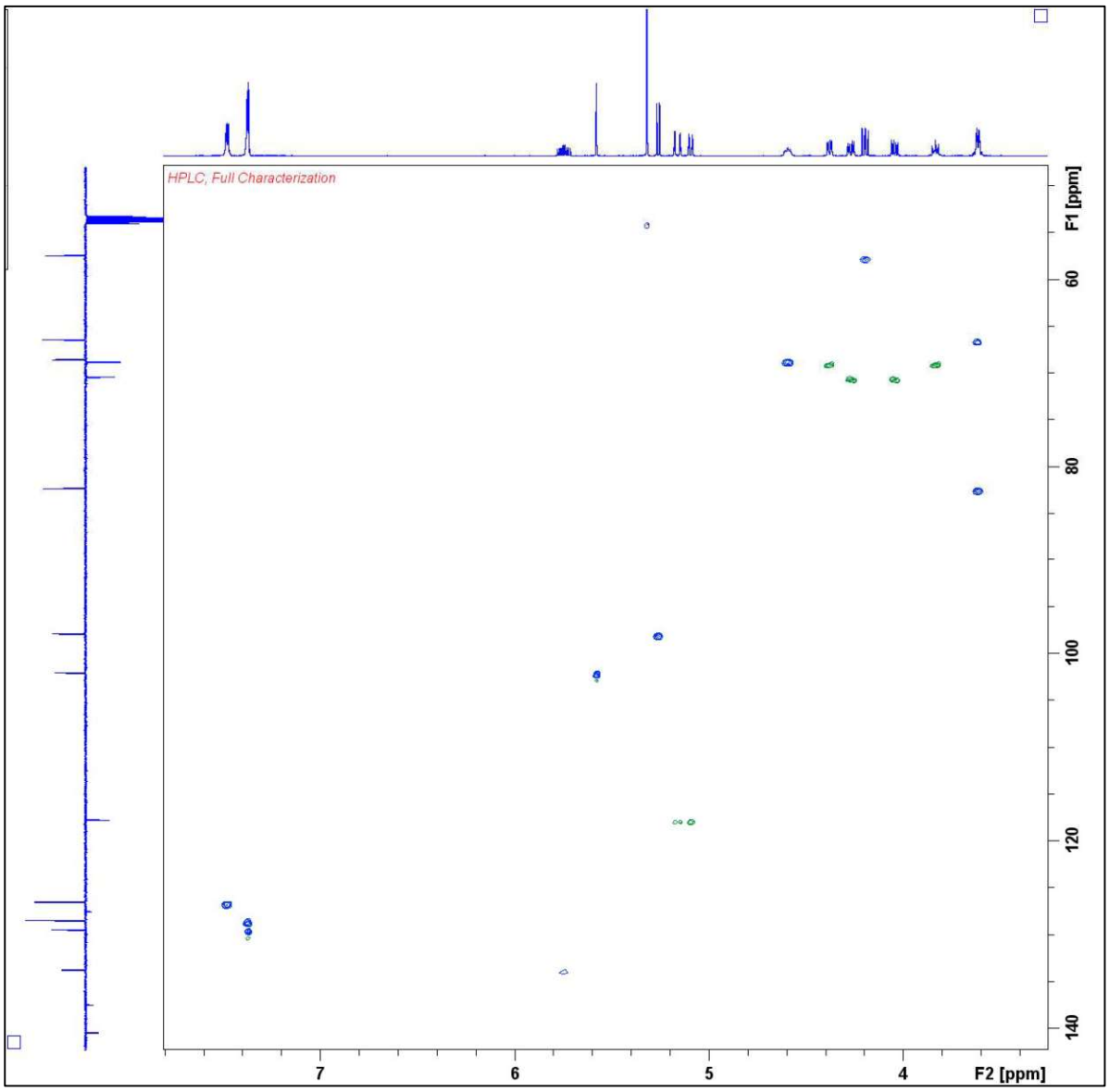

9.5 Compound **28**

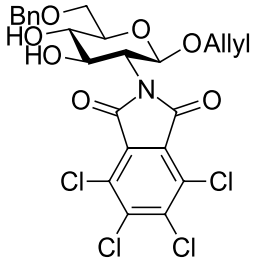

$C_{24}H_{21}Cl_4NO_7$
577.232 amu

28

9.5.1 ^{1}H NMR

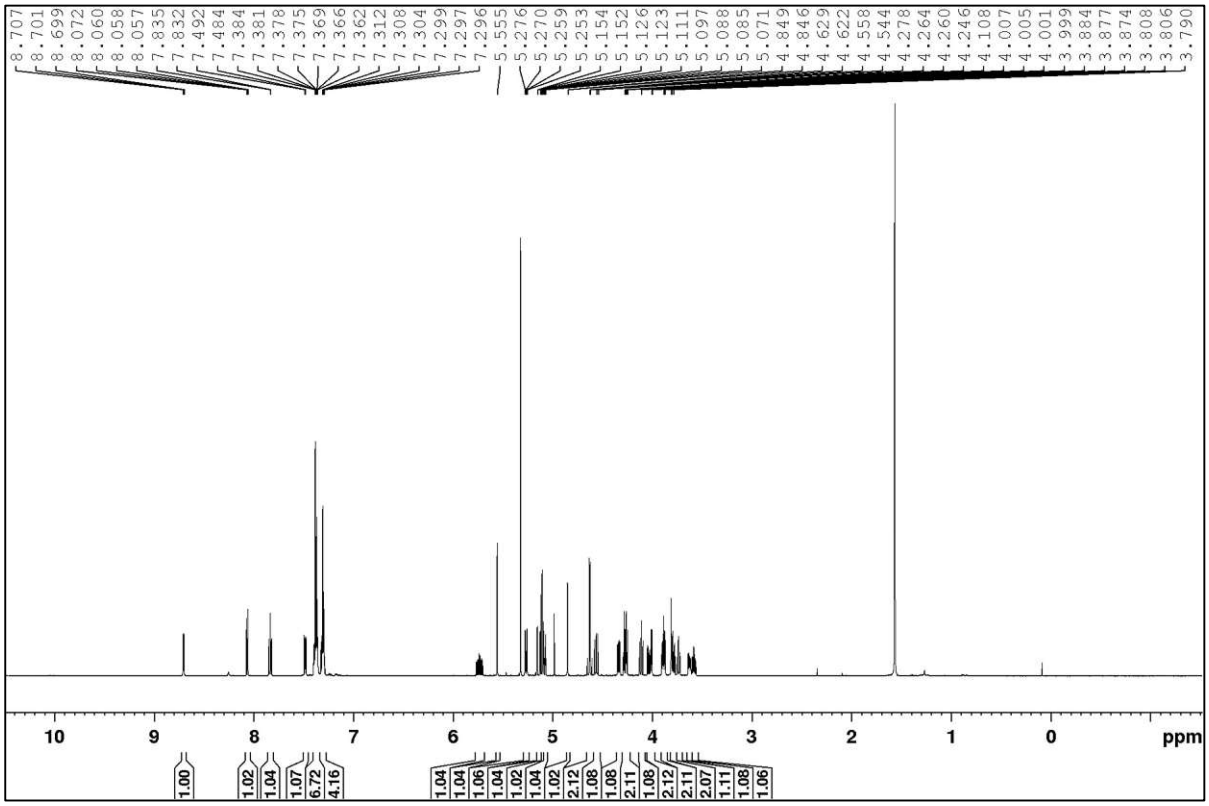

9.5.2 ^{13}C NMR

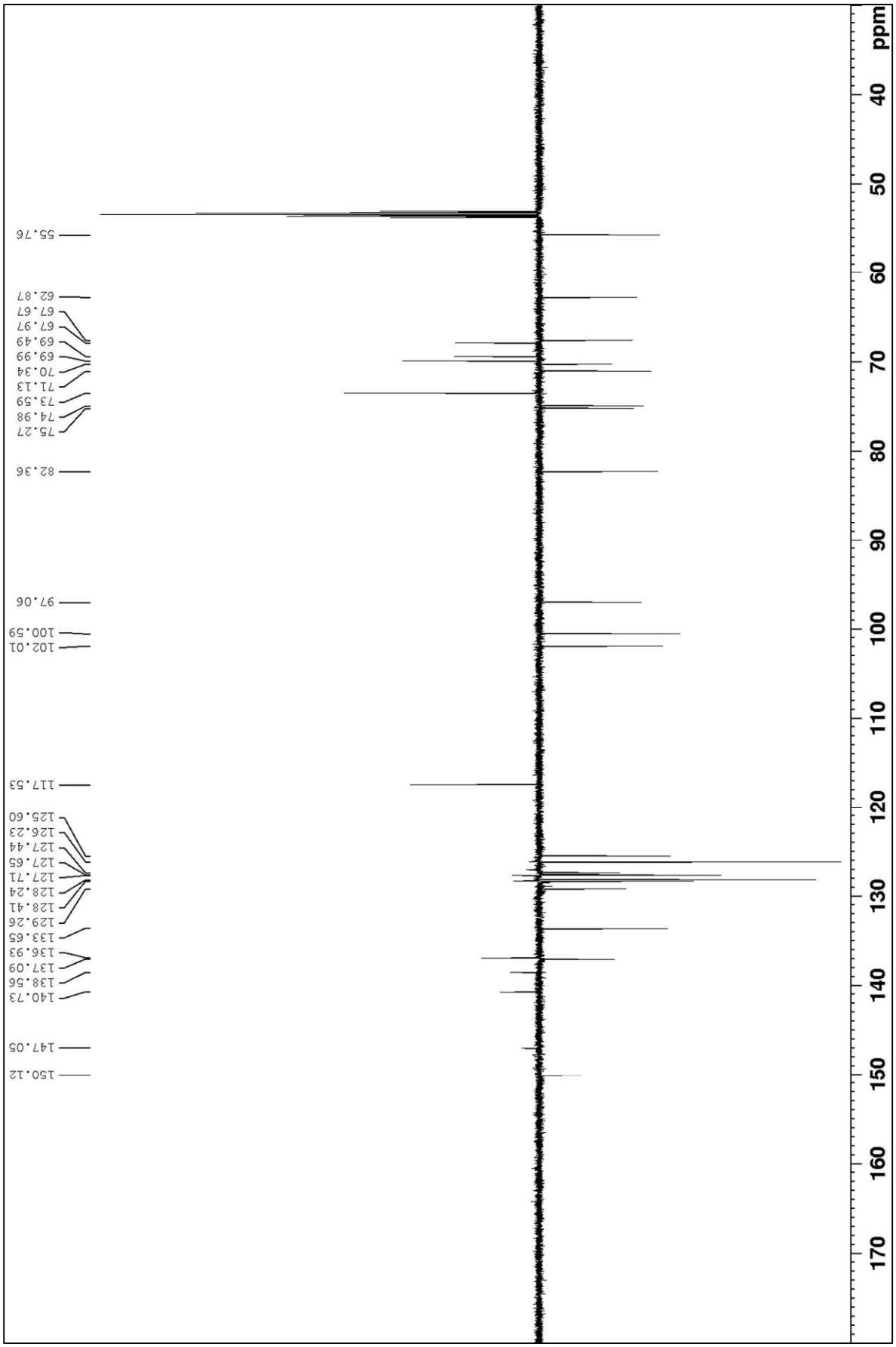

9.5.3 ^{1}H-^{13}C-HSQC

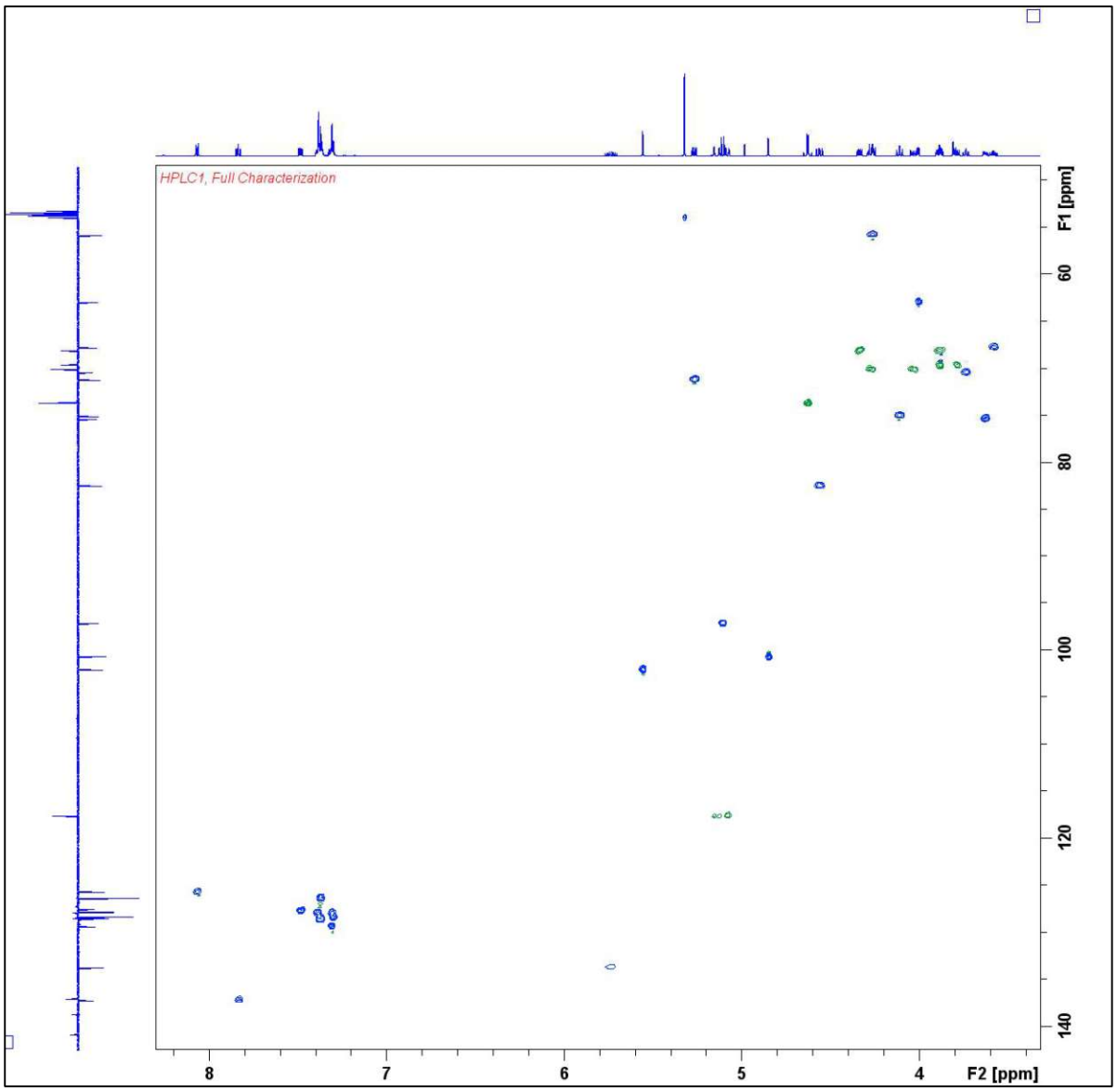

9.6 Compound **28a**

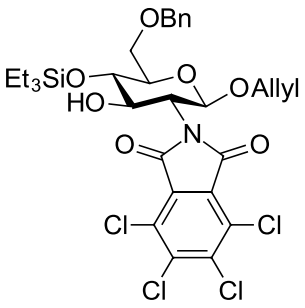

$C_{30}H_{35}Cl_4NO_7Si$
691.493 amu

28a

9.6.1 ^{1}H NMR

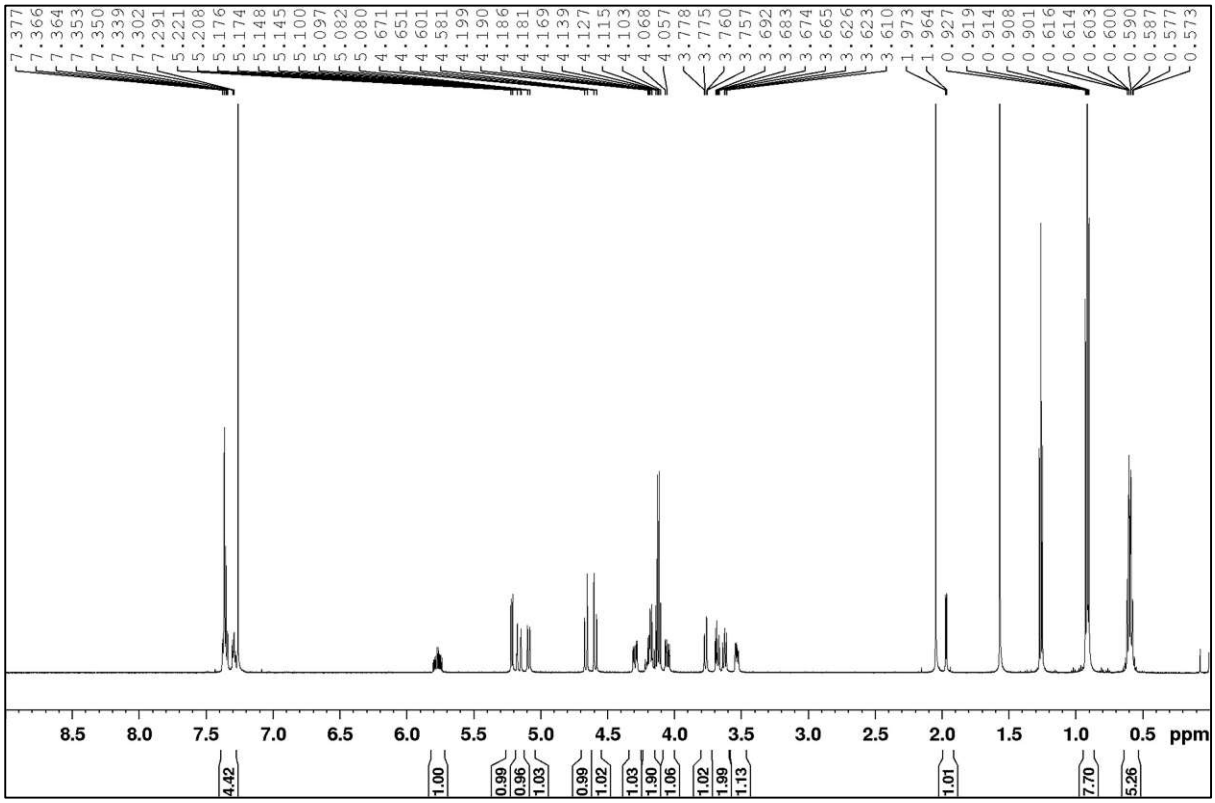

9.6.2 ^{13}C NMR

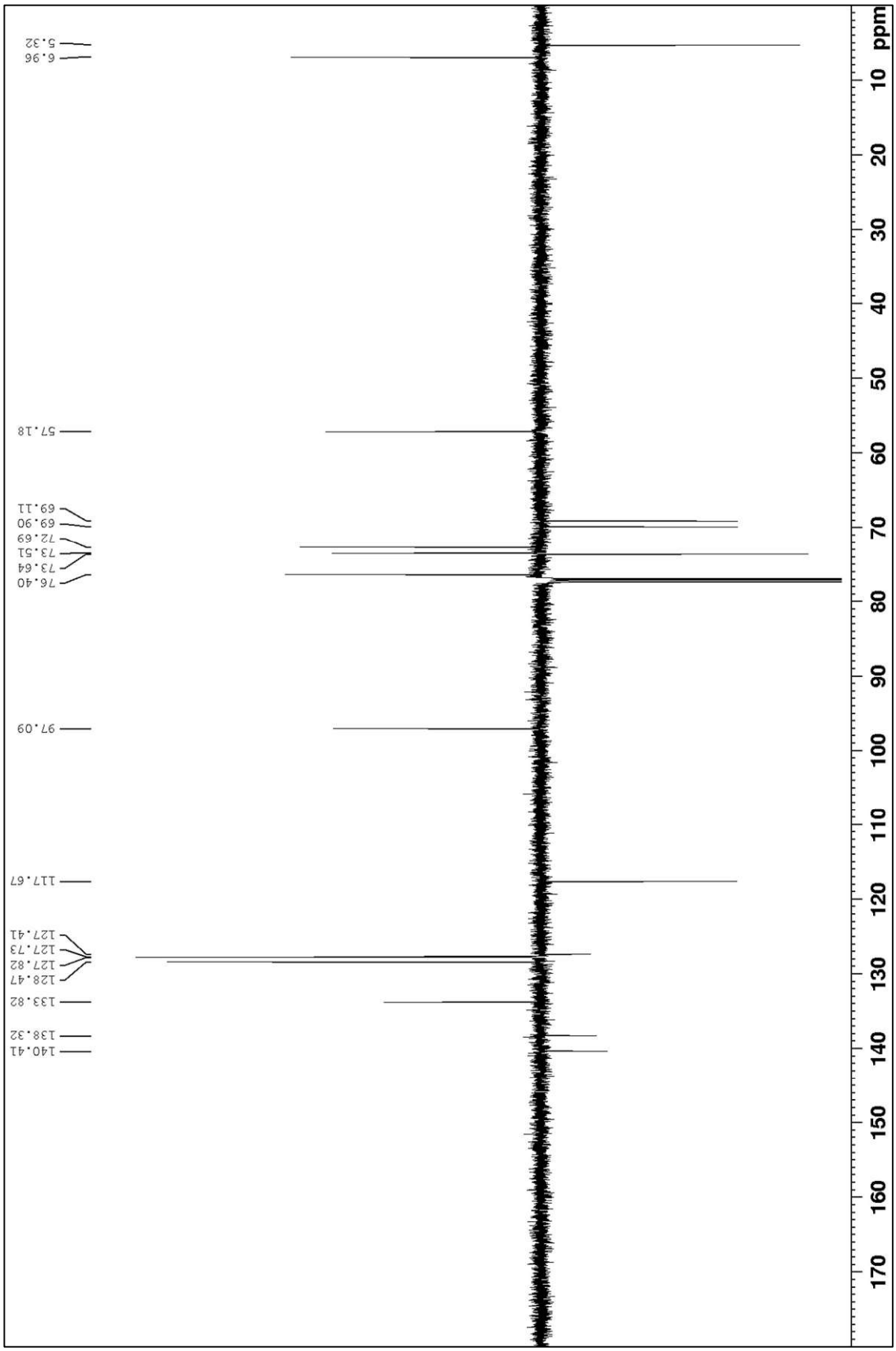

9.6.3 ^{1}H-^{13}C-HSQC

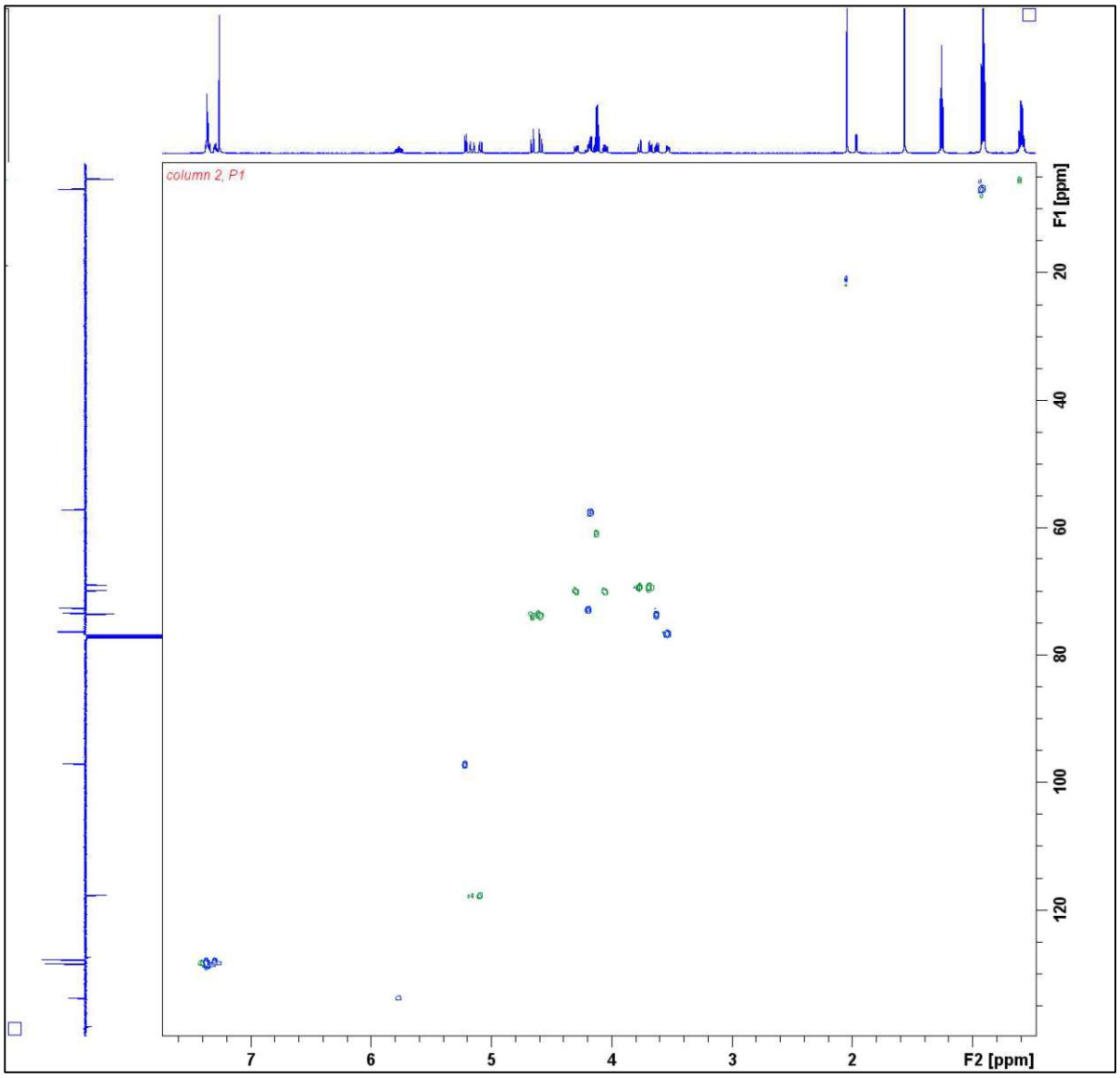

9.6.4 ^{1}H-^{29}Si-HMBC

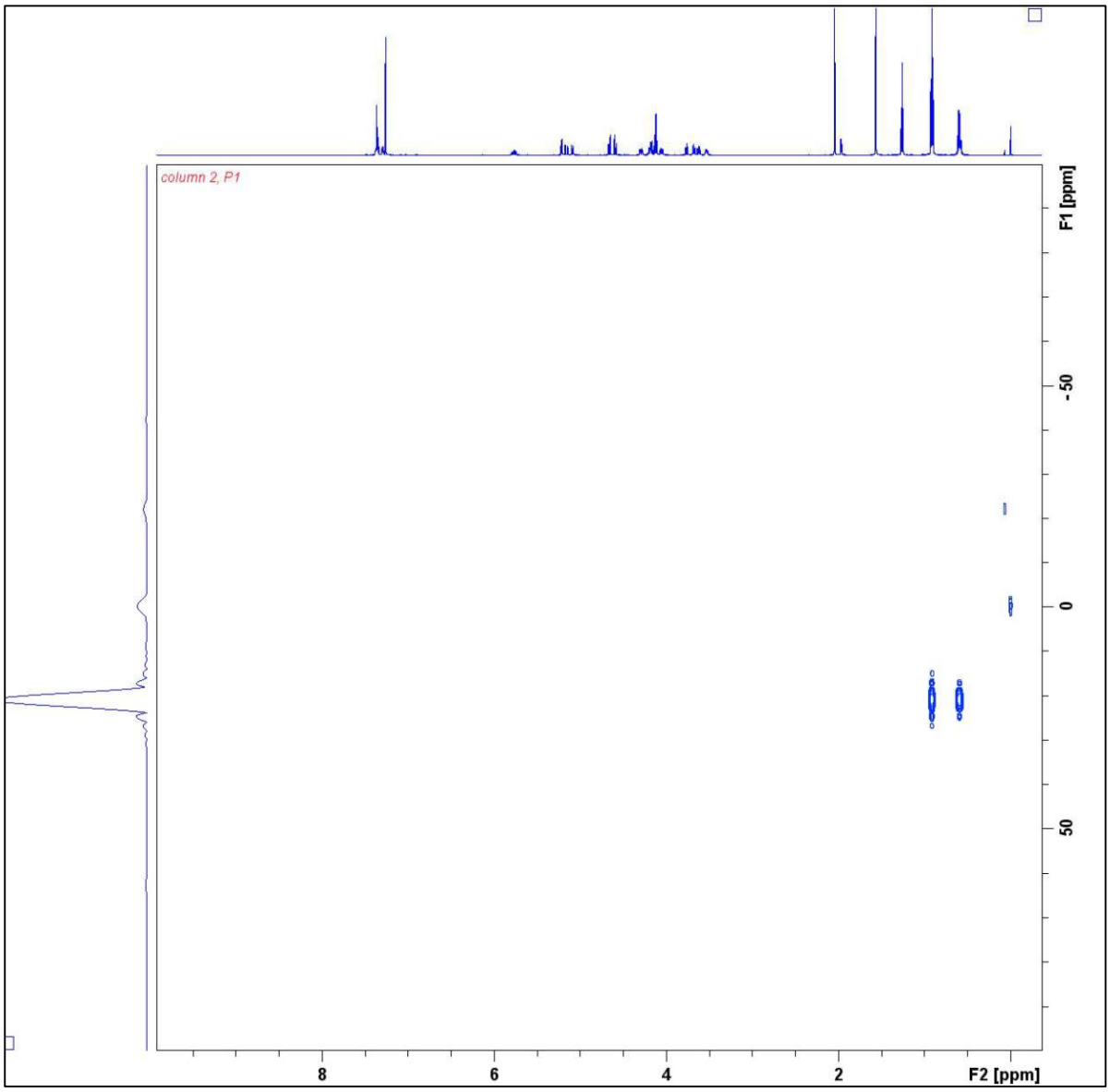

9.7 Compound **28b**

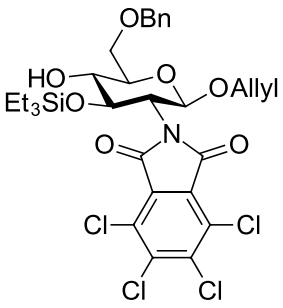

$C_{30}H_{35}Cl_4NO_7Si$
691.493 amu

28b

9.7.1 ^{1}H NMR

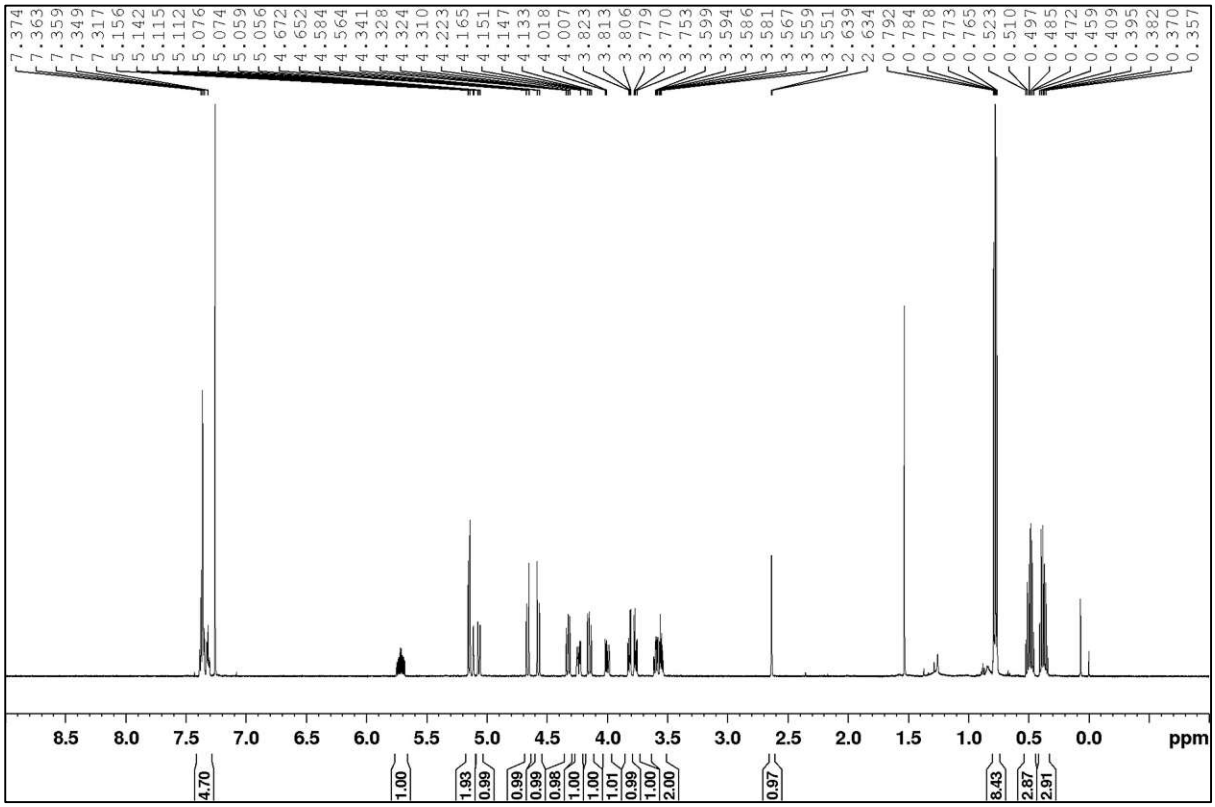

9.7.2 ^{13}C NMR

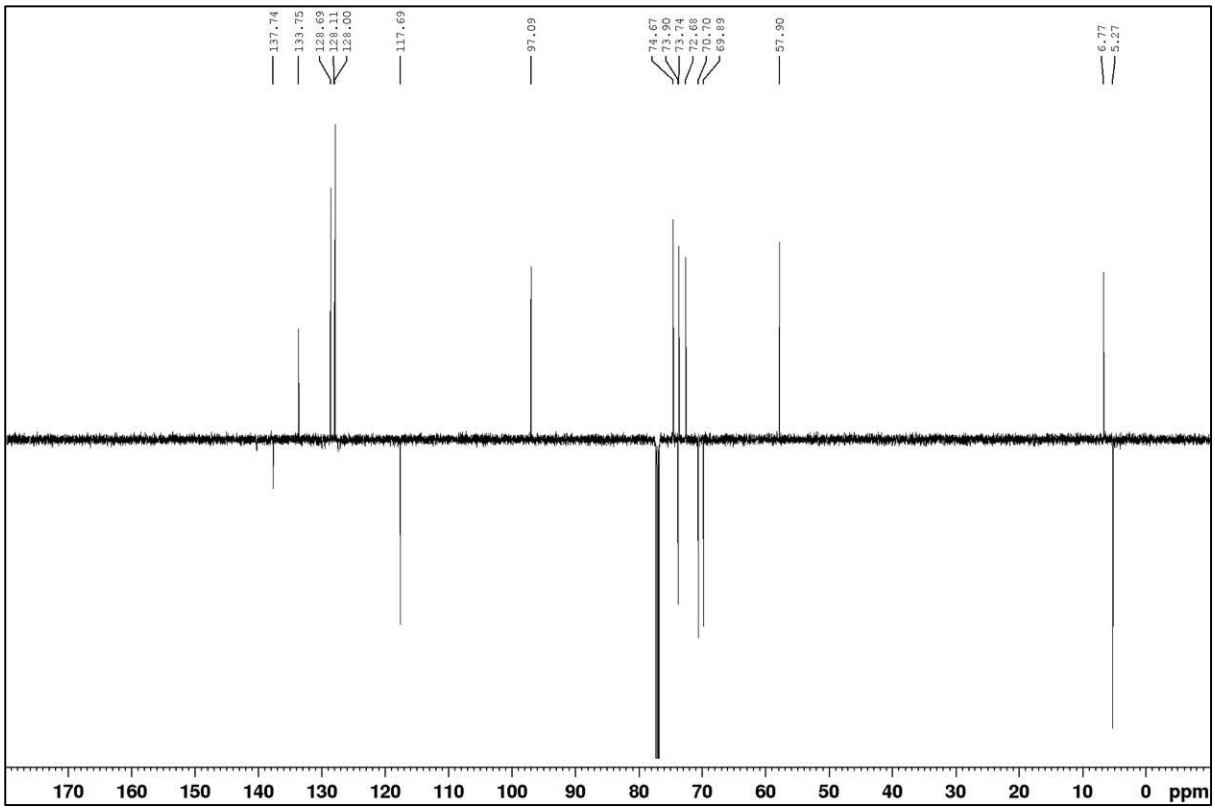

9.7.3 ^{1}H-^{13}C-HSQC

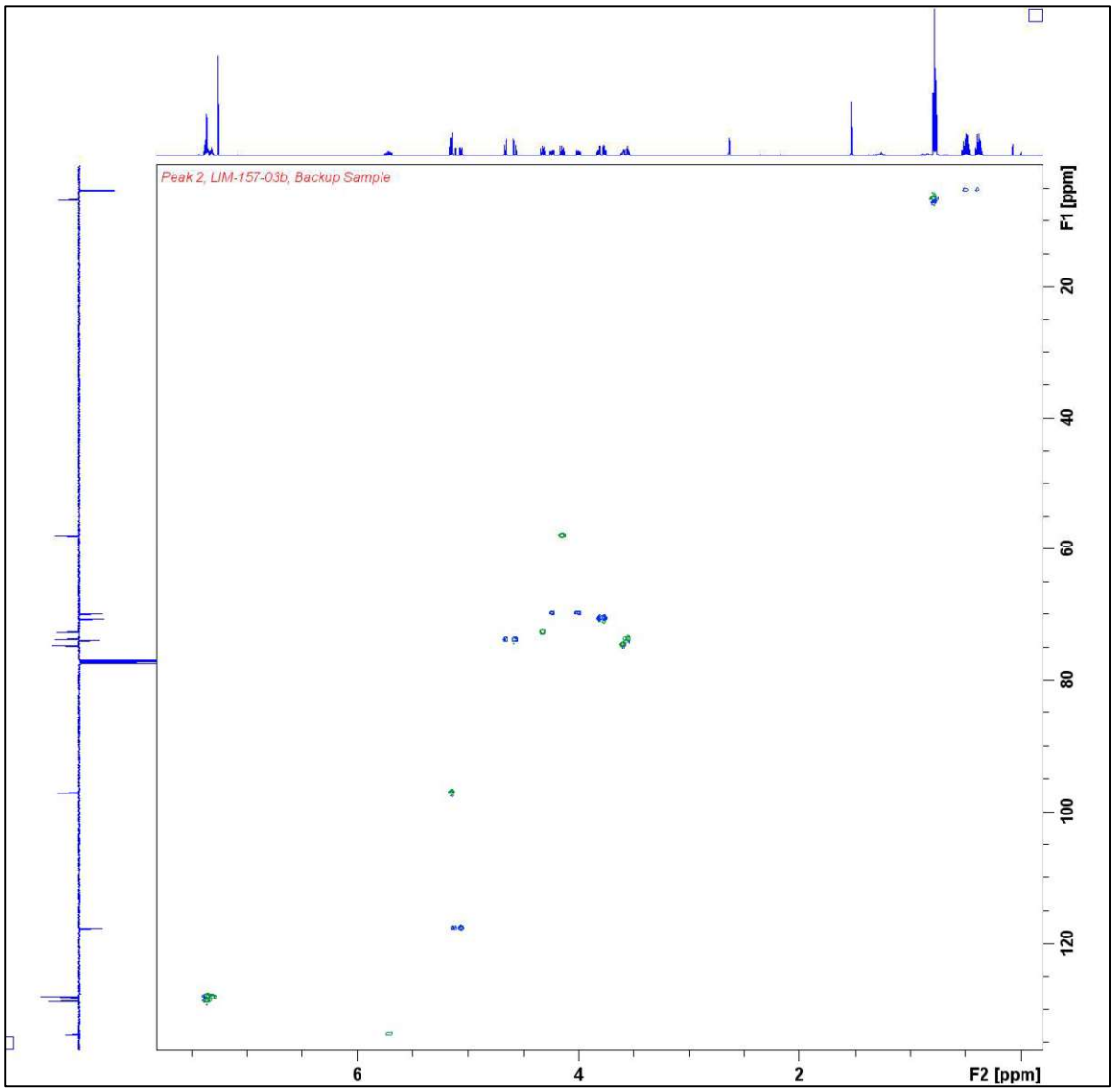

9.8 Compound **29**

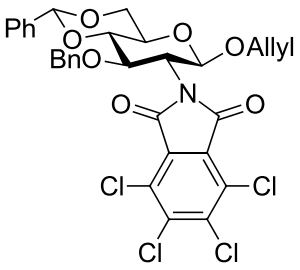

$C_{31}H_{25}Cl_4NO_7$
665.339 amu

29

9.8.1 ^{1}H NMR

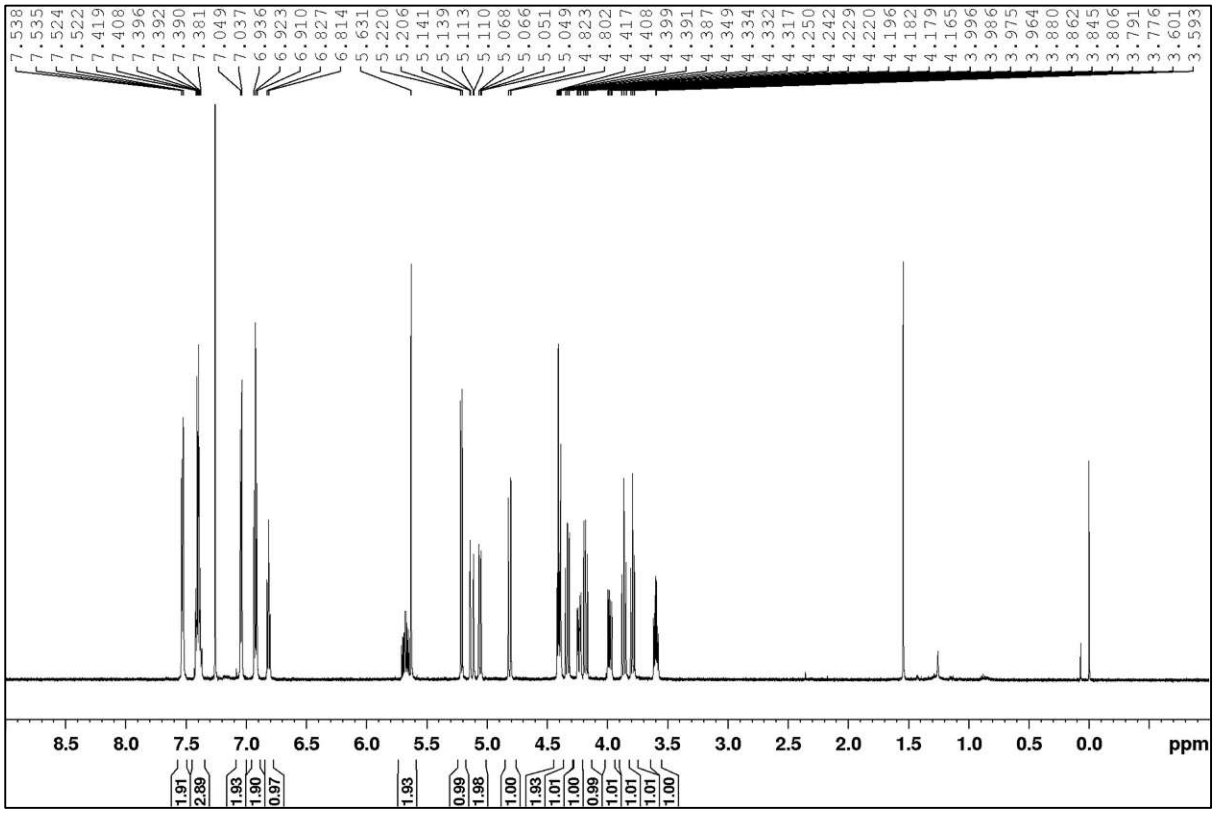

9.8.2 ^{13}C NMR

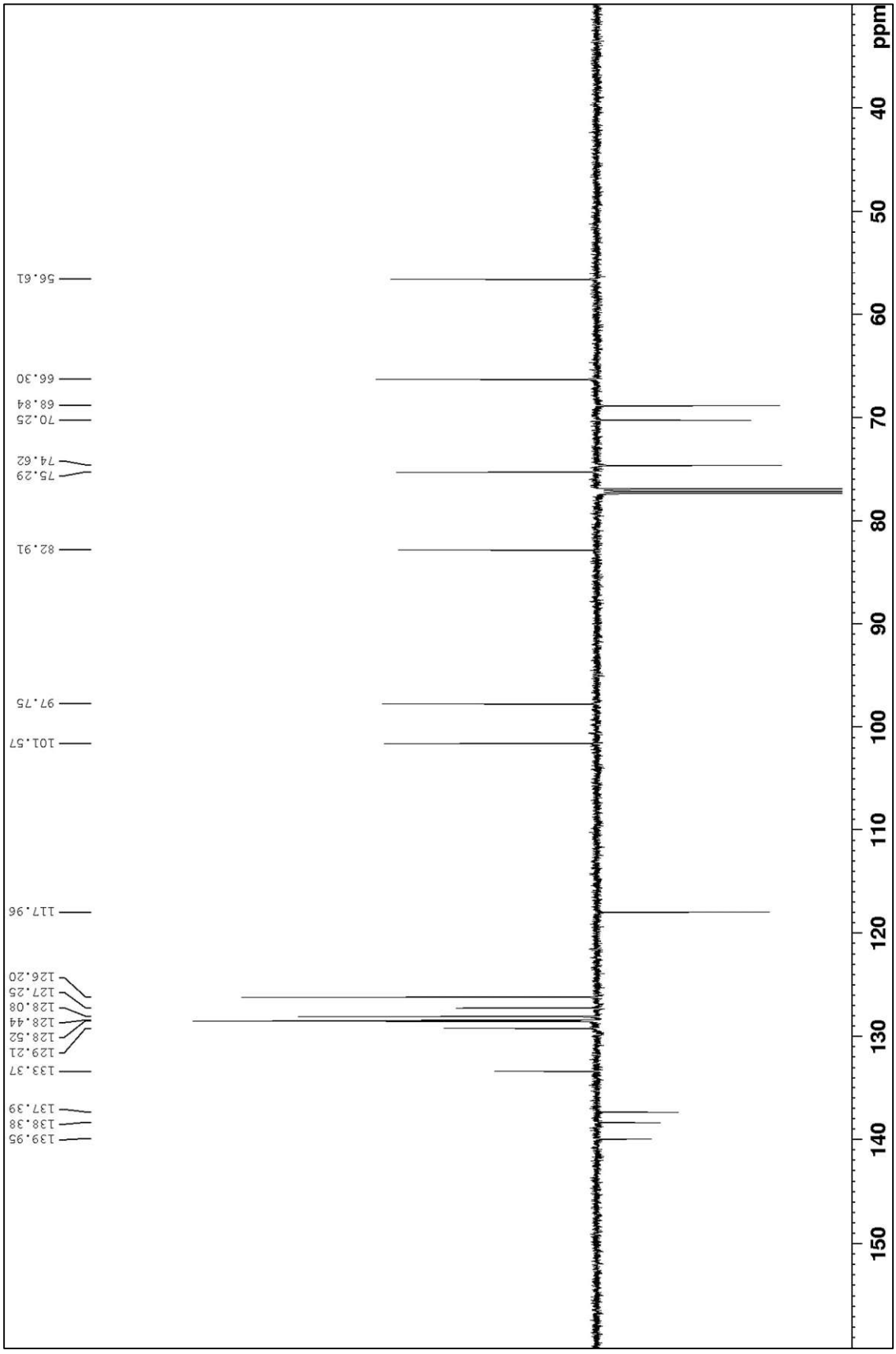

9.8.3 ^{1}H-^{13}C-HSQC

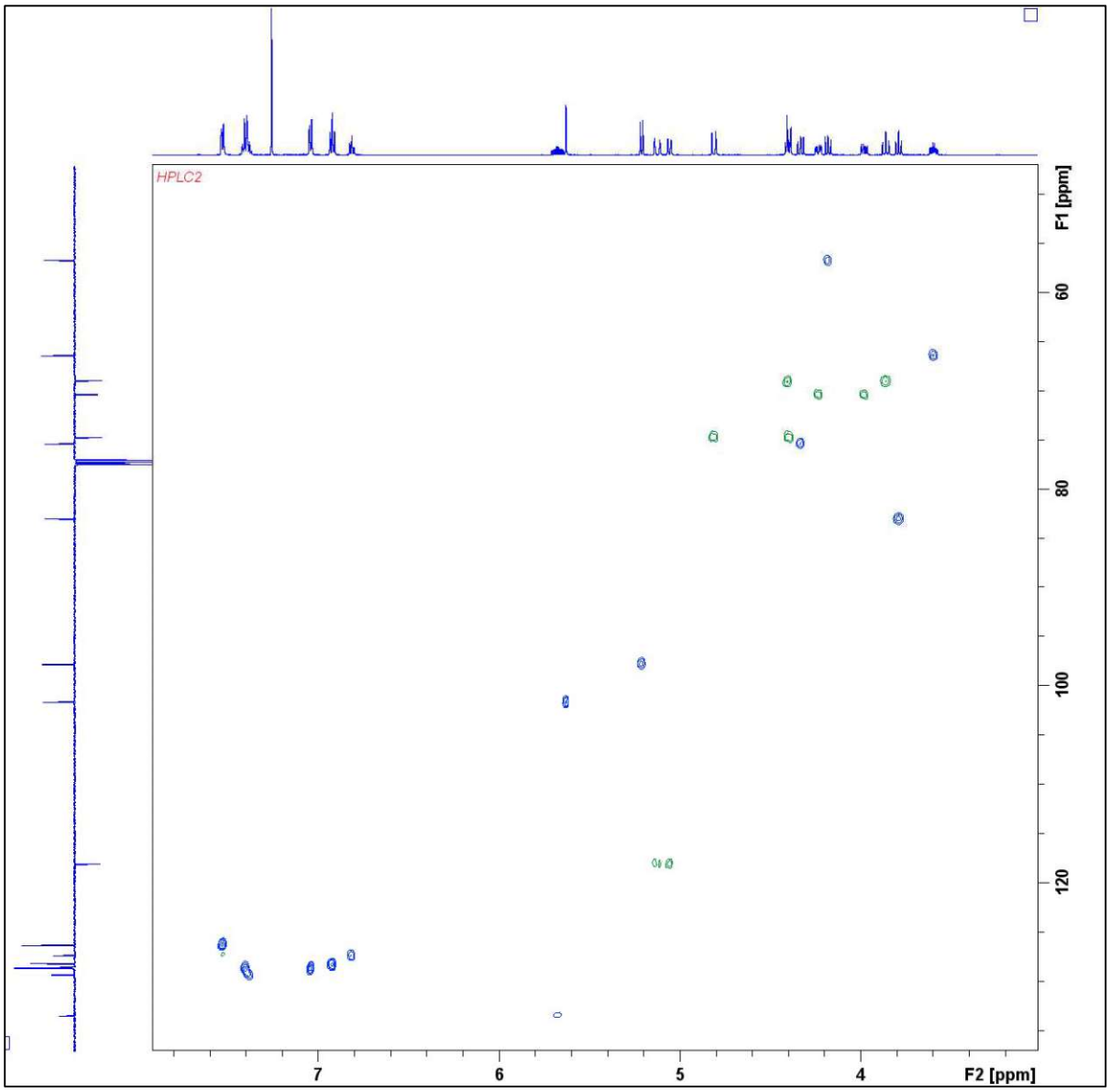

9.9 Compound **30**

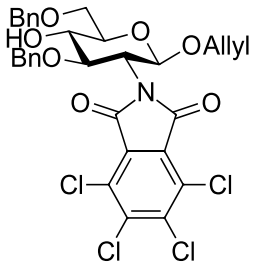

$C_{31}H_{27}Cl_4NO_7$
667.355 amu

30

9.9.1 ^{1}H NMR

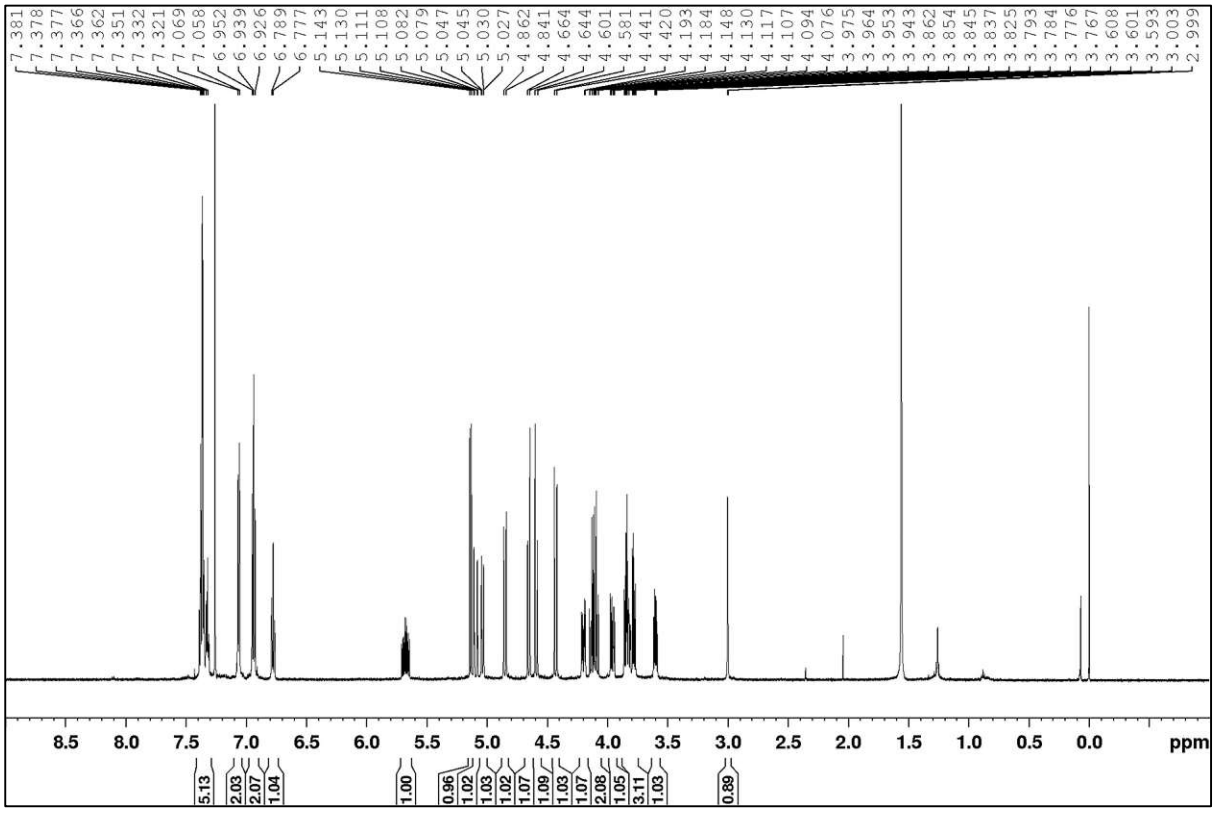

9.9.2 ^{13}C NMR

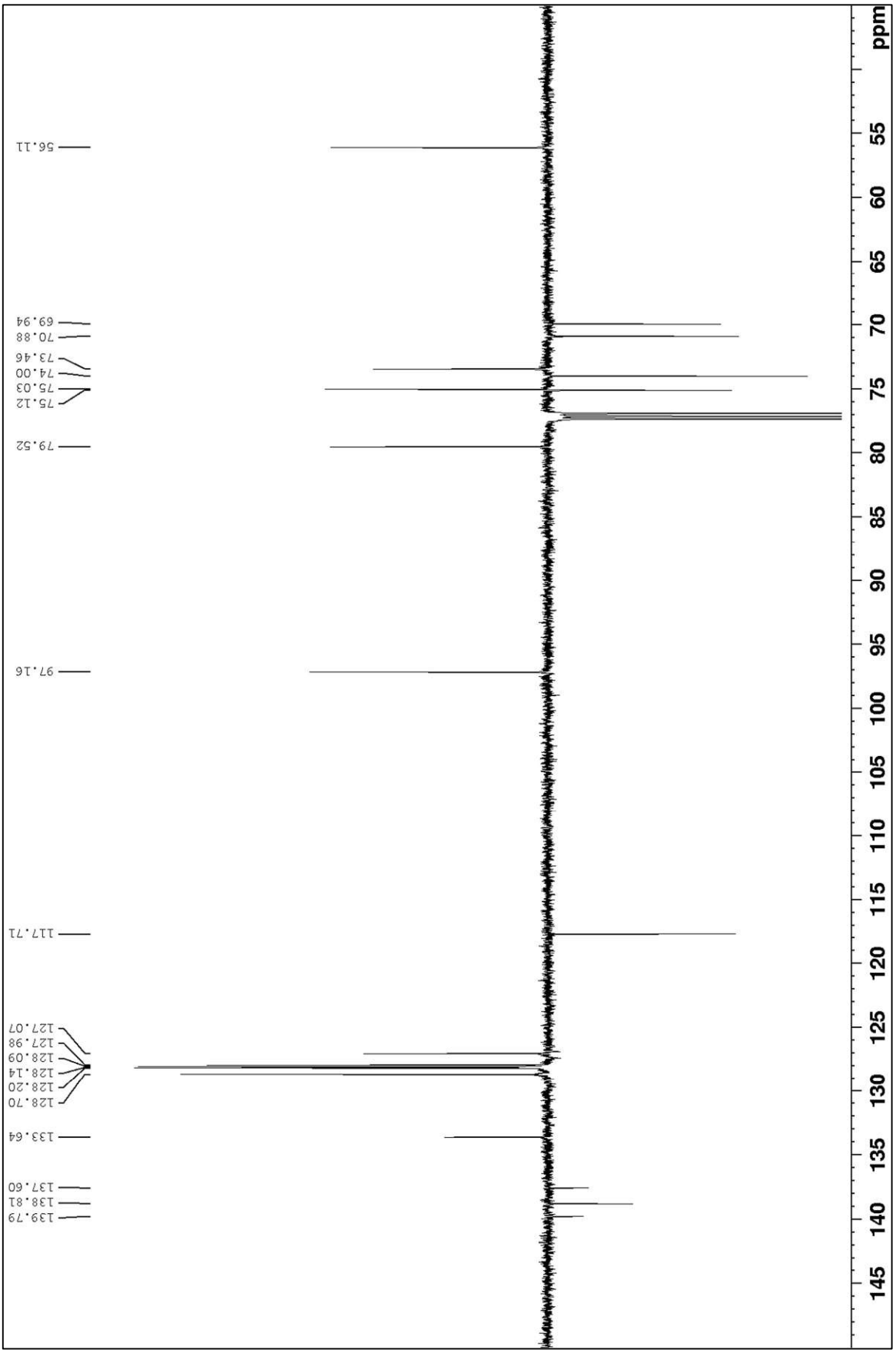

9.9.3 ^{1}H-^{13}C-HSQC

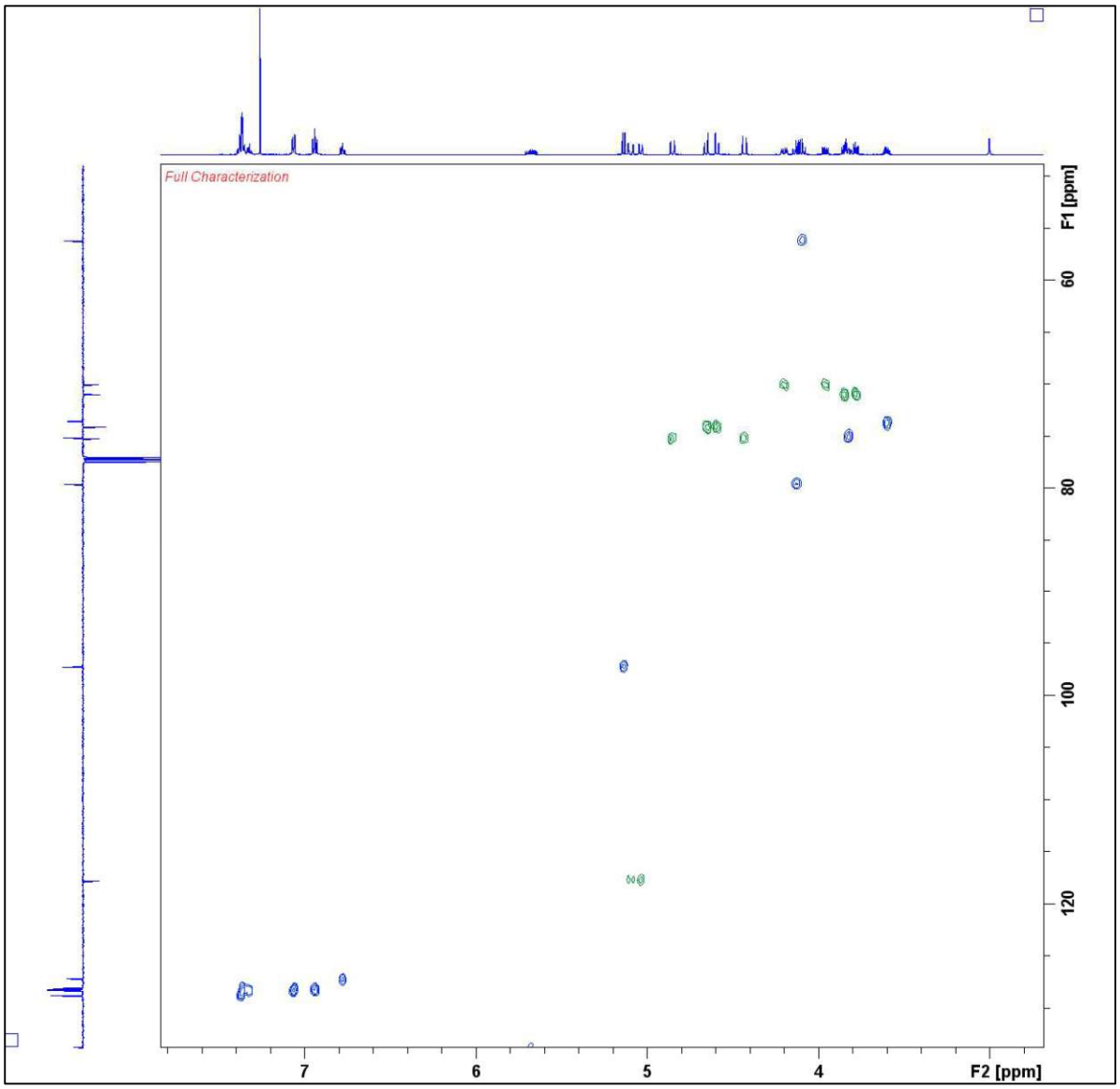

9.10 Compound **31a**

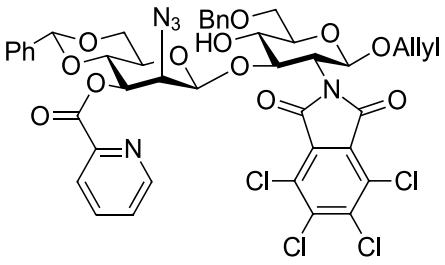

$C_{43}H_{37}Cl_4N_5O_{12}$
957.586 amu

31a

9.10.1 ^{1}H NMR

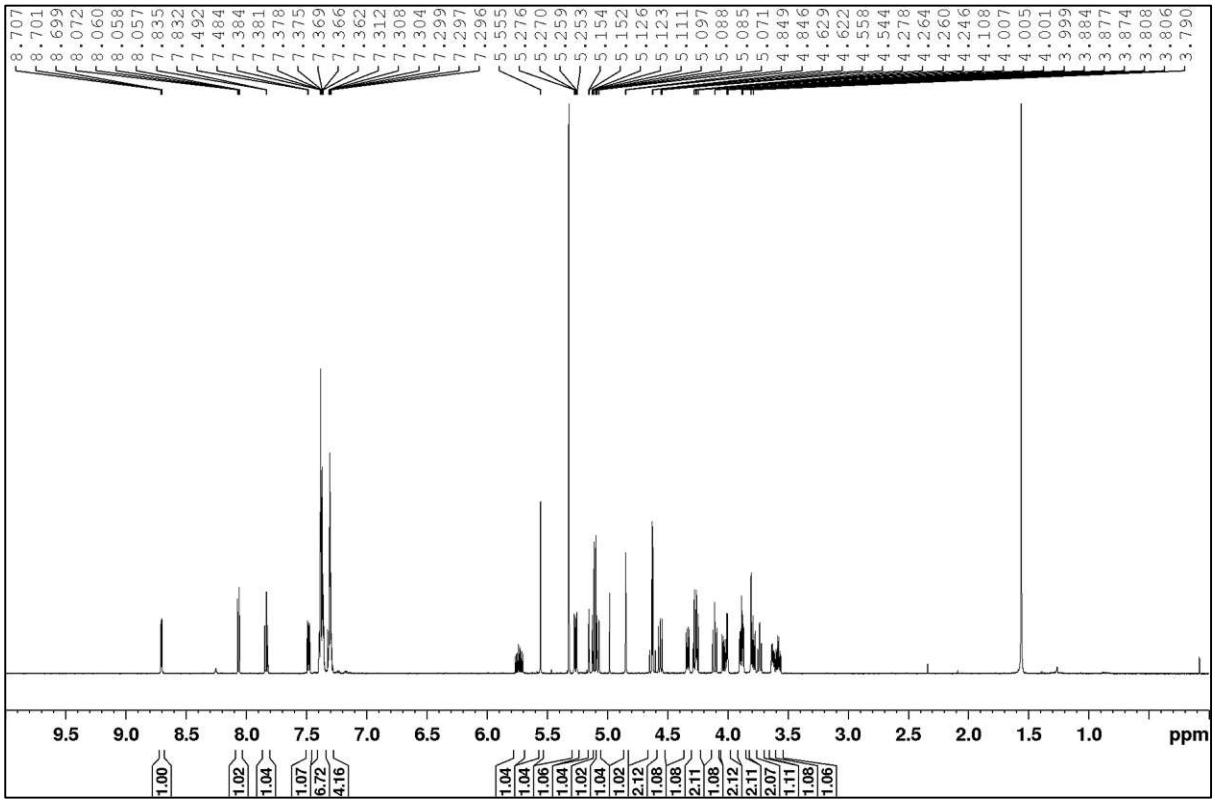

9.10.2 ^{13}C NMR

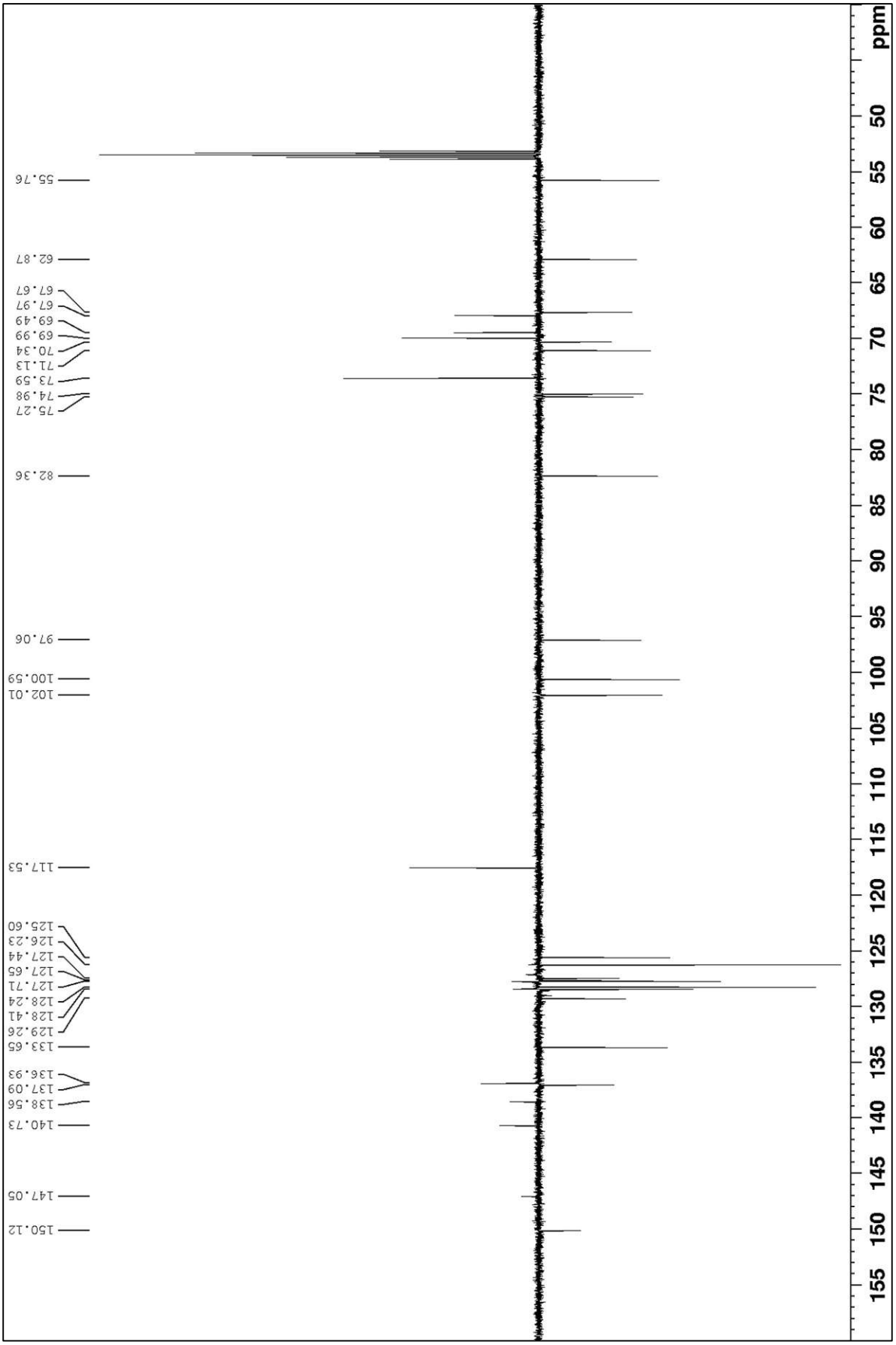

9.10.3 ^{1}H-^{13}C-HSQC

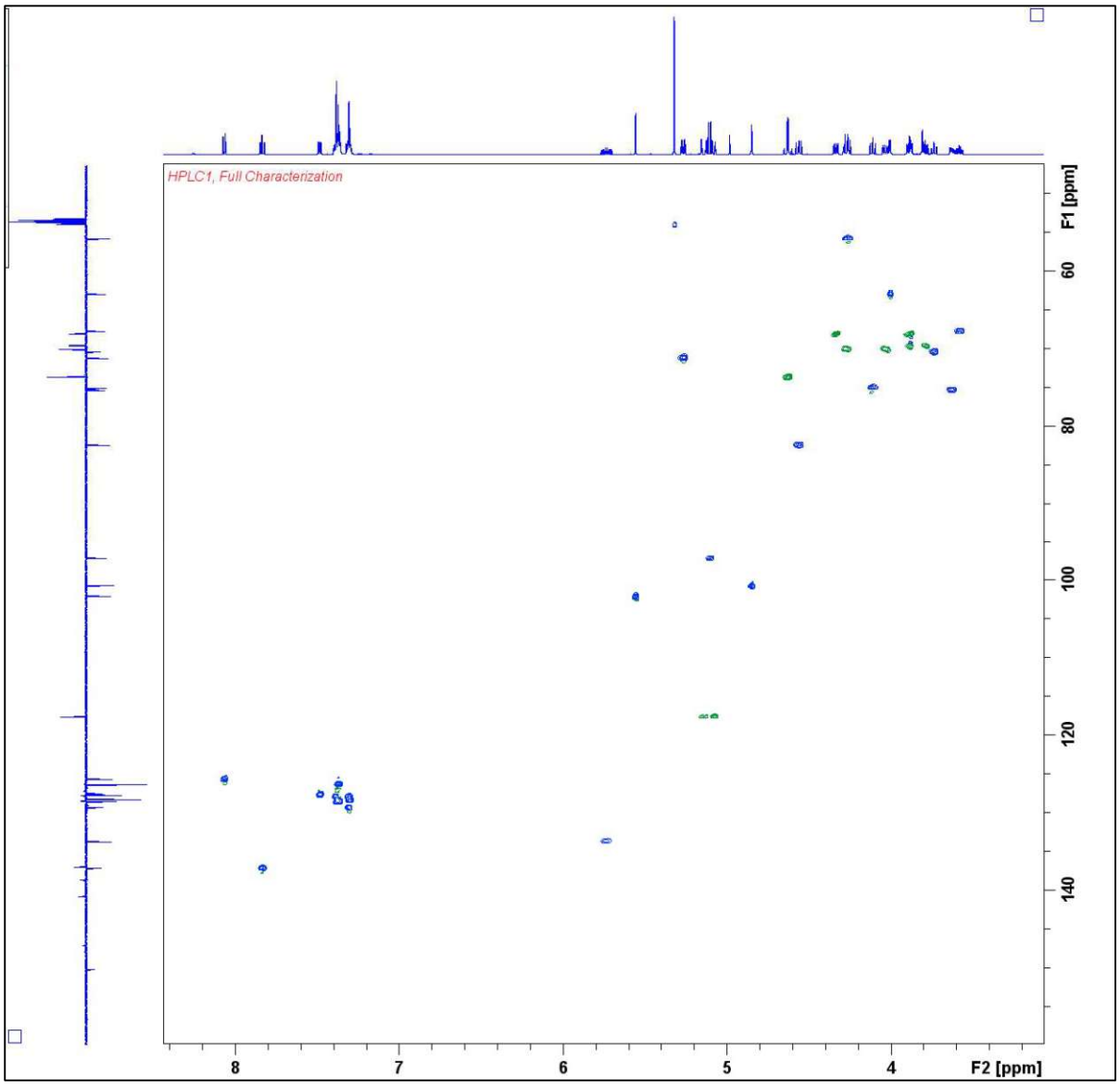

9.10.4 CLIP-HSQC

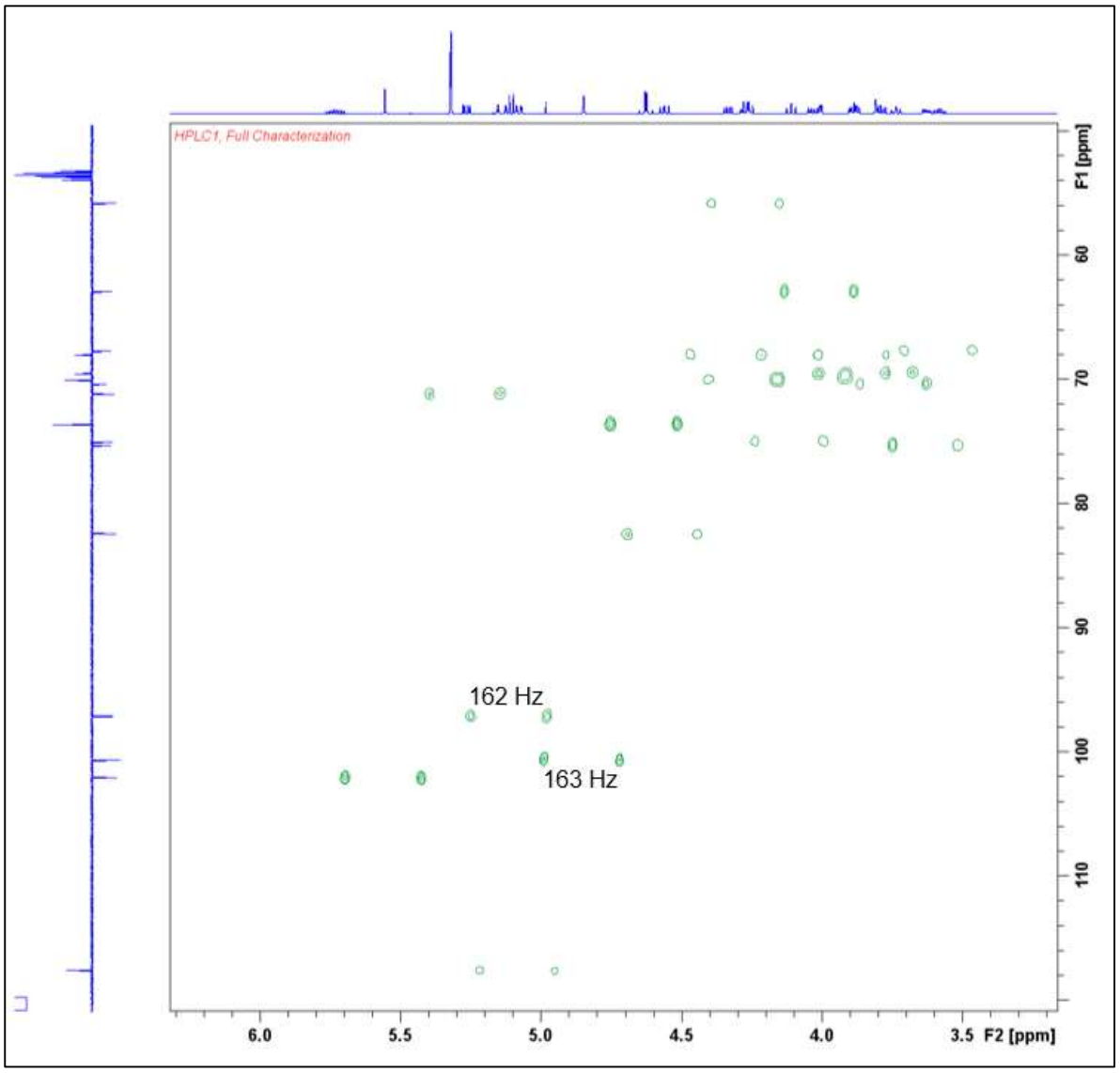

9.11 Compound **32**

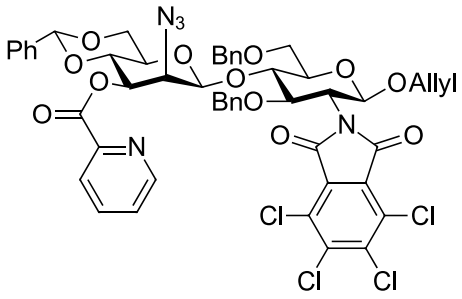

$C_{50}H_{43}Cl_4N_5O_{12}$
1047.708 amu

32

9.11.1 ^{1}H NMR

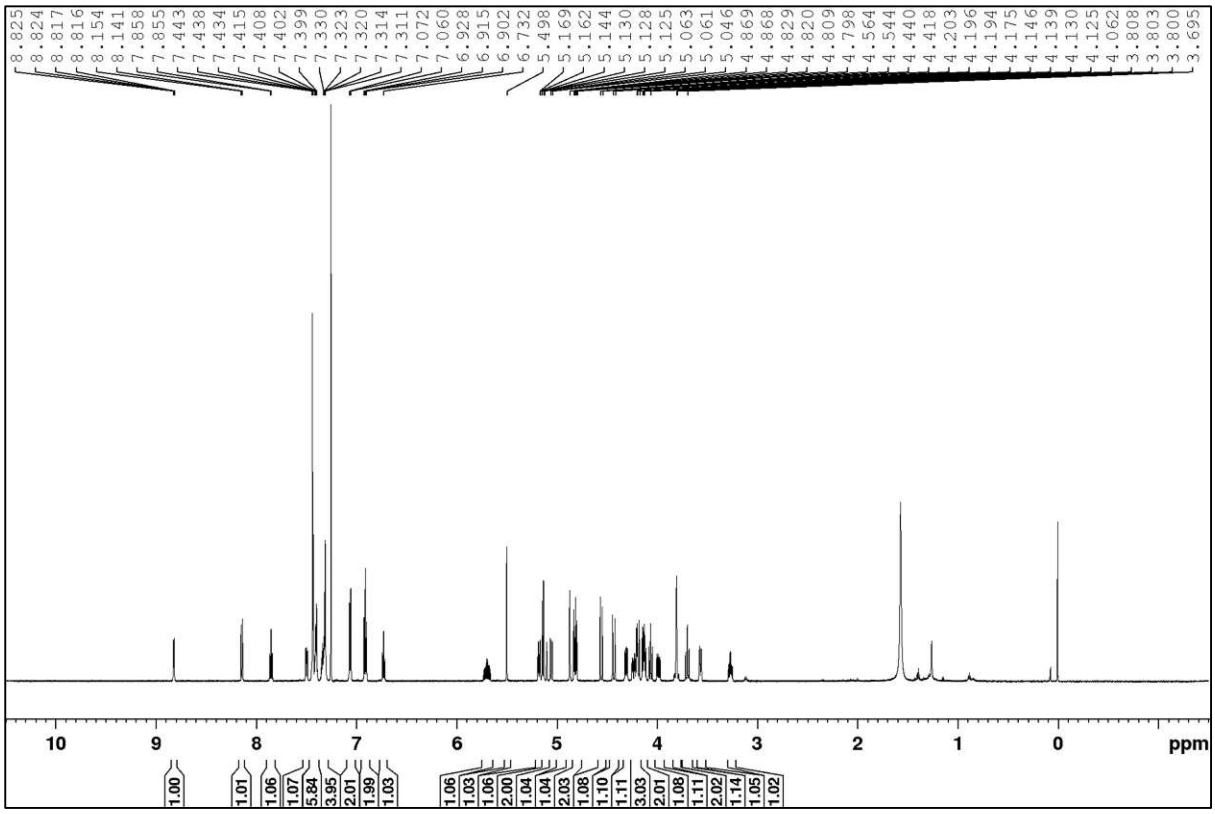

9.11.2 ^{13}C NMR

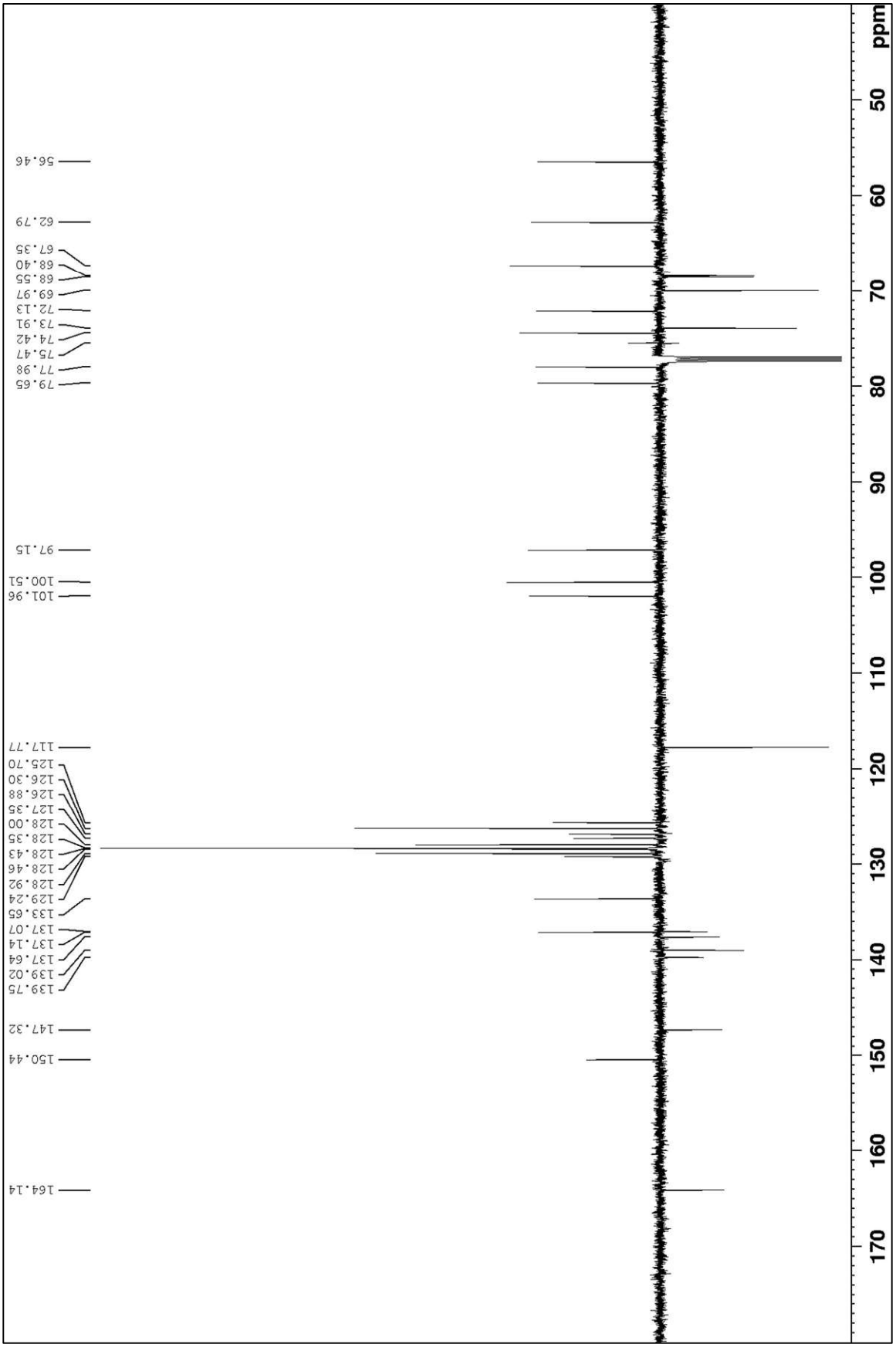

9.11.3 ^{1}H-^{13}C-HSQC

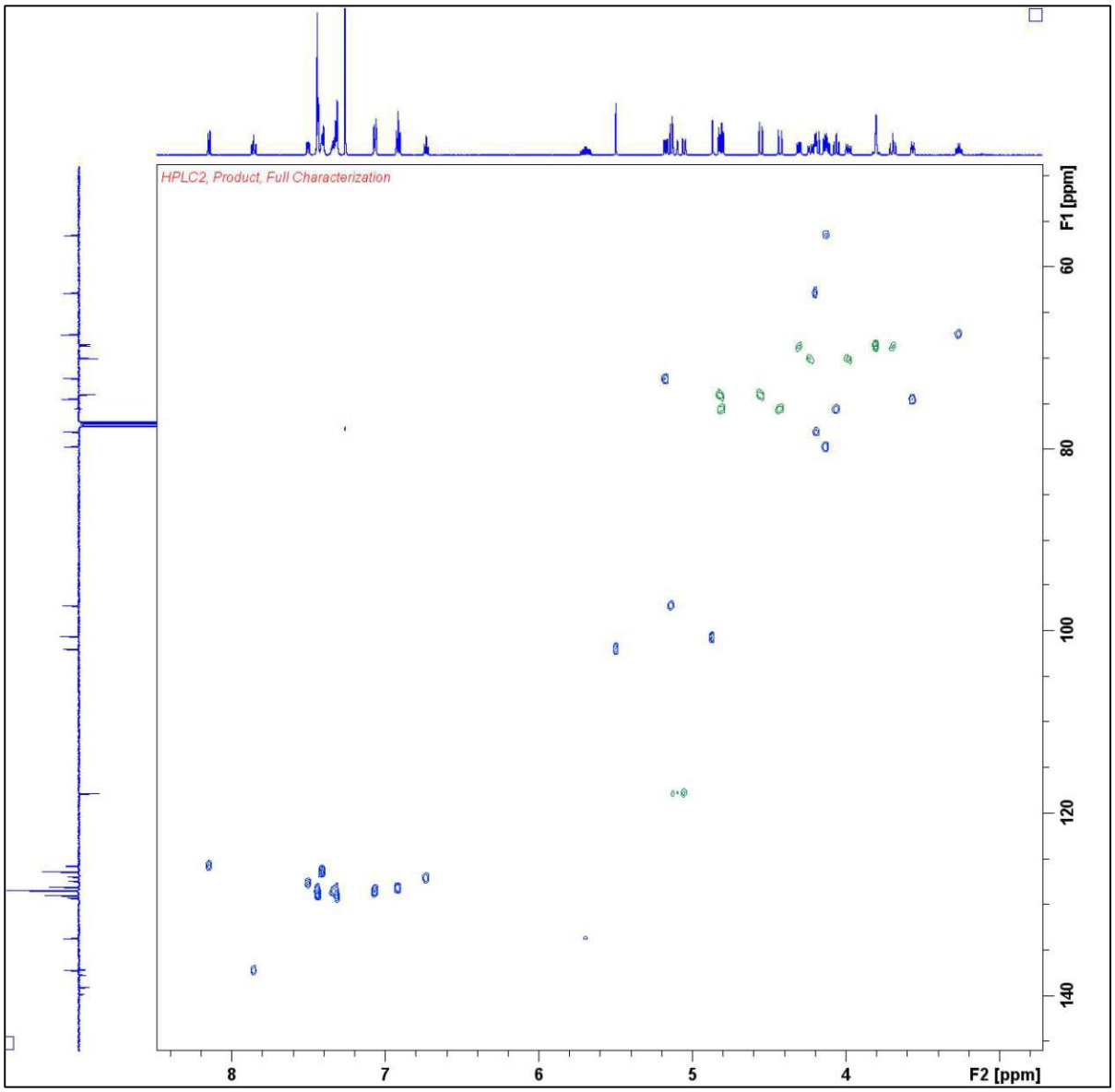

9.11.4 HSQC and HSQC/HMBC overlap

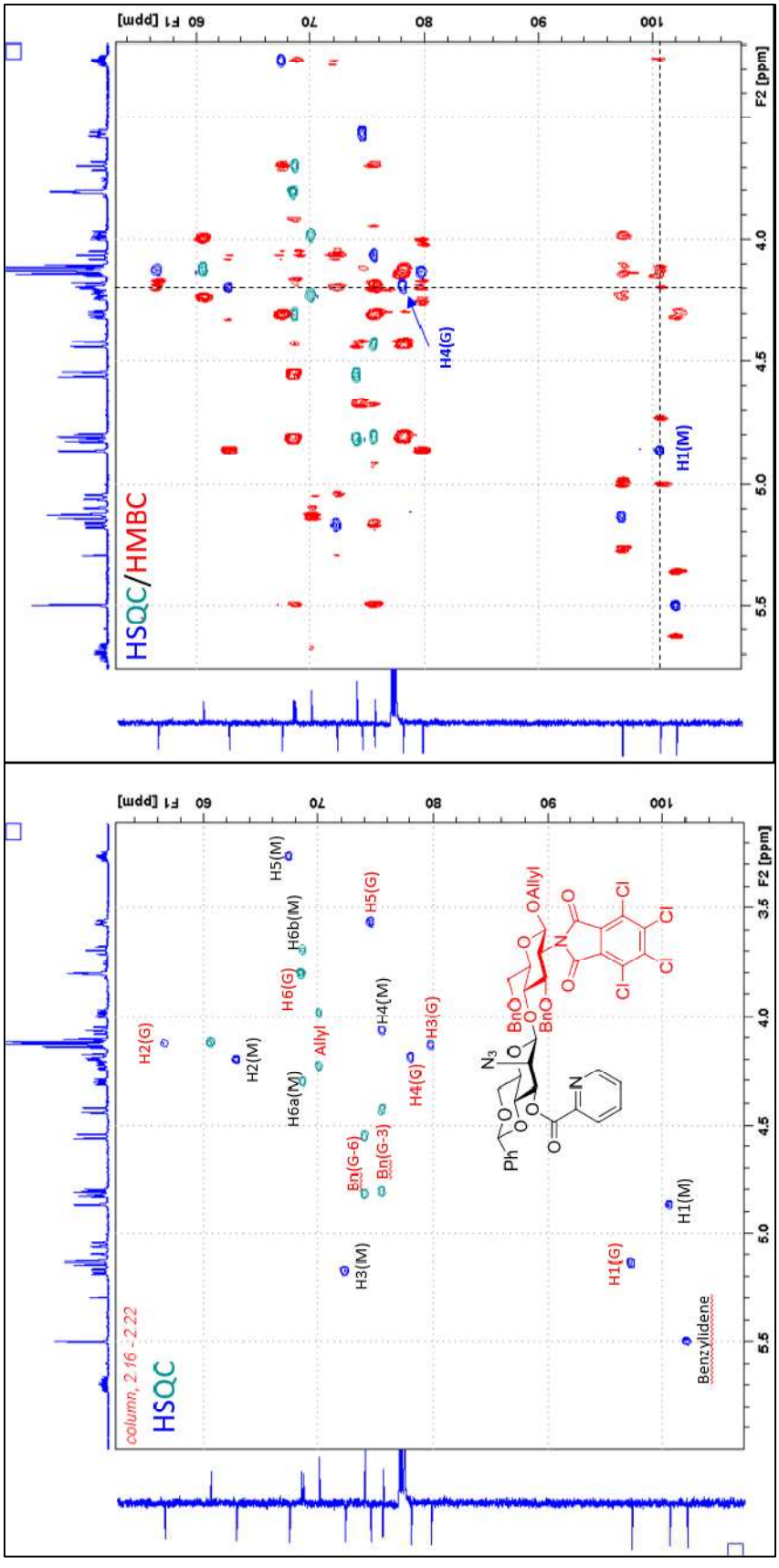

$^{1}J_{C1A,H1A}$ = 163 Hz

9.12 Compound **32a**

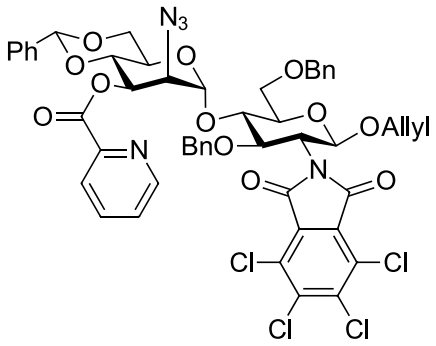

$C_{50}H_{43}Cl_4N_5O_{12}$
1047.708 amu

32a

9.12.1 ^{1}H NMR

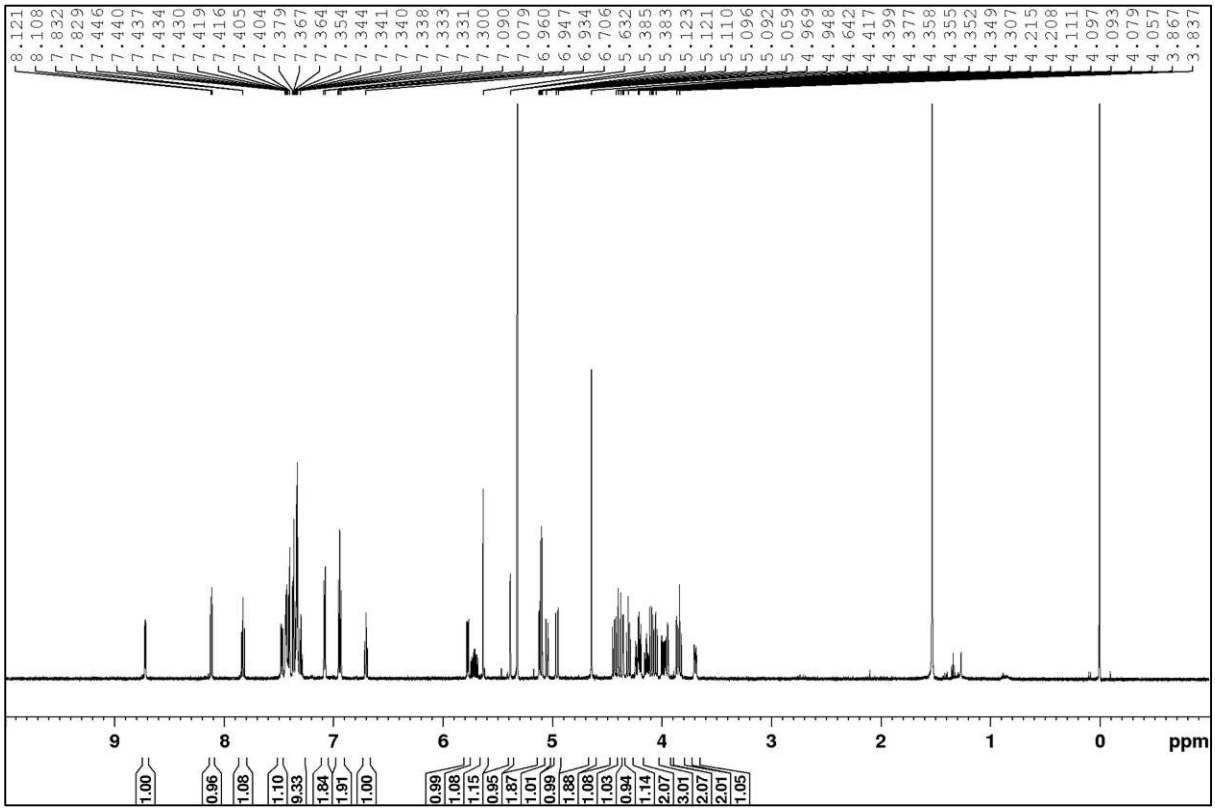

9.12.2 ^{13}C NMR

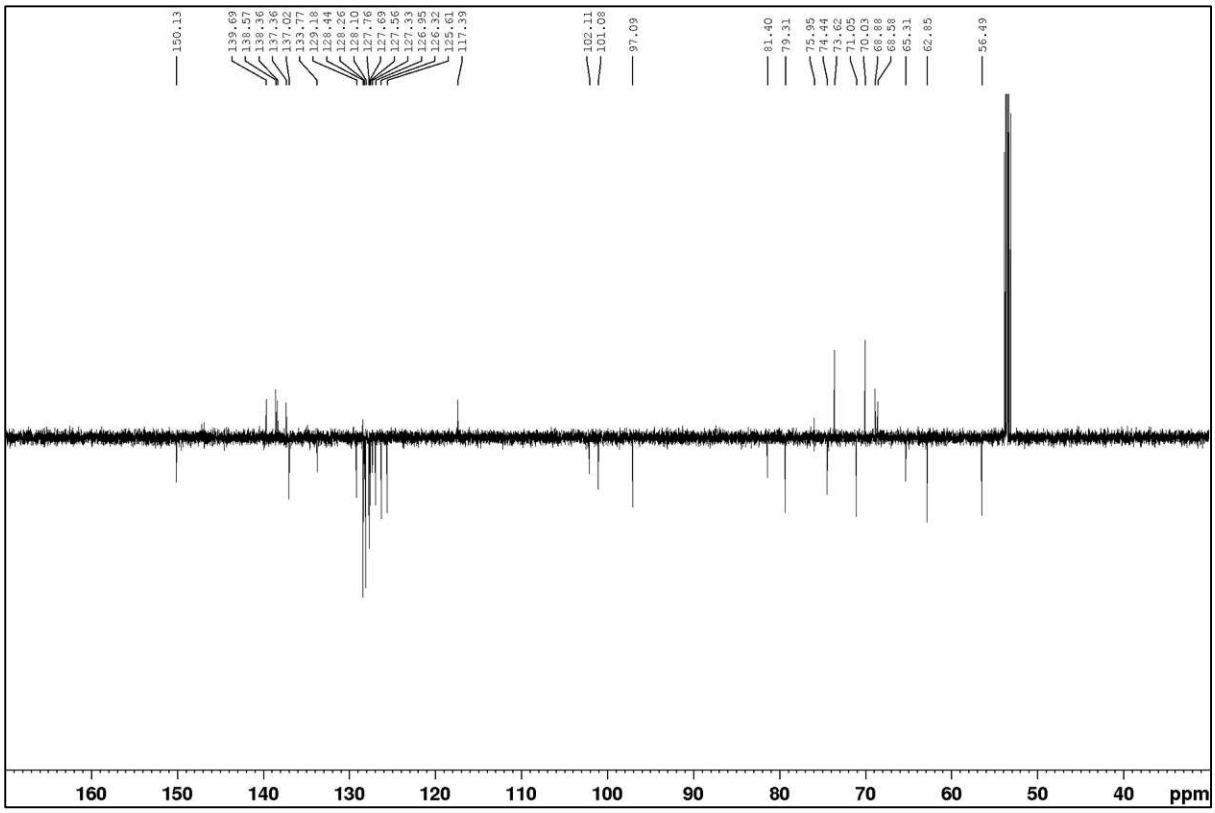

9.12.3 ^{1}H-^{13}C-HSQC

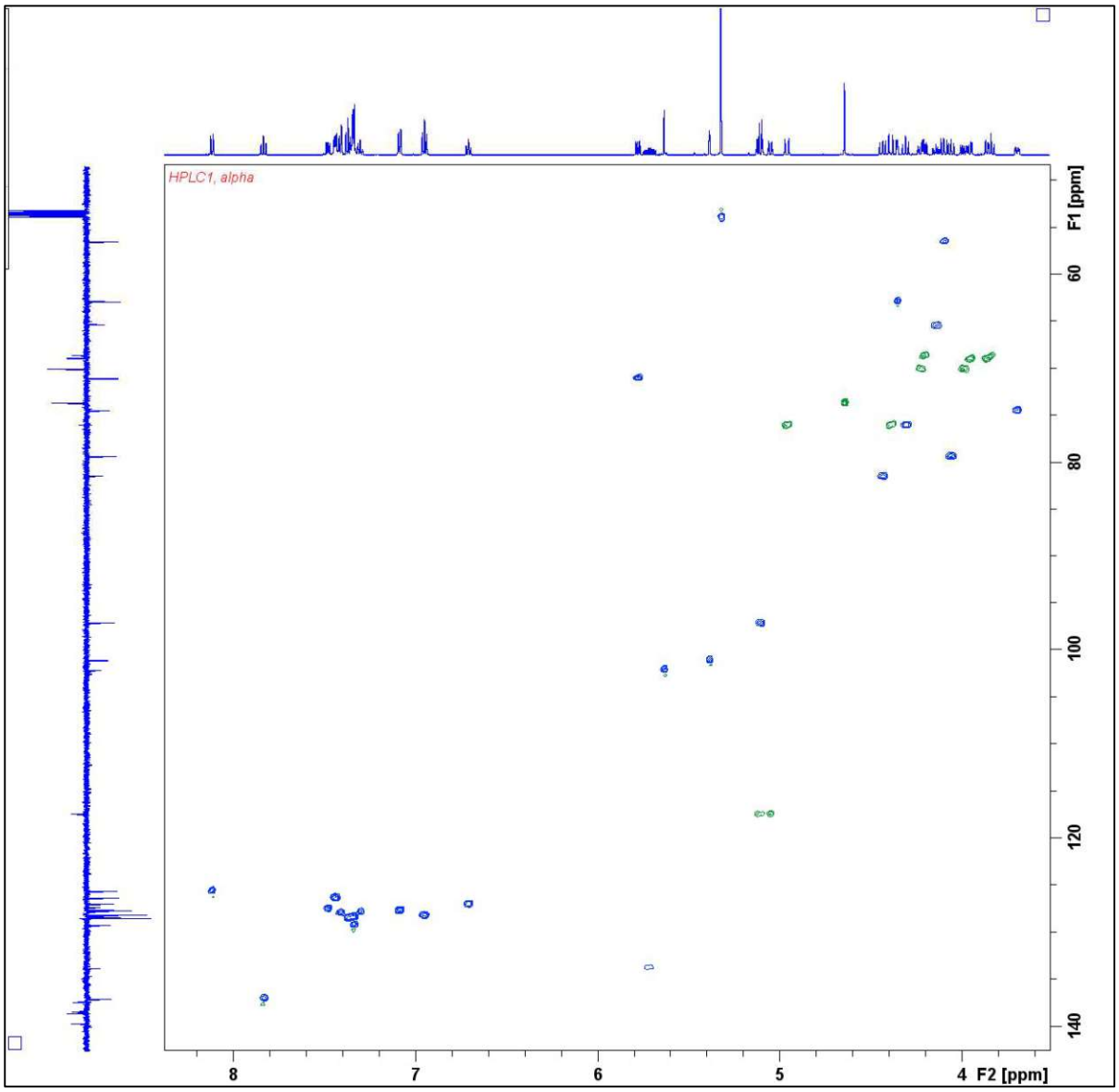

9.12.4 CLIP-HSQC

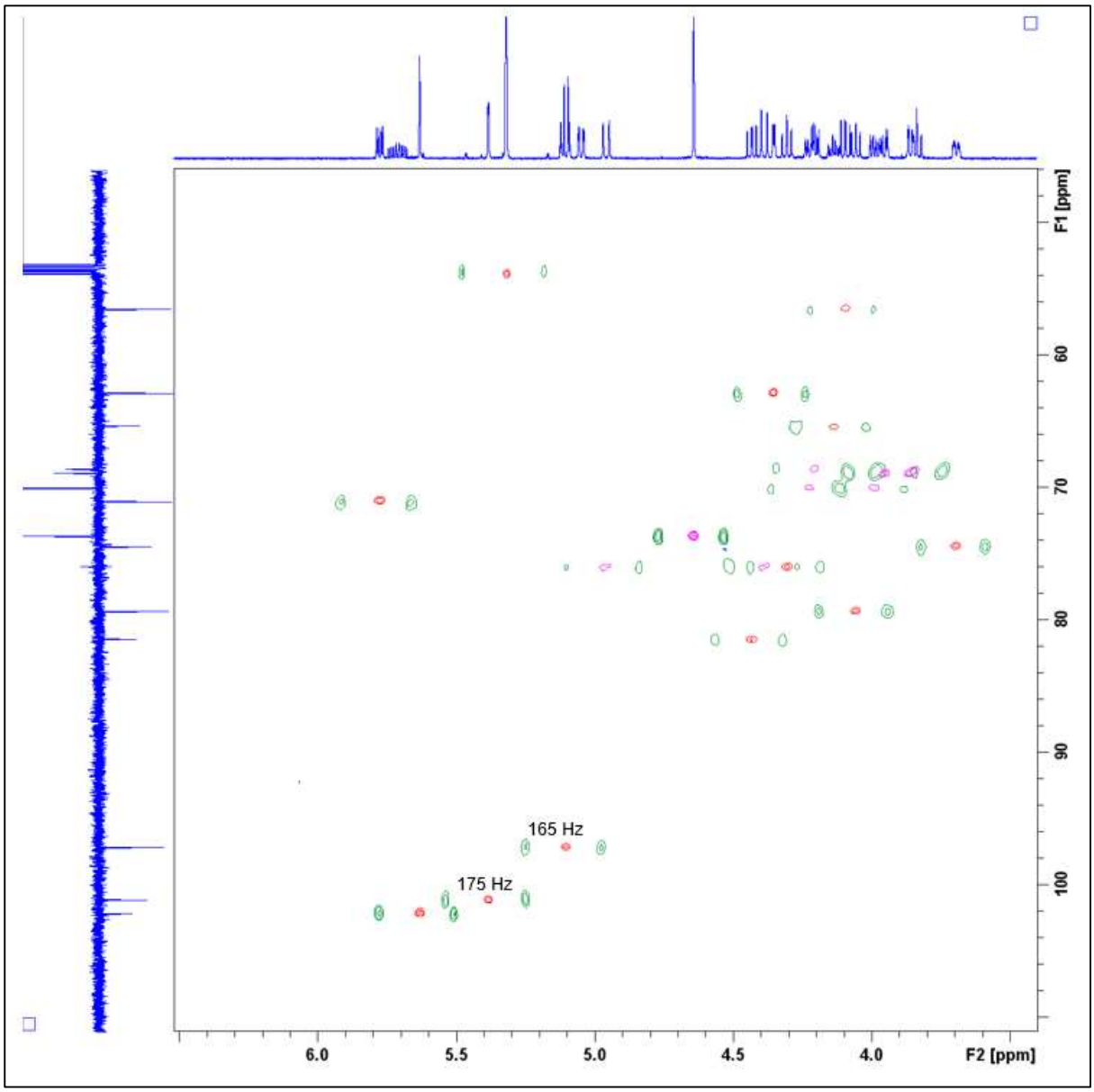

9.13 Compound **37**

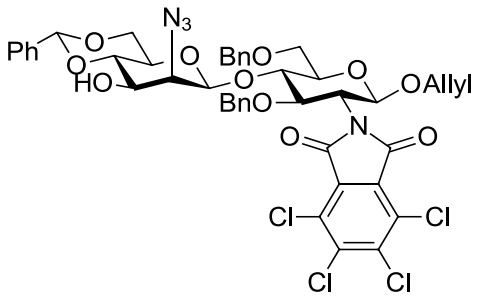

$C_{44}H_{40}Cl_4N_4O_{11}$
942.615 amu

37

9.13.1 ^{1}H NMR

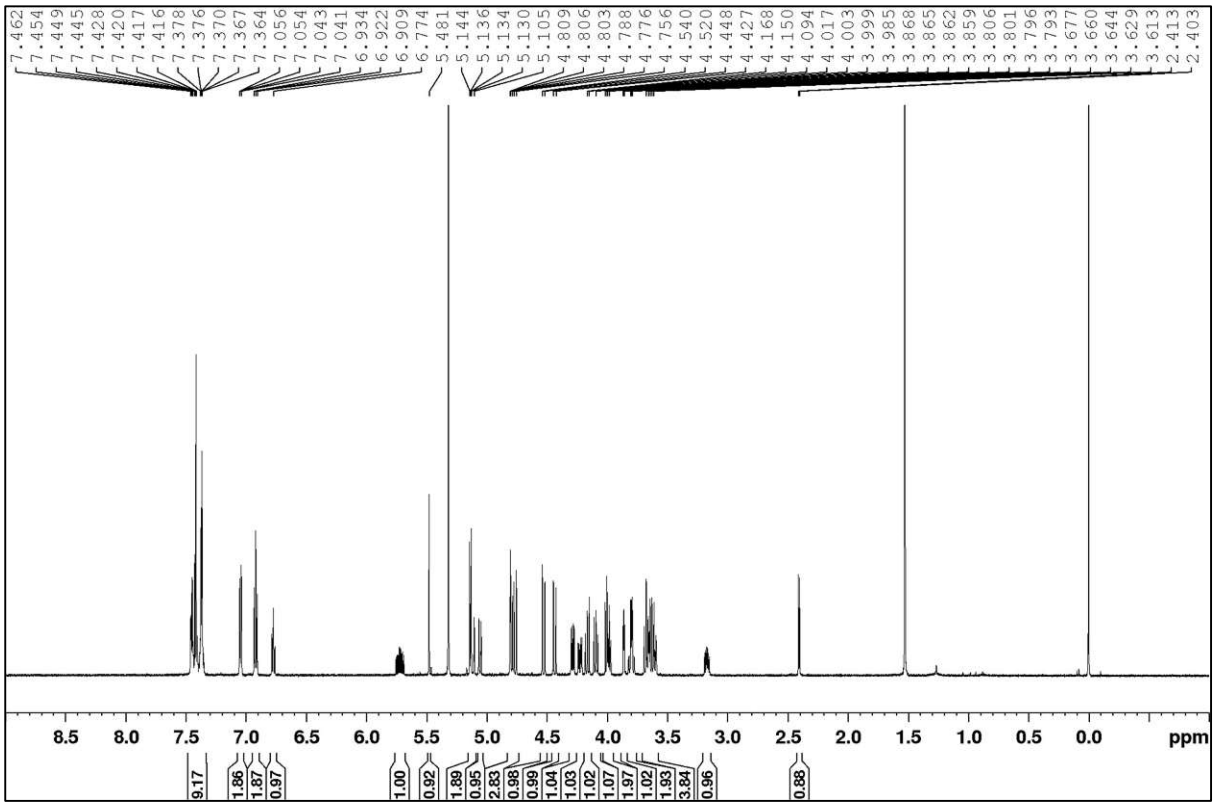

9.13.2 ^{13}C NMR

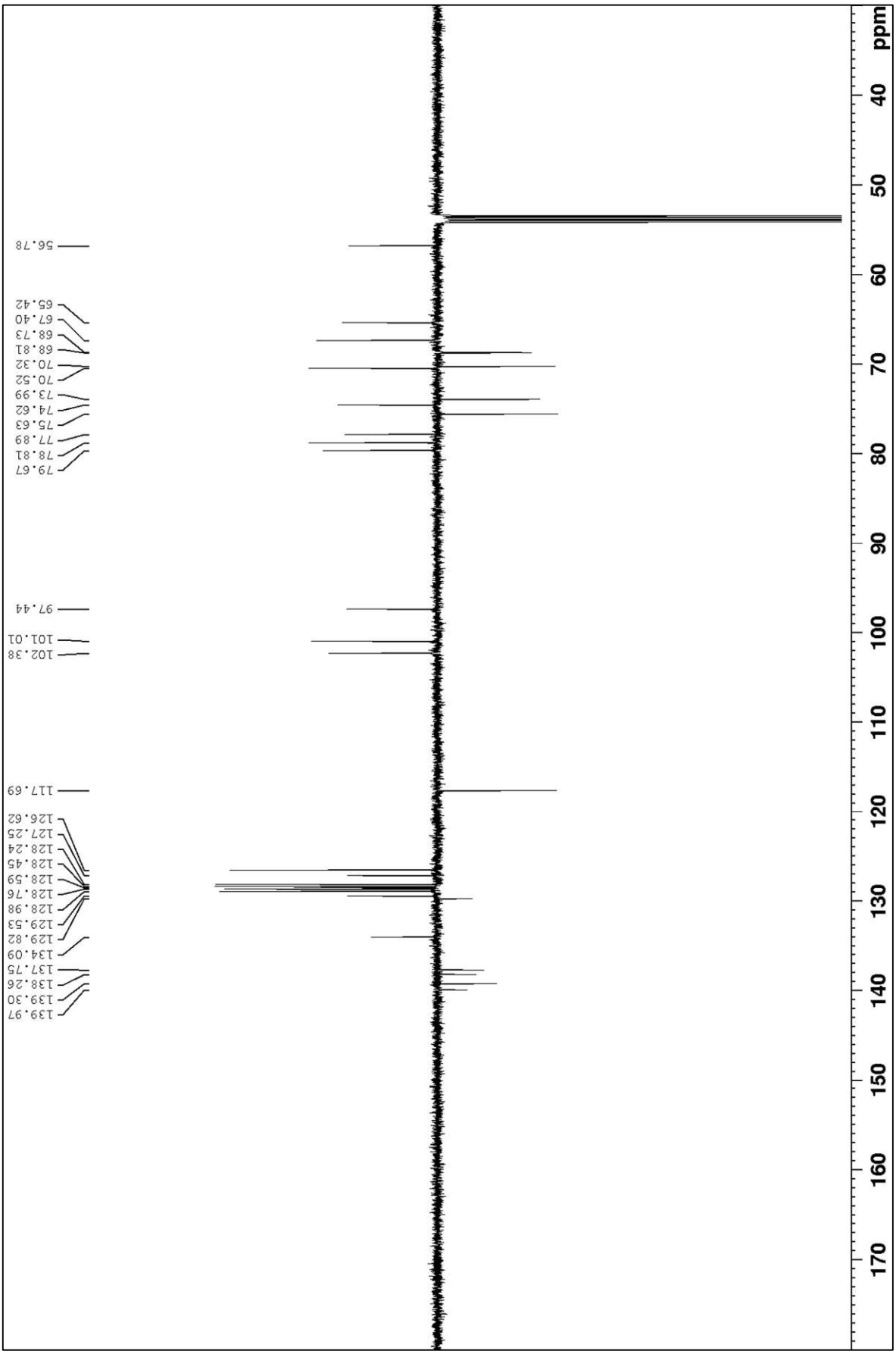

9.13.3 ^{1}H-^{13}C-HSQC

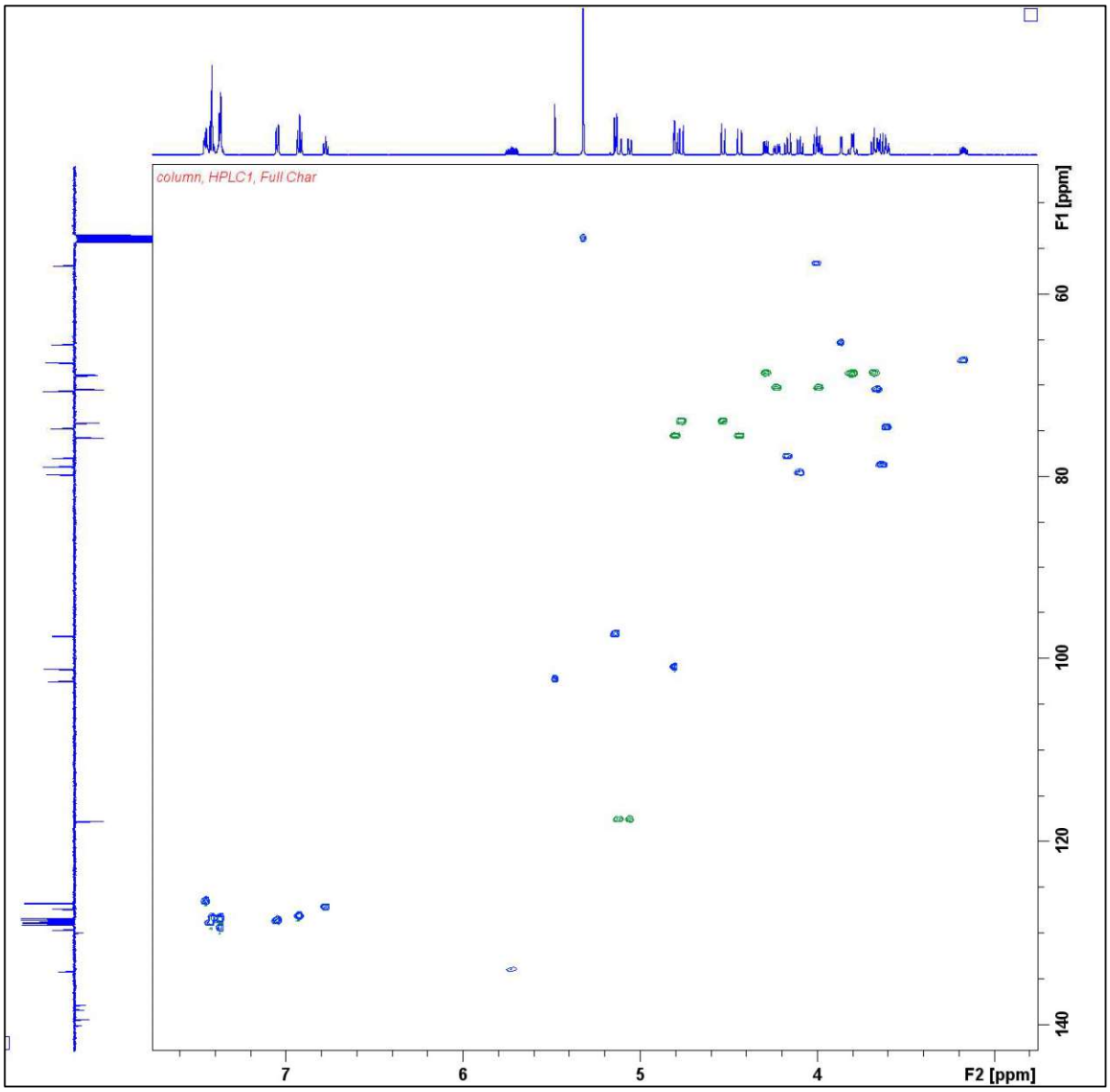

9.14 Compound **38**

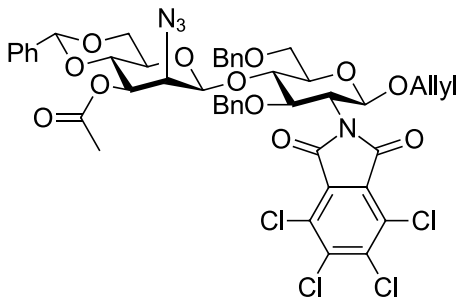

$C_{46}H_{42}Cl_4N_4O_{12}$
984.651 amu

38

9.14.1 ^{1}H NMR

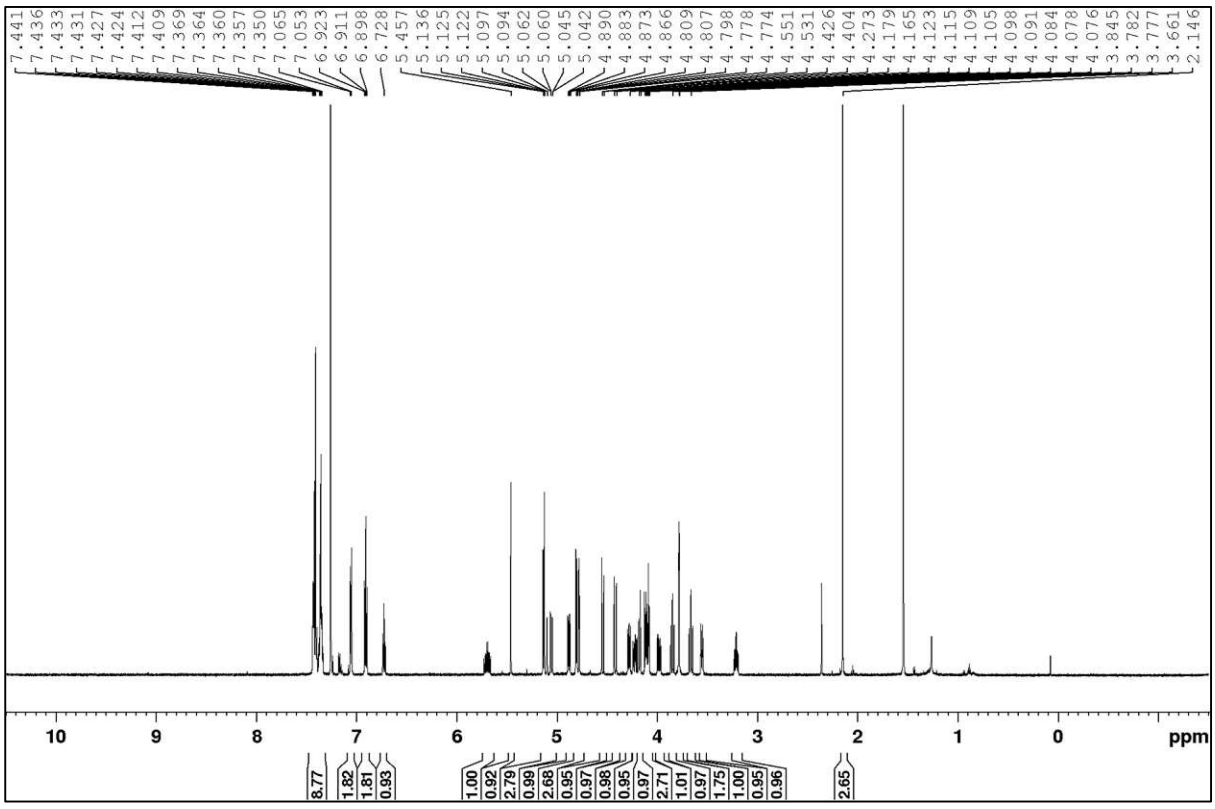

9.14.2 ^{13}C NMR

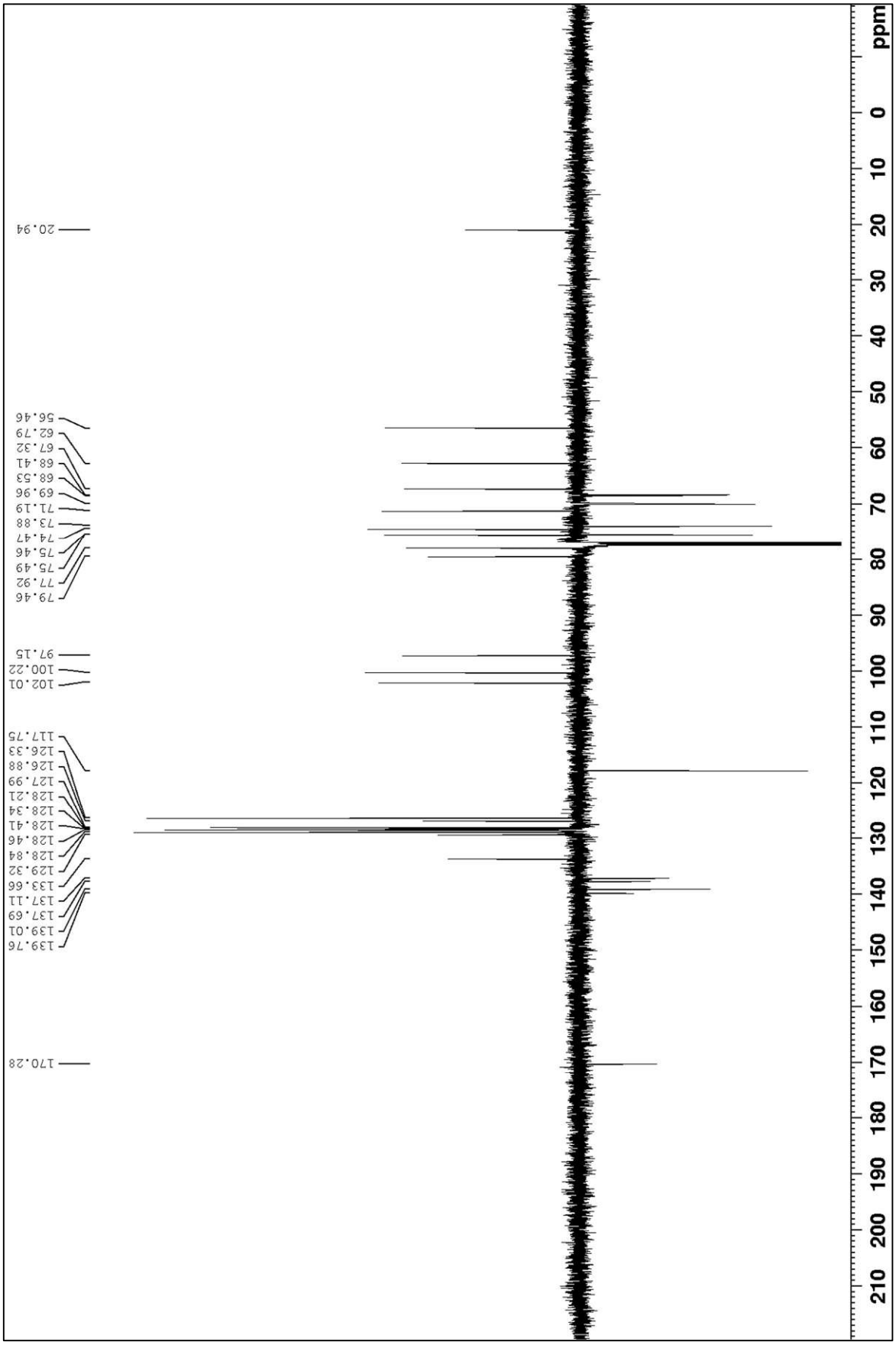

9.14.3 ^{1}H-^{13}C-HSQC

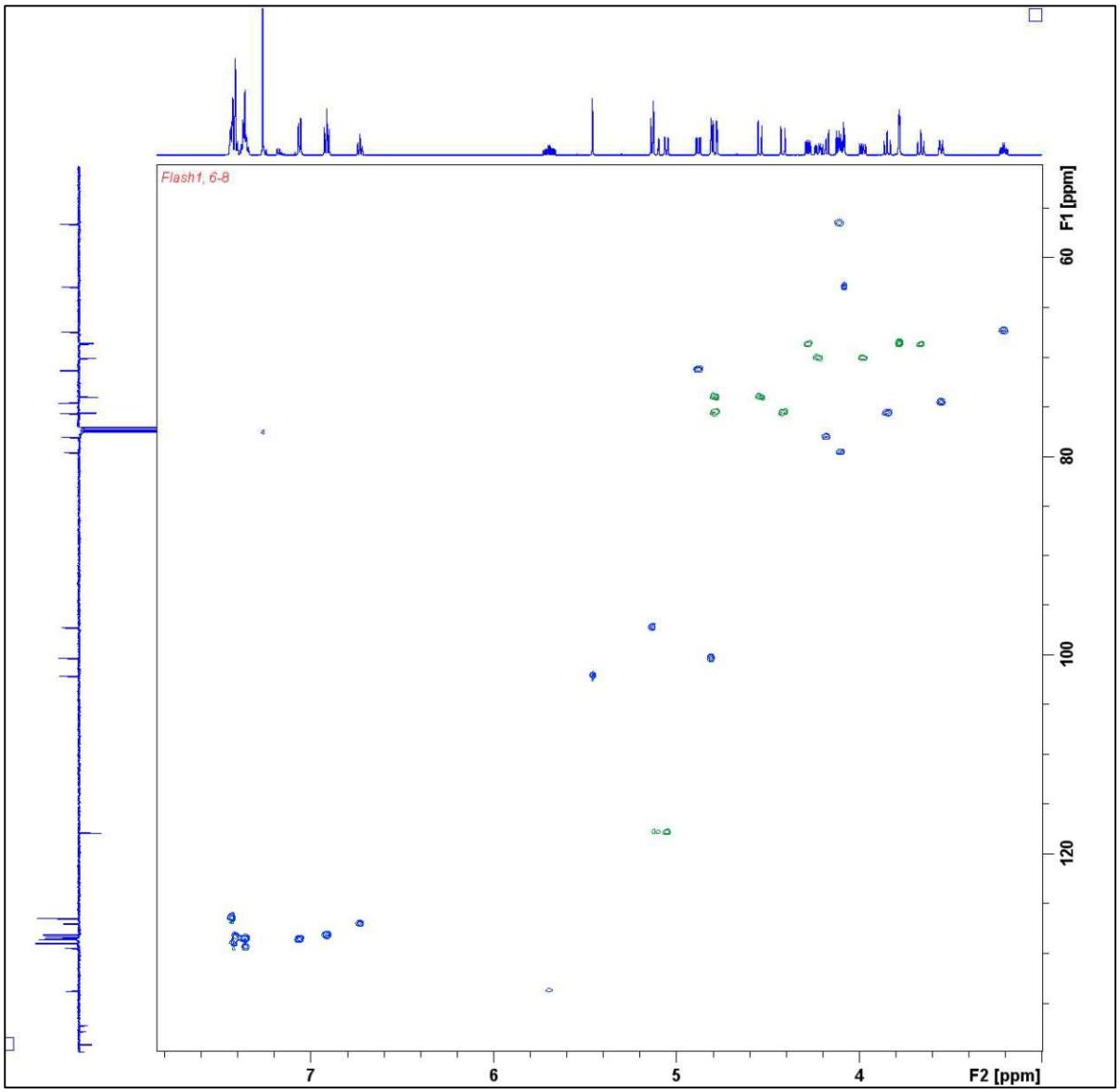

9.15 Compound **39**

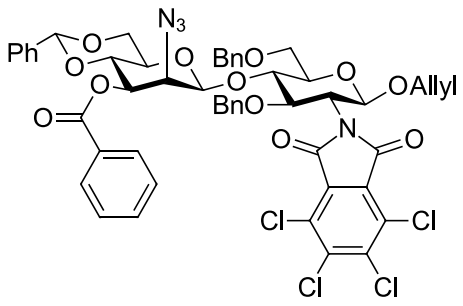

$C_{51}H_{44}Cl_4N_4O_{12}$
1046.720 amu

39

9.15.1 ^{1}H NMR

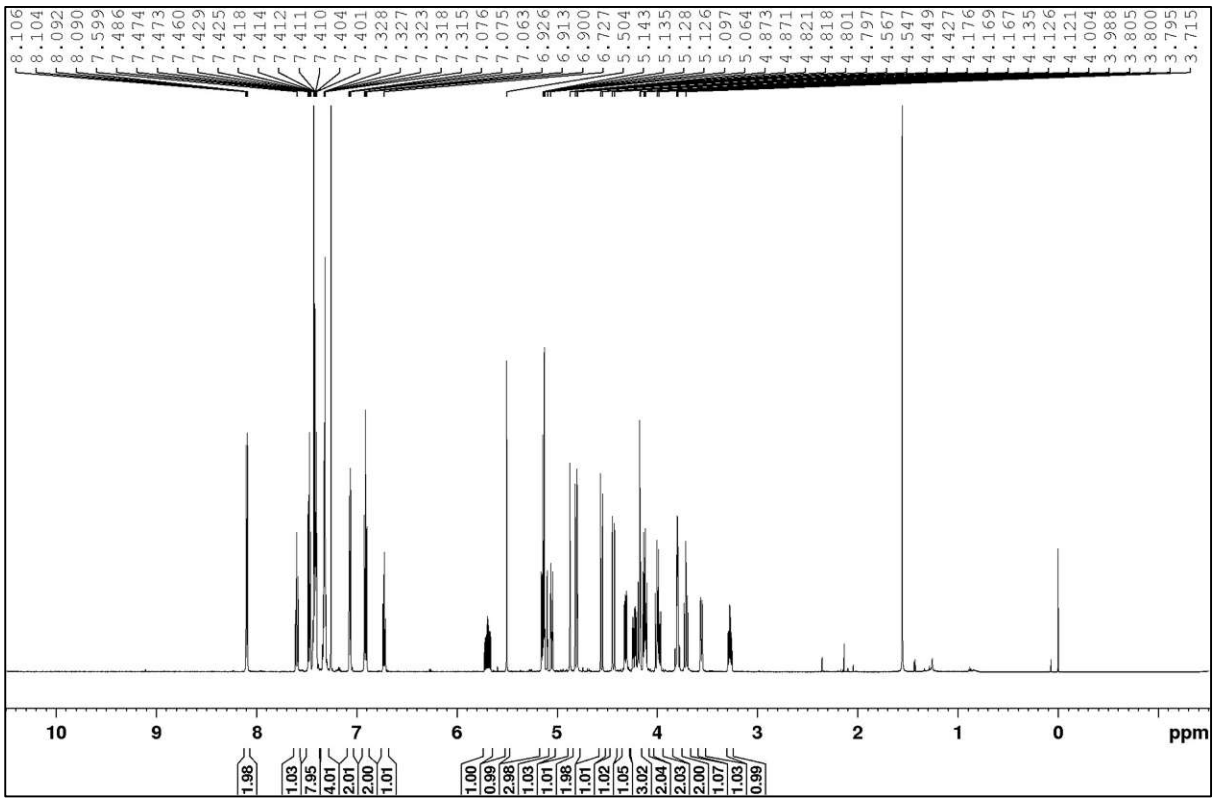

9.15.2 ^{13}C NMR

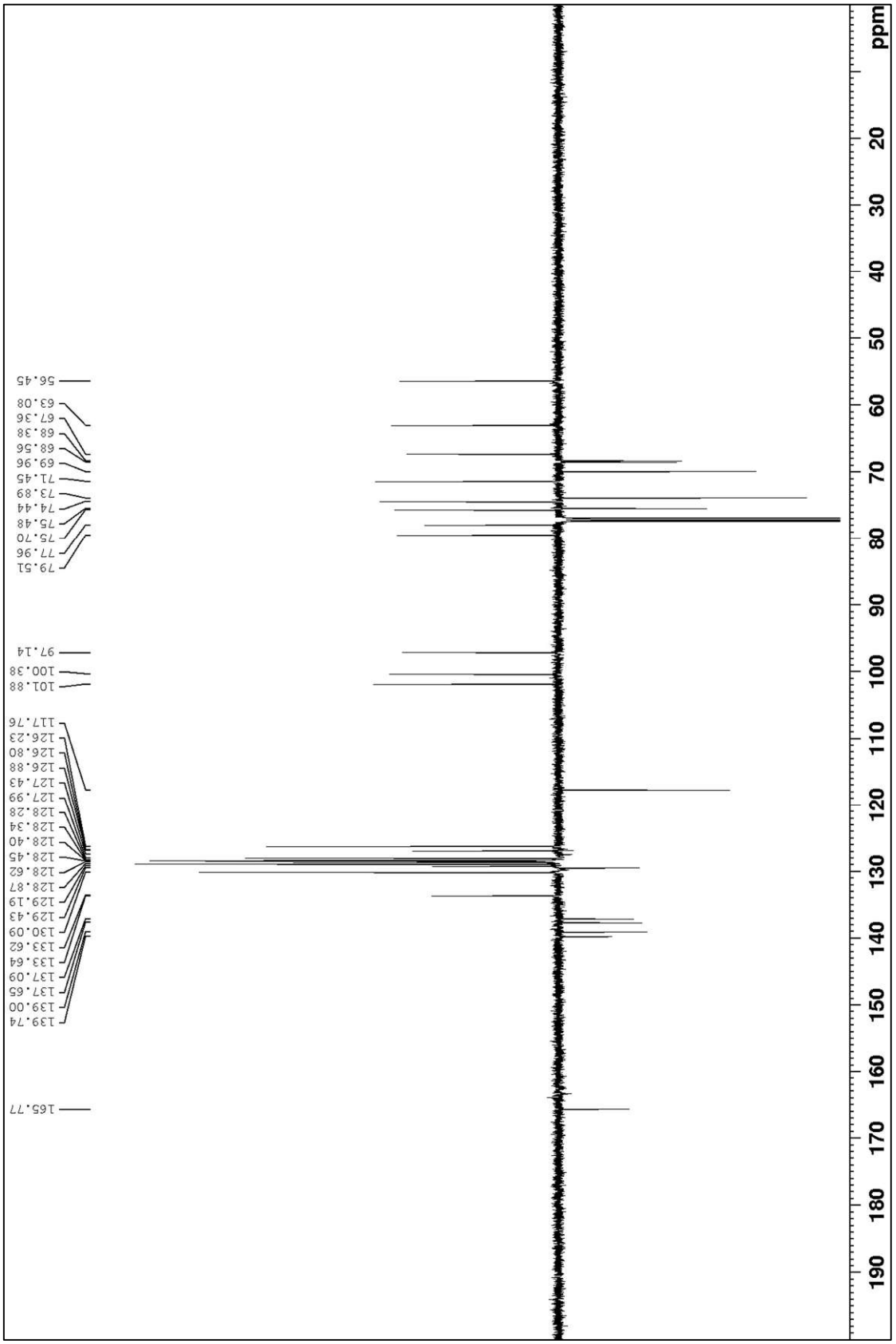

9.15.3 ^{1}H-^{13}C-HSQC

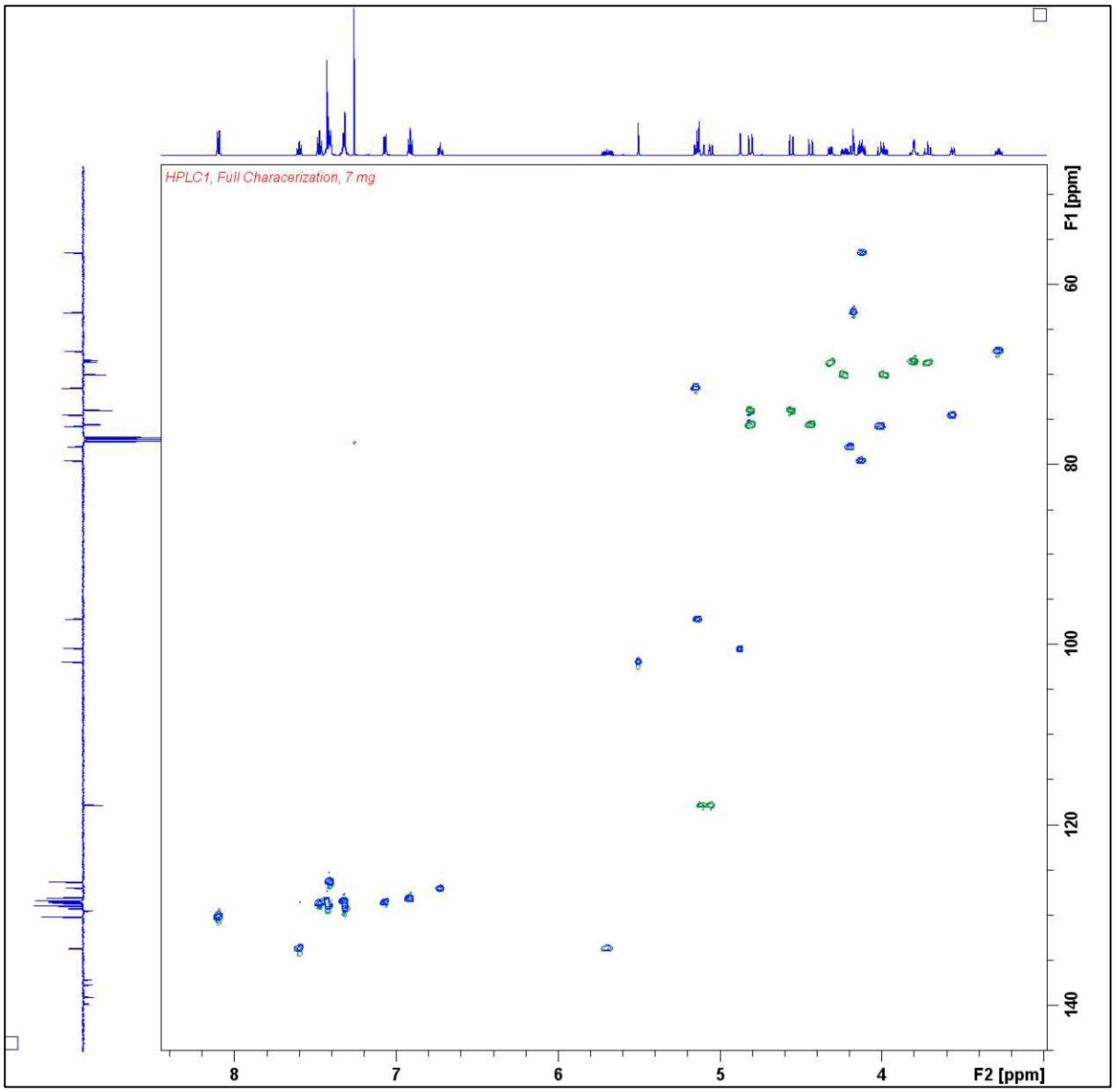

9.16 Compound **41**

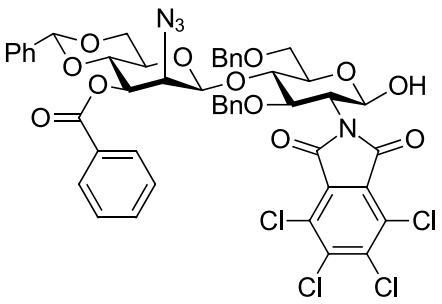

$C_{48}H_{40}Cl_4N_4O_{12}$
1006.657 amu

41

9.16.1 ^{1}H NMR

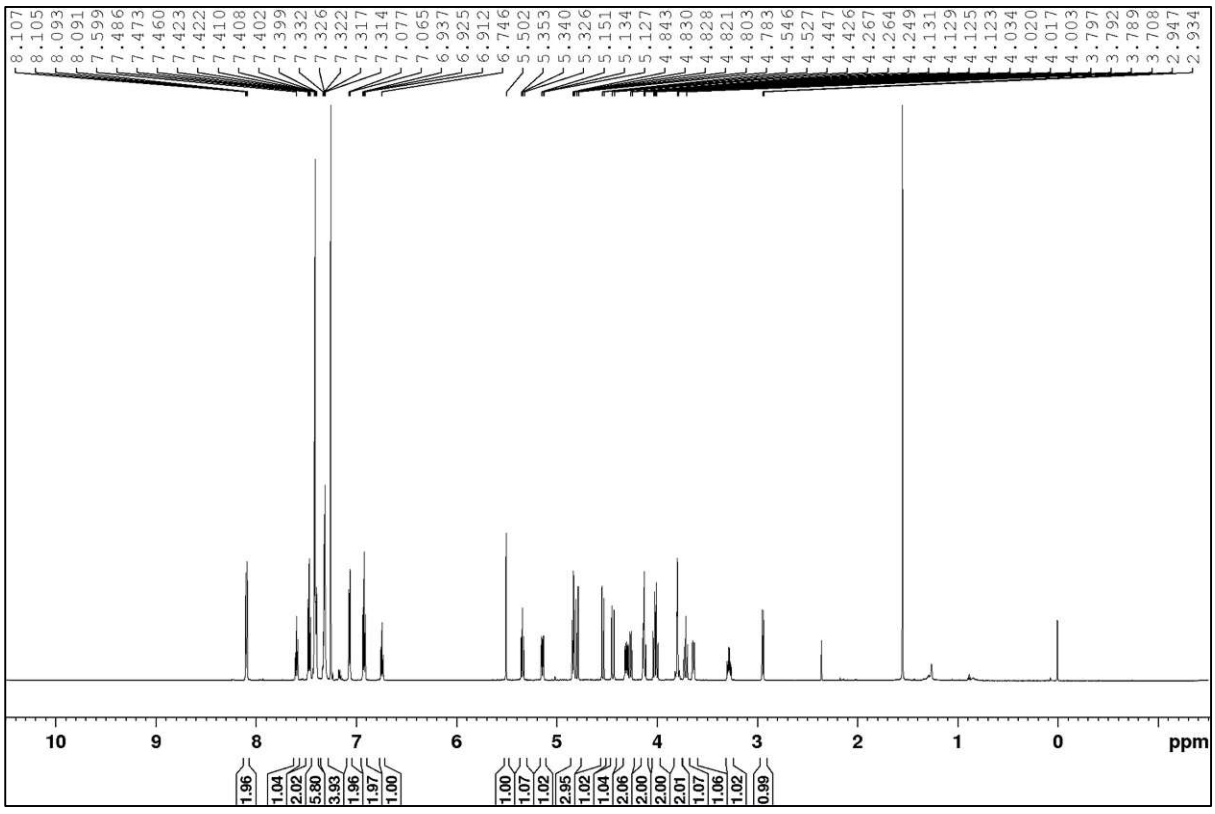

9.16.2 ^{13}C NMR

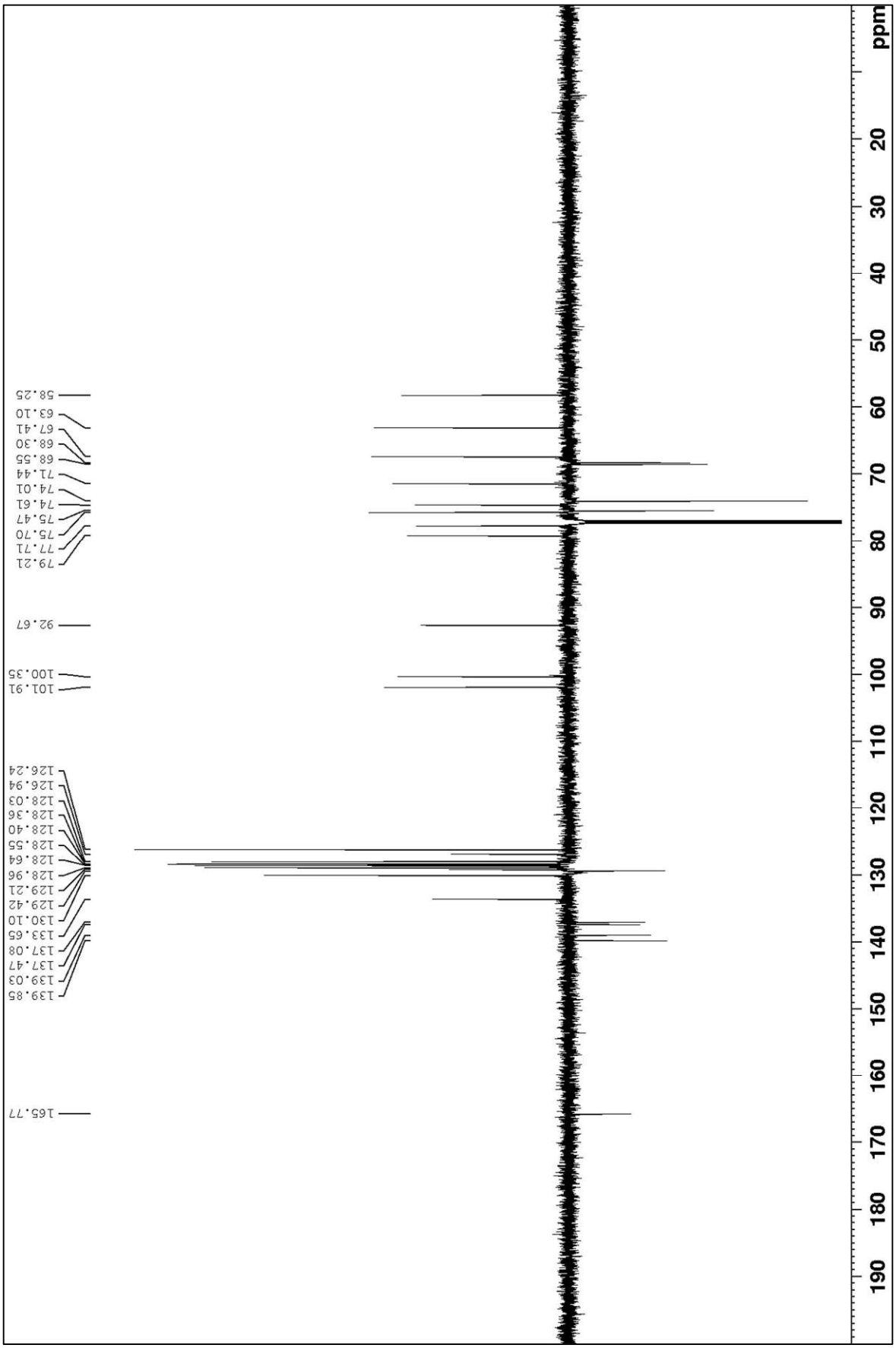

9.16.3 ^{1}H-^{13}C-HSQC

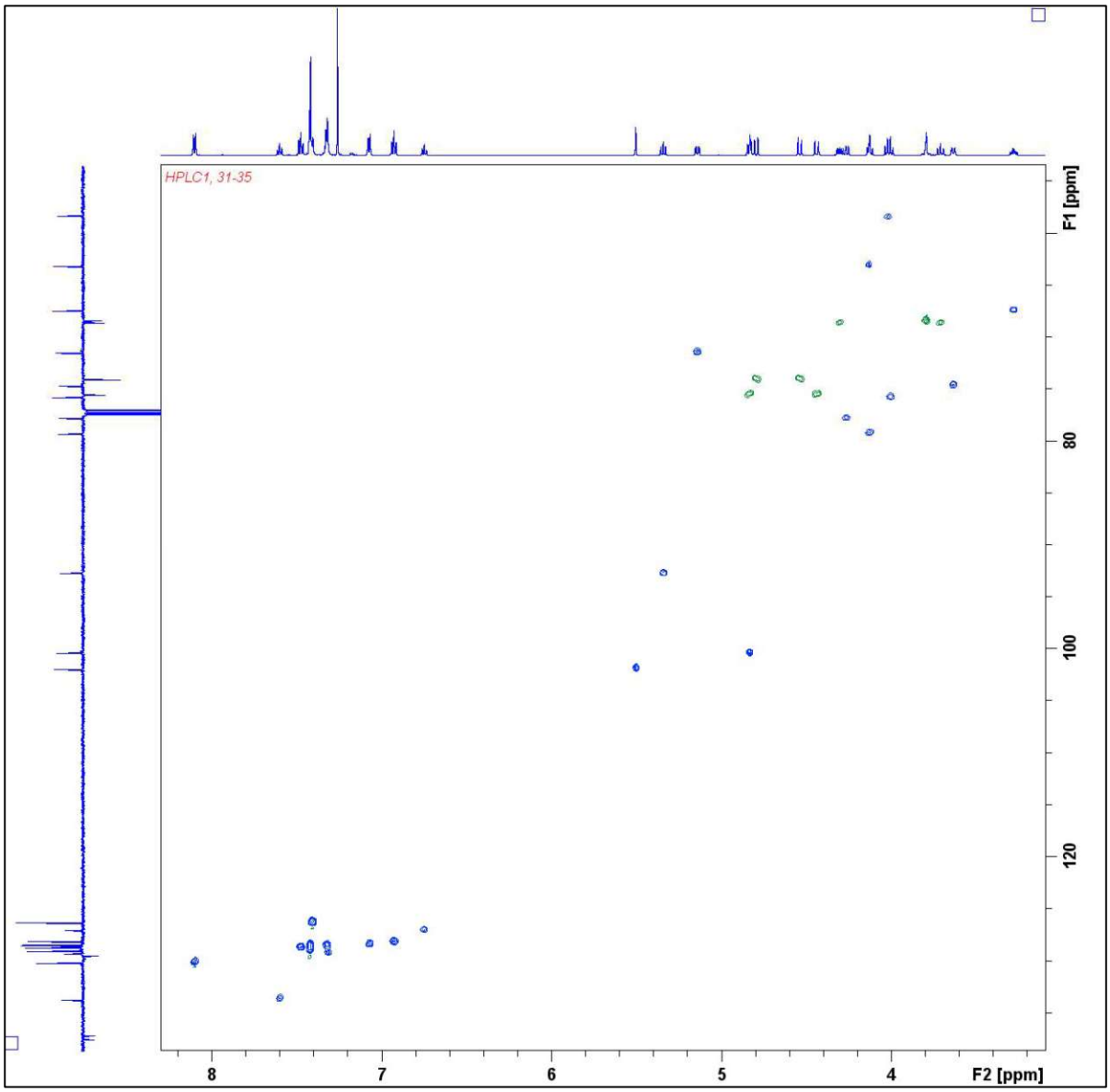

9.17 Compound **43**

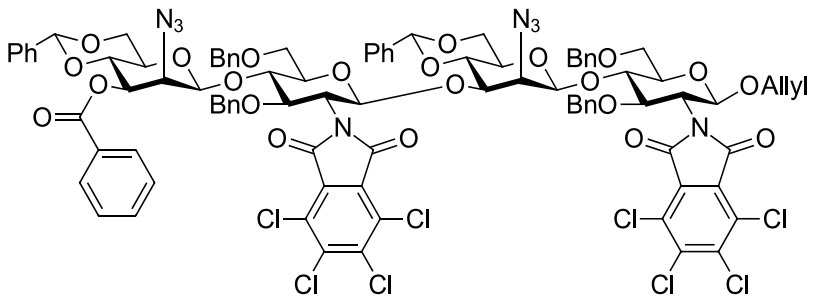

$C_{92}H_{78}Cl_8N_8O_{22}$
1931.255 amu

43

9.17.1 ^{1}H NMR

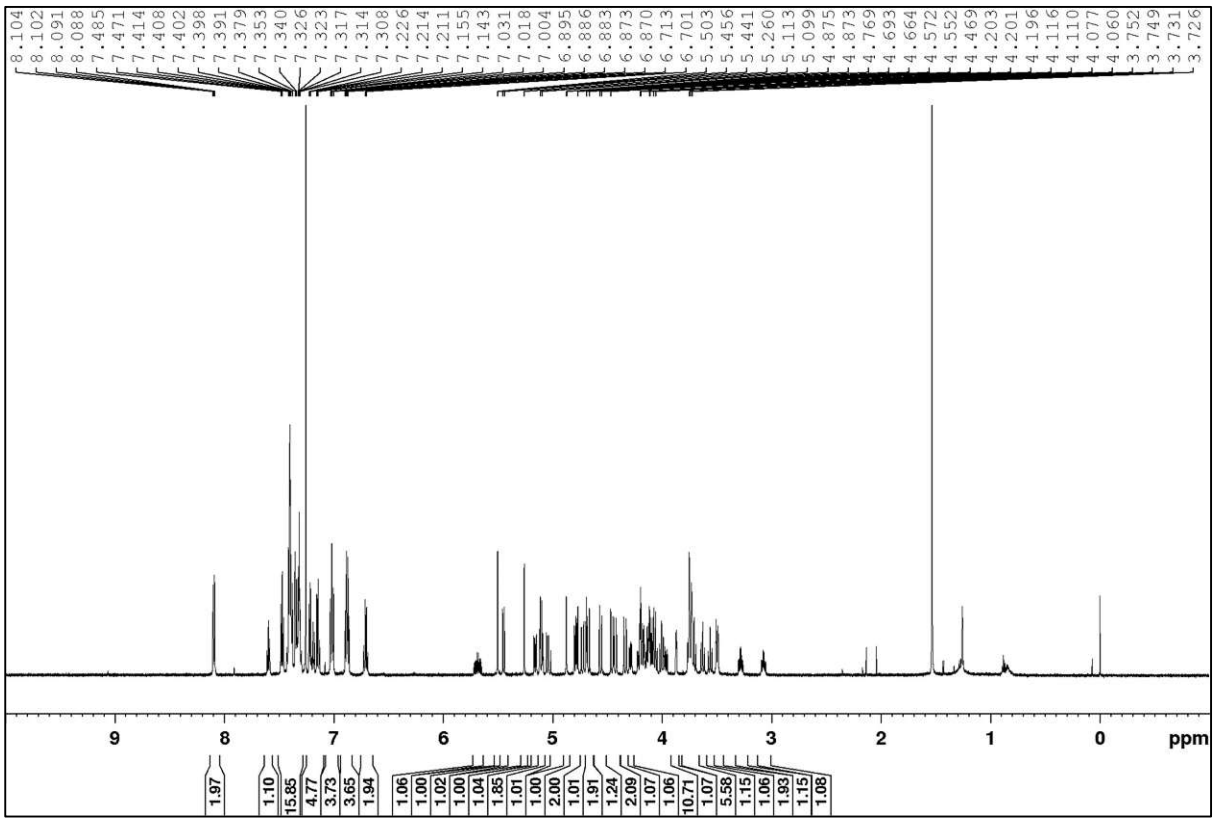

9.17.2 ^{13}C NMR

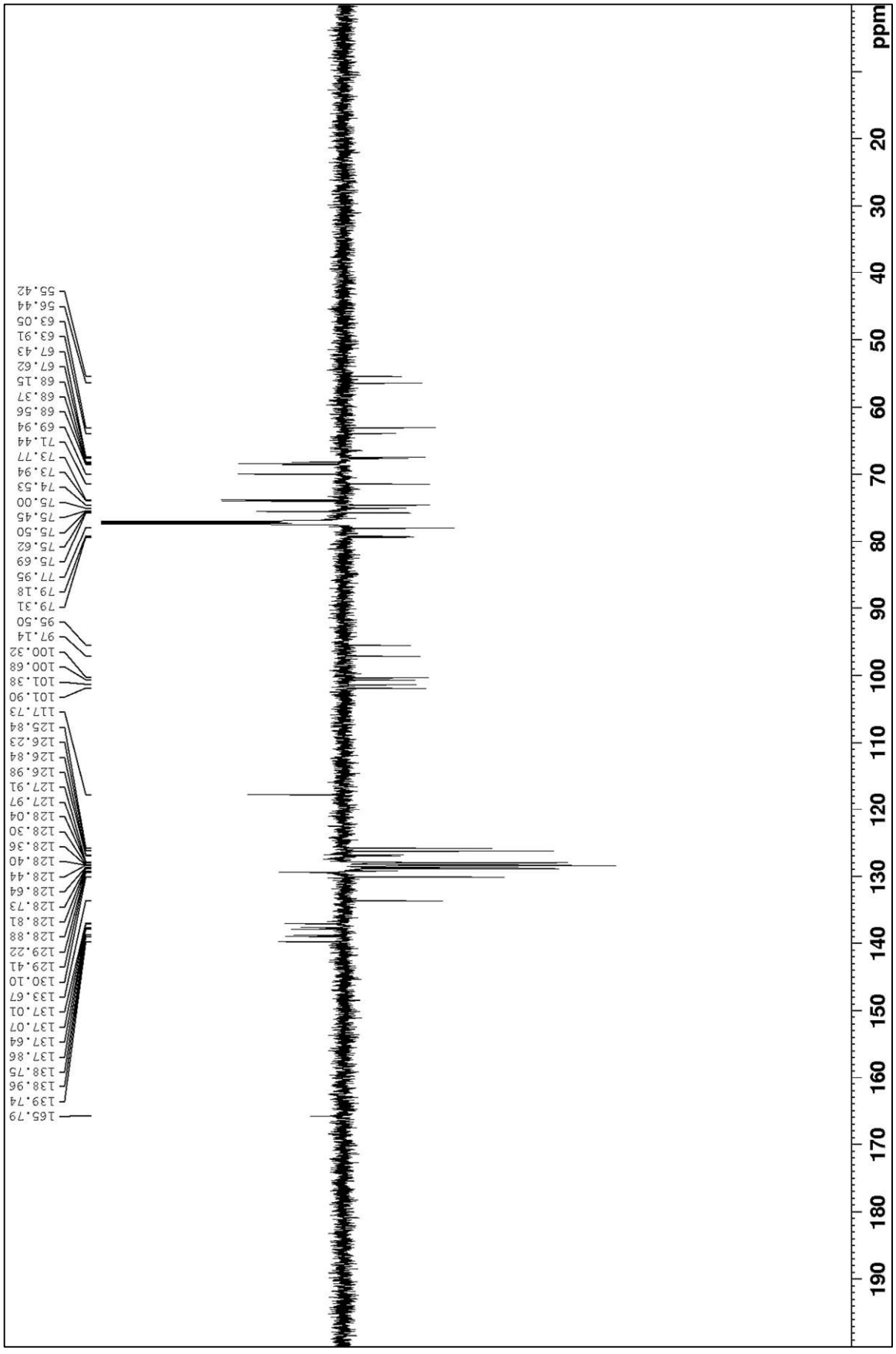

9.17.3 ^{1}H-^{13}C-HSQC

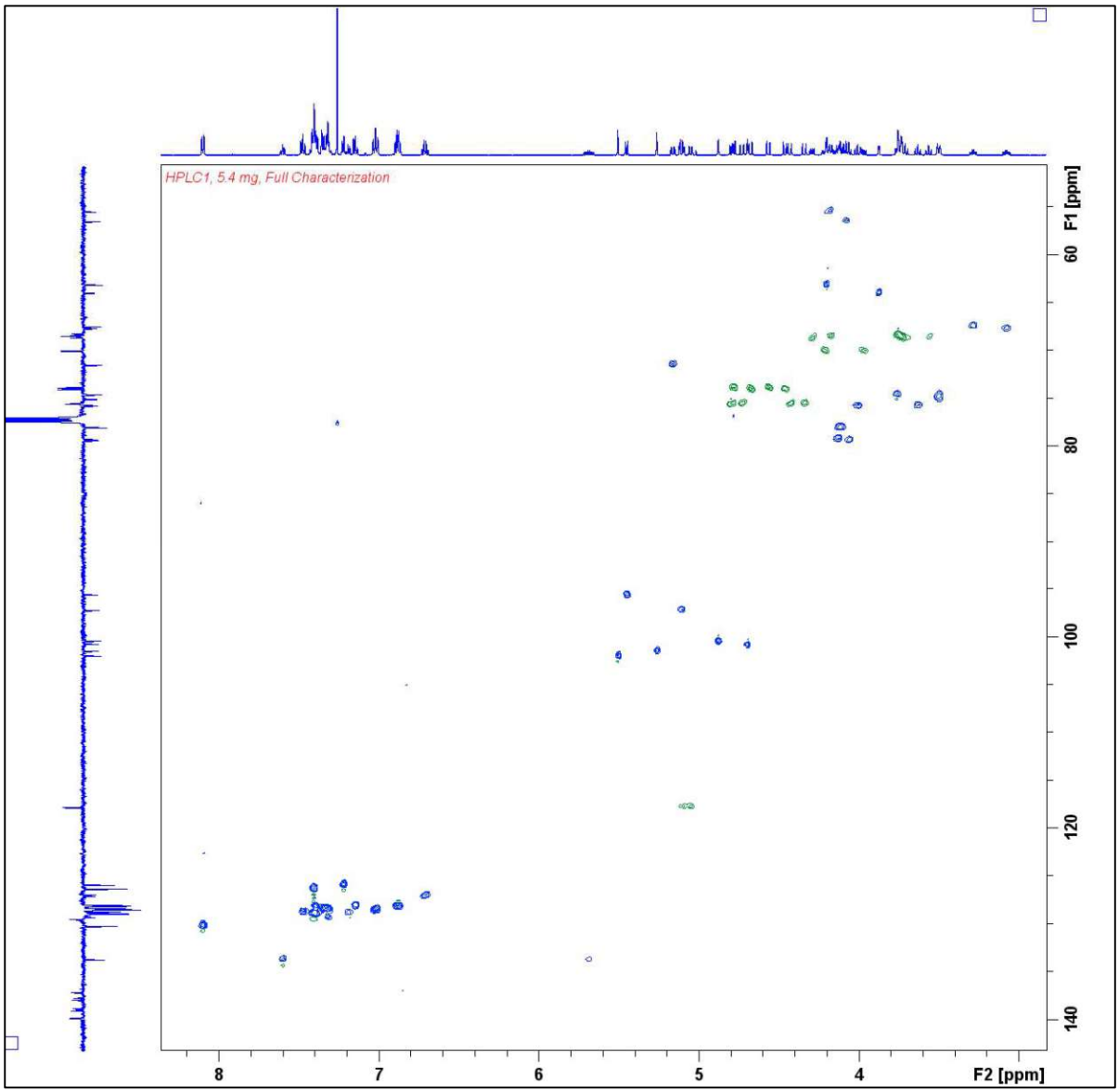

9.17.4 HSQC and CLIP-HSQC overlay

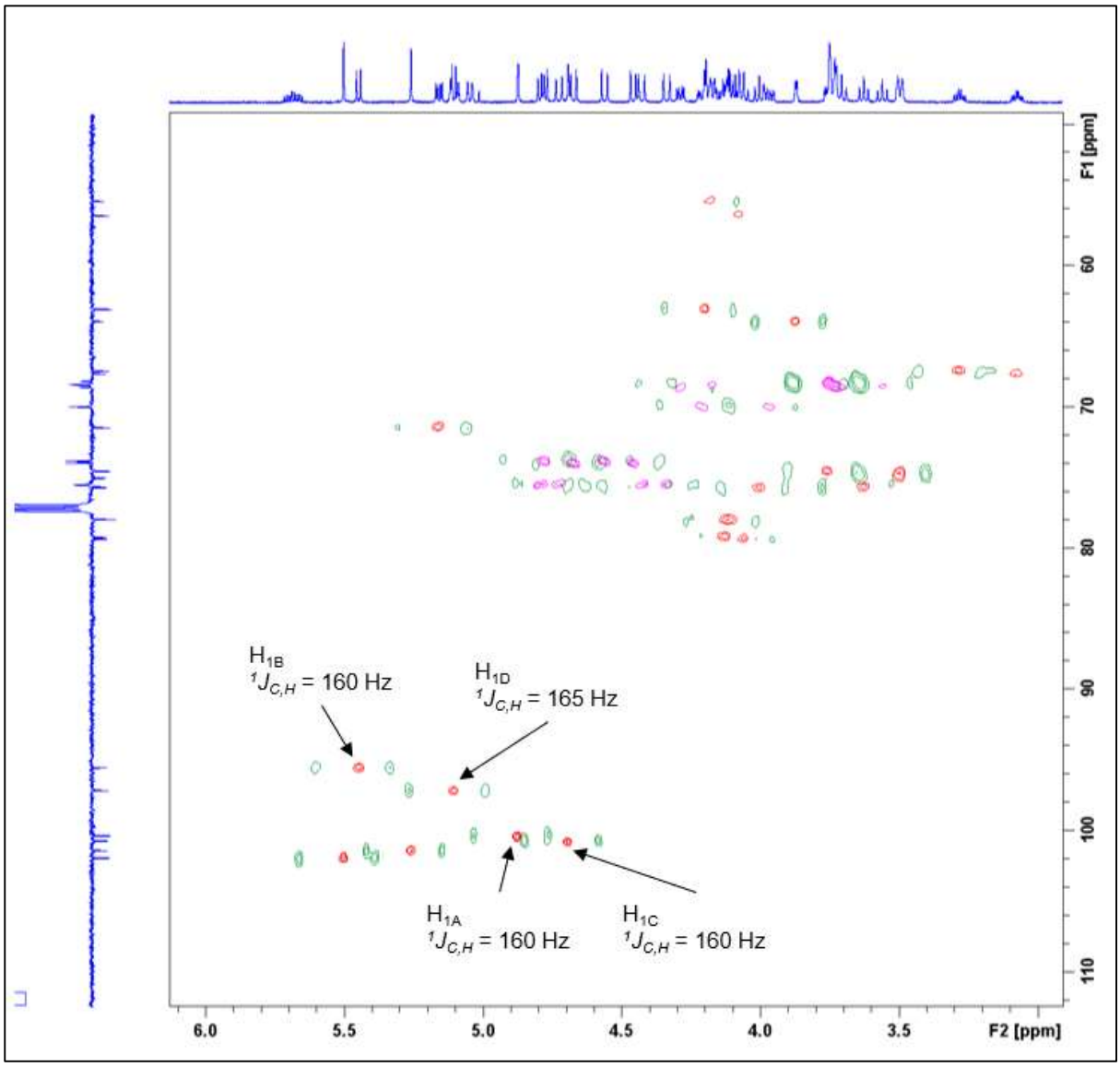

9.18 UDP-ManNAc **61**

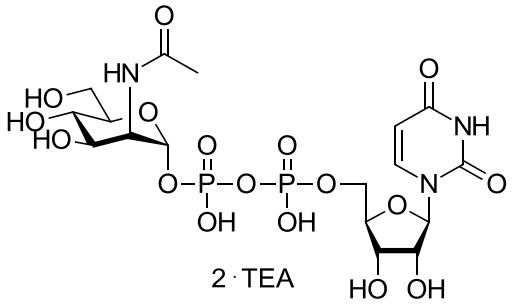

$C_{29}H_{61}N_5O_{17}P_2$
813.765 amu

61

9.18.1 ^{1}H NMR

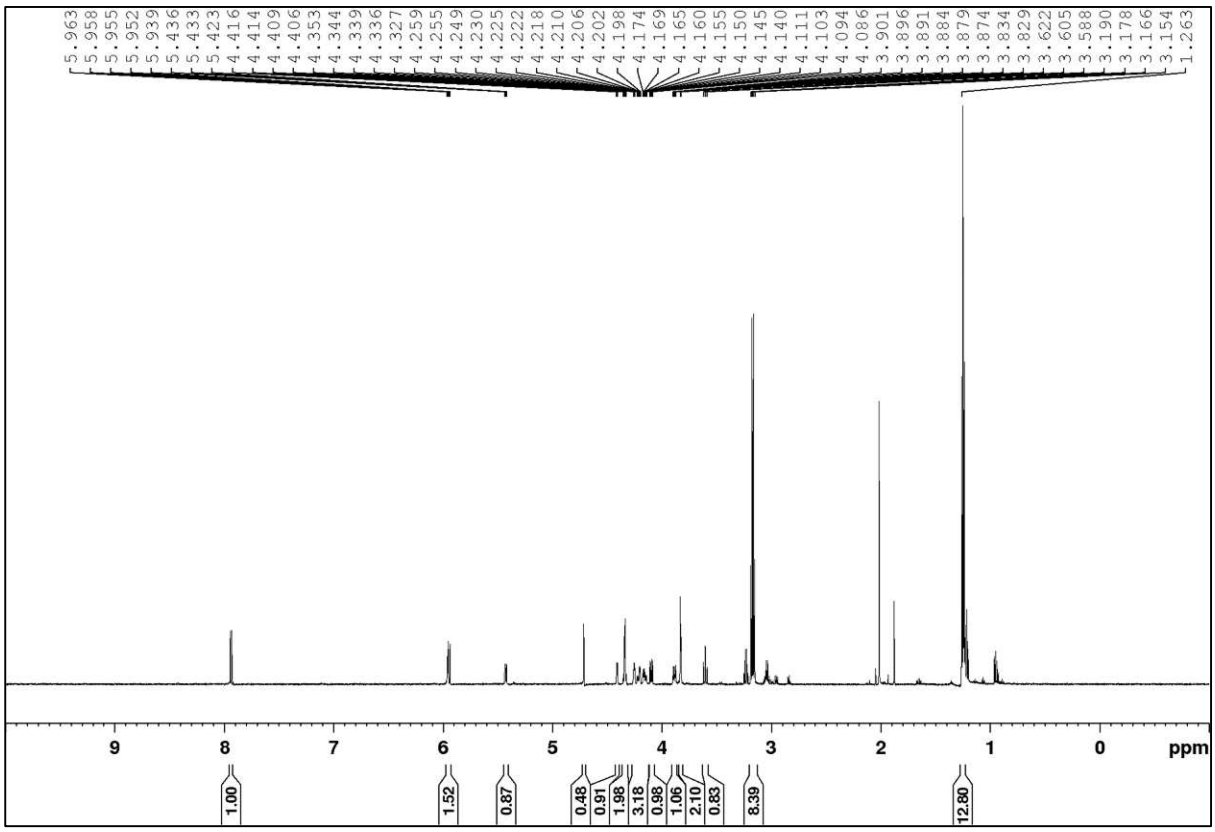

9.18.2 ^{1}H-^{31}P-HMBC